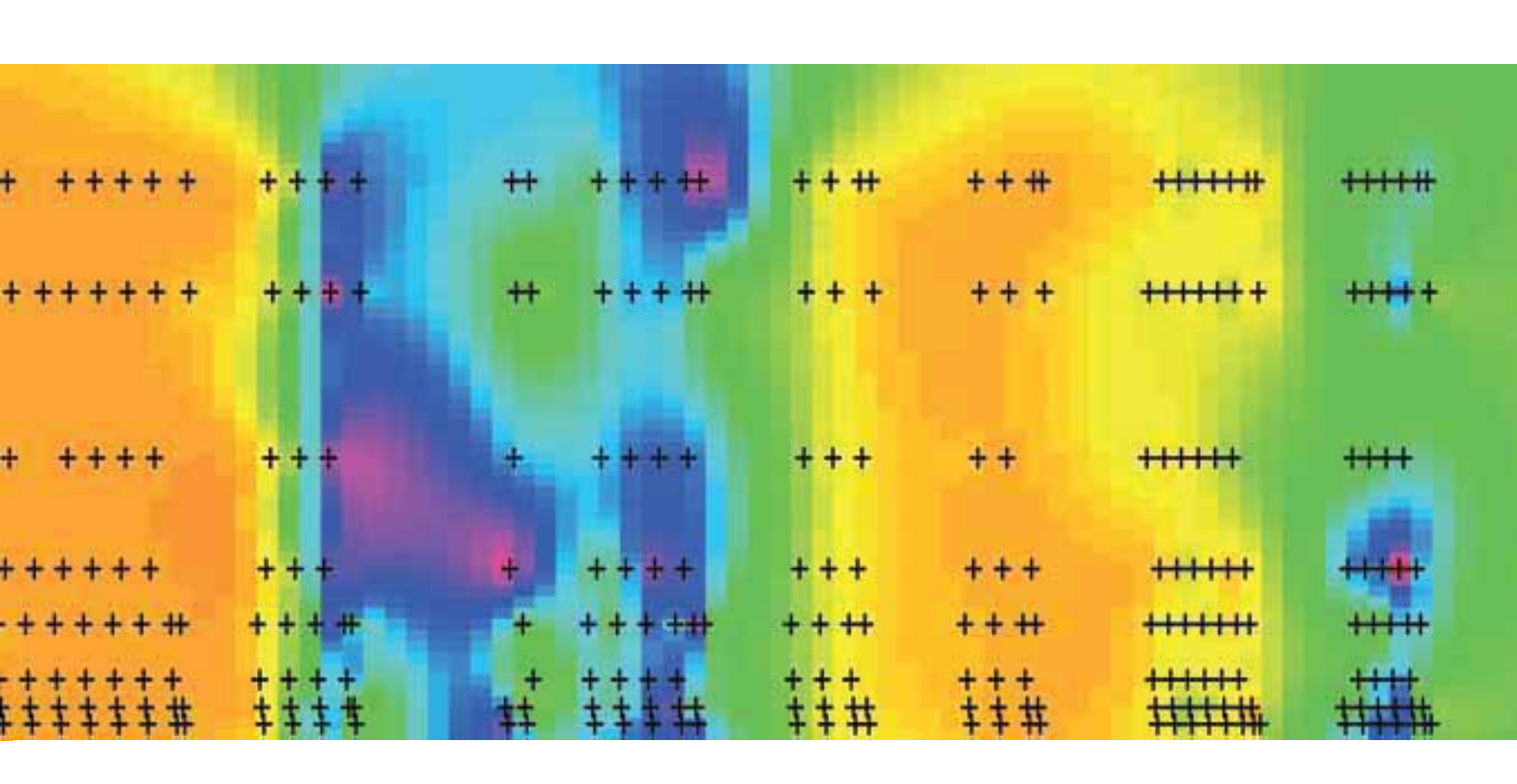
Methane emissions at farm and regional scales: origin, magnitude and spatio-temporal variability JACQUELINE V. STIEGER

ETH Zurich | 2013



Diss. ETH N°21538

Methane emissions at farm and regional scales: origin, magnitude and spatio-temporal variability

A dissertation submitted to ETH Zurich

for the degree of Doctor of Sciences

presented by

Jacqueline Stieger

Master of Science in Geography, University of Bern

14.02.1986 citizen of Oberriet-Holzrhode (SG)

Prof. Dr. Nina Buchmann
PD Dr. Werner Eugster
Prof. Dr. Euan Nisbet

2013

Dass ich nicht mehr, mit sauerm Schweiss,
Zu sagen brauche, was ich nicht weiss;
Dass ich erkenne, was die Welt
Im Innersten zusammenhält,
Schau alle Wirkenskraft und Samen,
Und tu nicht mehr in Worten kramen.

Faust – Der Tragödie erster Teil Johann Wolfgang Goethe

Abstract

Atmospheric methane (CH₄) is the second most important anthropogenic greenhouse gas after carbon dioxide (CO₂) and hence, an in-depth knowledge of methane sources and their emission strengths is of key importance for formulating mitigation strategies. Although the global methane budget is relatively well constrained, emission estimates by source sector are still substantially uncertain. As atmospheric methane originates from a variety of natural and anthropogenic sources, which in addition are spatially heterogeneously distributed, reliable emission estimates would require a dense measurement network. This is yet not achieved and methane emission estimates, hence, rely primariliy on model approaches, i.e., top-down and bottom-up approaches, which include only few direct measurements. Model estimates, however, do not only lack an experimental validation, but also do not take into account possible temporal variations of methane emissions, increasing overall estimation uncertainty. Particularly inventory emission estimates of agricultural methane, using a bottom-up approach based on livestock census data and default emission factors, are associated with high uncertainty levels. It is therfore crucial to experimentally investigate the spatio-temporal characteristics of atmospheric methane, in order to constrain methane budets and validate model estimates. This thesis aims to improve the understanding of the spatio-temporal pattern of atmospheric methane and its impact on the regional methane budget, with the main focus on methane emissions from agriculture.

We calculated methane budget fluxes from a typical farmstead in Switzerland from vertical concentration profiles in the nocturnal boundary layer (NBL) and compared them to inventory emission estimates of differing spatial resolution. The mean nocturnal budget flux of $1.59 \pm 0.22~\mu g$ CH₄ m⁻² s⁻¹ showed a good agreement with local inventory estimates of 1.29 ± 0.47 and $1.74 \pm 0.63~\mu g$ CH₄ m⁻² s⁻¹ for 2011 and for 2012, respectively, using current livestock numbers of the farmstead and default emission factors. Less agreement was found with the national inventory estimates and a spatially explicit inventory, due to the disaggregation of the emissions to different spatial scales. However, the results showed that the bottom-up approach used for inventory estimates is a valuable instrument to assess livestock methane emissions.

Spatially highly resolved near-surface transect measurements, conducted at the

Reuss Valley in Central Switzerland, revealed that point measurements of methane concentrations carried different information from the surrounding methane sources during day and night. Nighttime point measurements within the NBL showed a source influence of up to 9 km distance and, hence, can be used to constrain regional emission estimates of models. In contrast, daytime point measurements had a source influence distance of <1 km and are useful to exactly localize a methane source. The distribution of methane concentrations in the atmosphere, however, was not only affected by the source distribution itself but also by local wind patterns and the mixing efficiency of the atmospheric boundary layer. Thus, regional models need to include the atmospheric transport properties in order to reliably localize methane sources. These results showed that spatially highly resolved measurements are not only needed to identify the methane sources within a region, but are also essential to constrain high resolution inventories revealing inconsistencies in their source distribution.

A valuable tool to identify local methane sources from atmospheric methane measurements, without the need for measurements in the direct vicinity of the source, are measurements of δ^{13} C in CH₄. Spatio-temporally highly resolved measurements in the Reuss Valley revealed, that the nighttime methane build-up in the stable NBL was mainly caused by emissions from agriculture. Although non-biogenic sources had a minor contribution to the overall nighttime excess methane, their emission strengths were of similar magnitude compared to biogenic sources. During daytime, however, the contribution of non-biogenic methane sources to the total source mix in the Reuss Valley increased substantially to 22% and was attributed to the transport of δ^{13} C-enriched air masses from upwind lying agglomerations into the valley. Furthermore, it was shown that during the period of our measurements, the nighttime methane build-up was compensated during the day by convective dilution.

In summary, this thesis presents spatio-temporally highly resolved measurements of $\mathrm{CH_4}$ concentrations and $\delta^{13}\mathrm{C}$ in complex terrain, compares methane budget fluxes to inventory estimates and hence, contributes substantially to the scientific understanding of methane emissions and their temporal and spatial variations within the atmospheric boundary layer. The results underline that direct measurements are needed in order to constrain model estimates and to draw essential implications for methane budgets.

Zusammenfassung

Methan (CH₄) ist nach Kohlendioxid (CO₂) das wichtigste anthropogene Treibhausgas in der Atmosphäre, daher spielt das genaue Verständnis der Emissionsquellen und -stärken eine wichtige Rolle bei der Umsetzung von Klimaschutzmassnahmen. Die Abschätzungen der Methanemissionen aus einzelnen Quellen sind jedoch mit beträchtlichen Unsicherheiten verbunden, trotz der relativ genauen Berechnung der globalen Methanbilanz. Auf Grund der Vielfalt an natürlichen und anthropogenen Quellen und ihrer räumlich heterogenen Verteilung bedarf es eines dichten Netzwerkes an Messstationen für eine solide Einschätzung der Emissionen. Dies ist jedoch noch nicht erreicht, weshalb die Emissionen vorwiegend anhand von Modellen (mit sogenannten bottom-up und top-down Ansätzen) berechnet werden und selten auf direkten Messungen basieren. Auch die zeitliche Variabilität der Emissionen wird in den Modellen kaum berücksichtigt, was nebst der fehlenden experimentellen Überprüfung ein weiterer Grund für die hohen Unsicherheitsbereiche der Abschätzungen ist. Vor allem inventarbasierte, landwirtschafliche Abschätzungen, die vorwiegend auf statistischen Datenerhebungen und vorgegebenen Emissionsfaktoren innerhalb eines bottom-up Ansatzes basieren, weisen hohe Unsicherheitsbereiche auf. Um CH₄-Budgets einschränken und Modelleinschätzugnen validieren zu können, ist die Untersuchung des zeitlichen und räumlichen Musters von Methan in der Atmosphäre unverzichtbar. Das Ziel dieser Arbeit war es, das Verständnis über die räumlich und zeitliche Variabilität von Methan in der Atmosphäre zu verbessern und dessen Einfluss auf regionale CH₄-Budgets zu analysieren. Der Schwerpunkt lag dabei auf Methanemissionen aus landwirtschaflichen Quellen.

Anhand von vertikalen Konzentrationsprofilen in der nächtlichen Grenzschicht berechneten wir CH₄-Budgets für einen typisch schweizerischen Bauernhof und verglichen diese mit mehreren inventarbasierten Abschätzungen von unterschiedlicher räumlicher Ausdehnung. Das durchschnittliche CH₄-Budget von 1.59 \pm 0.22 μ g CH₄ m⁻² s⁻¹ stimmte gut mit der lokalen Inventarabschätzung überein, basierend auf dem aktuellen Tierbestand des untersuchten Bauernhofes (1.29 \pm 0.47 für 2011 und 1.74 \pm 0.63 μ g CH₄ m⁻² s⁻¹ für 2012). Eine weniger gute Übereinstimmung ergab der Vergleich zu den Abschätzungen des nationalen Inventars und eines räumlich hoch aufgelösten Inventars. Die Validierung der Inventarsabschätzungen zeigte dennoch, dass der bottom-up Ansatz, auf den die Inventarsabschätzungen basieren, ein

praktikables Instrument zur Abschätzung von Tieremissionen darstellt.

Räumlich hoch aufgelöste Konzentrationsmessungen im Reusstal (Zentralschweiz) zeigten, dass bodennahe Punktmessungen in der Nacht und am Tag unterschiedliche Informationen zu umliegenden Methanquellen beinhalteten. In der Nacht war der Einfluss einer Quelle (innerhalb der nächtlichen Grenzschicht) von bis zu 9 km Distanz nachweisbar. Messungen in der Nacht können somit zu Vergleichen mit regionalen Modellabschätzungen herangezogen werden. Hingegen zeigten bodennahe Punktmessungen am Tag, dass der Einfluss einer Quelle nur unter einer Distanz von 1 km nachweisbar ist und damit zur exakten Ortsbestimmung von Quellen dienen. Die räumliche Verteilung von Methan in der Atmosphäre hing hingegen nicht allein von der Quellenverteilung, sondern auch von den lokalen Windverhältnissen und der Durchmischung der Grenzschicht ab. Der Einbezug von Transportprozessen ist somit für eine verlässliche Lokalisierung der Quellen mittels Modellen unerlässlich. Räumlich hoch aufgelöste Messungen sind sowohl für die Ortsbestimmung der Methanquellen als auch für die Überprüfung von Unstimmigkeiten innerhalb hoch aufgelöster Modellabschätzungen und Inventare notwendig.

Messungen von den Kohlenstoff-Isotopenverhältnissen (δ^{13} C) in CH₄ stellen eine elegante Art der Quellenermittlung dar, da keine Messungen in der unmittelbaren Nähe der Quellen erforderlich sind. Räumlich und zeitlich hoch aufgelöste Messungen von δ^{13} C in CH₄ im Reusstal zeigten, dass vor allem landwirtschaftliche Emissionen zum nächtlichen Konzentrationsaufbau beitrugen. Obwohl abiogene Quellen nur geringfügig zum Aufbau beitrugen, hatten sie vergleichbare Emissionsstärken wie biogene Quellen. Am Tag stieg der Beitrag von abiogenen Quellen am Gesamtmethan in der Atmosphäre auf rund 22%, der aus der Advektion von 13 C-angereicherter Luft von windaufwärts liegenden Agglomerationen resultierte. In der Folge wurde der nächtliche Konzentrationsaufbau während unserer Messungen durch die konvektive Durchmischung am Tag kompensiert.

Diese Arbeit präsentiert räumlich und zeitlich hoch aufgelöste δ^{13} C- und CH₄ Konzentrationsmessungen in komplexem Gelände und vergleicht CH₄-Budgets mit inventarbasierten Abschätzungen. Sie leistet damit einen substanziellen Beitrag zum wissenschaftlichen Verständnis über Methanemissionen und ihrer zeitlichen und räumlichen Variabilität innerhalb der Grenzschicht. Die Ergebnisse heben hervor, dass direkte Messungen für die Begrenzung von Modellabschätzungen notwendig sind und wichtige Implikationen für Methanbilanzierung beinhalten.

Contents

Li	ist of Figures x			xii
Li	st of	Tables	S	xiv
1 Introduction				1
	1.1	Metha	ne from a global perspective	1
	1.2	Switze	erland's methane emission inventory estimates	2
	1.3	Measu	rement techniques	3
		1.3.1	Estimating methane emissions at different spatial scales	3
		1.3.2	Identifying methane sources	4
	1.4	Object	tives	5
	1.5	Thesis	soutline	6
	Refe	rences		7
_	3 7 19	1		
2			of farm-scale methane emissions using nocturnal bound-	
	·	v	budgets	11
	2.1	Introd	uction	13
	2.2	Mater	ials and Methods	15
		2.2.1	Site description	15
		2.2.2	Vertical balloon profiles and ground measurements	15
		2.2.3	Budget flux calculation	16
		2.2.4	Inventory estimates	18
		2.2.5	Data processing and general conventions	19
	2.3	Result	s	20
		2.3.1	Weather conditions and diel course of methane concentrations	20
		2.3.2	Vertical balloon profiles	21
		2.3.3	NBL budget fluxes and comparison to inventory estimates	22

X CONTENTS

	2.4	Discus	ssion	23
		2.4.1	Using the NBL budget approach in complex terrain	23
		2.4.2	Validating inventory estimates	25
	2.5	Concl	usion	26
	2.6	Tables	s and figures	27
	Refe	erences		32
3	Spa	tial va	riability of methane: Attributing atmospheric concentra-	
	tion	s to e	missions	37
	3.1	Introd	luction	36
	3.2	Mater	ials and Methods	40
		3.2.1	Site description and transect patterns	40
		3.2.2	Mobile measurement set-up	41
		3.2.3	Data analysis	42
	3.3	Result	ts	43
		3.3.1	Spatio-temporal variability of CH_4 concentrations	43
		3.3.2	Concentrations for constraining emission inventories	45
	3.4	Discus	ssion	47
		3.4.1	Processes driving the spatio-temporal CH ₄ concentration pat-	
			terns	47
		3.4.2	Constraining emission inventories using concentration mea-	
			surements	49
	3.5	Concl	usion	50
	3.6	Tables	s and figures	52
	Refe	erences		60
4	Sou	rce pa	rtitioning of atmospheric methane using carbon isotopes	63
	4.1	Introd	luction	65
	4.2	Mater	ials and Methods	66
		4.2.1	Study Area	66
		4.2.2	Stationary and mobile set-ups	67
		4.2.3	Isotope ratio analysis	68
		4.2.4	Nighttime source identification	68
		4.2.5	Daytime source identification	70
	43	Result	S	71

CONTENTS xi

		4.3.1	Mean diel cycles of CH_4 and $\delta^{13}C$		71
		4.3.2	Source identification		72
	4.4 Discussion				74
		4.4.1	Spatio-temporal varibility of $\mathrm{CH_4}$ and $\delta^{13}\mathrm{C}$		74
		4.4.2	Source partitioning		76
		4.4.3	Implications for methane emission budgets		77
	4.5	Conclu	usion		77
	4.6	Tables	s and figures		79
	Refe	rences			87
5	Syn	thesis			91
J	5.1		o-temporal dynamics of atmospheric CH ₄ in the Reuss Valley		91
		-	- · · · · · · · · · · · · · · · · · · ·		
	5.2	-	eations for model estimates		93
	5.3	Outloo	ok and research considerations		94
Aj	ppen	dices			97
A	Ant	hrono	genic and natural methane fluxes in Switzerland syntl	he-	
		- '	in a spatially-explicit inventory	110	97
В			ng response of grassland versus forest carbon and wa		
	flux	es to s	spring drought in Switzerland	1	121
\mathbf{C}	Larg	ge pea	ks of N_2O emissions following grassland restoration	1	135
A	cknov	wledge	ements	1	L 67
Cı	ırric	ulum '	Vitae	1	L 69

List of Figures

2.1	Meteorological conditions at Chamau during the balloon measure-	
	ments in 2011 and 2012	29
2.2	Kriged time-space interpolation (a) and diel course (b) of the methane	
	concentrations during 16/17 Aug 2011	30
2.3	Vertical profiles of potential temperature gradients (a), methane con-	
	centration (b) and wind direction (c) of the individual balloon mea-	
	surements	31
3.1	Routing of the valley and mountain transects in the Reuss Valley	53
3.2	Methane concentrations along the valley and mountain transects	54
3.3	Vertical profiles of air temperature (a) and methane concentration	
	(b) from the valley transect measurements	55
3.4	Vertical profiles of air temperature (a) and methane concentration	
	(b) from the mountain transect measurements	56
3.5	(a) Pearson correlation coefficients for the relationship between the	
	diurnal methane cycle at locations along the valley transect and	
	the diurnal cycle for the region, (b) regional average diurnal cycle	
	of methane concentrations including the average diurnal cycles of	
	methane at the (c) western and (d) eastern hillsides	57
3.6	(a) Source influence distances of point measurements at different	
	times of the day and (b) diurnal cycle of the displacement distances	
	for different source influence percentages	58
3.7	Quantile analysis between inventory emission estimates and concen-	
	tration measurements	59

4.1	Topographic map of the Reuss Valley with the stationary and mobile	
	set-up sites	82
4.2	Diel course of $\delta^{13}\mathrm{C}$ and $\mathrm{CH_4}$ concentrations at at the stationary set-up	
	site in 2011 and 2012	83
4.3	Diel courses of $\delta^{13}\mathrm{C}$ and $\mathrm{CH_4}$ concentrations at the mobile set-up sites	
	in 2012	84
4.4	Keeling plot of nighttime carbon isotopic data of observed CH_4 con-	
	centrations in 2011 and 2012	85
4.5	Source partitioning of daytime $\delta^{13}\mathrm{C}$ values into biogenic sources, non-	
	biogenic sources and sink processes	86

List of Tables

2.1	Overview of the balloon measurements in 2011 and 2012	27
2.2	Methane emission estimates from different inventories (NIR, SEI and	
	CHAI) and the NBL budget approach	28
3.1	Overview of the transect measurements during July 2012	52
4.1	Source types of methane in the Reuss Valley and their $\delta^{13}\mathrm{C}$ charac-	
	teristics	79
4.2	Nighttime source identification of $\delta^{13}\mathrm{C}$ values of (a) 2011 and (b) 2012	
	measurements	80

Introduction

1.1 Methane from a global perspective

Methane (CH₄) is the second most important anthropogenic greenhouse gas after carbon dioxide (CO₂). Despite its small atmospheric concentration and its short lifetime (approx. 9 years), methane's global warming potential is about 25 times larger compared to CO₂ (IPCC, 2007). Although in 1951, methane has been first considered as a 'non-variable component of atmospheric air' (Khalil, 2000), its concentration rose since 1750 by a factor of 2.5 to 1.745 ppm and it currently contributes about 20% to the anthropogenic radiative forcing (Lassey, 2007; Denmead, 2008). This increase in atmospheric methane is mainly attributed to the increase of anthropogenic emissions from fossil fuel energy production, agriculture, waste management systems and biomass burning (Lassey, 2007). Today's global methane budget is relatively well constrained and the total emissions are estimated to 500–600 Tg CH₄ yr⁻¹ (Dlugokencky et al., 2011). While anthropogenic emissions are the major contributor, natural sources, i.e., wetlands, oceans, lakes, termites, wild fires and wild ruminant animals, contribute only about one-third to the total methane emissions (Dalal et al., 2008). On a global scale, the main sink for atmospheric methane is the oxidation of CH₄ by the hydroxyl radical (OH⁻) in the troposphere and the stratosphere (94%), whereas the consumption by methanotrophic bacteria in aerobic soils (6%) is of minor, but significant importance (Dlugokencky et al., 2011; Miller, 2004). Currently, the removal of atmospheric methane balances the source emissions, making the methane budget highly sensitive to emission reductions or to sink 1. INTRODUCTION

strength changes (Heimann, 2011; Bousquet et al., 2006; Khalil, 2000). Reducing methane emissions will, thus, have a direct and quick effect on the global atmospheric methane burden. The formulation of effective mitigation strategies requires an in-depth knowledge about the spatio-temporal patterns of atmospheric methane and, due to the diversity of methane sources, well-constrained emission estimates by source sector (Dlugokencky et al., 2011).

1.2 Switzerland's methane emission inventory estimates

Yet, emission estimates by source sector are associated with large uncertainties (Keppler et al., 2009; Chanton, Liptay, 2000). The lack of a dense observation network impedes a feasible source partitioning and hence, constraining emission estimates at smaller scales, i.e., local to national scales (Dlugokencky et al., 2011). Consequential, methane emissions of different sources at smaller scales are often estimated using models, i.e, based on bottom-up and top-down approaches. Both of them are prone to large errors, either from up-scaling or down-scaling and they also lack direct experimental validation (Nisbet, Weiss, 2010; Keppler et al., 2009). Top-down methods assess emissions using atmospheric measurements and trace back the sources via transport trajectories (Schulze et al., 2009). In contrast, bottom-up approaches scale up measurements of CH₄ fluxes in space and time using statistical data and land-use information.

At the national level, greenhouse gas emissions are commonly estimated by a national inventory based on a simple and globally-applicable bottom-up approach (Lassey, 2007). In order to maintain consistency and comparability of reported greenhouse gas emissions among different nations, the inventory estimates follow the standard procedures recommended by the IPCC (Penman et al., 2000), using country-specific activity data, e.g., livestock population, multiplied with a specific emission factor, e.g., kg emitted CH₄ head⁻¹ year⁻¹ (Hsu et al., 2010; Soliva, 2006). The emission factors (EFs) rarely rely on direct measurements and are often derived from the default EFs provided by the IPCC guidelines. Inventory estimates still remain questionable, since EFs can vary spatially and temporally, due to different agricultural practices (e.g., animal type, diet, manure storage and application rate)

and climatic conditions (Wang et al., 2011). Consequently, the methane emission estimates assessed in Switzerland's national inventory report (NIR) are associated with high uncertainty levels ranging from 18% to 100% for enteric fermentation and waste management systems (FOEN, 2013). In order to reduce this uncertainty and improve the overall credibility of model estimates, measurements at different spatio-temporal scales are essential (Nisbet, Weiss, 2010).

1.3 Measurement techniques

1.3.1 Estimating methane emissions at different spatial scales

When estimating methane emissions at regional to national scales, assessing the small-scale variability of the emission sources is of key importance. Diverse measurement techniques are available to estimate the emission strength of different methane sources, however, all of them are based on concentration measurements combined with a particular flux calculation method. The most important measurement techniques for emission estimates of single methane sources, i.e., at small scales, include chamber and eddy covariance measurements, but also the flux-gradient techniques and the mass balance approach, which can likewise be used for larger scales. Chambers are a commonly used tool to quantify methane emissions from animals and surfaces, due to their simple operating principle (Harper et al., 2011). Because chambers only integrate fluxes over areas in the order of 1–5 m², several chambers are needed to obtain representative emission fluxes for surfaces (Denmead, 2008; Griffith, Galle, 2000). In contrast, eddy covariance measurements, flux-gradient techniques and mass balance approaches, integrate the emissions at landscape scale, i.e., $200 \text{ m}^2 - 1 \text{ km}^2$ (Harper et al., 2011; Lapitan et al., 1999). With respect to methane, they can either be used to assess the emissions of specific land-use types as grasslands, wetlands, forests, lakes and landfills (Baldocchi et al., 2012; Detto et al., 2011; Eugster, Plüss, 2010) or to evaluate livestock methane emissions over grazed pastures (Dengel et al., 2011; Laubach et al., 2008). Very small fluxes, e.g., methane exchange between the soil and the atmosphere, can still not be estimated with sufficient precision, due to the small gradients in methane concentrations rela4 1. INTRODUCTION

tive to their atmospheric background level (Griffith, Galle, 2000). These techniques are most suitable for uniform, high emitting and well defined source areas (Harper et al., 2011; Alifieri et al., 2010).

Farm, ecosystem and regional methane emissions are either estimated via the upscaling of these small-scale measurements using statistical land-use information or via direct measurements from airborne observations, using small aircrafts or tethered balloons. The measurements are mostly combined with a mass balance or a budgeting approach, integrating source emissions within the atmospheric boundary layer of up to 100 km² (Harper et al., 2011; Lapitan et al., 1999). These techniques require spatio-temporally highly resolved measurements within and above the boundary layer. Limitations are set by changing wind directions, unsuitable weather conditions and unfeasible predictions of the boundary-layer height (Denmead, 2008; Cleugh et al., 2004).

1.3.2 Identifying methane sources

Unknown methane sources can be identified either by spatially highly resolved measurements near the surface or by stable isotope ratio analysis of atmospheric CH₄, circumventing the need of measurements in the direct vicinity of methane sources. Stable isotope ratio analysis is used at different spatial scales: At small scales, the isotopic enrichment or depletion relative to the ambient background air helps identifying the sources responsible for the resulting methane concentration, whereas on a global scale, the isotopic composition of atmospheric methane is used to constrain the global methane budget (Dlugokencky et al., 2011; Chanton, 2005). The stable isotopes in CH₄ can be used to distinguish isotopically enriched sources from depleted sources, due to the different discrimination against the heavier isotope of C and H in various methane consumption and production processes. The primary method of stable isotope interpretation is the linear regression model of isotopic ratios against the inverse of the gas concentration, commonly illustrated in a Keeling plot (Pataki et al., 2003). The intercept of the regression is then interpreted as the source isotopic signature. However, there have also been attemps to derive emission estimates via boundary-layer budgets using stable isotopes (Lloyd et al., 2001). Due to the well defined isotopic signatures of different methane sources, measurements of $\delta^{13}\mathrm{C}$ and $\delta\mathrm{D}$ in CH_4 are a powerful tool for source partitiong of atmospheric 1.4. OBJECTIVES 5

methane.

Methane sources can be divided into three categories with fairly distinct isotopic signatures compared to the ambient background air, which has a $\delta^{13}{\rm C}$ and $\delta{\rm D}$ value of -47 and -85\%, respectively (Dlugokencky et al., 2011; Dalal et al., 2008; Levin et al., 1999). Within each category, the different sources can have distinct isotopic signatures. Methane of biogenic origin, e.g., bacterially produced methane from wetlands, landfills, sewage and enteric fermentation, has an average signature between -50 and -70% in δ^{13} C and -250 to -350% in δ D (Townsend-Small et al., 2012; Miller, 2004). The isotopic composition of biogenic methane, however, depends on the latitude and on the isotopic composition of the preceding substrate, i.e., C3 or C4 plants. Fossil fuel related methane from vehicle emissions, coal mines as well as natural gas range in its δ^{13} C values from -16 to -50\% and in its δ D value from -150 to -200\% (Lowry et al., 2001; Stevens, Wahlen, 2000). With respect to natural gas, the signature in $\delta^{13}\mathrm{C}$ also depends on the formation temperature, leading to distinguishable values of -50 and -30\% between natural gas from Siberia and the North Sea, respectively. The isotope ratio of methane from biomass burning is generally enriched in ¹³C and ¹D compared to the ambient background with δ^{13} C values from -18 to -26\% and δD values from -10 to -50\% (Dalal et al., 2008; Stevens, Wahlen, 2000). It also depends on the preceding substrate, due to the distinct photosynthetic pathways in C3 and C4 plants and resulting organic carbon isotope signatures. In contrast, the consumption of atmospheric methane by methanogenic bacteria in aerobic soils causes an enrichement in ${}^{13}C$ and ${}^{1}D$ of -21 and -80%, respectively (Miller, 2004; Snover, Quay, 2000). The remaining atmospheric methane after the oxidation with atmospheric radicals, e.g., OH⁻⁻, shows a mean enriched δ^{13} C value of -5.4\% and δD value of -220% (Miller, 2004; Snover, Quay, 2000).

1.4 Objectives

Due to the poorly known spatio-temporal pattern of methane sources and emissions at local to regional scales, the FasMeF (Farm-scale Methane Fluxes) project was implemented within this PhD study to contribute to the scientific understanding of atmospheric methane and its spatio-temporal variability. The overall goals of this project were (1) to understand the spatio-temporal variability of livestock methane

1. INTRODUCTION

emissions at a regional scale and (2) to constrain inventory estimates via direct measurements. Based on spatio-temporally highly resolved measurements of CH_4 concentrations and $\delta^{13}C$ values, this thesis specifies the following main research objectives:

- 1. Quantify farm-scale methane budget fluxes.
- 2. Compare farm-scale budget fluxes with methan emission inventory estimates at different spatial scales.
- 3. Assess the temporal variability and the spatial heterogeneity of atmospheric methane and its δ^{13} C value within the lower boundary layer.
- 4. Identify different methane sources and quantify their contributions to the overall source mix.
- 5. Assess the potential of highly resolved measurements to constrain model estimates at the farm to regional scale.

1.5 Thesis outline

6

This thesis is composed of three manuscripts. In the first manuscript (Chapter 2) farm-scale methane fluxes are quantified using a nocturnal boundary layer budgeting approach. The resulting fluxes are compared to three inventory estimates, whose estimates are based on the same bottom-up approach but differ in their spatial resolution. The second manuscript (Chapter 3) investigates the processes driving the spatio-temporal pattern of atmospheric methane and compares highly resolved concentration measurements to methane emission estimates of a spatially explicit inventory. In the third manuscript (Chapter 4) the spatio-temporal variability of δ^{13} C in CH₄ is elucidated and the contributions of different methane sources to the night- and daytime source mix are assessed. The findings are used to draw implications for the interpretation of regional-scale methane budgets.

Appendix A presents the first high-resolution (500 m x 500 m) $\rm CH_4$ emission inventory for Switzerland, synthesizing anthropogenic and natural methane emissions. Appendix B presents a comparison of the responses of grassland and forest carbon and water fluxes to the 2011 spring drought in Switzerland. Appendix C presents a full year greenhouse gas emission budget after grassland restoration.

References

- Alifieri S, Amato U, Carfora M, Esposito M, Magliulo V (2010) Quantifying trace gas emissions from composite landscapes: A mass-budget approach with aircraft measurements. *Atmospheric Environment* 44(15):1866–1876.
- Baldocchi D, Detto M, Sonnentag O, Verfaillie J, The Y, Silver W, Kelly N (2012) The challenges of measuring methane fluxes and concentrations over a peatland pasture. *Agricultural and Forest Meteorology* 153:177–187.
- Bousquet P, Ciais P, Miller J, Dlugokencky E, Hauglustaine D, Prigent C, Van der Werf G, Peylin P, Brunke E, Carouge C, Langenfelds R, Lathiere J, Papa F, Ramonet M, Schmidt M, Steele L, Tyler S, White J (2006) Contribution of anthropogenic and natural sources to atmospheric methane variability. *Nature* 443(7110):439–443.
- Chanton J (2005) The effect of gas transport on the isotope signature of methane in wetlands. Organic Geochemistry 36(5):753–768.
- Chanton J, Liptay K (2000) Seasonal variation in methane oxidation in a landfill cover soil as determined by an in situ stable isotope technique. *Global Biogeochemical Cycles* 14(1):51–60.
- Cleugh H, Raupach M, Briggs P, Coppin P (2004) Regional-scale heat and water vapour fluxes in an agricultural landscape: An evaluation of CBL budget methods at OASIS. *Boundary-Layer Meteorology* 110(1):99–137.
- Dalal R, Allen D, Livesley S, Richards G (2008) Magnitude and biophysical regulators of methane emission and consumption in the australian agricultural, forest, and submerged landscapes: a review. *Plant and Soil* 309(1-2):43–76.
- Dengel S, Levy P, Grace J, Jones S, Skiba U (2011) Methane emissions from sheep pasture, measured with an open-path eddy covariance system. *Global Change Biology* 17(12):3524–3533.
- Denmead O (2008) Approaches to measuring fluxes of methane and nitrous oxide between landscapes and the atmosphere. *Plant and Soil* 309(1-2):5–24.

8 REFERENCES

Detto M, Verfaillie J, Anderson F, Xu L, Baldocchi D (2011) Comparing laser-based open-and closed-path gas analyzers to measure methane fluxes using the eddy covariance method. *Agricultural and Forest Meteorology* 151(10):1312–1324.

- Dlugokencky E, Nisbet E, Fisher R, Lowry D (2011) Global atmospheric methane: budget, changes and dangers. *Philosophical Transactions of the Royal Society A:* Mathematical, Physical and Engineering Sciences 369(1943):2058–2072.
- Eugster W, Plüss P (2010) A fault-tolerant eddy covariance system for measuring CH₄ fluxes. Agricultural and Forest Meteorology 150(6):841–851.
- FOEN (2013) Switzerland's Greenhouse Gas Inventory 1990-2011: National Inventory Report 2013. page 483. Submission of 15 April 2013 under the United Nations Framework Convention on Climate Change and under the Kyoto Protocol. Federal Office for the Environment (FOEN), Bern, Switzerland.
- Griffith D, Galle B (2000) Flux measurements of NH₃, N₂O and CO₂ using dual beam FTIR spectroscopy and the flux–gradient technique. *Atmospheric Environment* 34(7):1087–1098.
- Harper L, Denmead O, Flesch T (2011) Micrometeorological techniques for measurement of enteric greenhouse gas emissions. *Animal Feed Science and Technology* 166:227–239.
- Heimann M (2011) Atmospheric science: Enigma of the recent methane budget. *Nature* 476(7359):157–158.
- Hsu Y, VanCuren T, Park S, Jakober C, Herner J, FitzGibbon M, Blake D, Parrish D (2010) Methane emissions inventory verification in southern California. *Atmospheric Environment* 44(1):1–7.
- IPCC W (2007). The physical science basis. Contribution of working group I to the fourth assessment report of the Intergovernmental Panel on Climate Change. In Solomon S, Qin D, Manning M, Chen Z, Marquis M, Averyt K, Tignor M, Miller H, editors, Climate Change 2007. Cambridge University Press Cambridge.
- Keppler F, Boros M, Frankenberg C, Lelieveld J, McLeod A, Pirttilä A, Röckmann T, Schnitzler J (2009) Methane formation in aerobic environments. *Environmental Chemistry* 6(6):459–465.
- Khalil M (2000) Atmospheric Methane: An Introduction. In: Atmospheric methane: its role in the global environment, (eds) Mohammad Aslam Khan Khalil, *Springer-Verlag Berlin Heidelberg*, Chapter 1, pp. 1–8.
- Lapitan R, Wanninkhof R, Mosier A (1999) Methods for stable gas flux determination in aquatic and terrestrial systems. *Developments in Atmospheric Science* 24:29–66.

REFERENCES 9

Lassey K (2007) Livestock methane emission: from the individual grazing animal through national inventories to the global methane cycle. Agricultural and Forest Meteorology 142(2):120–132.

- Laubach J, Kelliher F, Knight T, Clark H, Molano G, Cavanagh A (2008) Methane emissions from beef cattle a comparison of paddock-and animal-scale measurements. *Animal Production Science* 48(2):132–137.
- Levin I, Glatzel-Mattheier H, Marik T, Cuntz M, Schmidt M (1999) Verification of German methane emission inventories and their recent changes based on atmospheric observations. *Journal of Geophysical Research: Atmospheres* 104(D3):3447–3456.
- Lloyd J, Francey R, Mollicone D, Raupach M, Sogachev A, Arneth A, Byers J, Kelliher F, Rebman C, Valentini R, Wong S, Bauer G, Schulze E (2001) Vertical profiles, boundary layer budgets, and regional flux estimates for CO₂ and its 13 C/ 12 C ratio and for water vapor above a forest/bog mosaic in central Siberia. Global Biogeochemical Cycles 15(2):267–284.
- Lowry D, Holmes C, Rata N, O'Brian P, Nisbet E (2001) London methane emissions: Use of diurnal changes in concentration and δ^{13} C to identify urban sources and verify inventories. *Journal of Geophysical Research: Atmospheres* 106(D7):7427–7448.
- Miller J (2004) The carbon isotopic composition of atmospheric methane and its constraint on the global methane budget. In: Stable isotopes and biosphere-atmosphere interactions: processes and biological controls, (eds) Lawrence B. Flanagan, *Elsevier Academic Press*, Chapter 16, pp. 288–310.
- Nisbet E, Weiss R (2010) Top-down versus bottom-up. *Science* 328(5983):1241–1243.
- Pataki D, Ehleringer J, Flanagan L, Yakir D, Bowling D, Still C, Buchmann N, Kaplan J, Berry J (2003) The application and interpretation of Keeling plots in terrestrial carbon cycle research. *Global Biogeochemical Cycles* 17(1).
- Penman J, Kruger D, Galbally I, Hiraishi T, Nyenzi B, Emmanual S, Buendia L, Hoppaus R, Martinsen T, Mejer J, others (2000). Good practice guidance and uncertainty management in national greenhouse gas inventories. IPCC National Greenhouse Cost Inventories programme, Technical Support Unit.
- Schulze E, Luyssaert S, Ciais P, Freibauer A, Janssens I, Soussana J, Smith P, Grace J, Levin I, Thiruchittampalam B, Heimann M, Dolman A, Valentini R, Bousquet P, Peylin P, Peters W, Rödenbeck C, Etiope G, Viuchard N, Wattenbach M, Nabuurs G, Poussi Z, Nieschulze J, Gash J (2009) Importance of methane and nitrous oxide for Europe's terrestrial greenhouse-gas balance. *Nature Geoscience* 2(12):842–850.

10 REFERENCES

Snover A, Quay P (2000) Hydrogen and carbon kinetic isotope effects during soil uptake of atmospheric methane. Global Biogeochemical Cycles 14(1):25–39.

- Soliva C (2006) Report to the attention of IPCC about the data set and calculation method used to estimate methane formation from enteric fermentation of agricultural livestock population and manure management in Swiss agriculture. Institute of Animal Science, ETH Zurich, Switzerland. On behalf of the Fereal Office for the Environment (FOEN), Bern, Switzerland, pp. 14.
- Stevens C, Wahlen M (2000) The isotopic composition of atmospheric methane and its sources. In: Atmospheric methane: its role in the global environment, (eds) Mohammad Aslam Khan Khalil, *Springer-Verlag Berlin Heidelberg*, Chapter 3, pp. 25–40.
- Townsend-Small A, Tyler S, Pataki D, Xu X, Christensen L (2012) Isotopic measurements of atmospheric methane in Los Angeles, California, USA: Influence of "fugitive" fossil fuel emissions. *Journal of Geophysical Research: Atmospheres* 117(D07308):1451–1476.
- Wang J, Cardenas L, Misselbrook T, Gilhespy S (2011) Development and application of a detailed inventory framework for estimating nitrous oxide and methane emissions from agriculture. *Atmospheric Environment* 45(7):1454–1463.

Validation of farm-scale methane emissions using nocturnal boundary layer budgets

Jacqueline Stieger, Ines Bamberger, Nina Buchmann, Werner Eugster
Institute of Agricultural Sciences, ETH Zurich, Zurich, Switzerland

This manuscript is intended for submission to:

Agricultural and Forest Meteorology

Abstract

This study provides the first experimental validation of agricultural methane emission estimates at a farm scale in Switzerland. We measured CH₄ concentrations at a Swiss farmstead during intensive field campaigns in August 2011 and July 2012 to (1) assess the source strength of livestock methane emissions using a tethered balloon system, and (2) to validate inventory emission estimates via nocturnal boundary layer (NBL) budgets. Vertical profiles of air temperature, CH₄ concentration, wind speed and wind direction showed that the nocturnal boundary layer was strongly influenced by local transport processes and by the valley wind system. Resulting NBL budget fluxes, i.e., average surface fluxes, revealed a pronounced nocturnal course with highest fluxes in the middle of the night due to the establishment of a NBL. The mean NBL budget flux of 1.59 \pm $0.22 \mu g \text{ CH}_4 \text{ m}^{-2} \text{ s}^{-1}$ was in good agreement with local inventory estimates based on current livestock number and default emission factors, with 1.29 ± 0.47 and $1.74 \pm 0.63 \ \mu g \ \mathrm{CH_4 \ m^{-2} \ s^{-1}}$ for 2011 and for 2012, respectively. Estimates from a spatially explicit CH₄ emission inventory underestimated the CH₄ emissions at least by 26%. Our results show that the NBL budget approach can be a useful tool to validate statistical assessments and that further improvements are needed for the spatial disaggregation of inventory estimates. In addition, our direct validation via independent atmospheric measurements increases the overall credibility of the estimation methodology used by the inventories.

13

2.1 Introduction

Switzerland's methane emissions from agriculture are reported annually in the national inventory report (NIR), but have so far never been experimentally validated. To assess agricultural methane emissions in Switzerland, we used nocturnal boundary layer budgets and validated the methane emission inventory estimates at the farm scale. The official inventory estimates are based on standard procedures recommended by the IPCC (Heimann, 2011; Wang et al., 2011; Nisbet, Weiss, 2010; Lassey, 2008), e.g., national livestock numbers multiplied with default emission factors (EFs) derived from the IPCC Guidelines and Guidances (Penman et al., 2000). Despite considerable uncertainty of these default values, this estimation methodology has become commonly used in order to ensure conformity and comparability of reported greenhouse gas emissions among different nations (Lassey, 2007). Although an experimental validation of such inventory estimates by independent means would be highly beneficial to improve their overall credibility, the assessment of agricultural methane emissions by direct atmospheric measurements is still lacking for Switzerland.

Because of methane's high global warming potential and due to its relatively short atmospheric residence time, already a small reduction of CH₄ emissions will have a high impact on the global methane budget (Dlugokencky et al., 2011; Wang et al., 2011). But in order to formulate feasible mitigation strategies, a deeper understanding and a precise quantification of emission variability and source strength are needed (Dengel et al., 2011; Ulyatt et al., 2002; Lowry et al., 2001). Besides emissions from animal husbandry, emissions from the energy sector and from solid waste disposals are important methane sources in most European countries (Pulles, Van Amstel, 2010). Switzerland's CH₄ emissions, however, are dominated by the agricultural sector (84.6%), followed by emissions from waste treatment (8.3%) and from the energy sector (6.8%) (FOEN, 2013). Yet, due to the lack of direct field experiments and poorly known EFs (Lassey, 2007; Lowry et al., 2001), the NIR estimates are associated with uncertainties of $\pm 18.2\%$ and $\pm 54.3\%$ for enteric fermentation and manure management, respectively (FOEN, 2013). Although recent studies conducted at the animal husbandry level in Switzerland (Staerfl et al., 2012; Zeitz et al., 2012) showed that using country-specific EFs would not substantially alter the total estimate of livestock methane emissions, high uncertainty remains, as differing farming practices can have significant impacts on the EFs (Christie et al., 2012; Saggar et al., 2004; Lowry et al., 2001). In addition, the inventory estimates do not account for the large spatial heterogeneity and the temporal variability of methane sources (Wang et al., 2011). While spatially explicit inventories (SEI) improve the overall spatial representativeness of NIR, the accuracy of the estimates still remains unclear. This underpins the need for detailed local to regional-scale measurements.

Little is known about the temporal variability and spatial heterogeneity of different CH₄ sources, although an increasing number of studies show the importance of assessing methane budgets via atmospheric measurements (Baldocchi et al., 2012; Harper et al., 2011; Detto et al., 2010; Pendall et al., 2010; Pattey et al., 2006; Zinchenko et al., 2002; Ulyatt et al., 2002; Beswick et al., 1998; Fowler et al., 1996). Unfortunately, only few studies compare their results to inventory estimates (Hiller, 2012; Hsu et al., 2010; Lowry et al., 2001; Levin et al., 1999), and only one project, so far, has directly validated livestock methane emission estimates via atmospheric concentration measurements (Denmead et al., 2000). Using different budgeting approaches (e.g., convective and nocturnal boundary layer budgets, mass balance method), Denmead et al. (2000) found a good agreement of budget estimates with the respective inventory estimates, but they also pointed out problems related to the inherent uncertainty of the approaches used.

Up to now, there is no standardised procedure to compare experimental data to statistical assessments. Studies dealing with inventory validation modify their spatial focus according to the spatial extent of the methane source under examination (Levin et al., 1999). In this study, we focus on the farm scale, and (1) evaluate the source strength of a typical Swiss farmstead (0.5–5 km²), and (2) assess methane budget fluxes (average surface fluxes) using vertical methane concentration profiles within the atmospheric boundary layer. In addition, we use experimentally derived NBL budget fluxes for inventory validation at different spatial resolutions, i.e., the NIR and the SEI as well as a direct inventory estimate at the farm scale.

2.2 Materials and Methods

2.2.1 Site description

We performed intensive measurement campaigns during 16-17 August 2011 and 24–27 July 2012 at the ETH research station Chamau (47° 12′ 37″ N, 8° 24′ 38″ E at 393 m a.s.l.), which is located in the lower Reuss Valley in central Switzerland. 56.5% of the Reuss Valley is used for agriculture (FSO, 2012), which is the most dominant land use category besides forests (22.5%). 72.4% of the station's total area (62.03 ha) is covered by grassland used for grazing and forage production (Suter, 2011; Zeeman et al., 2010). Cropland used for silage corn production, forests and farm infrastructure cover 11.07%, 8.28% and 8.25%, respectively. The grasslands are intensively managed (cut and fertilized about 5 to 6 times a year) and dominated by mixed ryegrass-clover vegetation (Gilgen, Buchmann, 2009). With respect to methane, the grasslands have shown negligible soil methane fluxes on a daily timescale while acting as a small sink on an annual timescale (Imer et al., 2013). Livestock populations at Chamau vary according to the seasonal three-stage farming system. During summer, most cattle are moved to higher altitudes, whereas swine, goats and sheep stay stationary at the farm. During our measurement periods, cattle and swine were inside the barns, while goats and sheep were located outside at the meadows. Our measurement periods did not include management events (e.g., cutting or fertilization).

Local meteorology in the Reuss Valley is dominated by a prominent valley wind regime, where prevailing NNW-winds towards the Alps during the day are replaced by cold air drainage flows from SSE during the night, promoting the development of a shallow nocturnal boundary layer. Our measurement periods were restricted to fair weather conditions with a predominant high-pressure system and clear skies during night.

2.2.2 Vertical balloon profiles and ground measurements

Tethered balloon measurements were performed during the night in two years (2011 and 2012) with different temporal coverage (see Table 1 for details). A helium-filled blimp (7.2 m³, The Blimp Works Inc., Statesville, NC, USA) with a net lift of

4.35 kg carried a polyethylene inlet tube of 220 m length (Maagtechnic, Dübendorf, Switzerland) connected to a ground measurement station. The air sampled was drawn with a flow rate of ∼1 L min⁻¹ to a fast greenhouse gas analyzer (FGGA, Los Gatos Research Inc., Mountain View, CA, USA), which was installed at the ground.

Complementary measurements of air temperature, atmospheric pressure, relative humidity, wind speed and wind direction were carried out with the meteorological probe TS-5A-SEN (Atmospheric Instrument Research, Inc., Boulder, USA) which was attached to the tether line. These meteorological measurements were transmitted via an AIR IS-5A-RCR radio receiver (395–410 MHz) to a computer using the home-built A.I.R. Tethersonde Communication Program and stored. A GPS unit (eflight, SM-Modellbau.de, Germany) provided positioning and height information of the balloon system. In total, 18 soundings were conducted, of which 16 were used for further analysis, while two balloon soundings (16/17 Aug 2011 during 04:48 and 05:56 UTC+1) were rejected due to unfavorable meteorological conditions. Each ascent and descent of the remaining 16 soundings gave a mean vertical profile and a mean NBL budget flux (Table 1).

Furthermore, a guy-wired extension mast was installed next to the FGGA. Inlet tubes (Maagtechnic, Dübendorf, Switzerland) were installed at eight different heights (0.2 m, 0.5 m, 1 m, 2 m, 3 m, 5 m, 8 m and 10 m a.g.l.), leading the air into a home-built air inlet selection unit (Zeeman et al., 2008). The extension mast measurements were performed between the balloon soundings and each height was measured for three minutes. A nearby eddy covariance station provided further micrometeorological measurements of air temperature, relative humidity, wind speed, wind direction, photosynthetic active radiation (PAR) and turbulence (Zeeman et al., 2010), also used for cross-referencing the meteorological tether probes.

2.2.3 Budget flux calculation

The NBL budget technique is applied at night during favorable weather conditions with clear skies and low wind speeds. The budget flux F_s , i.e., the average surface flux, can be expressed as followed (Denmead et al., 1996):

$$F_s = \int_0^{z_i} \frac{\partial \bar{c}}{\partial t} \, \mathrm{d}z \tag{2.1}$$

where $\frac{\partial \bar{c}}{\partial t}$ is the rate of change in concentration with time, and z_i is the NBL height. The resulting budget flux describes the accumulation of a scalar within the stable boundary layer at consecutive time steps. The NBL budget method is based on the idea that during nights with ideal weather conditions, a stable nocturnal boundary layer develops, which is capped by a strong temperature inversion at its top and acts as a natural atmospheric chamber, accumulating all emissions of underlying sources (Pattey et al., 2006; Mathieu et al., 2005). Thus, the top of the NBL and hence z_i will be characterised by $\frac{\partial \bar{c}}{\partial t} = 0$ ppm s⁻¹ due to a neutral to unstable stratification with $\frac{\partial \bar{\theta}}{\partial z} \leq 0$ K m⁻¹. In our case, the budget flux computed with Eq. (1) is an integral measurement of the net flux from all relevant sources and sinks within the footprint of the balloon measurements. These relevant components can be specified in more detail by:

$$F_s = F_{soil} + F_{ENT} + F_{HA} + F_{other} \tag{2.2}$$

where F_{soil} is the soil exchange flux, F_{ENT} the entrainment flux at the top of the NBL, F_{HA} the horizontal advection, and F_{other} the flux resulting from emissions of other sources in the footprint. Under stationary conditions with a constant NBL height, F_{ENT} becomes negligible. At the Chamau site, earlier eddy covariance flux measurements showed that F_{soil} is very small compared to the other terms and hence can be neglected in Eq. (2). This minor role of the source and sink strengths of upland grasslands in the total farm greenhouse gas budget has already been reported by Imer et al. (2013) and Hartmann et al. (2011). Furthermore, the advection term can be neglected if measurements are taken over a horizontally sufficient large and flat terrain with a homogeneous source distribution (Pattey et al., 2006; Mathieu et al., 2005; Cleugh et al., 2004; Denmead et al., 2000; Beswick et al., 1998; Fowler et al., 1996; Choularton et al., 1995; Raupach et al., 1992). With these simplifications, Eq. (2) can be reduced to:

$$F_s \approx F_{other}$$
 (2.3)

where F_{other} in our case represents the Chamau farmstead.

Nevertheless, it has been shown that even under stable conditions, small advective effects and wind direction play an important role in determining the NBL budget (Hsu et al., 2010; Zinchenko et al., 2002; Lowry et al., 2001). Advected air parcels can include pollutants from sources lying in the upwind fetch and hence can bias the local methane concentrations, resulting in an overestimation of the NBL budget. Particularly nighttime measurements can include regional information of up to several kilometers upwind (Bamberger et al., 2013). In order to avoid the impact of emissions from upwind sources and to reduce the measurement footprint to an extent, which only includes the barn buildings of the Chamau farmstead, the integration height was set to the height where $\frac{\partial \bar{\theta}}{\partial z} \leq 0$ K m⁻¹ (Pattey et al., 2006; Mathieu et al., 2005). In addition, only measurements with a prevailing wind direction from the SSE-SW sector were used for the flux calculation, i.e., where the main barn building of the Chamau station and the grazed pastures are located.

2.2.4 Inventory estimates

Two inventory estimates of methane emissions exist for Switzerland (i.e., NIR and SIE), which both use the same estimation methodology, but differ in their spatial resolution. While the NIR evaluates methane emissions on an annual basis for entire Switzerland (FOEN, 2013), the recently developed SEI (Hiller et al., 2013) distributes the methane emissions, based on the 2007 year stocking census data (FSO, 2009), onto a 500 m x 500 m grid according to Swiss land use statistics (FSO, 2007). Both inventories estimate the CH₄ emissions from national livestock numbers multiplied with animal-specific conversion factors, i.e., the methane conversion rate for enteric fermentation y_m and the methane conversion factor for manure management (MCF), which are both given by the IPCC Good Practice Guidance (ART, 2012; Soliva, 2006).

The SEI accounts for the large spatial heterogeneity of methane sources which the NIR cannot resolve. In the SEI, the Chamau research station, is explicitly resolved by several grid cells with methane emissions ranging from 6 kg CH₄ ha⁻¹ yr⁻¹ to 820 kg CH₄ ha⁻¹ yr⁻¹. This large variation among the individual grid cells arises due to the standarized assessment process of the SEI: about 80% of the methane

emissions are assigned to the grid cell with the main building of a farmstead, while the remaining emissions are evenly distributed to the pasture area of the whole municipal (Hiller et al., 2013). In order to compare inventory estimates to budget fluxes, the NIR estimates of enteric fermentation (119 \pm 21.5 Gg CH₄ yr⁻¹) and manure management (31 \pm 17 Gg CH₄ yr⁻¹) for the year 2011 were disaggregated to the area used for pastures (here 5685.8 km²) according to the CORINE land use map (FSO, 1998). For the SEI, the grid cell representing the main building of the research station was used for comparison.

To overcome the inconsistencies in spatial resolution and temporal representativeness of both, the NIR and the SEI, we estimated methane emissions for the Chamau farmstead (in the following called CHAI) using the same EFs but multiplied with current stocking data of the respective measurement periods. This simplified the validation, as livestock represents the main methane source at the Chamau station and hence, the emission of the whole farmstead is included in the CHAI estimates without the need for spatial disaggregation. Since no uncertainty estimates exist for the SEI and CHAI, we assumed the same methodological-based uncertainty as for NIR. The uncertainty due to the spatial disaggregation of the SEI is not known. The standard deviation of all three inventory estimates (i.e., NIR, SEI and CHAI) was calculated as the average uncertainty estimates of enteric fermentation (18.2%) and manure management (54.3%) from NIR (FOEN, 2013), thus 36.25%.

2.2.5 Data processing and general conventions

Data processing, analysis and flux calculations were done with the statistics software package R, version 2.15.1 (R Development Core Team 2009, www.r-project.org). Nighttime data were defined as PAR $<20~\mu\mathrm{mol~m^{-2}s^{-1}}$. Ordinary kriging using the geoR-package was performed for spatio-temporal interpolation of methane concentrations and served as a basis for flux calculations. NBL budget flux calculations were restricted to the above mentioned selection criteria and limited to the duration time ± 30 minutes of each balloon sounding. If not stated otherwise, reported values denote mean \pm standard deviations. The terms n1-n4 and s1-s16 refer to the different nights and soundings in their respective year (Table 1).

2.3 Results

2.3.1 Weather conditions and diel course of methane concentrations

During our measurements in 2011 and 2012, the weather was dominated by a high-pressure system over Central Europe. We experienced warm and dry daytime conditions with temperatures reaching 302.1 K in 2011 and 306.1 K in 2012, and a pronounced surface cooling with clear skies and low wind speeds during all nights (Figure 1). Radiative cooling (i.e., $\frac{\partial \bar{I}}{\partial t} \leq 0 \text{ K h}^{-1}$) was most pronounced right after sunset, providing sufficient atmospheric stability and stationarity for the build-up of an NBL. Later during the nights, temperature cooling rates remained negative and enabled the deepening of the stable NBL. The drop in air temperature was most pronounced during n1 in 2011 (286.1 K), whereas air temperature at n2–n3 in 2012 did not fall below 287.1 K, with the highest nighttime value during n4 of 288.7 K. All nights were dominated by low near-surface wind speeds <1 m s⁻¹, associated with a very weak turbulence <0.08 m $^{-1}$. In 2012, however, some measurement periods experienced slightly increased wind speeds and friction velocities, probably due to weak advection promoting mixing processes within the stable NBL.

The diel course of methane concentration mainly followed the meteorological conditions. Due to convective mixing during daytime, methane concentrations remained relatively low (\sim 1.9 ppm). At night, concentration values increased as the emissions were trapped within the stable NBL (exemplarily shown for n1, Figure 2a). Highest mixing ratios, here up to 3.1 ppm, were observed around 3 am local time at the lowest measurement height close to the surface (i.e., 0.2 m a.g.l.) due to inhibited vertical mixing. For lower measurement heights, the nighttime accumulation of methane started after sunset. Measurements taken from above 70 m a.g.l., however, showed an increase in methane concentrations only during the second half of the night, resulting in a less pronounced diel pattern compared to lower elevations (Figure 2b). Besides reaching the top of the NBL at about 70 m a.g.l., variable wind directions affected the increase in CH₄ concentrations. The nighttime methane build-up was most pronounced when air masses originated from the wind sector between 180° and 270°, including the cattle barn buildings (in Figure 2b, at heights below 50 m a.g.l. from 9 to 11 pm local time). In contrast, air masses with a northern wind com-

2.3. RESULTS 21

ponent, here above 100 m a.g.l., showed constant or decreasing CH₄ concentrations during the same measurement period.

2.3.2 Vertical balloon profiles

Potential temperature gradients of successive vertical balloon profiles indicated stable conditions during all nights (i.e., $\frac{\partial \bar{T}}{\partial m} > 0$ K m⁻¹) and hence the establishment of a stable NBL (Figure 3a). However, the height of this NBL, where a transition from stable to unstable or neutral conditions is expected strongly differed among the individual profiles. Half of the profiles revealed a temperature inversion at or above 100 m a.g.l. (i.e., s1 and s3 of n1; s7 and s8 of n2; s12 of n3; s14, s15 and s16 of n4). The other half exhibited multiple transition heights, pointing to the development of multiple stable layers within the NBL. Only few of the soundings (i.e., s5 of n1; s6 of n2; s13 of n4) showed a clear temperature inversion (at 50–60 m a.g.l.), followed by a second stable layer with positive temperature gradients at increasing elevations. Other profile soundings were rather marked by a gradual transition from stable to neutral conditions (e.g., s10 and s11 of n3). However, temperature gradients among individual soundings differed markedly, indicating a temporal evolution (e.g. growth, consolidation or separation) of the different layers within the NBL.

In contrast, the methane concentration profiles showed quite different patterns between the two years. In 2011, the profiles exhibited a clear increase in mixing ratios from s1 to s5 within the lowest 100 m, and all profiles reached a background value of ~2 ppm above 100 m a.g.l., pointing to the main NBL inversion height (Figure 3b). This drop in concentration was associated with a change in wind direction from SSW to N and an increase in wind speeds up to 4 m s⁻¹ (Figure 3c). In 2012 (s6 to s16), all profiles indicated a well-mixed NBL with small or even absent vertical concentration gradients, but with an substantial increase in concentration over time (Figure 3a & b). Even though temperature inversions were present, none of the methane concentration profiles reached a background value at or above the inversion height. The same well-mixed conditions were found for the two rejected soundings in 2011. However, no clear changes in wind direction could be observed in the profiles for 2012. Most wind profiles meandered between a WSW sector in the lower part of the NBL and a ESE sector in the upper part of the NBL. Only s3 of n3 showed an abrupt change in wind direction from SE to N at 50 m a.g.l. Wind

speed in 2012 showed a slightly different picture compared to 2011 as well (data not shown). Except s6 and s8 of n2, all profiles revealed increasing wind speeds with height. Some soundings also showed a peak with maximum wind speeds (i.e. s9 of n2 at 80 m a.g.l.; s11 of n3 at 130 m a.g.l.; s14 and s15 of n4 at 140 m a.g.l. and 50 m a.g.l., respectively) pointing to a low-level jet.

2.3.3 NBL budget fluxes and comparison to inventory estimates

The observed CH₄ mixing ratio and potential temperature gradients showed that the overall NBL at Chamau was not merely influenced by local emissions from the farmstead. The well-mixed methane concentration profiles in 2012 suggested that the NBL was primarily influenced by emissions from sources further upwind, which were already well mixed with ambient air and that local sources had a minor influence. Applying the NBL budget flux calculation to the whole NBL height would therefore represent regional scale emission fluxes and include significant advection terms. Restricting the NBL budget either to the height where $\frac{\partial \theta}{\partial z} \leq 0$ and/or to wind directions originating from the SSE-SW sector allows separation of emissions from the Chamau station vs. emissions from upwind lying sources (see Section 2.3). The resulting NBL budget fluxes of the individual profiles varied between 0.79 ± 0.13 and $2.88 \pm 0.61 \ \mu g \ CH_4 \ m^{-2} \ s^{-1}$ for the different nights (Table 1), with an overall mean of 1.59 \pm 0.22 μ g CH₄ m⁻² s⁻¹. All nights showed a clear nocturnal course of NBL fluxes, with higher fluxes in the middle of the night and lower fluxes shortly after sunset and before sunrise. This nocturnal course was most enhanced during n2 and n3 in 2012 due to a more pronounced gradient of consecutive temperature and CH_4 profiles.

The estimates varied markably among the different inventories (Table 2). Highest values were derived for CHAI with 1.29 \pm 0.47 and 1.74 \pm 0.63 μ g CH₄ m⁻² s⁻¹ in 2011 and in 2012, respectively. Lower emission fluxes of 0.83 \pm 0.3 μ g CH₄ m⁻² s⁻¹ (for all nights) resulted from the spatial disaggregation of the NIR estimates. The SEI emission flux estimate for the grid cell including the main building of the farmstead, however, was only 0.42 \pm 0.15 μ g CH₄ m⁻² s⁻¹, significantly lower than the CHAI estimates. These CHAI estimates, representing the same spatial extent as the main SEI grid cell, are therefore at least three times higher than the SEI,

2.4. DISCUSSION 23

although 80% of total methane emissions from the Chamau farmstead were covered by this main grid cell. Mean NBL budget fluxes for the different nights ranged from 1.4 ± 0.5 to $2.05 \pm 0.45~\mu g$ CH₄ m⁻² s⁻¹ and were comparable to the CHAI estimates (Table 2). A small difference between NBL and CHAI of $0.04~\mu g$ CH₄ m⁻² s⁻¹ was found for 26/27 July 2012.

2.4 Discussion

2.4.1 Using the NBL budget approach in complex terrain

In contrast to other studies using the NBL budget approach at horizontally homogeneous and flat sites, our measurements were located in complex terrain with variable NBL structures. Temperature, concentration and wind profiles showed that the NBL in the Reuss Valley underwent a significant temporal evolution, with the establishment of multiple stable layers and with a high dependency on wind direction. With its location north of the Swiss prealps, the NBL was primarily affected by the valley wind system and the resulting thermodynamic processes in the atmosphere. The complex temporal evolution of our temperature, wind direction and wind speed profiles (Figure 3) suggested different disturbances (e.g., advection of air with higher methane concentration, pulsating down-valley flows, cold air drainage), leading to turbulent mixing events within the lower and upper parts of the NBL. These disturbances finally resulted in well-mixed methane concentration profiles throughout the NBL in 2012 and in some (rejected) profiles in 2011, although clear vertical concentration gradients were expected due to the observed temperature inversions. These findings suggest that advection and mixing processes played a prominent role during our measurements. In addition, turbulence and wind speed measurements of our eddy-covariance system suggested that intermittent turbulent processes affected the thermodynamic structure of the boundary layer. Although local meteorological conditions favoured the build-up of a stable and stratified NBL, turbulent processes within the NBL have also been reported by other studies (Wang et al., 2006; Mahrt, Vickers, 2002; Holden et al., 2000; Parker, Raman, 1993). In addition, some of our wind speed profiles indicated the presence of a low-level jet, which - besides cold air drainages - had a significant impact on vertical transport within an NBL (Sun et al., 2007; Pinto et al., 2006; Mathieu et al., 2005). Hence, similar to Dorninger et al.

(2011), the the temporal evolution of the NBL in the Reuss Valley was primarily affected by local-scale mixing processes.

Besides intermittent turbulence, advection processes challenge the applicability of the NBL budget approach for a feasible estimation of farm-scale methane emissions. Although studies so far have focused at the regional scale with homogenously distributed sources and hence neglected the advection term in the methane budget, advection has also been reported in other studies as an important impact factor of the resulting budget flux (Pattey et al., 2006; Kuck et al., 2000). Assuming $F_{HA} \approx$ 0, our NBL budget fluxes were expected to represent F_{other} . The methane concentration and wind direction profiles, however, suggested that CH₄ concentrations largely depended on wind direction (Figure 2b). This indicated a heterogeneous distribution of methane sources in the Reuss Valley, even though major parts of its relatively broad basin are used for agriculture. In addition, it has been shown that nighttime observations even measured at very low elevations above ground (2 m a.g.l.) carry regional information up to 25 km² (Bamberger et al., 2013). A one-to-one application of the NBL budget approach used in other studies will thus result in budgets, which represent an enlarged spatial extent compared to the Chamau farmstead. Furthermore, the fluxes will include horizontally advected air parcels which might not necessarily have been affected by the same amount of agricultural emissions. In order to estimate emissions at a farm scale, we minimized uncertainties caused by horziontal advection from sources further upwind of the Chamau farmstead by carefully selecting the integration height of the NBL budget flux calculation using specific wind direction and wind speed conditions. This ensured that the main factor affecting the measurements was kept to the Chamau farmstead and hence reduced the influence of upwind lying sources through advection. The good agreement of the NBL fluxes with the CHAI estimates showed that our emission estimates not only represented the emissions produced at the farm (Table 2), but also confirmed our selection criteria. Still, not all advective effects and external sources could be accounted for, as the NBL fluxes showed a clear intra- and interday variability (Tables 1 and 2), which could not merely be explained by the diel course of livestock methane production. Thus, the NBL budget approach not only integrates over a larger spatial scale but can also be used to resolve mixing processes on smaller, i.e., hourly time scales.

2.4. DISCUSSION 25

2.4.2 Validating inventory estimates

The validation of inventorial emission estimates via atmospheric measurements is not atrivial task. The main challenge lies in matching the different spatial and temporal scales of the inventories and the measurements. The inventory estimates represent annual values, which deviate substantially from the measurements taken at various times. Seasonally changing farming practices and temporal variability in methane emissions are not resolved within a typical inventory so far and are only covered by direct measurements. Furthermore, both the NIR and SEI estimates are affected by the low spatial resolution of the underlying census data and simplified assumptions, resulting in an underestimation of current methane emissions. Especially the coarse resolution of the statistical database in SEI impaired a reliable comparison with atmospheric measurements. Thus, improving the representativeness of temporal variations of methane emissions in both annual NIR and SEI estimates will require long-term measurements at different spatial scales.

In addition a differentiation is needed between the validation of livestock methane emission estimates and the verification of emission factors used for inventory estimates. Most studies adress the verification of EFs via direct measurements at animal level (Zeitz et al., 2012; Ulyatt et al., 2002). However, our study aims to validate the livestock methane emission estimates, by examining the appropriateness of the methodology used in the inventory, and test whether the estimates are consistent with direct atmospheric measurements (Lassey, 2007; Lowry et al., 2001). Using current livestock data (CHAI), the inventory estimates were in the same order of magnitude as atmospheric measurements. Therefore, statistical assessments/inventories are indeed able to reliably estimate methane emissions from livestock, even though the estimates are based on given default values. Beside that, the study showed that the methodology used in the inventory estimates is a practicable instrument for resolving current livestock methane emissions at farm scale and can, for the period of data collection, be applied at higher scales as well, e.g., regional to national scales.

2.5 Conclusion

Direct inventory estimates (CHAI: $1.29 \pm 0.47 \,\mu g$ CH₄ m⁻² s⁻¹ and $1.74 \pm 0.63 \,\mu g$ CH₄ m⁻² s⁻¹) and mean NBL budget fluxes (ranging between 1.22 ± 0.1 and $2.05 \pm 0.45 \,\mu g$ CH₄ m⁻² s⁻¹) agreed well when used to estimate the source strength of a typical Swiss farmstead. Thus, estimates based on current livestock data and default emission factors showed that statistical assessments/inventories give plausible results supporting the methodology used by such inventories to be 'best practice'. Furthermore, statistical assessments can also be applied at different spatial scales, i.e., from regional to continental levels, to compare the livestock methane emissions at a given point in time. Our study also raises confidence that the NIR reliably resolves national livestock methane emissions on an annual scale.

Acknowledgements

Funding for this project was provided by the Swiss National Science Foundation under the grant agreement no. 2.77771.10. We thank Peter Pluess and Thomas Baur for technical support, and Hans-Rudolf Wettstein and his team for their great efforts and support during the measurement campaigns at the ETH Research station Chamau. Many thanks to Dr. Rebecca Hiller and Prof. Dr. Mathias Rotach for fruitful discussions and valuable comments. The spatially explicit inventory of ME-TEOTEST was developed within the MAIOLICA project of the ETH Competence Center Environment and Sustainability (CCES).

2.6 Tables and figures

Date	Night	Sounding	Time	max. Height	Int. Height	NBL Flux
3		0	$[\mathrm{UTC}+1]$	[m a.g.l.]	[m a.g.l.]	$\mu g CH_4 m^{-2} s^{-1}$
16/17 Aug 2011	$^{\mathrm{n1}}$	s_1	20.47 - 21.26	140	20	1.27 ± 0.85
		$^{\mathrm{s}2}$	21:26-22:01	150	20	1.85 ± 0.07
		83	22:01-22:41	150	20	1.55 ± 0.48
		s4	22:41-23:30	160	70	1.19 ± 1.05
		2	00:48-01:47	150	50	1.13 ± 0.06
24/25 Jul 2012	n_2	9s	20:51-21:24	150	09	1.73 ± 0.14
		22	23:27-23:58	150	20	2.37 ± 0.72
		88	01:05-01:37	130	110	2.88 ± 0.61
		89	05:07-05:37	130	80	1.21 ± 0.34
25/26 Jul 2012	n3	810	20.56 - 21.16	170	20	1.18 ± 0.11
		s11	23:03-23:23	160	20	1.68 ± 0.05
		s12	01:06-01:22	130	40	0.79 ± 0.13
26/27 Jul 2012	$^{\mathrm{n4}}$	s13	20.53 - 21.14	190	09	1.93 ± 0.06
		s14	23:03-23:23	180	120	1.84 ± 0.09
		s15	01:01-01:25	180	50	1.52 ± 0.01
		$^{\mathrm{s}16}$	03:07-03:29	170	09	1.53 ± 0.12

Table 2.2: Methane emission estimates from different inventories (NIR, SEI and CHAI) and the NBL budget approach. The inventory estimates are based on the methodology recommended by the IPCC (see text for details). CHAI estimates use current stocking census data, whereas NIR and SEI estimates are based on 2011 and 2007 stocking census data, respectively. NBL budget fluxes are denoted as the mean of all budget fluxes from the individual balloon profiles of the respective nights. The fluxes are in μ g CH₄ m⁻² s⁻¹ (mean \pm sd).

Methodology	16/17 Aug 2011	24/25 Jul 2012	25/26 Jul 2012	26/27 Jul 2012
NIR	0.83 ± 0.30	0.83 ± 0.30	0.83 ± 0.30	0.83 ± 0.30
SEI	0.42 ± 0.15	0.42 ± 0.15	0.42 ± 0.15	0.42 ± 0.15
CHAI	1.29 ± 0.47	1.74 ± 0.63	1.74 ± 0.63	1.74 ± 0.63
NBL	1.40 ± 0.50	2.05 ± 0.45	1.22 ± 0.10	1.70 ± 0.07

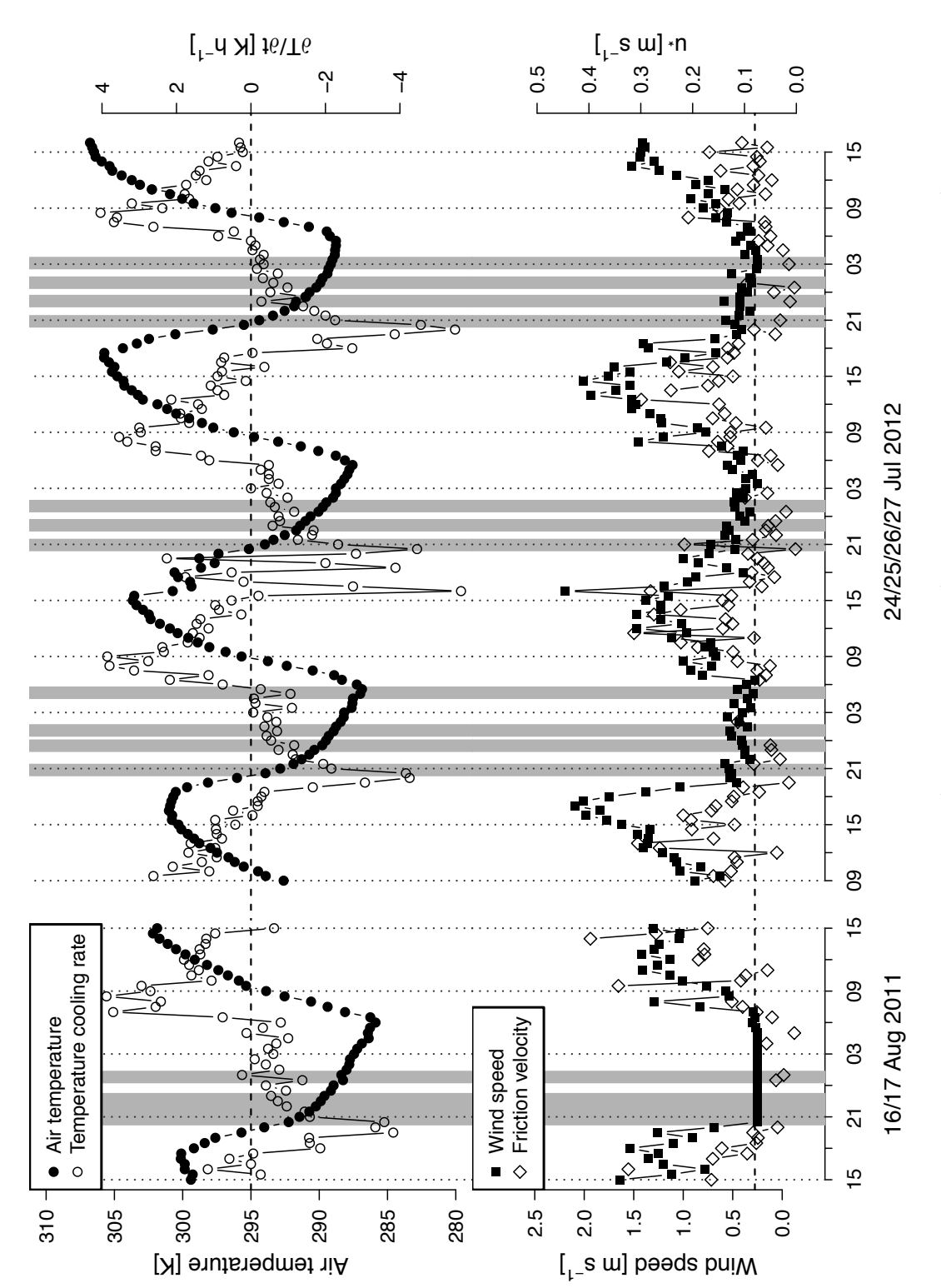


Figure 2.1: Meteorological conditions at Chamau (30-minute averages) during the balloon measurements (gray shaded areas) in 2011 and 2012. Top panel: Air temperature and cooling rates $\frac{\partial \vec{T}}{\partial t}$ at 2 m a.g.l. Bottom panel: Wind speed and friction velocity u_{*} at 2 m a.g.l. Dashed horizontal lines show the temperature cooling rate threshold of K s⁻¹ in the top panel and the threshold of low mechanical turbulence $<0.08 \text{ m s}^{-1}$ (Zeeman et al., 2010) in the lower panel.

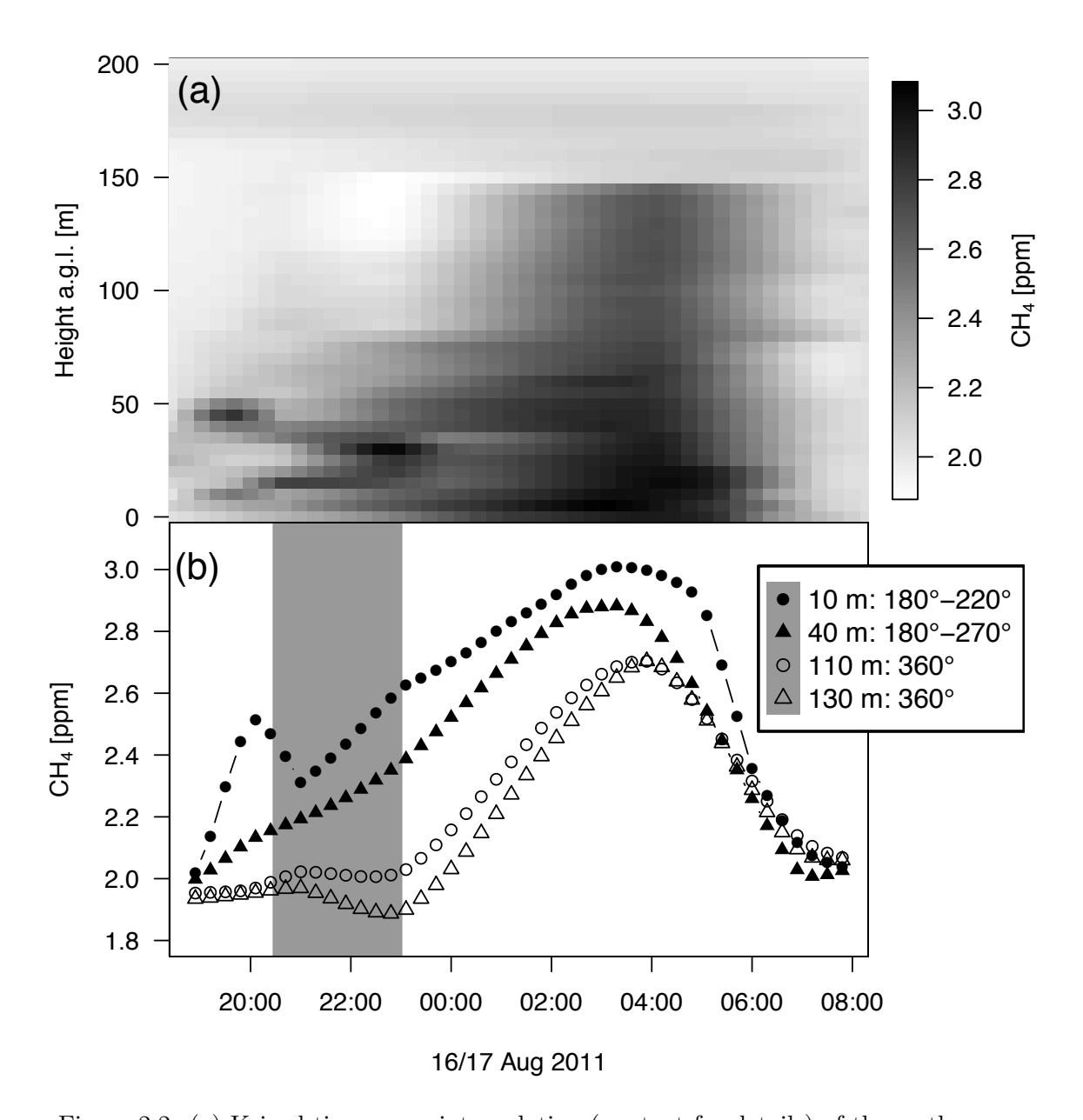


Figure 2.2: (a) Kriged time-space interpolation (see text for details) of the methane concentrations obtained from the balloon measurements during 16/17 Aug 2011. (b) Diel course of methane concentrations at 10 m, 40 m, 110 m and 130 m a.g.l. The gray shaded time periods show the impact of different wind directions, i.e., north winds (360°) and south-west winds $(180-270^{\circ})$, on the CH₄ concentration from the balloon profiles included in the NBL budget flux calculation in 2011.

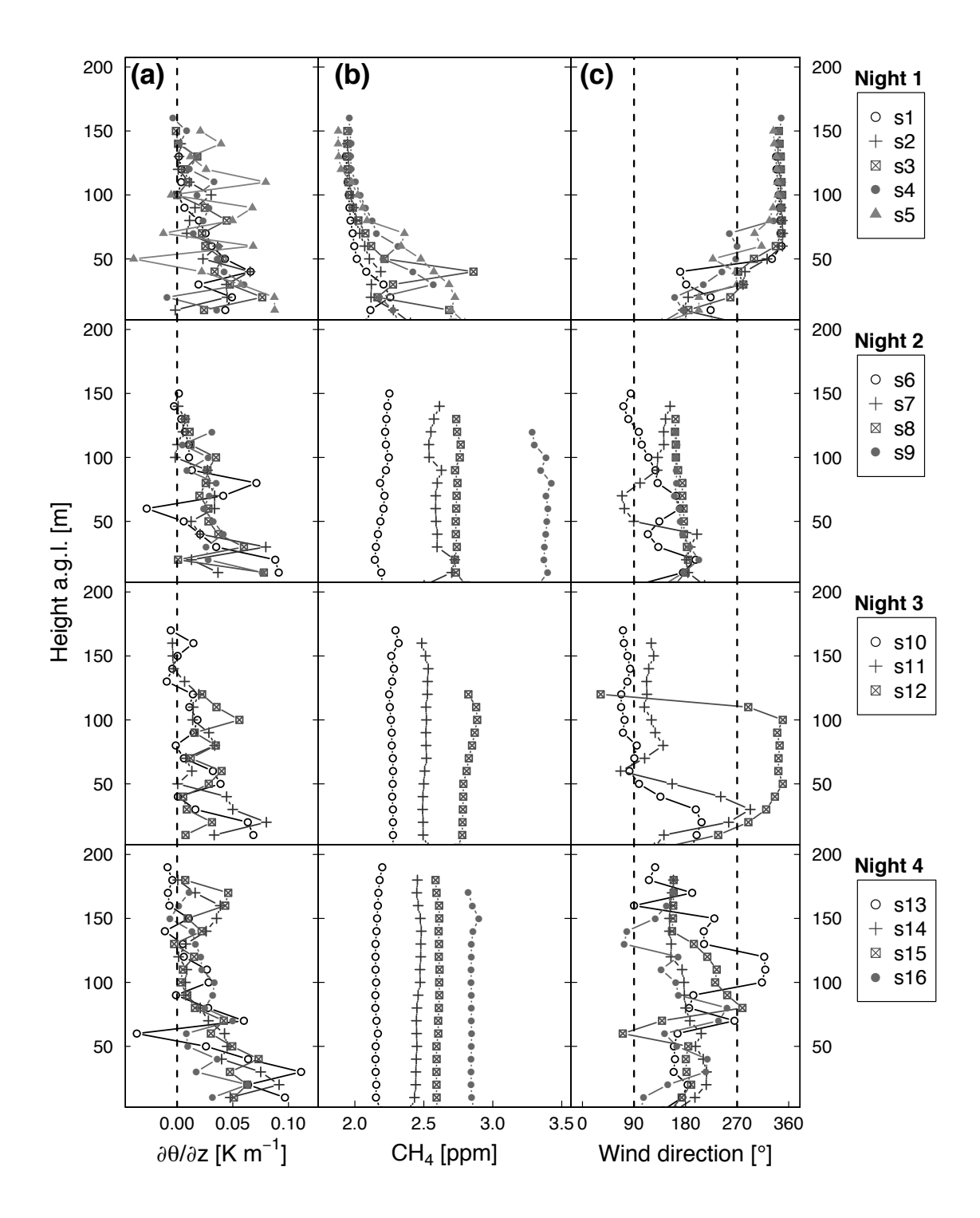


Figure 2.3: Vertical profiles of potential temperature gradients (a), methane concentration (b) and wind direction (c) of the individual balloon measurements. The dashed vertical lines indicate neutral stratification in (a), and lower and upper wind direction limits used for the NBL budget flux calculation, including the cattle barn buildings and grazed pastures at Chamau farmstead, in (c).

References

- ART (2012) Agricultural CH₄ and N₂O emissions in Switzerland. Agroscope Reckenholz Tänikon Research Station (ART), QA/QC Internal Report, Zurich, Switzerland, pp. 61.
- Baldocchi D, Detto M, Sonnentag O, Verfaillie J, The Y, Silver W, Kelly N (2012) The challenges of measuring methane fluxes and concentrations over a peatland pasture. *Agricultural and Forest Meteorology* 153:177–187.
- Bamberger I, Stieger J, Eugster W, Buchmann N (2013) Spatial variability of methane: Attributing atmospheric concentrations to emissions. *In prep.*
- Beswick K, Simpson T, Fowler D, Choularton T, Gallagher M, Hargreaves K, Sutton M, Kaye A (1998) Methane emissions on large scales. *Atmospheric Environment* 32(19):3283–3291.
- Choularton T, Gallagher M, Bower K, Fowler D, Zahniser M, Kaye A, Monteith J, Harding R (1995) Trace Gas Flux Measurements at the Landscape Scale Using Boundary-Layer Budgets. *Philosophical Transactions of the Royal Society of London. Series A: Physical and Engineering Sciences* 351(1696):357–369.
- Christie K, Gourley C, Rawnsley R, Eckard R, Awty I (2012) Whole-farm systems analysis of Australian dairy farm greenhouse gas emissions. *Animal Production Science* 62:998–1011.
- Cleugh H, Raupach M, Briggs P, Coppin P (2004) Regional-scale heat and water vapour fluxes in an agricultural landscape: An evaluation of CBL budget methods at OASIS. *Boundary-Layer Meteorology* 110(1):99–137.
- Dengel S, Levy P, Grace J, Jones S, Skiba U (2011) Methane emissions from sheep pasture, measured with an open-path eddy covariance system. *Global Change Biology* 17(12):3524–3533.
- Denmead O, Leuning R, Griffith D, Jamie I, Esler M, Harper L, Freney J (2000) Verifying inventory predictions of animal methane emissions with meteorological measurements. *Boundary-Layer Meteorology* 96(1-2):187–209.

Denmead O, Raupach M, Dunin F, Cleugh H, Leuning R (1996) Boundary layer budgets for regional estimates of scalar fluxes. *Global Change Biology* 2(3):255–264.

- Detto M, Baldocchi D, Katul G (2010) Scaling properties of biologically active scalar concentration fluctuations in the atmospheric surface layer over a managed peatland. *Boundary-Layer Meteorology* 136(3):407–430.
- Dlugokencky E, Nisbet E, Fisher R, Lowry D (2011) Global atmospheric methane: budget, changes and dangers. *Philosophical Transactions of the Royal Society A:* Mathematical, Physical and Engineering Sciences 369(1943):2058–2072.
- Dorninger M, Whiteman C, Bica B, Eisenbach S, Pospichal B, Steinacker R (2011) Meteorological events affecting cold-air pools in a small basin. *Journal of Applied Meteorology and Climatology* 50(11):2223–2234.
- FOEN (2013) Switzerland's Greenhouse Gas Inventory 1990-2011: National Inventory Report 2013. page 483. Submission of 15 April 2013 under the United Nations Framework Convention on Climate Change and under the Kyoto Protocol. Federal Office for the Environment (FOEN), Bern, Switzerland.
- Fowler D, Hargreaves K, Choularton T, Gallagher M, Simpson T, Kaye A (1996) Measurements of regional CH₄ emissions in the UK using boundary layer budget methods. *Energy Conversion and Management* 37(6):769–775.
- FSO (1998) CORINE Land cover map. Swiss Federal Statistical Office (FSO), Neuchatel, Switzerland.
- FSO (2007) Land use statistics (Arealstatisik) 1992/97, NOAS92. Swiss Federal Statistical Office (FSO), Neuchatel, Switzerland.
- FSO (2009) Data extract of census of agricultural entreprises 2007. Swiss Federal Statistical Office (FSO), Neuchatel, Switzerland.
- FSO (2012) Land use statistics (Arealstatisik) 2004/09, NOLU04/20120821. Swiss Federal Statistical Office (FSO), Neuchatel, Switzerland.
- Gilgen A, Buchmann N (2009) Response of temperate grasslands at different altitudes to simulated summer drought differed but scaled with annual precipitation. *Biogeosciences Discussions* 6(3):5217–5250.
- Harper L, Denmead O, Flesch T (2011) Micrometeorological techniques for measurement of enteric greenhouse gas emissions. *Animal Feed Science and Technology* 166:227–239.
- Hartmann A, Buchmann N, Niklaus P (2011) A study of soil methane sink regulation in two grasslands exposed to drought and n fertilization. *Plant Soil* 342(1-2):265–275.

Heimann M (2011) Atmospheric science: Enigma of the recent methane budget. *Nature* 476(7359):157–158.

- Hiller R (2012) Greenhouse gases: from the ecosystem scale to a regional integration. ETH PhD thesis No. 20183, ETH Zurich, Switzerland, pp. 179.
- Hiller R, Bretscher D, DelSontro T, Diem T, Eugster W, Henneberger R, Hobi S, Hodson E, Imer D, Kreuzer M, Künzle T, Merbold L, Niklaus P, Rihm B, Schellenberger A, Schroth M, Schubert C, Siegrist H, Stieger J, Buchmann N, Brunner D (2013) Anthropogenic and natural methane fluxes in Switzerland synthesized within a spatially-explicit inventory. Biogeosciences Discussions 10(9):15181–15224.
- Holden J, Derbyshire S, Belcher S (2000) Tethered balloon observations of the nocturnal stable boundary layer in a valley. *Boundary-Layer Meteorology* 97(1):1–24.
- Hsu Y, VanCuren T, Park S, Jakober C, Herner J, FitzGibbon M, Blake D, Parrish D (2010) Methane emissions inventory verification in southern California. *Atmospheric Environment* 44(1):1–7.
- Imer D, Merbold L, Eugster W, Buchmann N (2013) Temporal and spatial variations of CO₂, CH₄ and N₂O fluxes at three differently managed grasslands. *Biogeosciences* 10:5931–5945.
- Kuck L, Smith Jr T, Balsley B, Helmig D, Conway T, Tans P, Davis K, Jensen M, Bognar J, Arrieta R, others (2000) Measurements of landscape-scale fluxes of carbon dioxide in the Peruvian Amazon by vertical profiling through the atmospheric boundary layer. *Journal of Geophysical Research* 105(D17):22137–22.
- Lassey K (2007) Livestock methane emission: from the individual grazing animal through national inventories to the global methane cycle. *Agricultural and Forest Meteorology* 142(2):120–132.
- Lassey K (2008) Livestock methane emission and its perspective in the global methane cycle. *Animal Production Science* 48(2):114–118.
- Levin I, Glatzel-Mattheier H, Marik T, Cuntz M, Schmidt M (1999) Verification of German methane emission inventories and their recent changes based on atmospheric observations. *Journal of Geophysical Research: Atmospheres* 104(D3):3447–3456.
- Lowry D, Holmes C, Rata N, O'Brian P, Nisbet E (2001) London methane emissions: Use of diurnal changes in concentration and δ^{13} C to identify urban sources and verify inventories. *Journal of Geophysical Research: Atmospheres* 106(D7):7427–7448.

Mahrt L, Vickers D (2002) Contrasting vertical structures of nocturnal boundary layers. Boundary-Layer Meteorology 105(2):351–363.

- Mathieu N, Strachan I, Leclerc M, Karipot A, Pattey E (2005) Role of low-level jets and boundary-layer properties on the NBL budget technique. *Agricultural and Forest Meteorology* 135(1):35–43.
- Nisbet E, Weiss R (2010) Top-down versus bottom-up. Science 328(5983):1241–1243.
- Parker M, Raman S (1993) A case study of the nocturnal boundary layer over a complex terrain. *Boundary-Layer Meteorology* 66(3):303–324.
- Pattey E, Strachan I, Desjardins R, Edwards G, Dow D, MacPherson J (2006) Application of a tunable diode laser to the measurement of CH₄ and N₂O fluxes from field to landscape scale using several micrometeorological techniques. *Agricultural and Forest Meteorology* 136(3):222–236.
- Pendall E, Schwendenmann L, Rahn T, Millers J, Tans P, White J (2010) Land use and season affect fluxes of CO₂, CH₄, CO, N₂O, H₂ and isotopic source signatures in Panama: evidence from nocturnal boundary layer profiles. *Global Change Biology* 16(10):2721–2736.
- Penman J, Kruger D, Galbally I, Hiraishi T, Nyenzi B, Emmanual S, Buendia L, Hoppaus R, Martinsen T, Mejer J, others (2000). Good practice guidance and uncertainty management in national greenhouse gas inventories. IPCC National Greenhouse Cost Inventories programme, Technical Support Unit.
- Pinto J, Parsons D, Brown W, Cohn S, Chamberlain N, Morley B (2006) Coevolution of down-valley flow and the nocturnal boundary layer in complex terrain. *Journal of Applied Meteorology and Climatology* 45(10):1429–1449.
- Pulles T, Van Amstel A (2010) An overview of non-CO₂ greenhouse gases. *Journal of Integrative Environmental Sciences* 7(S1):3–19.
- Raupach M, Denmead O, Dunin F (1992) Challenges in linking atmospheric CO₂ concentrations to fluxes at local and regional scales. *Australian Journal of Botany* 40(5):697–716.
- Saggar S, Bolan N, Bhandral R, Hedley C, Luo J (2004) A review of emission of methane, ammonia, and nitrous oxide from animal excreta deposition and farm effluent application in grazed pastures. New Zealand Journal of Agricultural Research 47:513–544.
- Soliva C (2006) Report to the attention of IPCC about the data set and calculation method used to estimate methane formation from enteric fermentation of agricultural livestock population and manure management in Swiss agriculture. Institute

of Animal Science, ETH Zurich, Switzerland. On behalf of the Fereal Office for the Environment (FOEN), Bern, Switzerland, pp. 14.

- Staerfl S, Zeitz J, Kreuzer M, Soliva C (2012) Methane conversion rate of bulls fattened on grass or maize silage as compared with the IPCC default values, and the long-term methane mitigation efficiency of adding acacia tannin, garlic, maca and lupine. Agriculture, Ecosystems & Environment 148:111–120.
- Sun J, Burns S, Delany A, Oncley S, Turnipseed A, Stephens B, Lenschow D, LeMone M, Monson R, Anderson D (2007) CO₂ transport over complex terrain. *Agricultural and Forest Meteorology* 145(1):1–21.
- Suter F (2011) Greenhouse gases from managed ecosystems: a farm scale perspective. Insights from a consolidated greenhouse gas budgets of a typical Swiss three-stage grassland farming system. ETH Master thesis, ETH Zurich, Switzerland, pp. 69.
- Ulyatt M, Lassey K, Shelton I, Walker C (2002) Seasonal variation in methane emission from diary cows and breeding ewes grazing ryegrass/white clover pasture in New Zealand. New Zealand Journal of Agricultural Research 45:217–226.
- Wang J, Cardenas L, Misselbrook T, Gilhespy S (2011) Development and application of a detailed inventory framework for estimating nitrous oxide and methane emissions from agriculture. *Atmospheric Environment* 45(7):1454–1463.
- Wang S, Ackermann R, Stutz J (2006) Vertical profiles of O_3 and NO_x chemistry in the polluted nocturnal boundary layer in Phoenix, AZ: I. Field observations by long-path DOAS. *Atmos. Chem. Phys* 6:2671–2693.
- Zeeman M, Hiller R, Gilgen A, Michna P, Plüss P, Buchmann N, Eugster W (2010) Management and climate impacts on net CO₂ fluxes and carbon budgets of three grasslands along an elevational gradient in Switzerland. *Agricultural and Forest Meteorology* 150(4):519–530.
- Zeeman M, Werner R, Eugster W, Siegwolf R, Wehrle G, Mohn J, Buchmann N (2008) Optimization of automated gas sample collection and isotope ratio mass spectrometric analysis of δ^{13} C of CO₂ in air. Rapid Communications in Mass Spectrometry 22(23):3883–3892.
- Zeitz J, Solvia C, Kreuzer M (2012) Swiss diet types for cattle: how accurately are they reflected by the Intergovernmental Panel on Climate Change default values? Journal of Integrative Environmental Sciences 9:199–216.
- Zinchenko A, Paramonova N, Privalov V, Reshetnikov A (2002) Estimation of methane emissions in the St.Petersburg, Russia, region: An atmospheric nocturnal boundary layer budget approach. *Journal of Geophysical Research: Atmospheres* 107(D20):1451–1476.

Spatial variability of methane: Attributing atmospheric concentrations to emissions

Ines Bamberger, Jacqueline Stieger, Werner Eugster, Nina Buchmann Institute of Agricultural Sciences, ETH Zurich, Zurich, Switzerland

This manuscript is intended for submission to: $Environmental\ Pollution$

Abstract

Spatial variations in methane concentrations were quantified along transects using a mobile system in order to identify the spatio-temporal patterns of atmospheric methane and their controlling factors. The measurements from an agriculturally dominated area in Switzerland including vertical profiles, and the diurnal cycles of methane concentrations revealed three main aspects being responsible for the regional distribution of atmospheric methane; (1) the magnitude and distribution of methane sources within the region, (2) the efficiency of vertical exchange, and (3) local wind patterns within the complex topography. An autocorrelation analysis of measured methane concentrations showed that nighttime measurements close to the ground provide information about regional sources. At night, concentration is also a better indicator for emissions obtained from a spatially explicit methane emission inventory and for identifying inconsistencies in an emission inventory than during the day.

3.1 Introduction

The spatial variability of atmospheric methane concentrations and their temporal variations are still insufficiently known, despite the prominent role of methane in atmospheric chemistry, its major contribution (15%) to anthropogenic radiative forcing (IPCC, 2007) and an increasing number of measurement stations in deployment (Dlugokencky et al., 2011). With the advent of spatially explicit emission inventories, it becomes increasingly important to find empirical methods for field validation of such inventories. Using an instrumented car for transect measurements, as was done in and agriculturally dominated area of Switzerland in this study, is a promising technique that is a first step in that direction.

Since conventional measurement systems for methane concentrations and fluxes mostly rely on point measurements at specific sites, spatial interpolation is difficult. Especially in regions with multiple methane sources, the concentrations of atmospheric methane are expected to exhibit significant deviations from the global atmospheric background of 1.77 ppm (IPCC, 2007) and to give essential information about the emission strength of regional methane sources. Although there are studies which evaluated the regional distribution of methane in the upper atmosphere using aircraft measurements, e.g., Beck et al. (2012); Schuck et al. (2012); Xiong et al. (2010), there are only few studies so far, which evaluated the regional variability close to the ground. Phillips et al. (2013) found methane hotspots (up to 28.6 ppm) along the roads of Boston due to leakages in the gas distribution network. Methane concentrations also varied substantially in the greater area of Los Angeles (Townsend-Small et al., 2012). Still, the temporal fluctuations of the spatial variability and the underlying driving processes remained unresolved.

In addition, emission budgets of atmospheric methane are mainly based on modeling approaches and rarely include direct measurements. Currently two modeling approaches, i.e., top-down and bottom-up, are used to assess methane fluxes (Nisbet, Weiss, 2010). In top-down or backward modeling, often implemented for global methane budgets, atmospheric methane concentrations are traced back to regional sources using transport models (Bousquet et al., 2006). Uncertainties in those models arise from assumptions regarding the methane emissions, the use of atmospheric transport models (Tarasova et al., 2009; Gerbig et al., 2008; Lin, Gerbig, 2005) and a lack of direct measurements for validation. Although a reliable quantification of

regional-scale methane emissions using top-down models is not yet possible, global flux patterns are relatively well constrained (Dlugokencky et al., 2011; Bergamaschi et al., 2010). For regional-scale estimates a dense measurement network would be required (Villani et al., 2010; Tarasova et al., 2009), which is currently not existing. In contrast, bottom-up models estimate methane emissions via the up-scaling of emission factors or small-scale flux calculations using statistical land-use and live-stock information. However, the results from bottom-up models are still associated with considerable uncertainties (Gerbig et al., 2009; Jagovkina et al., 2000), which originate from the high variability in reported emission factors (Bergamaschi et al., 2010) and the questionable representativeness of small-scale flux calculations for regional scales. Thus, direct atmospheric measurements at regional scales and a better understanding how the heterogeneous patterns in atmospheric methane concentrations arise would help to reliably validate or constrain bottom-up and top-down emission estimates and to reduce associated uncertainties.

Our study aims to improve the understanding of spatio-temporal methane concentration patterns using highly resolved, mobile measurements in an agriculturally dominated area in Switzerland. The objectives of our study are (1) to identify the spatio-temporal methane patterns, (2) to investigate the processes controlling such patterns of methane concentrations in complex terrain, and (3) to assess the potential of methane concentration measurements to constrain regional scale emission estimates.

3.2 Materials and Methods

3.2.1 Site description and transect patterns

We used a mobile set-up for methane concentration measurements in the Reuss Valley, situated in Central Switzerland. The Reuss Valley is a river valley aligned in a northerly direction, with an altitudinal difference of approximately 440 m between the surrounding hilltops and the valley bottom. Agriculture is with 56.5% of the total area the dominant land-use type (FSO, 2012). Diurnal wind patterns within the valley are dominated by up-valley winds during daytime and down-valley winds during nighttime. The concentration measurements were performed during three

consecutive days and nights under fair weather conditions in July 2012, covering two predefined transects, i.e., the valley transect and the mountain transect (Figure 1).

The valley transect measurements were performed eight times (transect t1–t8) during 24^{th} – 25^{th} July 2012 and included the Reuss Valley bottom and the surrounding hillsides, covering altitudes between 380 and 716 m above sea level (a.s.l.). During 26^{th} of July, additional measurements (four transects t9 – t12) were taken along the mountain transect, including the Zugerberg mountain ridge at 1077 m a.s.l. located east of Lake Zug to extend the vertical profiles (Table 1).

3.2.2 Mobile measurement set-up

The mobile measurement set-up consisted of a DLT-100 Fast Methane Analyzer (FMA, Los Gatos Research, CA, USA), installed in the luggage compartment of a car. An Airmar weather station (AIRMAR® Technology Corporation, Milford, NH USA), providing meteorological data and GPS coordinates, was installed on a rod fixed to the roof rack of the car at approximately 2 m above ground. Through an inlet tube (Synflex 1300, ID 3.8 mm, Eaton, Eaton Hydraulics Group Europe, Morges, Switzerland), whose air inlet was placed next to the Airmar, the ambient air was drawn into the methane analyzer at a flow rate of 0.65 standard liter per minute. The methane analyzer, the Airmar weather station and a portable computer were attached to 12-Volt batteries (NPL65-12I, YUASA Battery Sales LTD, Swindon, UK) in series, connected to a power inverter (Sine Wave Inverter, Nordic Power, Järfälla, Sweden).

Methane concentrations were recorded on the analyzer's hard disk, while data from the infrared gas analyzer and the weather station were saved at the hard disk of the portable computer. A time lag correction using the flow rate of the pumps and the inner volume of the intake tubes was applied to the measurements of the FMA, to account for inlet tubing residence time. Time offsets originating from the reaction time of the GPS while driving, and from the distance between inlet and GPS were thought to be small and therefore neglected in the georeferencing of the measured time series.

3.2.3 Data analysis

Post-processing of the data was performed using the commercial MAT-LAB® software (Math Works®), Natick, MA, USA). We determined a methane background concentration of 1.92 ppmv from the 5^{th} percentile of all measured concentrations from the transects. For the vertical profiles, we bin-averaged the temperature and methane concentration measurements by altitude using smaller bin sizes (down to 20 m) for the altitudes where plenty measurement points were available and increased bin sizes to 100 m towards the highest elevations of the transects. In order to explore the diurnal patterns of methane concentrations as a function of the measurement location, we calculated Pearson correlation coefficients between the average diurnal cycle (averaged over all locations) and the diurnal cycle at a specific location (within a 150 m x 150 m grid cell) for every measurement location along the transect. The representativeness of point measurements for different spatial scales was assessed using an autocorrelation analysis on an equidistant data series of our measurements, which was obtained by nearest neighbor interpolation from the georeferenced time series.

The measured methane concentrations were compared to the emission estimates of a spatially explicit methane emission inventory (Hiller et al., 2013; METEOTEST, 2011). The inventory is based on a bottom-up approach and default emission factors were multiplied with lifestock census data and activity data from point sources (industry, waste water treatment) to receive estimates of the methane emission strength. Then, these emission estimates were disaggregated tonto a regular grid with a spatial resolution of 500 x 500 m using best available land use census data (Hiller et al., 2013; METEOTEST, 2011). We calculated day-and nighttime average concentrations of valley transect measurements lying in the respective grid cells of the spatially explicit inventory and compared them to the inventory estimates using quantile regressions (Koenker, 2005; Koenker, Basset, 1978). Transects 3 and 7 included transitions from day to night and were therefore excluded from this analysis.

3.3. RESULTS 43

3.3 Results

3.3.1 Spatio-temporal variability of CH₄ concentrations

Regional distribution of atmospheric methane concentrations

Along the valley transects (transects t1-t8), methane concentrations ranged from 1.91 ppmv up to a peak value of 5.80 ppmv and were heterogeneously distributed within the region (Figure 2a). While daytime transects (t1, t2, t5, t6) showed a relatively low variability in methane concentrations, i.e. between 1.92 ppmv and 4.06 ppmy, peak concentrations during nighttime transects (t4, t8) were generally higher. Transects measured during evening transitions showed methane concentrations spanning a range from 1.91 ppmv to 4.06 ppmv. Peak methane concentrations during daytime were locally confined, and could be associated with methane sources in direct vicinity of the measurements (such as farmsteads). In contrast, methane concentrations at night at the valley bottom were clearly higher than the daytime background levels, showing a mean value of 2.98 ppmv and maximum values of 5.80 ppmv within the valley (transect t4). During nighttime, however, lowest methane concentrations at the hillsides were close to the calculated background concentration and peak concentrations up there were slightly higher than during daytime but locally confined to the location of nearby sources as well (i.e. between 1.92 ppmv and 4.04 ppmv, for transect t4).

The mountain transects (t9 – t12, Table 1) showed slightly lower minimum methane concentrations than for valley transects (1.88 –1.89 ppmv). Minimum concentrations were generally observed at the mountaintop at altitudes ranging from 952 to 1059 m a.s.l. Methane concentrations along the mountain transects showed a very heterogeneous distribution and spanned a range from 1.88 ppmv to 7.66 ppmv (Table 1). Similar to the valley transects, methane concentrations during the night were higher within the valley than during daytime (compare Figure 2c, d). Peak concentrations, however, were not substantially lower during the daytime transects (t9, t10) than during the nighttime transect (t12), which contrasts strongly with conditions seen in the valley transects. Peak concentrations along transects t9 and t10 were observed close to a biogas plant (Figure 2c). The maximum concentration of transect t11 (Table 1), measured during the evening transition phase, was probably due to manure management in the upwind fetch at Zugerberg (data not

shown). During the night transect t12, the methane concentration maximum of 4.65 ppmv was observed at a lower altitude within the valley (424 m a.s.l, Figure 2d).

Nocturnal vertical temperature and CH₄ concentration profiles

Vertical temperature profiles showed the development of a nocturnal boundary layer with two inversion layers (Figure 3), the first starting at the valley bottom (around 350 m a.s.l) and the second inversion layer lying on top of the first one (at around 600 m a.s.l). Temperatures in the lower, strong inversion layer raised by 2.4°C from 14.6 °C at the valley bottom to 17.0 °C at an altitude of approximately 480 m a.s.l. during the first night of the valley transect measurements while the temperature difference was only 1°C from 16°C to 17°C (Figure 3a) between the lower (600 m a.s.l) and upper (640 m a.s.l) altitude of the second inversion layer. During the second night, the temperature difference across the boundaries of the first inversion layer was substantially lower (1.2 $^{\circ}$ C). As opposed to the previous night, the top of the second inversion layer with a lower boundary of 600 m a.s.l. was beyond the altitudinal range covered by the valley transect (Figure 3a). Methane accumulated to almost 2.98 ppmv (first night) and 2.82 ppmv (second night) predominantly in the first inversion layer on the valley bottom during both nights and declined rapidly to values close to 2.04 ppmv (first night) and 2.06 ppmv (second night) at higher altitudes (Figure 3b).

The vertical temperature profiles along the mountain transect (Figure 4) were similar to the profiles from the valley transect, exhibiting a first inversion layer, where temperatures raised from 16.8°C at an altitude of 405 m a.s.l to 20.1°C at the upper boundary (625 m a.s.l., Figure 4a). Above, a second, weaker inversion layer was observed, with a temperature difference of only 1.1°C between its lower (700 m a.s.l.) and upper (800 m a.s.l.) boundaries. Similar to the valley transect, methane concentrations of the mountain transect significantly increased to 2.76 ppmv close to the valley bottom (Figure 4b), and declined rapidly to values around 2.02 ppm with increasing altitude until the lower boundary of the second inversion layer was reached at 700 m a.s.l. Methane concentrations in the second inversion layer were slightly higher again (2.11 ppmv) and dropped back to values around 2.00 ppmv at an altitude of nearly 1000 m a.s.l (Figure 4).

3.3. RESULTS 45

Diurnal cycles of CH₄ concentrations

To identify differences in the spatio-temporal patterns, methane diurnal cycles at each sampling site of the valley transect were analyzed and compared to the regional average diurnal cycle (Figure 5a). While diurnal cycles for sampling sites at the bottom of the valley showed a similar behavior (expressed by high correlation coefficients R>0.7, p<0.05) compared to the regional average diurnal cycle at the sampling sites, the diurnal cycles at the hillsides showed insignificant correlations (p<0.05) with the regional average diurnal cycle (Figure 5a). The regional average diurnal cycle of CH₄ concentrations showed a strong day to night variation, with increased concentrations (up to 2.58 ± 0.52 ppmv) from dusk till dawn and lowest concentrations (down to 1.97 \pm 0.07 ppmv) during the day (Figure 5b). At the western hillside (Figure 5c) the average diurnal pattern was less distinct compared to the diurnal cycles at the valley bottom, but showed elevated methane concentrations (>2.2 ppmv) even in late morning (9:30), lowest values in the afternoon around 15:00, and increasing concentrations afterwards. At the eastern hillside, however, methane concentrations always remained below 2.2 ppmv and no distinct (Figure 5d) diurnal pattern was observed.

3.3.2 Concentrations for constraining emission inventories

Representativeness of point measurements

An autocorrelation analysis of the different valley transects showed that the distance of influence from a local point source (source influence) varied considerably between different times of day (Figure 6a). During the afternoon, the source influence, expressed as the coefficient of determination of the autocorrelation function, decreased to 20% already within a displacement distance of 250 m between source and measurement location. This clearly differed from conditions during night and at dawn, when a much stronger influence from point sources was detectable (>20%) over much longer separation distances of 2.1 km and 9.2 km, respectively (Figure 6a). The source influence also revealed a diurnal pattern, very similar to the average diurnal cycle, with peak values before dawn and lowest values during daytime (Figure 6b). The minimal displacement distance between source and measurement location at which the source influence was at least 25% (green curve)

was highest before dawn (8.3 km, which corresponds to an area of approximately 5000 ha around a source) and declined to values around 240 m during daytime (Figure 6b). The displacement distances at which the influence was at least 10%, 50%, 75%, and 90% showed similar diurnal patterns, with highest values at dawn and lowest during the day, but with increasing and decreasing distances for the lower and higher source influences (in %), respectively.

Concentrations versus inventory emissions

Methane concentration measurements show a large spatial variability, but also the spatial variability in methane inventory estimates at 500 m x 500 m resolution is high. Although there was no simple linear relationship between methane concentrations and inventory fluxes, an exponential relationship between the two variables was found via quantile regression analysis. The quantile regression approach (Koenker, 2005; Koenker, Basset, 1978) divides the dataset into quantiles in such a way that the relationship between inventory fluxes and concentrations are investigated for data quantiles instead of the ensemble of all data. Each line in a quantile regression actually separates a given percentage of data that lie above the line from those below the line, to indicate how this separation line depends on the independent variable. We used a power law function, $y = b * 10^{s*x}$ with x the measured methane concentration, y the corresponding inventory emission rate, s the growth rate of the relationship between y and x, and b is the emission rate which distinguishes the lower emission limit without significant impact on ambient methane concentrations (Figure 7). Concentration measurements were separated into daytime and nighttime values (Figure 7 a, c) which were then analyzed separately. In both cases lower to intermediate flux quantiles showed the strongest response of methane emissions with concentration measurements, whereas for the higher quantiles (>75\% probability of exceedance) no robust relationship was found between concentrations and emission inventory fluxes (Figure 7c, d). During the day a methane concentration increase of 1 ppmv comes along with a hundred-fold (10^2) increase in inventory emissions for the 55% flux quantile. This means that daytime methane concentration measurements are a reasonably good indicator for lower and intermediate methane emissions, but the highest emission fluxes appear to be poorly related to ambient concentrations. This is seen in the strongly decreasing growth rates towards higher flux quantiles (Figure 7b) where they reach values below 0.5 ppbv^{-1} (>75\% flux quantiles). A

3.4. DISCUSSION 47

growth rate of 0.5 ppbv⁻¹ corresponds to a three-folding of emissions for each ppmv increase in methane concentration measurements. Towards lower flux quantiles the growth rate decreases steadily to 0.7 ppbv⁻¹ (corresponding to a five-folding of emissions for each ppmv), but increases again for the lowest flux percentiles. At night, the relationships between measured concentrations and inventory fluxes showed a comparable pattern but were generally stronger than during the day (lower uncertainty ranges for the rate of growth) although the growth rates were smaller than during the day, with values around 0.8 ppbv⁻¹ (corresponding to a six-folding of emissions for each ppmv increase in concentration measurements). These findings from the quantile regression analysis are in line with what can be expected from the spatial autocorrelation analysis: at night the relationship between concentration measurements and associated methane emissions is stronger and clearer than during the day.

3.4 Discussion

3.4.1 Processes driving the spatio-temporal CH_4 concentration patterns

Except for locations very close to local methane sources, methane concentrations were around the calculated background concentration due to strong turbulent mixing during daytime. Thus, differences in atmospheric methane concentrations during daytime were mainly controlled by the location and strength of methane sources within the region, a behavior also seen in the study by Phillips et al. (2013). During the night, a stable nocturnal boundary layer (NBL) developed, indicated by the temperature inversion close to the valley bottom, resulting in elevated methane concentrations. It is well known that at night, the efficiently mixed convective (daytime) layer is replaced by the NBL, which suppresses vertical mixing (Stull, 1988). This process led to nighttime accumulation of methane at the valley bottom, while horizontal dispersion distributed the methane enriched air across the entire valley bottom. The low vertical mixing during nighttime also caused characteristic diurnal cycles within the valley, with increased methane concentrations in the night compared to values during the day. During the summer months under fair weather

conditions, similar diurnal patterns were also observed by other studies for methane (Wang et al., 2013; Shipham et al., 1998) but also for other VOCs like monoterpenes (Kaser et al., 2013; Bamberger et al., 2011). These findings clearly indicate that besides the source distribution, the efficiency of turbulent mixing in the boundary layer plays an important role for the spatio-temporal patterns of methane concentrations.

However, methane concentrations at the western and eastern hillsides showed a significantly different diurnal course. Especially at the western hillside, which received direct sunlight in the morning on clear-sky days, morning methane concentrations were clearly higher compared to afternoon concentrations. At sunrise, temperature gradients between the warmer hillsides (in our case the western hillside) and the colder valley bottom initiate up-slope winds (Whiteman, 2000). The diurnal concentration patterns at the western hillsides suggest that methane-enriched air masses, which had been trapped at the valley bottom within the NBL, were transported along the western hillside by the up-slope wind in the morning. As a consequence this led to the observed high morning concentrations which decreased to background concentrations with the complete breakup of the NBL later during the day. This interpretation agrees well with the study by Gohm et al. (2009) and Schnitzhofer et al. (2009), who conducted gas (CO, NO₂) and particle pollution measurements within an Austrian Alpine valley during wintertime and described one-sided vertical transport of pollutants with up-slope winds along the warmer mountain slope. Although our study was conducted in a non-Alpine valley, the measured profiles suggested that these wind systems also develop over river valleys, in agreement with current knowledge about mountain meteorology that such wind systems are strongly driven by the pressure gradient between the mountain tops and their foothills and foreland (Whiteman, 2000).

Thus, our study suggests that there are three main processes, affecting the spatiotemporal patterns of methane concentrations in complex terrain: (1) the source distribution, (2) the efficiency of turbulent mixing in the boundary layer, and (3) local wind patterns like valley wind systems. This finding is especially important with regard to atmospheric transport models, since uncertainties in wind measurements and vertical mixing heights lead to significant uncertainties in the transport of greenhouse gases even over homogeneous and flat terrain (Gerbig et al., 2008; Lin, Gerbig, 2005). 3.4. DISCUSSION 49

3.4.2 Constraining emission inventories using concentration measurements

In order to investigate the suitability of atmospheric concentration measurements to constrain emission inventories, it is important to know how representative point measurements close to the ground are for the understanding regional scale processes. The autocorrelation analysis implied that (1) measurements taken close to the ground (at ca. 2 m altitude) in the valley carry regional source information of up to of 5000 ha around the measurement location during nighttime; (2) due to efficient vertical mixing, methane measurements during daytime (if not taken in the direct vicinity of sources) are representative for regional background methane concentrations but do not carry information about regional sources; and (3) during the day, a slight difference in the displacement distance may result in a considerable deviation in methane concentrations. These findings demonstrated that nighttime measurements of methane concentrations are useful to derive information about regional source strengths within the valley and therefore suited to constrain regional emission estimates. In contrast, daytime measurements provided information about regional methane background concentrations and allow the localization of point sources as was reported by Phillips et al. (2013). These findings might be especially useful regarding the attribution of methane sources on a regional scale, which is often a substantial source of uncertainty for top-down models (Bergamaschi et al., 2009; Tarasova et al., 2009).

Concentration measurements obtained along a spatial transect can be used to predict fluxes in areas with small to intermediate fluxes according to the emission inventory, but grid cells with the highest emission inventory fluxes were not clearly reflected in the concentration measurements (Figure 7). The weak relationship between methane concentrations and highest inventory estimates cannot be explained by the three processes discussed in Section 4.1 and hence needs special attention. A closer look at the dominating methane source in the Reuss Valley, animal husbandry, shows that for the inventory 80% of total livestock emissions were attributed to farmsteads in the inventory and only 20% to the agricultural areas within the local community (Beat Rihm, pers. comm.). This may be a good approximation for annual average emissions, but because our measurements were taken during the summer period, we assume that most cattle were actually grazed on pasturelands and not kept

in barns of the farmsteads. Hence, a misallocation due to lack of more detailed cattle census information is likely. Especially for bigger farmsteads pasturelands are not necessarily located within the same grid cells as the farmsteads they belong to. This may explain the weak relationship between concentrations and inventory emissions for the highest flux percentiles. Contrastingly, the lower to intermediate inventory fluxes are more likely to originate either from smaller farmsteads or from stationary sources and are therefore rather well captured by the spatially highly resolved concentration measurements.

3.5 Conclusion

Our study clearly showed that the distribution of sources, the efficiency of vertical mixing in the boundary layer and local wind patterns are controlling factors for the spatio-temporal distribution of methane concentrations within the region. Atmospheric methane measurements close to the ground hence provided very useful insights into regional scale processes affecting the spatial variation of methane concentrations.

Thus, it is suggested that regional to continental transport models, need to account for topography and the local wind patterns, in order to reliably attribute emissions to source areas. Moreover, spatially highly resolved atmospheric methane measurements using a ground-based, mobile measurement approach have a high potential for monitoring regional air quality and to localize methane sources. The identification of disagreements between mobile measurements and spatially highly resolved inventory estimates can be used to identify errors in the spatial allocation of diffuse emissions to inventory grid cells as well as the existence of locally relevant methane sources that were considered negligible in emission inventories.

Acknowledgements

The study was financially supported by the Swiss National Science Foundation under the contract numbers 2.77771.10 and 200021_129866. The spatially explicit methane inventory was developed during two projects funded by the Competence Center of 3.5. CONCLUSION 51

Environment and Sustainability (CCES) at ETH Zurich. The authors acknowledge Peter Pluess and Thomas Baur for their technical support during the preparation and execution of the measurement campaign. Furthermore, we thank the Grassland Sciences Group and the staff members of the ETH research station for their support at the field site. Prof. Dr. Mathias Rotach is thanked for his valuable contribution to the discussion of the results from a meteorological point of view.

3.6 Tables and figures

Table 3.1: Time, duration, location as well as average temperatures and methane concentration ranges for each transect during July 2012.

Transect Number	Start Time [UTC]	Duration [Hours]	Transect Pattern	Average Temperature	Methane Concentration
	L J			[°C]	Range [ppmv]
$ \begin{array}{c} \text{t1} \\ \text{(day)} \end{array} $	24.07.2012 07:23:44	3:16:48	valley transect	19.7	1.98-3.35
$ \begin{array}{c} \text{t2} \\ \text{(day)} \end{array} $	24.07.2012 13:10:30	3:48:18	valley transect	25.9	1.93-2.82
t3 (transition)	24.07.2012 19:08:07	5:10:51	valley transect	17.9	1.92-4.06
$ \begin{array}{c} $	$\begin{array}{c} 25.07.2012 \\ 00:56:17 \end{array}$	4:08:43	valley transect	14.6	1.92 – 5.80
$ \begin{array}{c} t5 \\ (day) \end{array} $	25.07.2012 05:32:04	3:34:22	valley transect	19.4	1.98-4.06
t6 (day)	$\begin{array}{c} 25.07.2012 \\ 10.02.27 \end{array}$	4:00:23	valley transect	27.4	1.92-3.89
t7 (transition)	25.07.2012 17:21:10	2:17:13	valley transect	22.5	1.91-3.89
$ \begin{array}{c} t8 \\ (\text{night}) \end{array} $	$\begin{array}{c} 25.07.2012 \\ 21:55:51 \end{array}$	2:53:28	valley transect	16.2	1.91 – 5.18
t9 (day)	26.07.2012 05:24:56	3:00:52	mountain transect	18.9	1.88-4.65
t10 (day)	26.07.2012 11:14:20	2:10:24	mountain transect	27.5	1.88-5.99
t11 (transition)	26.07.2012 16:50:11	3:14:28	mountain transect	23.8	1.89-7.66
t12 (night)	26.07.2012 22:54:05	2:35:23	mountain transect	17.5	1.89-4.65

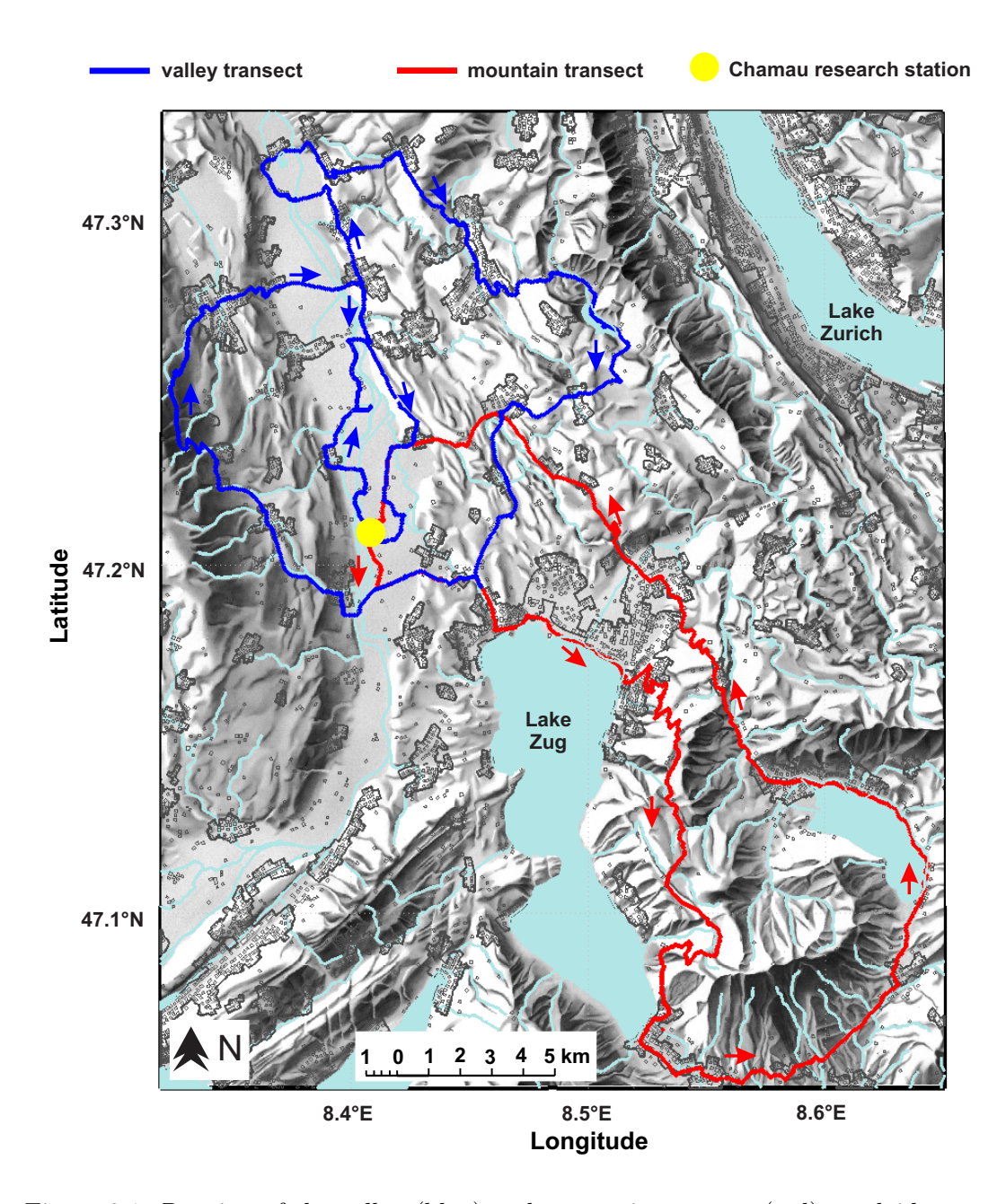


Figure 3.1: Routing of the valley (blue) and mountain transect (red) overlaid on a relief map of the measurement area. The relief map was provided by the Federal Office of Topography swisstopo (Art. 30 GeoIV): 5704 000 000.

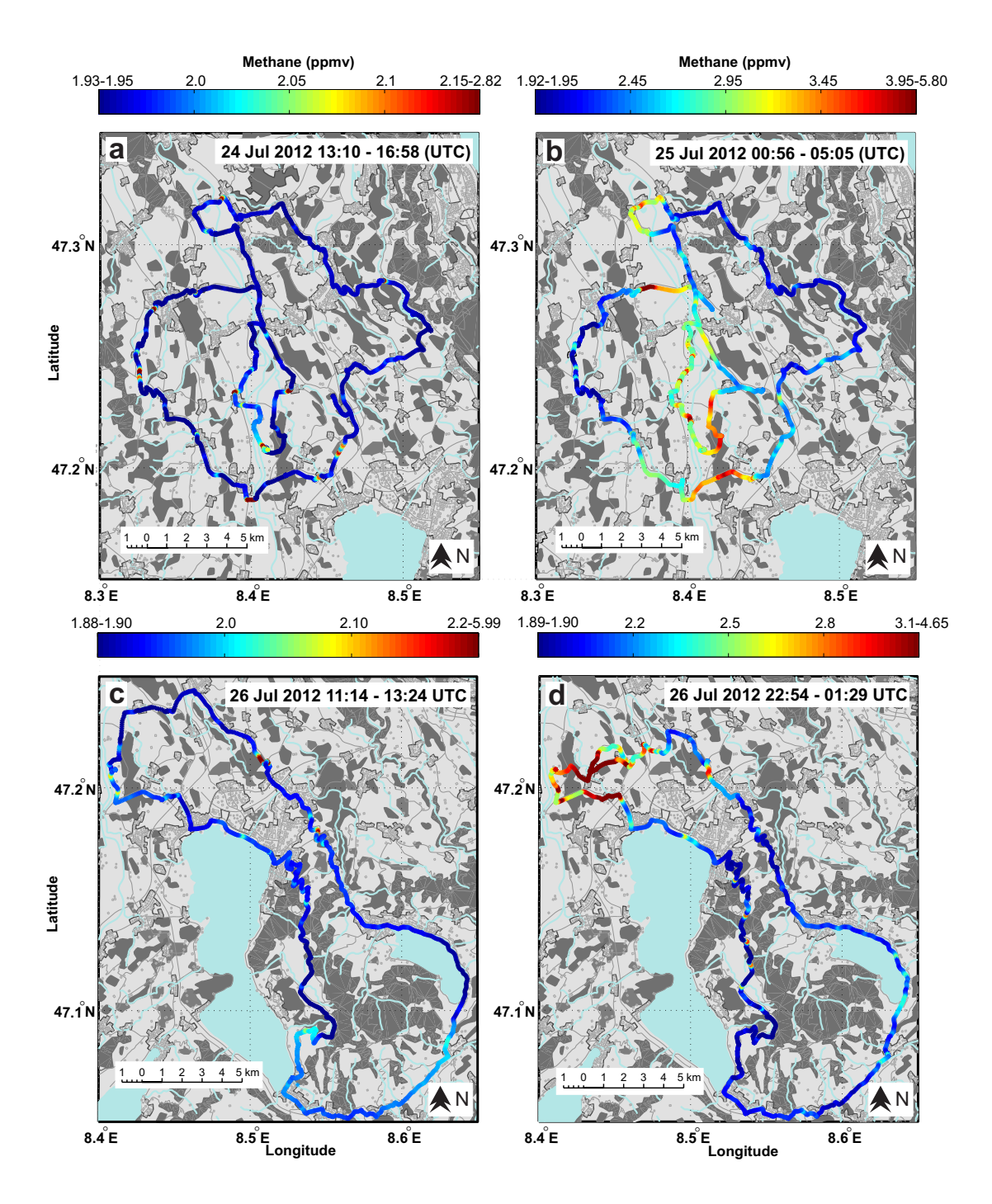


Figure 3.2: Methane concentrations (color axis and colored symbols) along the valley transect during the afternoon (a, t2) and night (b, t4) and along the mountain transect during midday (c, t10) and night (d, t12). Land cover maps were provided by the Federal Office of Topography swisstopo (Art. 30 GeoIV): 5704 000 000.

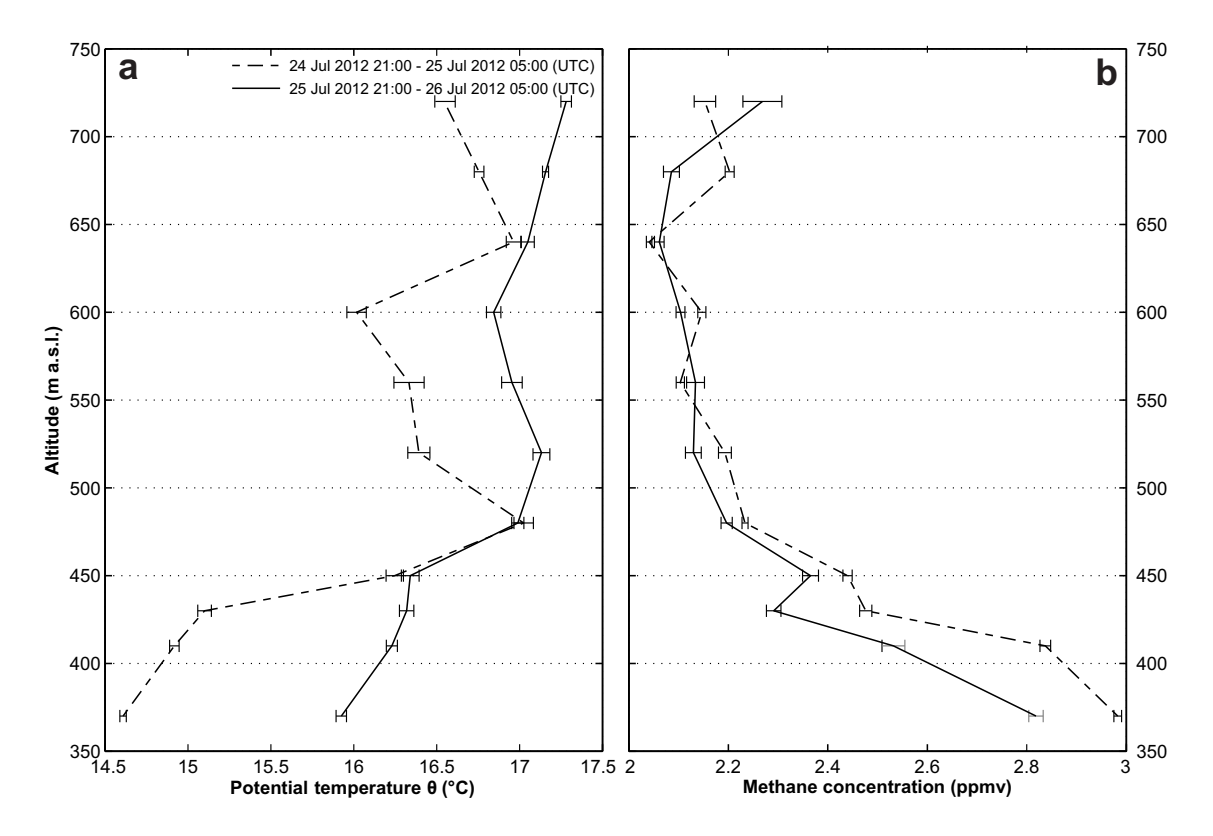


Figure 3.3: Vertical nighttime profiles of bin-averaged temperature (a) and methane concentration (b) from the valley transect during two consecutive nights, i.e., 24–25 July 2012 and 25–26 July 2012. The standard errors for methane and temperature measurements are given.

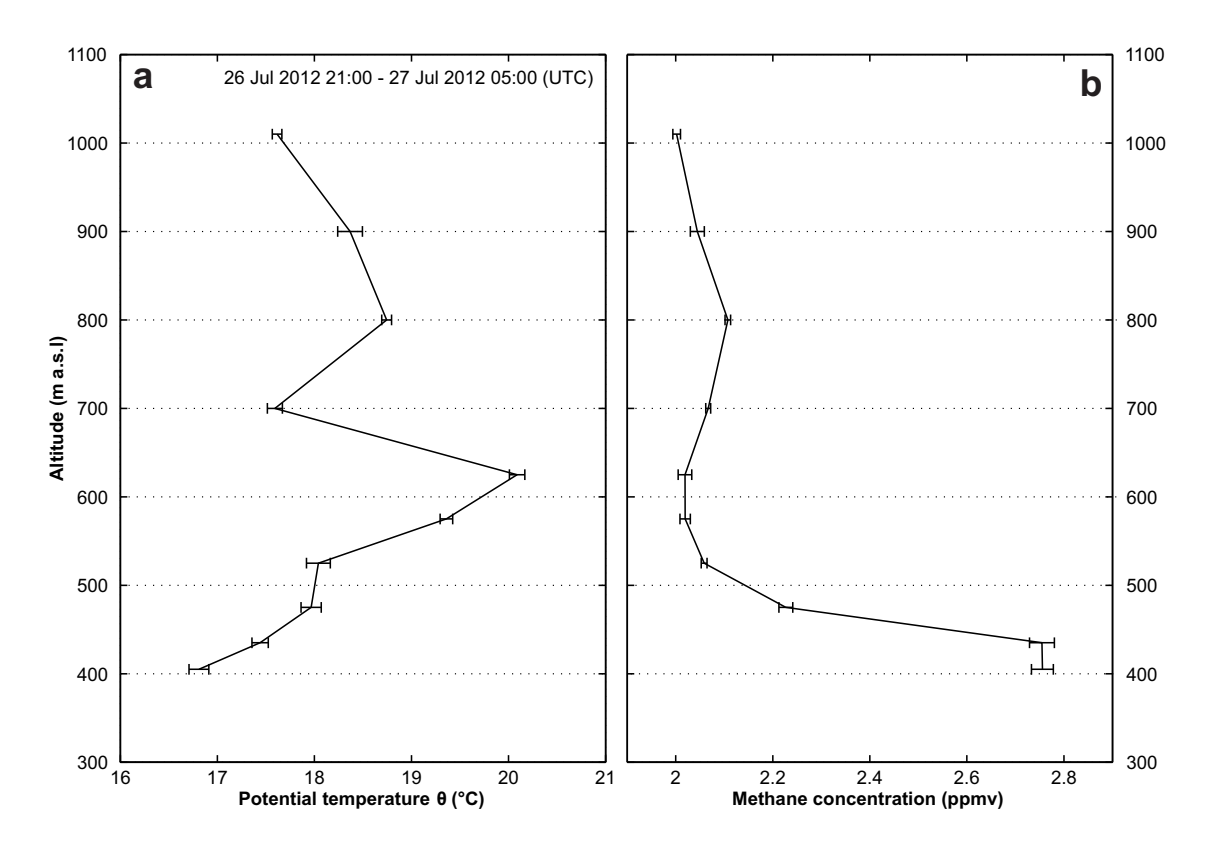


Figure 3.4: Vertical nighttime profiles of bin-averaged temperature (a) and methane concentration (b) from the mountain transect for the night from 26 to 27 July 2012. The standard errors for methane and temperature measurements are given.

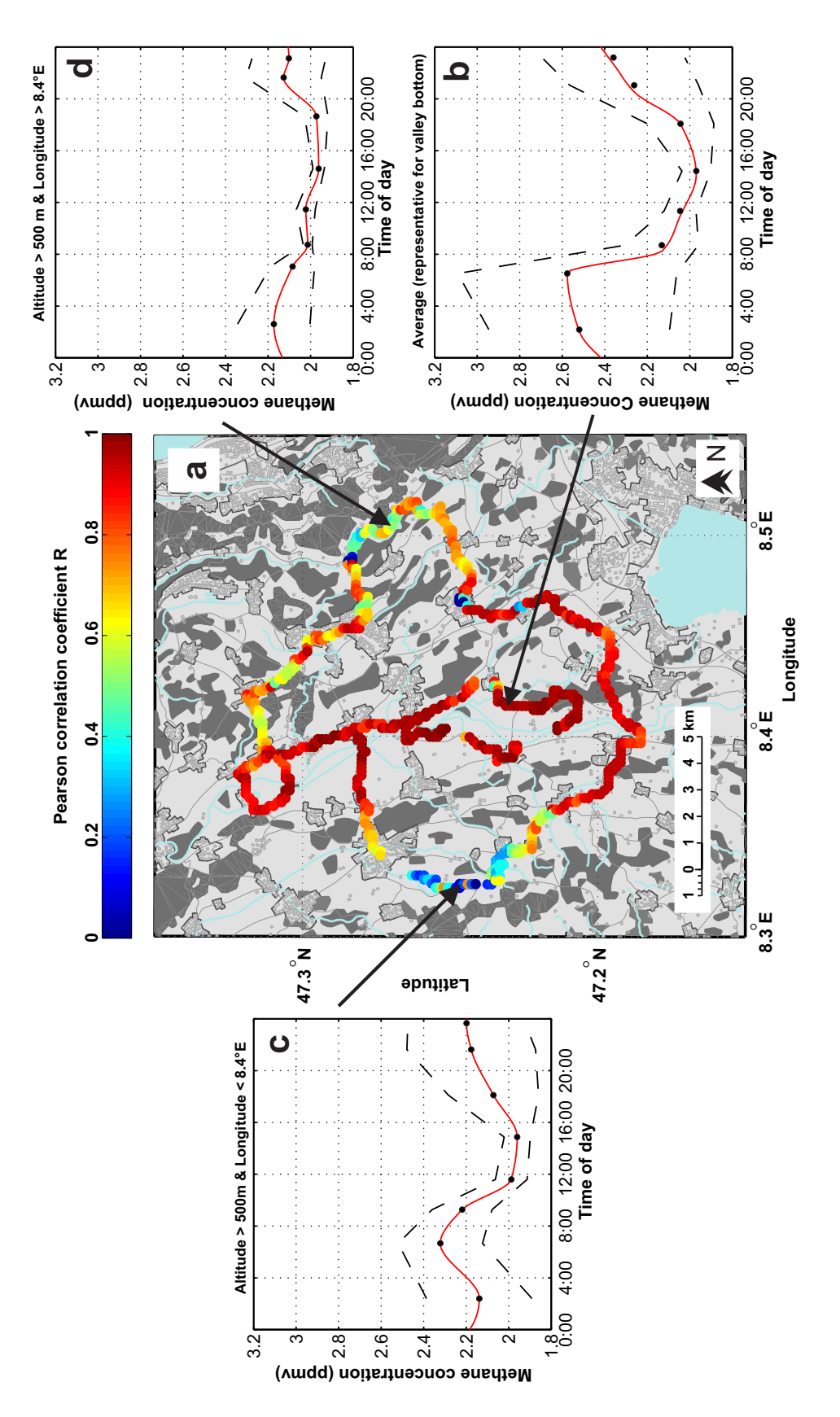


Figure 3.5: (a) Pearson correlation coefficients R for the relationship between the diurnal methane cycle at locations along the valley transect (colored circles) and the diurnal cycle for the region, (b) regional average diurnal cycle of methane concentrations including the average diurnal cycles of methane at the (c) western and (d) eastern hillsides, respectively. Solid black circles symbols denote measurement points, grey dashed lines denote the ranges given by the standard deviation and solid red lines denote the diurnal cycle pattern received from a cubic spline interpolation.

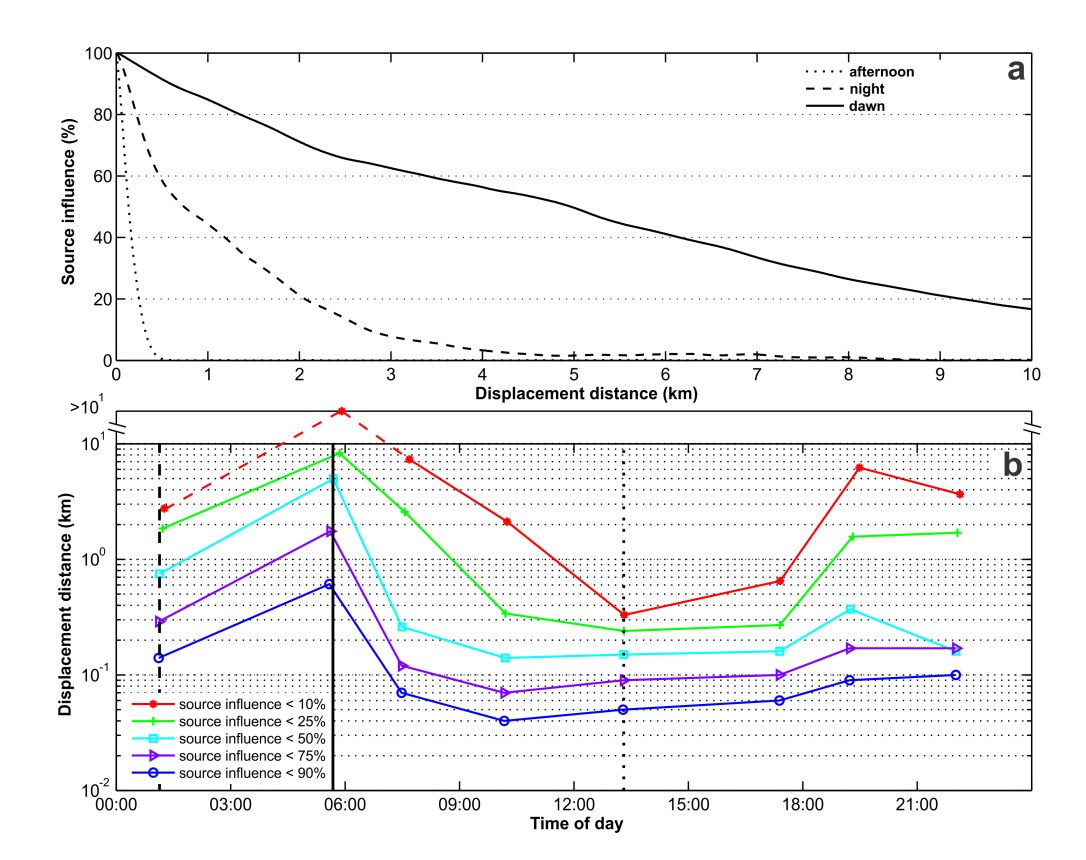


Figure 3.6: (a) The influence of a methane point source on methane concentrations as a function of distance between source and the measurement location shown exemplarily for valley transects in the afternoon, at night and before dawn. (b) Diurnal cycle of the displacement distances at which influence from a point source is below 90%, 75%, 50%, 25%, and 10%.

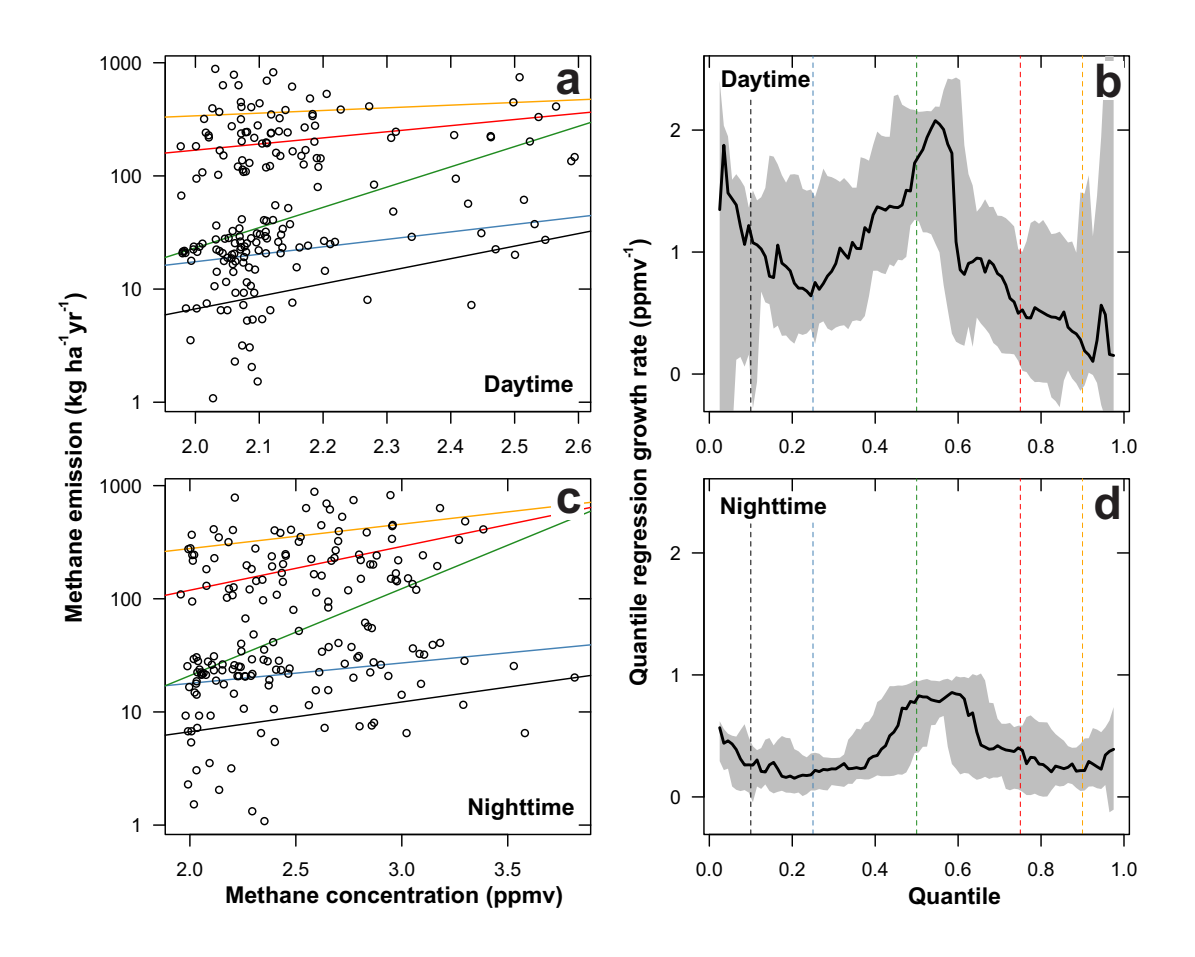


Figure 3.7: Scatter plot of methane fluxes (given by a high resolution emission inventory) against the corresponding atmospheric average methane concentrations including the regression lines for the 0.10 (orange), 0.25 (red), 0.50 (green), 0.75 (blue) and 0.90 (black) quantiles of the inventory fluxes for daytime (a) and nighttime (b). The growth rate and its related error ranges received by an exponential fit $(y = b * 10^s * x)$ between concentrations and the different flux quantiles of the inventory for daytime (c) and nighttime (d).

References

- Bamberger I, Hörtnagl L, Ruuskanen T, Schnitzhofer R, Müller M, Graus M, Karl T, Wohlfahrt G, Hansel A (2011) Deposition fluxes of terpenes over grassland. Journal of Geophysical Research: Atmospheres 116(D14).
- Beck V, Chen H, Gerbig C, Bergamaschi P, Bruhwiler L, Houweling S, Röckmann T, Kolle O, Steinbach J, Koch T (2012) Methane airborne measurements and comparison to global models during BARCA. *Journal of Geophysical Research:* Atmospheres 117(D15).
- Bergamaschi P, Frankenberg C, Meirink J, Krol M, Villani M, Houweling S, Dentener F, Dlugokencky E, Miller J, Gatti L (2009) Inverse modeling of global and regional CH4 emissions using SCIAMACHY satellite retrievals. *Journal of Geophysical Research* 114(D22):D22301.
- Bergamaschi P, Krol M, Meirink J, Dentener F, Segers A, Van Aardenne J, Monni S, Vermeulen A, Schmidt M, Ramonet M (2010) Inverse modeling of European CH₄ emissions 2001–2006. *Journal of Geophysical Research: Atmospheres* 115(D22).
- Bousquet P, Ciais P, Miller J, Dlugokencky E, Hauglustaine D, Prigent C, Van der Werf G, Peylin P, Brunke E, Carouge C, Langenfelds R, Lathiere J, Papa F, Ramonet M, Schmidt M, Steele L, Tyler S, White J (2006) Contribution of anthropogenic and natural sources to atmospheric methane variability. *Nature* 443(7110):439–443.
- Dlugokencky E, Nisbet E, Fisher R, Lowry D (2011) Global atmospheric methane: budget, changes and dangers. *Philosophical Transactions of the Royal Society A:* Mathematical, Physical and Engineering Sciences 369(1943):2058–2072.
- FSO (2012) Land use statistics (Arealstatisik) 2004/09, NOLU04/20120821. Swiss Federal Statistical Office (FSO), Neuchatel, Switzerland.
- Gerbig C, Dolman A, Heimann M (2009) On observational and modelling strategies targeted at regional carbon exchange over continents. *Biogeosciences* 6(10):1949–1959.

Gerbig C, Körner S, Lin J (2008) Vertical mixing in atmospheric tracer transport models: error characterization and propagation. *Atmospheric Chemistry and Physics* 8(3):591–602.

- Gohm A, Harnisch F, Vergeiner J, Obleitner F, Schnitzhofer R, Hansel A, Fix A, Neininger B, Emeis S, Schäfer K (2009) Air pollution transport in an Alpine valley: Results from airborne and ground-based observations. *Boundary-Layer Meteorology* 131(3):441–463.
- Hiller R, Bretscher D, DelSontro T, Diem T, Eugster W, Henneberger R, Hobi S, Hodson E, Imer D, Kreuzer M, Künzle T, Merbold L, Niklaus P, Rihm B, Schellenberger A, Schroth M, Schubert C, Siegrist H, Stieger J, Buchmann N, Brunner D (2013) Anthropogenic and natural methane fluxes in Switzerland synthesized within a spatially-explicit inventory. Biogeosciences Discussions 10(9):15181–15224.
- IPCC W (2007). The physical science basis. Contribution of working group I to the fourth assessment report of the Intergovernmental Panel on Climate Change. In Solomon S, Qin D, Manning M, Chen Z, Marquis M, Averyt K, Tignor M, Miller H, editors, *Climate Change 2007*. Cambridge University Press Cambridge.
- Jagovkina S, Karol I, Zubov V, Lagun V, Reshetnikov A, Rozanov E (2000) Reconstruction of the methane fluxes from the west Siberia gas fields by the 3D regional chemical transport model. *Atmospheric Environment* 34(29):5319–5328.
- Kaser L, Karl T, Schnitzhofer R, Graus M, Herdlinger-Blatt I, DiGangi J, Sive B, Turnipseed A, Hornbrook R, Zheng W (2013) Comparison of different real time VOC measurement techniques in a ponderosa pine forest. *Atmospheric Chemistry and Physics* 13(5):2893–2906.
- Koenker R (2005) Quantile regression. Cambridge University Press, New York, USA.
- Koenker R, Basset G (1978) Regression quantiles. Econometrica 46:33–50.
- Lin J, Gerbig C (2005) Accounting for the effect of transport errors on tracer inversions. Geophysical Research Letters 32(1):L01802.
- METEOTEST (2011) Methan-Emissionskataster Schweiz. Aufbereitung von Datengrundlagen, Berechnung eines räumlich hoch aufgelösten Katasters. Internal Report, Genossenschaft METEOTEST, Bern, Switzerland, pp. 18.
- Nisbet E, Weiss R (2010) Top-down versus bottom-up. *Science* 328(5983):1241–1243.
- Phillips N, Ackley R, Crosson E, Down A, Hutyra L, Brondfield M, Karr J, Zhao K, Jackson R (2013) Mapping urban pipeline leaks: Methane leaks across Boston. *Environmental Pollution* 173:1–4.

Schnitzhofer R, Norman M, Wisthaler A, Vergeiner J, Harnisch F, Gohm A, Obleitner F, Fix A, Neininger B, Hansel A (2009) A multimethodological approach to study the spatial distribution of air pollution in an Alpine valley during wintertime. *Atmospheric Chemistry and Physics* 9(10):3385–3396.

- Schuck T, Ishijima K, Patra P, Baker A, Machida T, Matsueda H, Sawa Y, Umezawa T, Brenninkmeijer C, Lelieveld J (2012) Distribution of methane in the tropical upper troposphere measured by CARIBIC and CONTRAIL aircraft. *Journal of Geophysical Research: Atmospheres* 117(D19).
- Shipham M, Bartlett K, Crill P, Harriss R, Blaha D (1998) Atmospheric methane measurements in central New England: An analysis of the long-term trend and the seasonal and diurnal cycles. *Journal of Geophysical Research* 103(D9):10621–10.
- Stull R (1988) Stable Boundary Layer. In: An Introduction to Boundary Layer Meteorology, Vol. 13, (eds) Roland B. Stull, *Kluwer Academic Publishers*, Chapter 12, pp. 499–543.
- Tarasova O, Houweling S, Elansky N, Brenninkmeijer C (2009) Application of stable isotope analysis for improved understanding of the methane budget: comparison of TROICA measurements with TM3 model simulations. *Journal of Atmospheric Chemistry* 63(1):49–71.
- Townsend-Small A, Tyler S, Pataki D, Xu X, Christensen L (2012) Isotopic measurements of atmospheric methane in Los Angeles, California, USA: Influence of "fugitive" fossil fuel emissions. *Journal of Geophysical Research: Atmospheres* 117(D07308):1451–1476.
- Villani M, Bergamaschi P, Krol M, Meirink J, Dentener F (2010) Inverse modeling of European CH₄ emissions: Sensitivity to the observational network. *Atmospheric Chemistry and Physics* 10(3):1249–1267.
- Wang J, Murphy J, Geddes J, Winsborough C, Basiliko N, Thomas S (2013) Methane fluxes measured by eddy covariance and static chamber techniques at a temperate forest in central Ontario, Canada. *Biogeosciences* 10(6):4371–4382.
- Whiteman C (2000) Diurnal mountain winds. In: Mountain meteorology: fundamentals and applications, (eds) C. David Whiteman, Oxford University Press, New York, Chapter 11, pp. 171–202.
- Xiong X, Barnet C, Zhuang Q, Machida T, Sweeney C, Patra P (2010) Mid-upper tropospheric methane in the high Northern Hemisphere: Spaceborne observations by AIRS, aircraft measurements, and model simulations. *Journal of Geophysical Research* 115(D19):D19309.

Source partitioning of atmospheric methane using carbon isotopes

Jacqueline Stieger¹, Ines Bamberger¹, Rolf T.W. Siegwolf ², Nina Buchmann¹, Werner Eugster¹

 $^1{\rm Institute}$ of Agricultural Sciences, ETH Zurich, Zurich, Switzerland 2 Laboratory for Atmospheric Chemistry, Paul Scherrer Institute, Villigen, Switzerland

This manuscript is intended for submission to Journal for Geophysical Research: Atmospheres

Abstract

Today's understanding of the spatio-temporal variability of atmospheric methane is very limited, due to the heterogeneous pattern of methane sources and their emissions. Particularly budget estimates of regions with diverse methane sources are associated with considerable uncertainty levels as the individual contributions of the different sources are rarely separated. In order to quantify the contributions of different methane sources to the atmospheric CH₄ source mix and to elucidate the variability of the emissions, we conducted spatio-temporally highly resolved measurements of methane concentrations and $\delta^{13}\mathrm{C}$ values in the agricultural dominated Reuss Valley in Switzerland during August 2011 and July 2012. The results showed, that the diel courses of CH₄ concentrations and δ^{13} C values were strongly affected by the valley wind patterns and the position within the local topography. We found that biogenic sources were the main contributor to the nighttime excess methane. The enrichment in daytime ¹³C relative to background, however, also revealed a mean contribution of 62% from biogenic methane sources, but was associated with an increased influece from non-biogenic sources (22%), while sink processes (16%) were of minor importance. Despite the dominant role of agricultural methane emissions in the Reuss Valley, the local nighttime methane build-up from biogenic sources were compensated by convective dilution during the day and non-biogenic methane emissions from upwind lying agglomerations revealed a comparable source strength. The results demonstrated that direct measurements of CH₄ concentrations and their respective δ^{13} C value are a valuable tool to assess the contributions of different sources and to constrain the interpretation of regional methane budgets.

65

4.1 Introduction

Despite being the second-most important greenhouse gas in the atmosphere after carbon dioxide, methane sinks and sources and their temporal variability are still poorly understood on local to regional spatial scales (Townsend-Small et al., 2012; Miller, 2004). The estimation of regional CH₄ budgets is often impeded by the heterogeneous spatial pattern of different sources and by the unresolved temporal variability of their underlying emissions (Tarasova et al., 2009; Bousquet et al., 2006; Jagovkina et al., 2000). Direct concentration measurements at different spatiotemporal scales are therefore essential for a reliable estimation of regional source distributions and intensities, putting significant constraints on CH₄ budget calculations (Miller, 2004; Jagovkina et al., 2000). Particularly top-down approaches are generally underconstrained, thus methane budgets remain substantially uncertain, since the small-scale variability is often smoothed out (Tarasova et al., 2009). But also for bottom-up approaches, measurements covering the spatio-temporal variability of methane emissions are scarce. In addition, measurements of atmospheric methane over hetereogenous areas represent a mixture of different sources, which is rarely partioned into the individual contributions resulting in uncertain emission estimates by source sector (Dlugokencky et al., 2011). Hence, a separation of individual sources is needed, due to their possible cumulative impact on the total methane budget.

However, based on concentration measurements alone, it remains difficult to separate the different components of a methane budget. In regions with diverse methane sources or sinks, combined measurements of CH_4 concentrations and $\delta^{13}C$ values can improve constraining major CH_4 sources and sinks, due to their enrichment or depletion in ^{13}C relative to the ambient backround value (Dlugokencky et al., 2011; Tyler et al., 2007; Conrad, 2005; Levin et al., 1999). The processes of methane production and methane oxidation discriminate against the heavier carbon isotope and the resulting isotopic ratios are used to differentiate microbial from thermogenic sources and sinks (Townsend-Small et al., 2012; Dalal et al., 2008; Whiticar, 1999). Microbial produced CH_4 , e.g., from enteric fermentation and manure, is charaterized by depleted $\delta^{13}C$ values (Table 1). In contrast, thermogenic produced CH_4 , e.g., at high temperature from fossil fuel combustion, and CH_4 resulting from methanogenic consumption or oxidation with atmospheric radicals are enriched in the heavier iso-

tope (Miller, 2004; Cicerone, Oremland, 1988). On the global scale, the use of δ^{13} C in methane is well established for long-term and present-day emission budgets (Dlugokencky et al., 2011; Kai et al., 2011; Neef et al., 2010; Mischler et al., 2009). Evaluations of small-scale emission budgets using δ^{13} C of atmospheric methane, however, are often limited to source strength estimations of specific land-use types as landfills, rice paddies, peatlands or pastures, where source signatures are well known and problems caused by multi-source systems can be avoided (Pendall et al., 2010; Chanton, Liptay, 2000; Chanton et al., 1999; Stevens, Engelkemeir, 1988). So far, only a few studies have identified multiple sources of atmospheric methane via δ^{13} C. Rural areas in New Zealand revealed a significant nocturnal depletion in δ^{13} C resulting from methane emissions from grazing sheeps (Harvey et al., 2002). Urban areas, in contrast, were mainly affected by emissions from landfills, gas leakages and waste water treatments, whose source position and strength could be assessed through δ^{13} C and wind direction analysis (Townsend-Small et al., 2012; Lowry et al., 2001; Levin et al., 1999). However, the heterogeneous character of source distributions, the low temporal resolution of methane concentration measurements and the complex atmospheric transport processes affected an unequivocal interpretation of the regional methane budget.

Thus, the objectives of our study were: (1) to elucidate the temporal evolution of δ^{13} C within the atmospheric boundary layer over an agriculture dominated valley in Switzerland, (2) to identify major sources and sinks using a two-component mixing model, (3) to quantify their contributions to the daytime CH₄ source mix, and (3) to discuss the resulting implications on the regional methane budget.

4.2 Materials and Methods

4.2.1 Study Area

The Reuss Valley in central Switzerland is aligned in a south-east to north-west direction and is surrounded by relatively low mountain ranges (up to 760 m a.s.l.). About 57% of its area is used for agriculture, around 23% and 18% are used for forests and urban areas (FSO, 2012). Lakes and unproductive areas are of minor importance (<3%). Under fair weather conditions, the wind patterns in the

Reuss Valley are dominated by the valley wind system: during the day, when a convective boundary layer (CBL) establishes, the wind trajectories are directed from the lowlands towards the alpine region. With the development of a stable nocturnal boundary layer (NBL) at night, these winds are replaced by opposite cold air drainage flows. We used two measurement approaches, a stationary set-up (during 16–18 August 2011 and 24–25 July 2012), using a tethered balloon system and a mobile set-up (during 24–25 July 2012 only), using a car.

4.2.2 Stationary and mobile set-ups

The stationary set-up site was located in the valley bottom at the ETH research station Chamau (47° 12′ 37″ N, 8° 24′ 38″ E at 393 m a.s.l., Figure 1). The station is mainly used for forage production and its livestock density changes over the year according to the seasonal three-stage farming system. During the winter the cattle stay at the base farm, i.e., at the Chamau research station, whereas during the summer months most of them are moved to higher located grazing pastures. We measured CH₄ concentrations within the atmospheric boundary layer at 0.2, 0.5, 2, 8 and 10 m a.g.l. using a guy-wired extension mast and at 25, 50, 100 and 160 m a.g.l. using a tethered balloon system. Inlet tubes installed at the different heights, and carried up with the balloon, led the air into a fast greenhouse gas analyzer (FGGA, Los Gatos Research Inc., Mountain View, CA, USA), placed at the ground and measuring at 1 Hz at a flow rate of ~ 1 L min⁻¹. These measurements were complemented with measurements of air temperature, atmospheric pressure, relative humidity, wind speed and wind direction using the meteorological probe TS-5A-SEN (Atmospheric Instrument Research, Inc., Boulder, USA) attached to the tether line. The extension mast measurements were complemented with wind direction as well as wind speed measurements at 10 m a.g.l. at the top of the mast using a wind monitor (05103LM, Campbell Scientific Inc., Loughborough, UK) and with measurements of air temperature and relative humidity (HydroClip S3, Rotronic AG, Bassersdorf, Switzerland) installed at 2 m a.g.l. in 2011 and at 0.2 m a.g.l. in 2012. Furthermore, air from the different heights was collected in 300 mL glass flasks for isotopic analysis (see below). At the stationary set-up site, we used 3 portable automatic air sampling units (ASA) with 33 glass flasks per unit (Zeeman et al., 2008). Each glass flask was filled for 5 minutes at a flow rate of $\sim 0.7 \text{ L min}^{-1}$.

The mobile set-up consisted of measurements at five predefined sampling sites (Figure 1, A-D) in and around the Reuss Valley, covering an altitudinal range from 380 m to 697 m a.s.l. A fast methane analyzer (FMA DLT-100, Los Gatos Research, CA, USA) and a Airmar weather station (AIRMAR Technology Corporation, Mirford, NH, USA), installed in a car, provided CH₄ concentrations (at 1 Hz and a mean flow rate of ~ 0.5 L min⁻¹), air temperature, relative humidity, air pressure, wind direction and wind speed measurements at each location. Each time a sampling site was visited (5x each in 2012), air samples were collected in an ASA unit (collection time 5 minutes, at ~ 1 L min⁻¹).

4.2.3 Isotope ratio analysis

The ASAs containing the glass flasks with the air samples were directly connected to a gas purifying methane conversion system (PRECON, Thermo Finnigan, Bremen, Germany). With a helium stream of 15 mL min⁻¹, the air samples were transferred from each individual flask through a scrubber (Ascarite, Hekatech, Germany) and water traps (Magnesium perchlorate, Merck, Germany) mounted in the PRECON into a first cold trap, which was permanently immersed in liquid nitrogen (LN2) to remove the residual CO₂ and H₂O from the helium stream. To convert methane to CO₂, the gas passed a micro combustion reactor, containing NiO wires, kept at 1010°C. The resulting CO₂ was captured in a second cold trap, submersed for 720 seconds in LN2. A third cold trap, submersed in LN2 for 360 seconds, was used to remove remaining gas species (N₂O, O₂, CO). The trapped CO₂ was then released to a gas chromatography column where the remaining N₂O and CO₂ were separated. Via an open split interface (GP-Interface, Thermo Finnigan, Bremen, Germany), the gas was transferred to the isotope ratio mass spectrometer (DeltaPlus XL, Thermo Finnigan, Bremen, Germany) to determine the ¹³C/¹²C isotope ratio of CH₄. The measurement precision was 0.5–0.7‰, based on repeated measurements of laboratory-working standards.

4.2.4 Nighttime source identification

We used a two-component mixing model to identify the source mix leading to a significant increase of atmospheric methane concentration, i.e., excess methane, over

a specific background (Tarasova et al., 2009; Lowry et al., 2001; Levin et al., 1999; Stevens, Engelkemeir, 1988):

$$\delta^{13}C_{source} = \frac{\delta^{13}C_{obs} \cdot c_{obs} - \delta^{13}C_{ref} \cdot c_{ref}}{c_{obs} - c_{ref}}$$

$$\tag{4.1}$$

where c_{ref} and $\delta^{13}\mathrm{C}_{ref}$ are the methane concentration and the $\delta^{13}\mathrm{C}$ value of the background, calculated from daytime observations at Chamau (see below) and further refered to as reference. The observed methane concentration and its $\delta^{13}\mathrm{C}$ value are denoted as c_{obs} and $\delta^{13}\mathrm{C}_{obs}$. Depending on the isotopic signature of the additional CH₄, which mixes into the background air, the $\delta^{13}\mathrm{C}_{obs}$ deviates from the $\delta^{13}\mathrm{C}_{ref}$ value. Using equation (1), the isotopic signature of the source can be calculated for each flask sample. The derived source signal describes an average isotopic signature of several sources and $\delta^{13}\mathrm{C}_{source}$ therefore characterizes a source mix. This two-component mixing model is based on two assumptions (Tarasova et al., 2009; Pataki et al., 2003): First, it assumes that only two gas components are involved in the mixing process, hence the source and the reference. Second, the isotopic signatures of the components are not changing during the time of sampling. However, the assumptions are rarely perfectly fulfilled, therefore, the model is mostly used for nighttime measurements when mixing processes can be neglected and sufficiently large concentration ranges are present (Pataki et al., 2003).

For both measurement years (2011 and 2012), we specified the reference values for $\delta^{13}C_{ref}$ and c_{ref} . They were determined as the mean of all profile measurements during well-mixed daytime conditions, when the methane concentrations at each height reached simultaneously their minima. The reference in 2011 for CH₄ and $\delta^{13}C$ was estimated as 1.929 ± 0.006 ppm and $-46.0 \pm 0.7\%$. For 2012, we calculated a mean CH₄ and $\delta^{13}C$ reference value of 1.965 ± 0.009 ppm and $-45.6 \pm 0.5\%$. Equation (1) was applied to nighttime isotopic signatures measured between 9 pm and 6 am local time and the resulting $\delta^{13}C_{source}$ values were compared to specific $\delta^{13}C$ signatures of methane sources and sinks in the Reuss Valley (Table 1).

4.2.5 Daytime source identification

For the identification of the source mix during daytime, we used an extended mass balance equation by solving the percentages of three *a priori* defined source categories (f_a, f_b, f_c) contributing to the observed isotopic signature δ_{obs} (Phillips, Gregg, 2003):

$$\delta_{obs} = f_a \delta_a + f_b \delta_b + f_c \delta_c \tag{4.2}$$

$$1 = f_a + f_b + f_c (4.3)$$

where δ_a , δ_b and δ_c denote the isotopic signature of the three source categories. For every observed isotopic signature, we created each possible combination of percentages of the three source components summing up to 100% by iteration steps (source increments) of 1% and then computed the predicted signatures of the mixture. The predicted mixture signatures falling into a mass balance tolerance of $\pm 1\%$ from the observed isotopic signature, i.e.:

$$f_a \delta_a + f_b \delta_b + f_c \delta_c = \delta_m \pm 1\% \tag{4.4}$$

provided the contribution estimates of the three source categories (in percentages) and were selected for further analysis.

In this study, we used the extended mass balance equation for measurements between 9 am and 9 pm local time. Three source categories were specified for the source mix identification during daytime, derived from typical source type signatures (Table 1): (1) An isotopic value of -61.26% was calculated for biogenic sources as the weighted average of the proportions from enteric fermentation and manure management emissions to total agricultural methane emissions in Switzerland, here 80% and 20%, respectively (FOEN, 2013); (2) An isotopic value of -25.55% was determined for non-biogenic sources by the unweighted average of δ^{13} C values for vehicle emissions, biomass burning and natural gas, and (3) an isotopic value of -5.4% was derived for the impact of sink processes from the sink strength estimation in Miller (2004). In addition, a sensitivity analysis was performed to test the effect of differing

4.3. RESULTS 71

source increments and mass balance tolerances on the contribution estimates of the three source categories. We used three levels of mass balance tolerance (0.5, 1 and 2‰) with a source increment fixed at 1% and three levels of source increment (0.5, 1 and 2%) with a mass balance tolerance fixed at 1‰.

4.3 Results

4.3.1 Mean diel cycles of CH_4 and $\delta^{13}C$

In both years, we observed clear diel cycles at Chamau for CH₄ concentrations and δ^{13} C isotopic signatures (Figure 2). The nighttime build-up in methane concentration at 0-10 m a.g.l. to 2.92 ppm in 2011 and to 3.83 ppm in 2012 was associated with a depletion in ¹³C relative to the reference values by -8.5 and -5.9\%, respectively. During the day, the concentrations and δ^{13} C values were closed to the respective reference values. Less pronounced diel patterns were found higher above ground, i.e. between 25–50 m and between 100–200 m a.g.l. In 2011, the nighttime methane build-up was at 25–50 m a.g.l. reduced to 2.84 ppm and above 100 m a.g.l. to 2.34 ppm and was associated with a mean depletion in nighttime ¹³C by $-4.8 \pm 0.1\%$ (both height ranges). While in 2011 the nighttime methane build-up was reduced with increasing height, no considerable differences in the diel course of CH₄ was found for the different heights in 2012, probably due to existing mixing processes. In general, highest methane concentration peaks within the diel course were observed in both years around 5 am at all measured height levels. Unlike CH₄ concentrations, the δ^{13} C values were highly variable at all measurement heights and no single peak could be assigned to a definite time within the diel course. Nevertheless, heights up to 50 m a.g.l. showed lowest δ^{13} C values between 0 and 5 am, whereas above 100 m, δ^{13} C decreased slightly after sunrise. With the replacement of the NBL by the CBL, the methane concentration decreased rapidly at all measured heights, reaching between 3 and 6 pm slightly enriched δ^{13} C values relative to the reference value. However, isotopic signatures showed a large variance during the day. Particularly in 2011, daytime δ^{13} C values were highly variable including also very high values above -40\% compared to daytime values in 2012, which were constantly close to the reference value.

The diel courses from the mobile measurement set-up sites were comparable to the observations from the stationary set-up, with a clear diel cycle of similar magnitude at the measurement locations in the valley bottom (Figure 3, A and C). At the location C in the south of the valley, the methane concentration reached 3.31 ppm before sunrise and was depleted by -8% in 13 C. At the northern measurement location A, we probably missed the peak before sunrise, therefore highest methane concentration were found after 7 am with 3.0 ppm and an associated decrease by -6.1% in δ^{13} C. No diel trend was found during the observations at the eastern hilltop (B) located next to a lake. At the western hilltop (D), where the measurements were located at a managed cropland closed to a farmstead, only small diel fluctuations were observed. There, a small methane peak occurred delayed at 10 am and the subsequent decrease in CH₄ mixing ratios was accompanied by an enrichment in the isotopic signature. However, all locations revealed δ^{13} C values above the reference during the day, while CH₄ reached its minimum.

Despite the less pronounced diel patterns of the observed isotopic signatures with increasing height, no correlation was found between δ^{13} C and height a.g.l. The median showed no significant decrease in δ^{13} C (slope: -0.005, p= 0.06) with increasing height above ground. In contrast, the interquartile range converged rapidly between 0 and 25 m a.g.l. from 4.6 to 2.3% and reached its minimum difference of 1.8% at 150 m a.g.l. No significant correlation was found between δ^{13} C and wind direction or wind speed. Not all wind sectors, however, have been covered with our measurements.

4.3.2 Source identification

 δ^{13} C values from nighttime measurements imply that biogenic methane sources are of major importance in the Reuss Valley (Figure 4): On a Keeling plot, the majority of the data fell into the biogenic source sector and originated from a combination of enteric fermentation, manure and waste management. Only 4 out of total 65 measurements were clearly influenced by non-biogenic sources, sink processes or a combination thereof. The calculated $\delta^{13}C_{source}$ values of nighttime isotopic signatures revealed a similar picture (Table 2). In 2011, biogenic source mixtures caused excess methane with a mean isotopic signature of -56.3% (removing all observations from non-biogenic sources, i.e. $\delta^{13}C_{obs} \geq \delta^{13}C_{ref}$). Not significantly different was the

4.3. RESULTS 73

mean $\delta^{13}C_{source}$ of -54.8% for all observations of biogenic origin in 2012. However, in 2012 about 40% of all nighttime excess CH₄ was not caused by biogenic source mixtures alone (compared to 5.8% in 2011). Despite the increased methane mixing ratios in 2012 compared to 2011 (Figure 4), the observed $\delta^{13}C$ values were closed to the reference value and are pointing to a combination of biogenic and non-biogenic methane sources. Highly enriched values for $\delta^{13}C_{source}$ (>-25%) were only observed during measurement periods before sunrise.

For the daytime $\delta^{13}{\rm C}$ observations, the calculated percentages of the three source categories contributing to the observed isotopic signature revealed that the contribution of biogenic sources to the source mixture also dominated during the day (Figure 5). The contribution range of biogenic sources was substantially more variable in 2011 (31–80%) than in 2012 (45–76%), although the mean daytime $\delta^{13}{\rm C}$ value showed no significant difference between the two measurement years (–44.8 \pm 2.8 and –45 \pm 1‰ in 2011 and 2012, respectively). The ranges of the other source types were relatively broad and included zero contributions. In 2011, non-biogenic sources contributed to the $\delta^{13}{\rm C}_{obs}$ between 0–69%, whereas a minor contribution range of 0–44% was found for the sink processes. In 2012, non-biogenic sources (0–55%) and sink processes (0–35%) contributed both less to the daytime source mixture compared to 2011. A reason for the likewise broad contribution ranges of non-biogenic sources and sink processes might be the relatively similar isotopic source signatures of –25.55‰ and –5.4‰, respectively, compared to the biogenic source type signature (–61.26‰).

With respect to different $\delta^{13}C_{obs}$ ranges, very narrow contribution ranges of the biogenic source percentage, expressed by the standard deviation (68.5 \pm 4.6 and 66 \pm 4.6% in 2011 and 2012, respectively), were found for $\delta^{13}C_{obs}$ values depleted in $^{13}C_{obs}$, i.e., between -47 and -50% (Figure 5). For enriched $\delta^{13}C_{obs}$ values, i.e., between -30 and -43%, the mean percentage of biogenic sources fell in both years below 60% and showed in 2011 a higher contribution range ($\pm 7.5\%$). The contribution ranges of non-biogenic sources and sink processes increased with the enrichment of $\delta^{13}C_{obs}$ in ^{13}C , e.g. in 2011 from $\pm 11.4\%$ to $\pm 17.0\%$ and in 2012 from $\pm 7.3\%$ to $\pm 10.9\%$, respectively. Although contribution ranges of the three source types to the observed isotopic signature broadened with increasing $\delta^{13}C_{obs}$ values, the mean contributions of non-biogenic sources and sink processes, however, remained relatively unaffected at 21.7% and 16%, respectively, in both measurement years.

Sensitivity analysis showed, that alterations in source increments from 0.5 to 2% had no effect on the contribution range of the different source types. Only a minimal effect on the range could be observed from alterations in the mass balance tolerance. At a 2% mass balance tolerance the contribution range of biogenic sources increased by 4-5% and between 1-3% regarding the remainder source contributions. However, median and $5\text{-}95^{th}$ percentile width stayed unaffected by the alterations in the mass balance tolerance for all source contributions.

4.4 Discussion

4.4.1 Spatio-temporal varibility of CH₄ and δ^{13} C

In both years, the diel course in the methane concentration at the valley bottom clearly showed the interplay between the nocturnal development of a stable boundary layer and the diurnal replacement by a convective mixing layer. Diel patterns with large concentration build-ups during the night were also observed in other studies with dominant anthropogenic methane sources (Laubach et al., 2013; Baldocchi et al., 2012). These studies, focusing on areas with a single methane source, e.g. ruminants, natural gas and landfills, also found a clear diel pattern in associated δ^{13} C isotopic values with a strong nighttime depletion/enrichment in 13 C and a daytime signal close to background (Harvey et al., 2002; Lowry et al., 2001). Our measurements, in contrast, showed a less pronounced diel pattern in δ^{13} C isotopic values compared to the methane concentrations, although enteric fermentation and manure management from agriculture have been identified as the main contributors to atmospheric CH₄ in the Reuss Valley.

With respect to the nighttime data, the nocturnal decrease in δ^{13} C values relative to the reference value, however, was rather small at the valley bottom. Particularly the nighttime measurements of 2012 showed clearly that enriched emission plumes resulted in equally high excess methane as the emissions from biogenic sources, probably due to stronger nighttime advective transport of enriched upwind air masses and following mixing processes with the local depleted NBL. Excess methane of clear non-biogenic origin, i.e., $\delta^{13}C_{source} > -25\%$, was only observed during limited time periods before sunrise in both years (Table 2), probably resulting from nighttime fan-

4.4. DISCUSSION 75

ning of local non-biogenic emissions. As these high δ^{13} C values were observed even at very low measurement heights (0.2, 2 and 10 m a.g.l.), the findings suggest that nearby non-biogenic sources do exist (with comparable source strength), but that their proportions in the Reuss Valley must be very low compared to the agricultural source proportion. Possible origins could be vehicular methane emission from less efficient combustion of farm machinery or vintage cars and emissions from biomass burning (e.g., grilling on charcoal). With respect to daytime data, the δ^{13} C values showed an enrichment at all measured heights, demonstrating that biogenic sources were not alone responsible for the observed diel pattern. The enriched signatures were found after sunrise (Figures 2 and 3), when under fair weather conditions prevailing NNW-winds from northern agglomerations penetrate into the valley, where leakages in gas pipelines are expected to be a major methane source (Hiller et al., 2013). Although no correlation has been found between δ^{13} C and wind direction, we argue that the valley wind system, carrying methane from upwind lying sources into the Reuss Valley, was responsible for the enriched daytime δ^{13} C values.

As expected, the mobile set-up measurements at the hilltop sites did not show a diel course in CH₄ concentrations and δ^{13} C values, as they were located above the NBL. Despite the near-ground measurements, i.e., at 2 m a.g.l., the diel pattern even remained unaffected by methane emissions of nearby farmsteads. However, we also observed the daytime enrichment in 13 C at these locations as can be seen in a transport-induced peak in δ^{13} C at the mobile measurement site D around 10 am. This observation is in agreement with other studies from the Reuss Valley, where with the onset of the valley wind system the upward transported air masses dominated the local diel concentration pattern (Bamberger et al., 2013).

The results showed that the diel patterns in δ^{13} C were strongly influeced by the local topography and by advective transport processes, which play a major role in atmospheric methane (Laubach et al., 2013; Baldocchi et al., 2012; Townsend-Small et al., 2012). Even locations above the NBL, which do not exhibit a diel course, are affected by the local wind patterns during the day. Furthermore, the impact of non-biogenic methane sources cause variations in the diel course of δ^{13} C values, but, however, not necessarily in the diel course of CH₄ concentrations. Hence, non-biogenic methane sources are assumed to have a comparable source strength, as their emissions resulted in similar high excess methane.

4.4.2 Source partitioning

Generally, the source partitioning of δ^{13} C in CH₄ was affected by the overabundance of possible non-biogenic sources and sink processes, expressed by the broad distribution range and the zero contributions (Figure 5). This resulted in a wide range of possible combinations of all three specified source categories, indicating a variety of possible explanations for the observed δ^{13} C values. Additional measurements of δD in CH_4 would probably help to reduce possible source categories, resulting from their relatively well constrained isotopic signatures for different biogenic and nonbiogenic sources (Tyler et al., 2007; Quay et al., 1999; Schoell, 1988), and improve the overall understanding of spatiotemporal methane emissions (Dlugokencky et al., 2011; Phillips et al., 2005; Pataki et al., 2003; Phillips, Gregg, 2003). Still, source partitioning analysis showed, that biogenic methane sources contributed most to the total source mix during day and night and that other sources or sinks were of minor importance in the Reuss Valley. During the day, however, a considerable contribution of non-biogenic sources and sink processes were found and disregarding different ranges of observations in δ^{13} C, the percentages of all source categories remained very robust.

Despite the suggested mean contribution of 16% from the mixing model, the effect of sink processes on the $\delta^{13}C_{obs}$ value remains questionable. The main methane sink, i.e., atmospheric OH, reacts on longer temporal and larger spatial scales (Tyler et al., 2007; Miller, 2004; Quay et al., 1999; Cicerone, Oremland, 1988) and the sink strengths of different soils, which largely depend on the land-use type, are yet not resolved on shorter temporal scales (Dalal et al., 2008). While methane uptake of grasslands with -0.21 mg CH₄ m⁻² d⁻¹ do not contribute significantly to the methane budget (Imer et al., 2013), forest uptake rates were estimated by up to -1.5 mg CH₄ m⁻² d⁻¹ (Hiller et al., 2013). Still, an enrichment of isotopic signatures alone by forest soils remains doubtful, but the net effect of soil uptake on the isotopic discrimination of atmospheric methane on a regional scale needs to be investigated in more detail. Thus, we assume that methane sinks played a minor role during our measurements in the Reuss Valley.

The effect of non-biogenic sources on the regional methane budget due to turbulent mixing during the day, however, has to our knowledge not been considered for model estimates, as biogenic methane from agriculture has been reported as the main 4.5. CONCLUSION 77

methane source in the Reuss Valley. With a mean contribution 21.7%, non-biogenic sources had a substantial effect on the local source mix and need to be quantitively assessed in detail, in order to reliably interpret their contribution to the regional methane budget.

4.4.3 Implications for methane emission budgets

It has been shown that during anticyclonic fair weather conditions, trends in background levels of methane concentration give information about the regional emission strength of major sources (Lowry et al., 2001). The impact of agricultural methane emissions from the Reuss Valley on the local background atmospheric CH₄ burden, however, was negigible. While no effect was found for background CH₄ concentrations, only a marginal depleting effect (-0.3\%) was observed for the δ^{13} C background value. Thus, nighttime methane emissions are compensated by convective dilution during the day. We therefore conclude that during the time of observation biogenic methane sources from the Reuss Valley had a comparable emission strength as nonbiogenic methane sources from upwind lying agglomerations, resulting in similar high excess methane but forcing background signatures towards slightly more depleted δ^{13} C values. These findings put significant implications on the interpretation of regional methane budgets and models: The impact of sources lying upwind is not necessarily visible in the local methane concentration, but due to generalized assumptions it is often included in the local emission budget, which might result in a overestimation of the local methane emission budget. In order to separate between the different sources and to constrain the formulation of mitigation strategies, the identification of different source types (e.g., via stable isotope analysis) is therefore essential.

4.5 Conclusion

This study showed that highly resolved measurements of CH_4 and $\delta^{13}C$ improve the understanding about the temporal and spatial emissions of different methane sources within a specific region. Such measurements are highly needed in order to improve the agreement between modeled and measured emissions and give relevant information about the interpretation of methane budgets. In the Reuss Valley, minor sources of non-biogenic origin had the same impact on excess methane as biogenic methane sources, but smoothing them out in models will result in an increased budget uncertainty. Attention should be paid to the question, whether the measurements reflect minor emissions from local sources or transport-induced emissions from upwind sources. Methane emissions from upwind sources, i.e., non-biogenic methane from northern agglomerations, were contributing up to 22% on average to the local source mix and have so far not been seperated from biogenic methane emissions in the case of the Reuss Valley. Leving the different source emissions unseparated will bias the local methane budget towards an overestimation. Furthermore, observations above the boundary layer showed that the biogenic methane emissions are compensated during daytime convective dilution, a process which can not be assessed using only localized measurements within the atmospheric boundary layer.

Acknowledgements

This research was supported by the Swiss National Science Foundation, grant no. 2-77771-10. We thank H.-R. Wettstein and his team for their logistic support at the ETH research station Chamau. Peter Pluess and Thomas Baur are thanked for their technical support.

4.6 Tables and figures

Table 4.1: Source types of methane in the Reuss Valley and their δ^{13} C characteristics. Weighted averages were used for the source identification of nighttime measurements (see text for details). No uncertainty ranges were available for the sink components.

Source / Sink	Isotopic signature δ^{13} C [‰]	Weighted average δ^{13} C [‰]	Reference
Sources			
Vehicle emissions			
American	-16.0 ± 6		Lowry et al. (2001)
European	-28.0 ± 3		Lowry et al. (2001)
Natural Gas		-39.7 ± 3^{a}	
North Sea	-34.0 ± 3		Dlugokencky et al. (2011); Lowry et al. (2001)
Siberia	-50.0 ± 3		Dlugokencky et al. (2011); Lowry et al. (2001)
$Biomass\ Burning$			
C4 vegetation	-18.0 ± 3		Dlugokencky et al. (2011); Lowry et al. (2001)
C3 vegetation	-26.0 ± 3		Dlugokencky et al. (2011); Lowry et al. (2001)
$Enteric\ fermentation$		-64.5 ± 1^{b}	
C4 diet	$-57.5 {\pm} 0.6$		Klevenhusen et al. (2010)
C3 diet	$-67.5 {\pm} 0.6$		Klevenhusen et al. (2010)
Manure Management		-48.2 ± 1^{b}	
C4 diet	$-49.1 {\pm} 0.5$		Klevenhusen et al. (2010)
C3 diet	$-46.0 {\pm} 0.5$		Klevenhusen et al. (2010)
Waste Management		-56.0 ± 3^{c}	
Landfills	-53.0 ± 2		Dlugokencky et al. (2011); Lowry et al. (2001)
Domestic Sewage	-57.0 ± 3		Dlugokencky et al. (2011); Lowry et al. (2001)
Animal Waste	-58.0 ± 3		Dlugokencky et al. (2011); Lowry et al. (2001)
Sinks		-5.4	Miller (2004)
Tropospheric OH	-3.9		
Soils	-21		
Stratosphere	-12		

^aWeighted average according to Switzerland's gas import statistics of the year 2011 (VSG, 2012).

^bCalculated according to the proportions of C4- and C3-vegetation in the forage mixture used at the Chamau research station, i.e., 30% and 70%, respectively (pers. comm. H.-R. Wettstein).

^cUnweighted average of δ^{13} C values from landfill, domestic sewage and animal waste.

Table 4.2: Nighttime source identification of $\delta^{13}\mathrm{C}$ values in 2011 and 2012. Not available wind direction measurements are indicated with n.a. The Reference values are determined as the mean of all profile measurements during well-mixed daytime conditions (see text for details on the reference value and on the calculation of $\delta^{13}\mathrm{C}_{source}$). Uncertainty estimation is determined by error propagation.

(a) Nighttime source identification of 2011 measurements.

Date	Time [UTC+1]	Height [m a.g.l.]	Wind direction [°]	CH ₄ [ppm]	$\begin{array}{ c c } \delta^{13}C_{obs} \\ [\%] \end{array}$	$\delta^{13}C_{source}$ [%]	Error ±[‰]
Reference value				1.92	-46.0		
Stationary measurements							
17 August	21:28	2	n.a.	2.52	-48.9	-58.3	0.2
17 August	21:30	0.5	n.a.	2.49	-47.9	-54.4	0.1
17 August	21:34	0.2	n.a.	2.30	-48.1	-58.7	< 0.1
17 August	21:37	10	217	2.27	-49.9	-71.9	< 0.1
17 August	21:40	8	n.a.	2.49	-47.5	-52.7	0.1
18 August	01:28	2	n.a.	2.70	-49.9	-59.6	< 0.1
18 August	01:31	0.5	n.a.	2.87	-51.7	-63.4	0.2
18 August	01:34	0.2	n.a.	2.97	-47.0	-48.8	0.1
18 August	01:37	10	80	2.99	-49.9	-56.9	< 0.1
18 August	01:40	8	n.a.	2.67	-50.4	-61.8	0.1
18 August	02:01	160	308	2.10	-46.1	-48.0	0.1
18 August	02:14	100	292	2.36	-47.8	-56.2	0.3
18 August	02:25	50	328	2.66	-44.2	-39.6	0.2
18 August	02:33	25	305	2.94	-46.9	-48.6	< 0.1
18 August	05:28	2	n.a.	2.47	-48.2	-56.3	< 0.1
18 August	05:31	0.5	n.a.	2.55	-47.0	-50.2	0.1
18 August	05:34	0.2	n.a.	2.53	-36.5	-6.1	< 0.1
18 August	05:37	10	211	2.76	-38.4	-21.0	0.1
18 August	05:40	8	n.a.	2.85	-47.9	-52.0	0.1
22 August	21:46	100	200	2.30	-45.9	-45.6	0.2
22 August	21:53	50	305	2.42	-45.0	-41.4	0.1
22 August	21:59	25	129	2.74	-47.5	-51.2	0.3
23 August	00:04	100	155	2.26	-49.5	-70.0	0.4
23 August	00:10	50	233	2.31	-49.5	-67.4	0.2
23 August	00:15	25	307	2.51	-47.5	-52.6	0.4
23 August	05:04	100	66	2.34	-41.4	-19.9	0.1
23 August	05:11	75	n.a.	2.35	-47.1	-52.0	0.1
23 August	05:17	50	n.a.	2.74	-49.2	-56.9	0.2
23 August	05:22	25	n.a.	2.94	-50.3	-58.5	0.2

(b) Nighttime source identification of 2012 measurements.

Date	Time [UTC+1]	Height [m a.g.l.]	Wind direction [°]	CH_4 [ppm]	$\begin{array}{c c} \delta^{13}C_{obs} \\ [\%] \end{array}$	$\delta^{13}C_{source}$ [%]	Error $\pm [\%]$
Reference value	[]	[0]		1.96	-45.6	[]	[, **]
				1.00	10.0		
Stationary measurements							
24 July	21:08	100	129	2.17	-44.7	-36.8	0.1
24 July	21:16	25	170	2.19	-44.7	-36.6	0.1
24 July	23:33	150	152	2.61	-46.0	-47.4	< 0.1
24 July	23:42	100	131	2.64	-46.7	-50.1	< 0.1
24 July	23:51	25	178	2.75	-45.0	-43.6	0.1
25 July	00:30	2	n.a.	2.77	-47.4	-52.0	< 0.1
25 July	00:33	0.5	n.a.	2.76	-47.3	-51.7	< 0.1
25 July	00:36	0.2	n.a.	2.78	-44.4	-41.5	0.1
25 July	00:39	10	268	2.87	-48.9	-56.2	< 0.1
25 July	00:42	8	n.a.	2.92	-44.8	-43.1	0.1
25 July	01:13	150	162	2.73	-48.1	-54.4	< 0.1
25 July	01:22	100	165	2.72	-45.0	-43.4	< 0.1
25 July	01:31	25	184	2.72	-46.0	-47.3	< 0.1
25 July	02:30	2	n.a.	2.83	-48.5	-55.3	< 0.1
25 July	02:33	0.5	n.a.	2.91	-51.0	-62.1	< 0.1
25 July	02:36	0.2	n.a.	2.84	-42.5	-35.6	< 0.1
25 July	02:39	10	265	2.84	-50.9	-62.6	< 0.1
25 July	02:42	8	n.a.	2.83	-52.5	-68.0	< 0.1
25 July	03:11	150	n.a.	3.23	-47.4	-50.2	< 0.1
25 July	03:20	100	n.a.	3.16	-47.5	-50.7	0.1
25 July	03:29	25	n.a.	3.14	-43.2	-39.1	< 0.1
25 July	04:30	2	n.a.	3.14	-37.0	-22.6	< 0.1
25 July	04:33	0.5	n.a.	3.19	-48.2	-52.3	< 0.1
25 July	04:36	0.2	n.a.	3.30	-51.3	-59.7	< 0.1
25 July	04:39	10	264	3.35	-42.5	-38.0	< 0.1
25 July	04:42	8	n.a.	3.38	-51.7	-60.3	< 0.1
25 July	05:14	150	163	3.26	-43.0	-39.2	< 0.1
25 July	05:22	100	163	3.42	-43.9	-41.6	< 0.1
25 July	05:30	25	174	3.41	-48.0	-51.2	< 0.1
Mobile Measurements							
24 July	23:39	402 [m a.s.l.]	144	2.46	-45.9	-47.2	< 0.1
25 July	00:09	694 [m a.s.l.]	248	2.20	-47.2	-60.4	0.1
25 July	02:53	387 [m a.s.l.]	270	2.96	-43.6	-39.8	< 0.1
25 July	04:19	402 [m a.s.l.]	162	3.31	-51.4	-59.9	< 0.1
25 July	04:52	694 [m a.s.l.]	254	2.16	-45.6	-45.9	0.1

■ Stationary set-up site ⋈ Mobile set-up sites

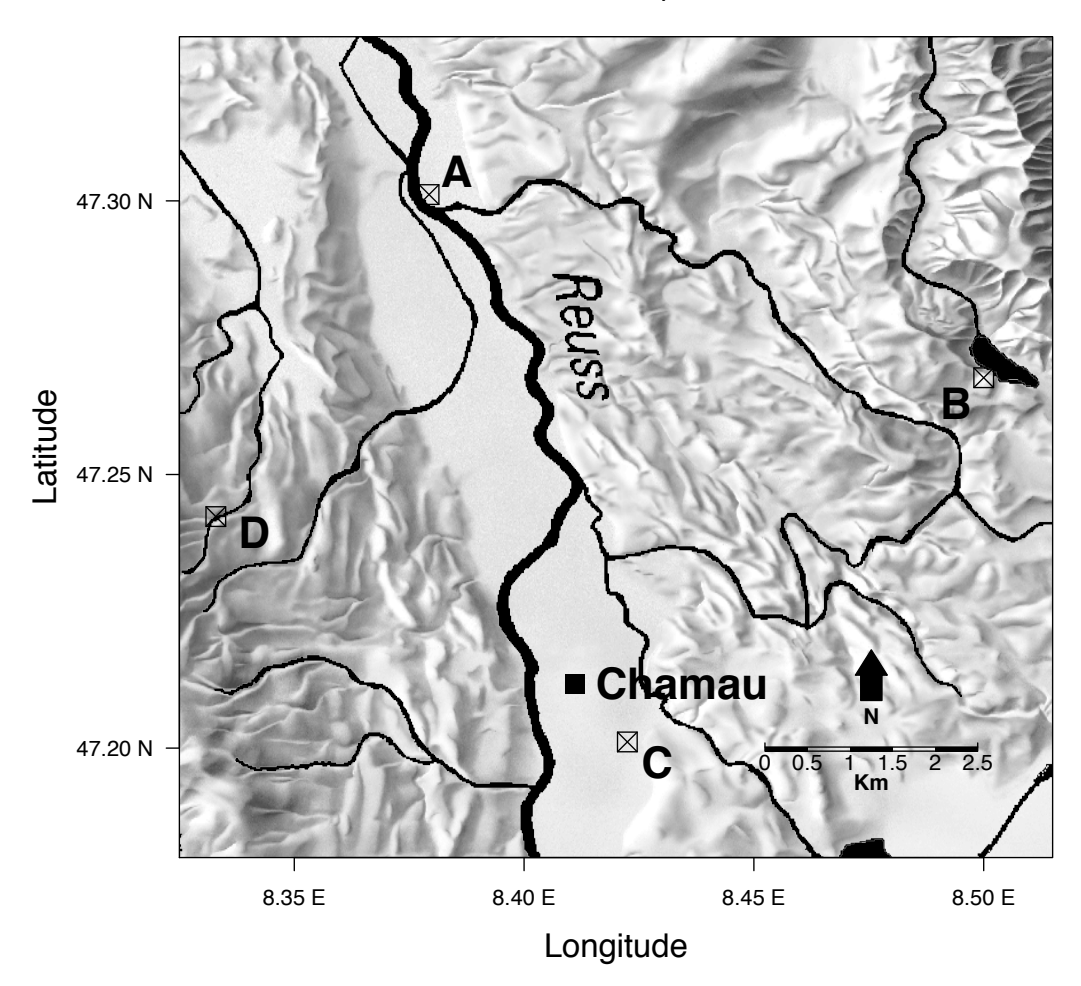


Figure 4.1: Topographic map of the stationary (Chamau) and mobile (A–D) set-up sites in the Reuss Valley, Switzerland (map source: © Federal Office of Topography, swisstopo (2011): JD100042).

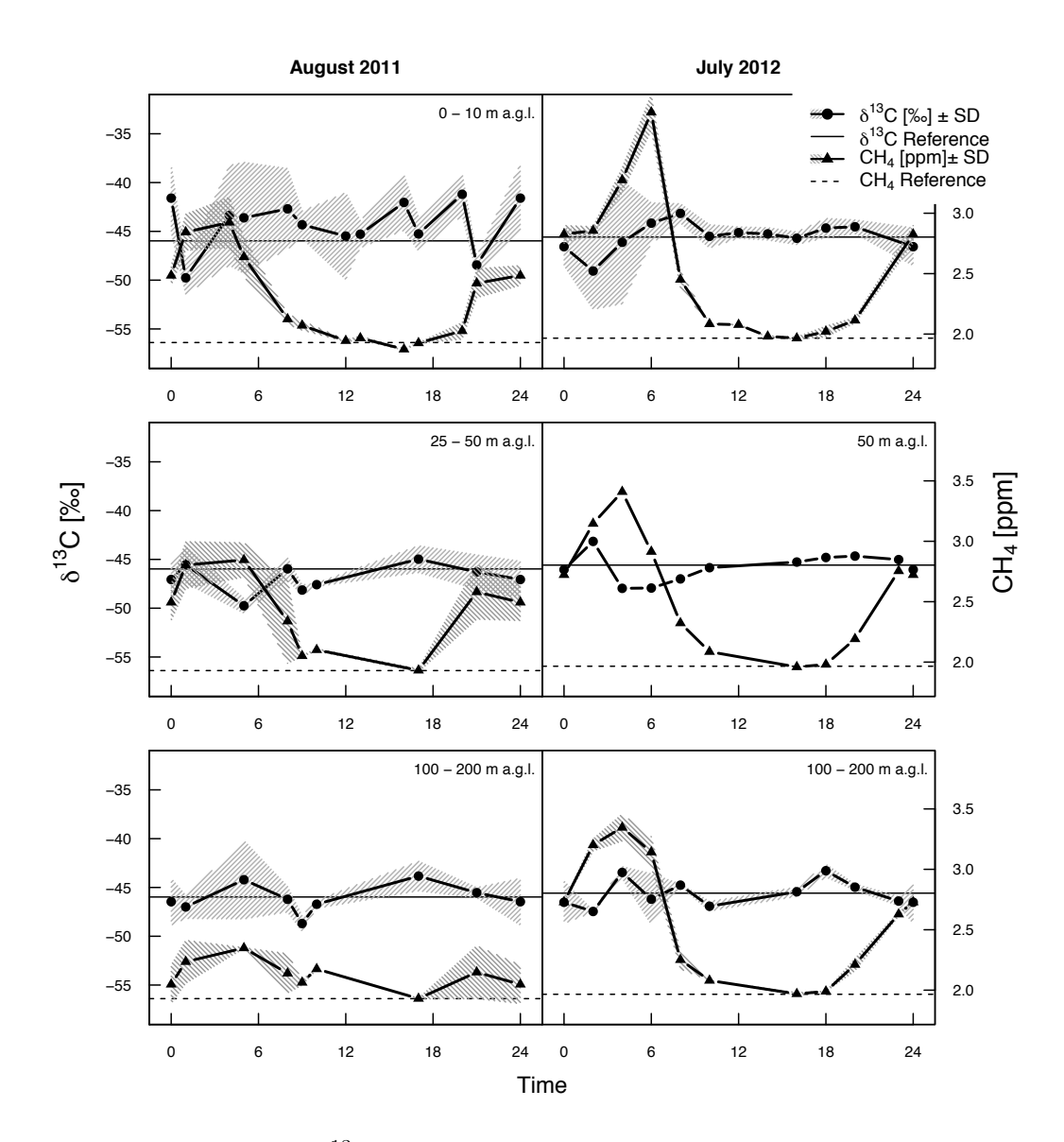


Figure 4.2: Diel course of δ^{13} C and CH₄ concentrations at the stationary set-up site ETH Research Station Chamau given in means and standard deviations (SD) for the respective height levels. The Reference values are determined as the mean of all profile measurements during well-mixed daytime conditions (see text for details).

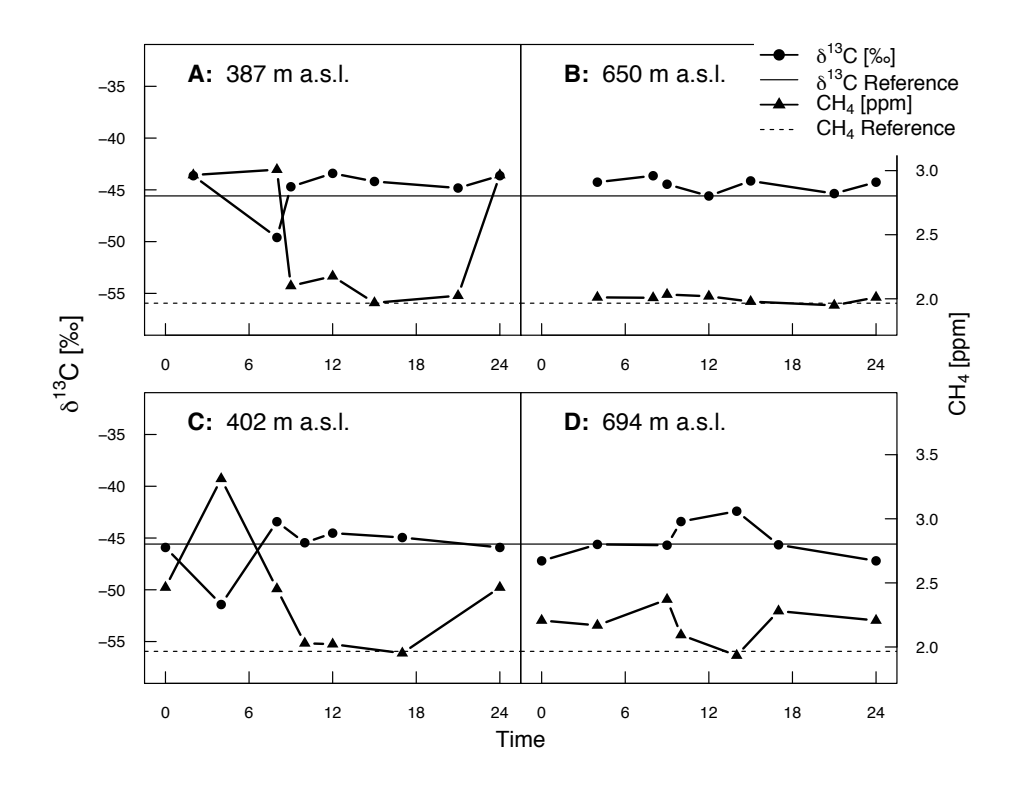


Figure 4.3: Diel courses of δ^{13} C and CH₄ concentrations of the mobile set-up sites during July 2012. The Reference values are determined as the mean of all profile measurements during well-mixed daytime conditions from stationary set-up site (see text for details).

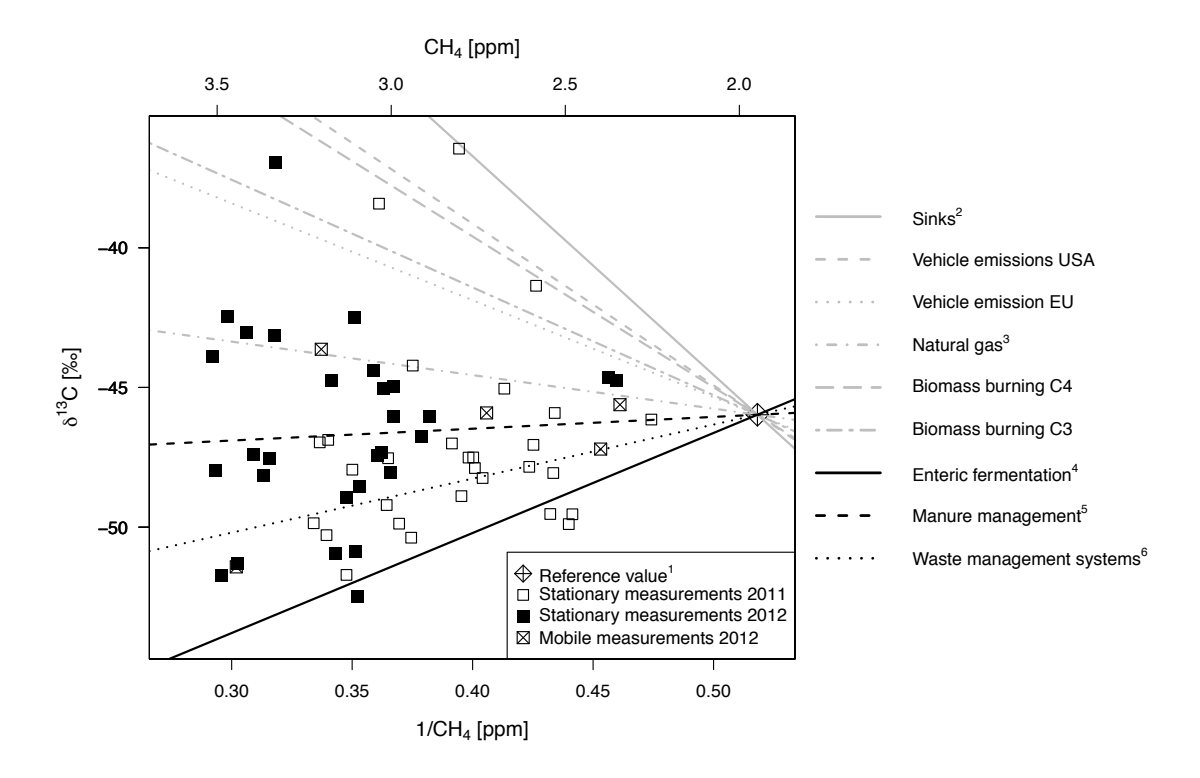
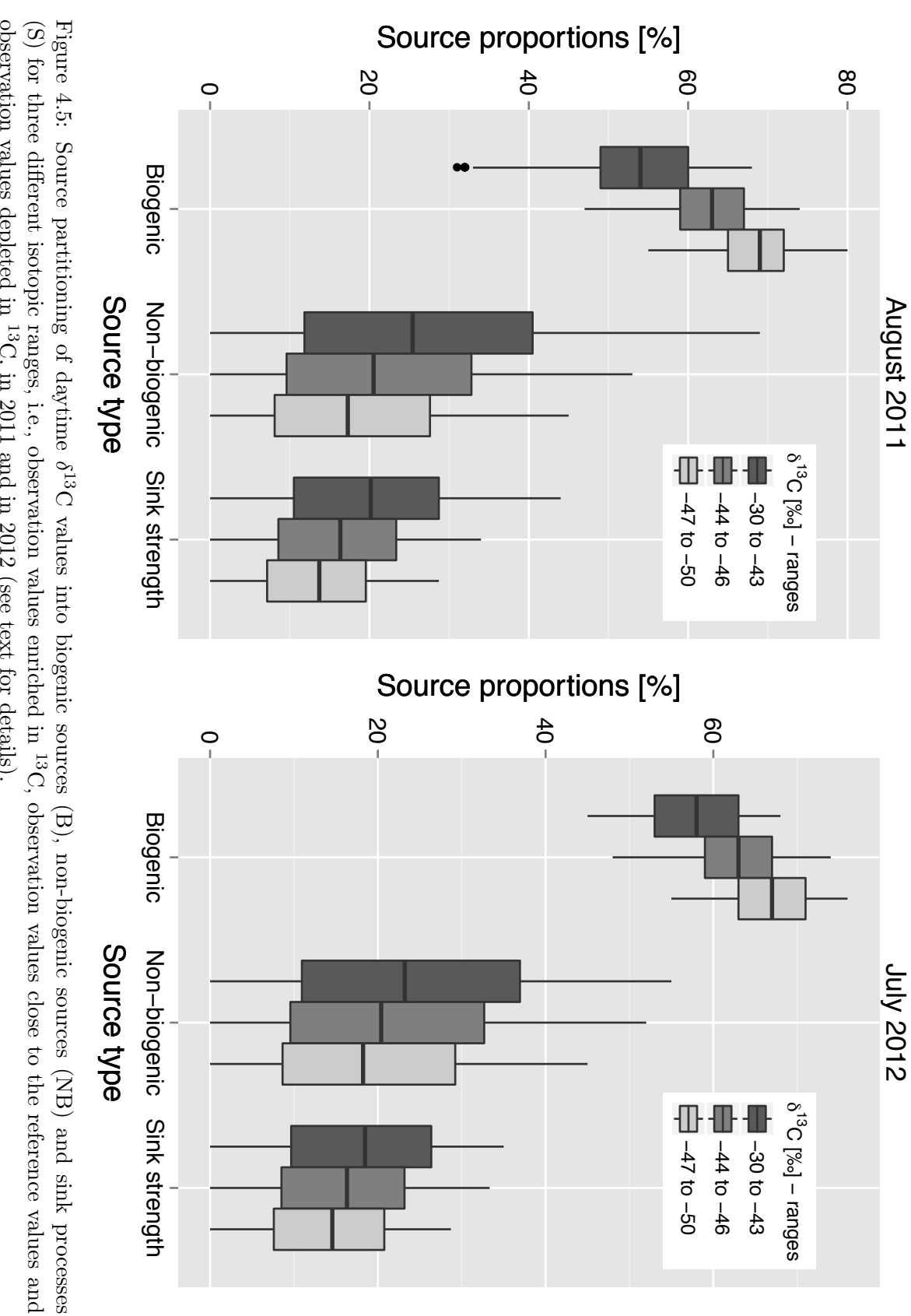


Figure 4.4: Keeling plot of nighttime carbon isotopic data of observed CH₄ concentrations (points) and different methane source types (lines). ¹Average of the reference values of 2011 and 2012, calculated as the mean of all profile measurements during well-mixed daytime conditions from the stationary set-up site (see text for details). ²Miller (2004). ³Weighted average according to Switzerland's gas import statistics of the year 2011 (VSG, 2012). ⁴⁺⁵Calculated according to the proportions of C4- and C3-vegetation in the forage mixture used at the Chamau research station, i.e., 30% and 70%, respectively (pers. comm. H.-R. Wettstein). ⁶Unweighted average of δ^{13} C values from landfill, domestic sewage and animal waste.



observation values depleted in ¹³C, in 2011 and in 2012 (see text for details). (S) for three different isotopic ranges, i.e., observation values enriched in ¹³C, observation values close to the reference values and

References

- Baldocchi D, Detto M, Sonnentag O, Verfaillie J, The Y, Silver W, Kelly N (2012) The challenges of measuring methane fluxes and concentrations over a peatland pasture. *Agricultural and Forest Meteorology* 153:177–187.
- Bamberger I, Stieger J, Eugster W, Buchmann N (2013) Spatial variability of methane: Attributing atmospheric concentrations to emissions. *In process*.
- Bousquet P, Ciais P, Miller J, Dlugokencky E, Hauglustaine D, Prigent C, Van der Werf G, Peylin P, Brunke E, Carouge C, Langenfelds R, Lathiere J, Papa F, Ramonet M, Schmidt M, Steele L, Tyler S, White J (2006) Contribution of anthropogenic and natural sources to atmospheric methane variability. *Nature* 443(7110):439–443.
- Chanton J, Liptay K (2000) Seasonal variation in methane oxidation in a landfill cover soil as determined by an in situ stable isotope technique. *Global Biogeochemical Cycles* 14(1):51–60.
- Chanton J, Rutkowski C, Mosher B (1999) Quantifying methane oxidation from landfills using stable isotope analysis of downwind plumes. *Environmental Science & Technology* 33(21):3755–3760.
- Cicerone R, Oremland R (1988) Biogeochemical aspects of atmospheric methane. Global Biogeochemical Cycles 2(4):299–327.
- Conrad R (2005) Quantification of methanogenic pathways using stable carbon isotopic signatures: a review and a proposal. *Organic Geochemistry* 36(5):739–752.
- Dalal R, Allen D, Livesley S, Richards G (2008) Magnitude and biophysical regulators of methane emission and consumption in the australian agricultural, forest, and submerged landscapes: a review. *Plant and Soil* 309(1-2):43–76.
- Dlugokencky E, Nisbet E, Fisher R, Lowry D (2011) Global atmospheric methane: budget, changes and dangers. *Philosophical Transactions of the Royal Society A:* Mathematical, Physical and Engineering Sciences 369(1943):2058–2072.

Federal Office of Topography, swisstopo (2011) Topographic land cover map (Art. 30 GeoIV): 5704 000 000. Federal Office of Topography swisstopo, Wabern, Switzerland.

- FOEN (2013) Switzerland's Greenhouse Gas Inventory 1990-2011: National Inventory Report 2013. page 483. Submission of 15 April 2013 under the United Nations Framework Convention on Climate Change and under the Kyoto Protocol. Federal Office for the Environment (FOEN), Bern, Switzerland.
- FSO (2012) Land use statistics (Arealstatisik) 2004/09, NOLU04/20120821. Swiss Federal Statistical Office (FSO), Neuchatel, Switzerland.
- Harvey M, Brailsford G, Bromley A, Lassey K, Mei Z, Kristament I, Reisinger A, Walker C, Kelliher F (2002) Boundary-layer isotope dilution/mass balance methods for measurement of nocturnal methane emissions from grazing sheep. *Atmospheric Environment* 36(29):4663–4678.
- Hiller R, Bretscher D, DelSontro T, Diem T, Eugster W, Henneberger R, Hobi S, Hodson E, Imer D, Kreuzer M, Künzle T, Merbold L, Niklaus P, Rihm B, Schellenberger A, Schroth M, Schubert C, Siegrist H, Stieger J, Buchmann N, Brunner D (2013) Anthropogenic and natural methane fluxes in Switzerland synthesized within a spatially-explicit inventory. Biogeosciences Discussions 10(9):15181–15224.
- Imer D, Merbold L, Eugster W, Buchmann N (2013) Temporal and spatial variations of CO₂, CH₄ and N₂O fluxes at three differently managed grasslands. *Biogeosciences* 10:5931–5945.
- Jagovkina S, Karol I, Zubov V, Lagun V, Reshetnikov A, Rozanov E (2000) Reconstruction of the methane fluxes from the west Siberia gas fields by the 3D regional chemical transport model. *Atmospheric Environment* 34(29):5319–5328.
- Kai F, Tyler S, Randerson J, Blake D (2011) Reduced methane growth rate explained by decreased Northern Hemisphere microbial sources. *Nature* 476(7359):194–197.
- Klevenhusen F, Bernasconi S, Kreuzer M, Soliva C (2010) Experimental validation of the intergovernmental panel on climate change default values for ruminant-derived methane and its carbon-isotope signature. *Animal Production Science* 50(3):159–167.
- Laubach J, Bai M, Pinares-Patiño C, Phillips F, Naylor T, Molano G, Cárdenas Rocha E, Griffith D (2013) Accuracy of micrometeorological techniques for detecting a change in methane emissions from a herd of cattle. *Agricultural and Forest Meteorology* 176:50–63.

Levin I, Glatzel-Mattheier H, Marik T, Cuntz M, Schmidt M (1999) Verification of German methane emission inventories and their recent changes based on atmospheric observations. *Journal of Geophysical Research: Atmospheres* 104(D3):3447–3456.

- Lowry D, Holmes C, Rata N, O'Brian P, Nisbet E (2001) London methane emissions: Use of diurnal changes in concentration and δ^{13} C to identify urban sources and verify inventories. *Journal of Geophysical Research: Atmospheres* 106(D7):7427–7448.
- Miller J (2004) The carbon isotopic composition of atmospheric methane and its constraint on the global methane budget. In: Stable isotopes and biosphere-atmosphere interactions: processes and biological controls, (eds) Lawrence B. Flanagan, *Elsevier Academic Press*, Chapter 16, pp. 288–310.
- Mischler J, Sowers T, Alley R, Battle M, McConnell J, Mitchell L, Popp T, Sofen E, Spencer M (2009) Carbon and hydrogen isotopic composition of methane over the last 1000 years. *Global Biogeochemical Cycles* 23(4).
- Neef L, van Weele M, van Velthoven P (2010) Optimal estimation of the present-day global methane budget. Global Biogeochemical Cycles 24(4).
- Pataki D, Ehleringer J, Flanagan L, Yakir D, Bowling D, Still C, Buchmann N, Kaplan J, Berry J (2003) The application and interpretation of Keeling plots in terrestrial carbon cycle research. *Global Biogeochemical Cycles* 17(1).
- Pendall E, Schwendenmann L, Rahn T, Millers J, Tans P, White J (2010) Land use and season affect fluxes of CO₂, CH₄, CO, N₂O, H₂ and isotopic source signatures in Panama: evidence from nocturnal boundary layer profiles. *Global Change Biology* 16(10):2721–2736.
- Phillips D, Gregg J (2003) Source partitioning using stable isotopes: coping with too many sources. *Oecologia* 136(2):261–269.
- Phillips D, Newsome S, Gregg J (2005) Combining sources in stable isotope mixing models: alternative methods. *Oecologia* 144(4):520–527.
- Quay P, Stutsman J, Wilbur D, Snover A, Dlugokencky E, Brown T (1999) The isotopic composition of atmospheric methane. *Global Biogeochemical Cycles* 13(2):445–461.
- Schoell M (1988) Multiple origins of methane in the earth. Chemical Geology 71(1):1–10.
- Stevens C, Engelkemeir A (1988) Stable carbon isotopic composition of methane from some natural and anthropogenic sources. *Journal of Geophysical Research:* Atmospheres 93(D1):725–733.

Tarasova O, Houweling S, Elansky N, Brenninkmeijer C (2009) Application of stable isotope analysis for improved understanding of the methane budget: comparison of TROICA measurements with TM3 model simulations. *Journal of Atmospheric Chemistry* 63(1):49–71.

- Townsend-Small A, Tyler S, Pataki D, Xu X, Christensen L (2012) Isotopic measurements of atmospheric methane in Los Angeles, California, USA: Influence of "fugitive" fossil fuel emissions. *Journal of Geophysical Research: Atmospheres* 117(D07308):1451–1476.
- Tyler S, Rice A, Ajie H (2007) Stable isotope ratios in atmospheric CH₄: Implications for seasonal sources and sinks. *Journal of Geophysical Research: Atmospheres* 112(D03303).
- VSG (2012) Erdgas in Zahlen. Ausgabe 2012. erdgas. Verband der Schweizerischen Gasindustrie (VSG), Zurich, Switzerland.
- Whiticar M (1999) Carbon and hydrogen isotope systematics of bacterial formation and oxidation of methane. *Chemical Geology* 161(1):291–314.
- Zeeman M, Werner R, Eugster W, Siegwolf R, Wehrle G, Mohn J, Buchmann N (2008) Optimization of automated gas sample collection and isotope ratio mass spectrometric analysis of δ^{13} C of CO₂ in air. Rapid Communications in Mass Spectrometry 22(23):3883–3892.

Synthesis

Due to the heterogeneous distribution patterns of the methane sources, it is still not well understood how atmospheric methane evolves temporally on regional scales. This thesis aims at improving the understanding of CH₄ dynamics in the atmospheric boundary layer regarding the agriculture-dominated Reuss Valley in Central Switzerland. The overall goal was to analyse spatio-temporally highly resolved measurements of atmospheric methane and to evaluate the potential of such measurements for constraining statistical assessments of emission estimates.

5.1 Spatio-temporal dynamics of atmospheric CH_4 in the Reuss Valley

At the bottom of the Reuss Valley, methane concentrations and δ^{13} C values followed a clear diel cycle (Chapter 3 and 4). Methane concentrations increased during the night with the establishment of a nocturnal boundary layer (NBL) and were associated with a general depletion in 13 C relative to the background value. In contrast, daytime methane concentrations were low and the associated δ^{13} C values were slightly above the background value. Such a diel course can be commonly seen in regions with major anthropogenic methane sources, in our case the Reuss Valley with its livestock methane emissions. In contrast to many natural methane sources, their emissions are independent of air temperature and soil moisture and relatively constant in time. Therefore, the emission strength can be best observed

92 5. SYNTHESIS

during the night, when the increase in concentration is caused by the trapping of methane within the stable NBL, whereas the emission signal gets diluted during the day due to the mixing of the convective boundary layer (CLB). This diel course got less pronounced with increasing height above ground and even disappeared on the surrounding hilltops of the Reuss Valley. There, the diel cycle was mainly affected by the local wind patterns and not necesserally by the proximity of the methane sources.

Besides the source distribution, transport processes were identified as the most important determinant for the atmospheric distribution of methane in complex terrain. Due to advection, the signal of methane sources can be seen over very long distances during day and night and hence, affects the local concentration dynamics and bias the regional emission budget (Chapter 3). During July 2012, cold-air drainage flows and intermittent turbulence resulted in a well-mixed NBL and constrained a oneto-one application of the NBL budget approach (Chapter 2). The integration of all vertical concentration gradients up to the top of the NBL would have led to a significant overestimation of the local methane emission budget. In order to reduce the impact of upwind source emissions, the integration height had to be set according to the atmospheric stability within the NBL. In addition, small-scale advection (i.e., horizontal fanning) of non-biogenic source emissions was observed during nighttime measurements, leading to exess methane similar to biogenic source emissions, but with substiantially enriched δ^{13} C values (Chapter 4). In contrast, large-scale advection processes were observed mainly during daytime, when the valley wind system brought ¹³C-enriched air masses from upwind agglomerations into the Reuss Valley. This resulted in a enrichement of the local air masses and a complete compensation of the trapped nighttime excess methane, due to convective dilution. Although nightime methane concentrations were mostly originating from livestock, an average source contribution of only 20% from non-biogenic sources was sufficient to equilibrate the local isotopic signature of atmospheric methane towards background values. Thus, non-biogenic methane sources are suggested to have similar source strengths compared to biogenic sources, despite their small contribution to the total source mix. We showed that sources which have so far been thought to be of minor importance can substatially contribute to the total emission budget. With respect to the spatial resolution and temporal variation, highly resolved CH₄ concentration and δ^{13} C measurements are needed to reliably assess methane sources and separate their impact on the regional methane budget.

5.2 Implications for model estimates

Direct measurements of atmospheric methane are essential to constrain and validate model outputs. However, with respect to the spatial resolution of the model, the measurement design has to be carfully selected. Models tracing methane sources, i.e., inverse or forward modelling, often smooth out the atmospheric signals of locally confined sources, which can have a significant cumulative impact on the emission budget. Mobile near-surface measurements provide a very powerful tool to identify the location of methane sources (Chapter 3). Depending on the spatial resolution needed for the localization of these sources, nighttime measurements will integrate a larger area than daytime measurements. An important aspect thereby is that local wind patterns are included in the air transport dynamics of the model, as increased methane concentrations have been found at sites without major sources in their vicinity.

Nighttime measurements within the NBL are especially useful to estimate the source strength of a specific area (Chapter 2 and 3) and hence, to validate model emission estimates. Within the NBL, which acts as a natural chamber, the emitted methane is trapped and the concentration gradients will give sufficient information about the emission strengths of underlying sources. The NBL budget flux for livestock methane emissions at the farm scale of 1.59 \pm 0.22 μ g CH₄ m⁻² s⁻¹ was in good agreement with the inventory estimates and can be seen as an appropriate instrument to validate model emission estimates. Furthermore, our results affirmed the assessment methodology for livestock methane emissions of the inventories to be 'best practice' for the respective assessment period. As it can be used at different spatial scales, i.e., from local to global spatial scales, the national inventories are suggested to give a reasonable annual estimate of their livestock emissions. Still, special consideration has to be given to spatially-explicit inventories, which disaggregate the annual estimates on a higher resolution, e.g., 500 m x 500 m. The validation via direct measurements remains a non-trivial task, since no temporal variation is included in the estimates and the measurements will be affect by the current farming practices and the local meteorological conditions. Particularly with respect to 94 5. SYNTHESIS

livestock, the emissions are temporally not bound to the position of the farmstead and therefore resulted in a low correlation between the concentration measurements and the inventory grid cells of high emission estimates (Chapter 3).

In contrast, nighttime measurements above the NBL and/or daytime measurements far off direct methane sources include information about the impact of a source area on the background atmspheric methane burden. While air masses are passing the source area of interest, the uptake of additional methane will cause an increase in the background concentration value. Monitoring the background methane concentration is of key importance for global climate but requires, however, longterm measurements which are so far represented by global emission models and satellite measurements. Nevertheless, during our observations in the Reuss Valley in August 2011 and July 2012, no significant impact of the methane emissions on the background concentration was found, but the large biogenic source contributions resulted in a slightly depleted δ^{13} C value compared to the background value (Chapter 4).

5.3 Outlook and research considerations

- Continuous measurements of CH₄ concentrations provide a valuable tool to constrain methane budgets on different spatial scales and to improve the understanding of atmospheric methane dynamics.
- Measurements of δ^{13} C and δ D in CH₄ will simplify the separation of the contribution of different methane sources to the resulting atmospheric concentration and reduce the uncertainties associated with emission estimates by source sector.
- With respect to different sources, the validation of model estimates, i.e., bottom-up and top-down, via direct measurements is essential to reduce the overall estimation uncertainty. It is crucial to carefully select the measurement design according to the spatial resolution of the model, as atmospheric concentrations are substantially affected by the vicinity of a source, the local transport processes and the respective time period of the measurements.

- Methane emission estimates for other sources, i.e., energy and waste, are still associated with high uncertainties for Switzerland. An evaluation of these emissions via direct measurements has yet to be done.
- Open questions remain with respect to sink processes of atmospheric methane. Methane budgets at all spatial scales will likely be affected by changes in sink strengths. Sink processes in the atmosphere and in the soil are to our knowledge poorly quantified and their spatio-temporal impact on local to regional scale budgets is highly unknown.

Appendix A

Anthropogenic and natural methane fluxes in Switzerland synthesized within a spatially-explicit inventory

```
R. V. Hiller<sup>1</sup>, D. Bretscher<sup>2</sup>, T. DelSotro <sup>3</sup>, 4, T. Diem<sup>3</sup>, W. Eugster<sup>5</sup>, R. Hennenberger<sup>4</sup>, S. Hobi<sup>6</sup>, E. Hodson<sup>6</sup>, D. Imer<sup>5</sup>, M. Kreuzer<sup>5</sup>, T. Künzle<sup>7</sup>, L. Merbold<sup>5</sup>, P.A. Niklaus<sup>8</sup>, B. Rihm<sup>7</sup>, A. Schellenberger<sup>9</sup>, M. H. Schroth<sup>4</sup>, C. J. Schubert<sup>3</sup>, H. Siegrist<sup>10</sup>, J. Stieger<sup>5</sup>, N. Buchmann<sup>5</sup>, D. Brunner<sup>1</sup>
```

¹Empa, Swiss Federal Laboratories for Materials Science and Technology, Duebendorf, Switzerland ²Agroscope Reckenholz-Tänikon Research Station ART, Zurich, Switzerland ³Eawag, Swiss Fedeal Institute of Aquatic Science and Technology, Kastanienbaum, Switzerland ⁴ETH Zurich, Institute for Biogeochemistry and Pollutant Dynamics, Zurich, Switzerland ⁵ETH Zurich, Institute of Agricultural Sciences, Zurich, Switzerland ⁶WSL, Swiss Federal Institute for Forest, Snow and Landscape Research, Birmensdorf, Switzerland ⁷Meteotest, Bern, Switzerland ⁸University of Zurich, Institute of Evolutionary Biology and Environmental Studies, Zurich, Switzerland ⁹FOEN, Federal Office for the Environment, Bern, Switzerland ¹⁰Eawag, Swiss Federal Institute of Aquatic Science and Technology, Duebendorf, Switzerland *now at:

This manuscript was published in: Biogeosciences Discussions, 2013, 10, 15181–15224

MeteoSwiss, Federal Office of Meteorology and Climatology, Zurich, Switzerland

Biogeosciences Discuss., 10, 15181–15224, 2013 www.biogeosciences-discuss.net/10/15181/2013/doi:10.5194/bgd-10-15181-2013 © Author(s) 2013. CC Attribution 3.0 License.



This discussion paper is/has been under review for the journal Biogeosciences (BG). Please refer to the corresponding final paper in BG if available.

Anthropogenic and natural methane fluxes in Switzerland synthesized within a spatially-explicit inventory

R. V. Hiller^{1,*}, D. Bretscher², T. DelSontro^{3,4}, T. Diem³, W. Eugster⁵, R. Henneberger⁴, S. Hobi⁶, E. Hodson⁶, D. Imer⁵, M. Kreuzer⁵, T. Künzle⁷, L. Merbold⁵, P. A. Niklaus⁸, B. Rihm⁷, A. Schellenberger⁹, M. H. Schroth⁴, C. J. Schubert³, H. Siegrist¹⁰, J. Stieger⁵, N. Buchmann⁵, and D. Brunner¹

15181

Received: 13 August 2013 - Accepted: 20 August 2013 - Published: 17 September 2013

Correspondence to: R. V. Hiller (hillerrv@gmail.com)

Published by Copernicus Publications on behalf of the European Geosciences Union.

¹Empa, Swiss Federal Laboratories for Materials Science and Technology, Duebendorf, Switzerland

²Agroscope Reckenholz-Tänikon Research Station ART, Zurich, Switzerland

³Eawag, Swiss Federal Institute of Aquatic Science and Technology, Kastanienbaum, Switzerland

⁴ETH Zurich, Institute for Biogeochemistry and Pollutant Dynamics, Zurich, Switzerland ⁵ETH Zurich, Institute of Agricultural Sciences, Zurich, Switzerland

⁶WSL, Swiss Federal Institute for Forest, Snow and Landscape Research, Birmensdorf, Switzerland

⁷Meteotest, Bern, Switzerland

⁸University of Zurich, Institute of Evolutionary Biology and Environmental Studies, Zurich, Switzerland

⁹FOEN, Federal Office for the Environment, Bern, Switzerland

¹⁰Eawag, Swiss Federal Institute of Aquatic Science and Technology, Duebendorf, Switzerland now at: MeteoSwiss, Federal Office of Meteorology and Climatology, Zurich, Switzerland

Abstract

We present the first high-resolution (500 m × 500 m) gridded methane (CH₄) emission inventory for Switzerland, which integrates the national emission totals reported to the United Nations Framework Convention on Climate Change (UNFCCC) and recent CH₄ flux studies conducted by research groups across Switzerland. In addition to anthropogenic emissions, we also include natural and semi-natural CH₄ fluxes, i.e., emissions from lakes and reservoirs, wetlands, wild animals as well as uptake by forest soils. National CH₄ emissions were disaggregated using detailed geostatistical information on source locations and their spatial extent and process- or area-specific emission factors. In Switzerland, the highest CH₄ emissions in 2011 originated from the agricultural sector (150 Gg CH₄ yr⁻¹), mainly produced by ruminants and manure management, followed by emissions from waste management (15 Gg CH₄ yr⁻¹) mainly from landfills and the energy sector ($12 \, \text{Gg} \, \text{CH}_4 \, \text{yr}^{-1}$), which was dominated by emissions from natural gas distribution. Compared to the anthropogenic sources, emissions from natural and semi-natural sources were relatively small (6 Gg CH₄ yr⁻¹), making up only 3 % of the total emissions in Switzerland. CH₄ fluxes from agricultural soils were estimated to be not significantly different from zero (between -1.5 and 0 Gg CH₄ yr⁻¹), while forest soils are a CH_4 sink (approx. $-2.8\,Gg\,CH_4\,yr^{-1}$), partially offsetting other natural emissions. Estimates of uncertainties are provided for the different sources, including an estimate of spatial disaggregation errors deduced from a comparison with a global (EDGAR v4.2) and a European CH₄ inventory (TNO/MACC). This new spatially-explicit emission inventory for Switzerland will provide valuable input for regional scale atmospheric modeling and inverse source estimation.

1 Introduction

Most of the atmospheric methane (CH₄) produced in Switzerland results from anthropogenic activities. These emissions are well documented in the Swiss Greenhouse 15183

Gas Inventory (SGHGI, FOEN, 2013) that is updated and communicated to the UN-FCCC on an annual basis. In contrast, the latest estimate for natural CH4 fluxes including lakes, wild animals, wetlands and forest soils (SAEFL, 1996) is outdated and was never compared with actual measurements taken in Switzerland. In 2011, the agri-5 cultural sector contributed 84.6 % to the total anthropogenic CH₄ emissions of 178 Gg CH₄ yr⁻¹, while the waste management and the energy sector added another 8.3% and 6.8 %, respectively (FOEN, 2013). Since 1990, CH₄ emissions have decreased by about 20% in Switzerland (FOEN, 2013). One reason is the decline in livestock numbers over the last 20 yr, mainly caused by changes in federal legislation. Emissions from natural gas distribution decreased due to the replacement of old infrastructure (Xinmin, 2004). However, this replacement process is now completed (Xinmin, 2004) and, combined with the projected higher demand for natural gas due to the new Swiss energy strategy (SFOE, 2012a), emissions are expected to increase again. Disposal of combustible waste in landfills has been prohibited since 2000 in Switzerland and therefore emissions from this source are decreasing (FOEN, 2013). Counteracting this trend, emissions from biogas production have more than doubled since 1990 and are projected to rise even further (FOEN, 2013). Thus, a reliable base-line inventory for CH₄ emissions from anthropogenic activities and natural processes is urgently needed. Inventory estimates such as those presented in the SGHGI are based on numerous assumptions and statistical data that are associated with large uncertainties in several categories. Hence, validation by independent means is essential. Attempts have been

made to constrain regional or national CH_4 emissions by atmospheric concentration measurements using boundary-layer budgets (Gallagher et al., 1994; Choularton et al., 1995; Fowler et al., 1996; Beswick et al., 1998; Wratt et al., 2001), inverse emission modeling (Vermeulen et al., 1999; Bergamaschi et al., 2005; Manning et al., 2011; Polson et al., 2011; Wennberg et al., 2012), or by discriminating individual sources with help of the isotopic signature of CH_4 (Levin et al., 1999; Lowry et al., 2001; Miller, 2005). Studies of CH_4 fluxes in Switzerland mainly concentrated on measurements at a few selected sites and typically focused on improving process-level understanding

rather than on providing representative numbers for national emission budgets. Only one single attempt has so far been made to upscale CH₄ flux measurements to national totals or to validate the Swiss CH₄ inventory with atmospheric measurements (Hiller, 2012).

In order to model the influence of CH₄ emissions on atmospheric concentrations, spatially-explicit inventories are needed in addition to total national emissions (Bun et al., 2010). To disaggregate emissions to a higher spatial resolution, detailed knowledge on the location and the activity of each source is required, leading to additional uncertainty (Ciais et al., 2010). In recent years, the increasing targeting of the atmospheric and inverse modeling community on the regional and urban scale led to a clear trend towards high-resolution inventories. Currently, four different CH₄ inventories include Switzerland. EDGARv4.2, EDGAR-HTAP and TNO-MACC focus on anthropogenic emissions, NatAir considers only natural and biogenic emissions (details are shown in Table 1); thus, no inventory combines all CH₄ sources. Although these inventories have benefited from a considerable increase in resolution (e.g. EDGAR changed in 2009 from 1° × 1° to 0.1° × 0.1°), they are still limited to cell sizes of about 10 km × 10 km. For a spatially heterogeneous country such as Switzerland, this resolution is still too coarse to capture local variations.

The goal of this study was to produce the first gridded, high-resolution (500 m×500 m) CH₄ inventory for Switzerland. Anthropogenic emission estimates followed the methodologies of the SGHGI (FOEN, 2013). National totals were either spatially disaggregated across Switzerland using respective correlated geostatistical data with at least 500 m × 500 m spatial resolution, or generated in a bottom-up approach using emission factors (EFs). The SAEFL (1996) fluxes were updated and total emissions for all relevant categories are reported together with their uncertainties. The additional uncertainty at the grid level introduced by the spatial disaggregation was estimated by comparing different inventories. For each source category, a brief review of recent research studies in Switzerland is presented and the results from field studies are compared with the inventory estimates where possible.

15185

2 Data collection and processing

Our spatially-explicit inventory is based on the SGHGI for anthropogenic emissions and additionally comprises natural fluxes. National emission totals were distributed onto a 500 m × 500 m grid according to correlated geostatistical data. Natural sources without up-to-date national totals available were up-scaled and spatially attributed using geostatistical data. Emission factors were adapted from the literature, including dedicated studies for Switzerland. The spatially-explicit inventory was generated for the year 2011, which is the latest year available from the SGHGI. Sources are represented by positive numbers, sinks by negative numbers.

10 2.1 Swiss anthropogenic greenhouse gas inventory (SGHGI)

The latest submission of the SGHGI to the UNFCCC on 15 April 2013 reports greenhouse gas (GHG) emissions by sources and removals by sinks between 1990 (base year) and 2011 (FOEN, 2013). A detailed description of the institutional arrangements for inventory preparation, data sources and methodologies, uncertainty evaluations as well as quality assurance/quality control (QA/QC) activities are given in the SGHGI (FOEN, 2013). The inventory preparation follows the reporting guidelines developed by the Intergovernmental Panel on Climate Change (IPCC) (IPCC, 1997, 2000, 2003, 2006). To estimate GHG emissions and removals following the IPCC methodology, three approaches differing in complexity (so-called tiers) can be used. The Tier 1 methodology uses generalized default equations and parameters provided by the IPCC guidelines. Tier 2 employs country-specific input data, providing more detail of the underlying processes with regional specificities. Tier 3 is the most complex approach in terms of capturing dynamic processes and their spatial stratification, involving domestic measurements and/or modeling. The UNFCCC encourages parties to develop Tier 3 methods for large sources and sinks as well as for those with temporal trends, the so-called key categories (IPCC, 2000). Switzerland is currently working to include more country-specific information for the next commitment period 2013-2020.

For the spatially-explicit inventory, the eight strongest CH_4 sources out of a total of 620 listed in the SGHGI (FOEN, 2013) were selected, adding up to about 90% of all anthropogenic CH_4 emissions. These eight sources include emissions from the agricultural sector (41% from enteric fermentation of dairy cattle, 17% from young cattle, 5% from suckler cows, 2% from sheep, 9% from manure of dairy cattle and 5% of swine), the waste sector (5% from landfills), and the energy sector (5% from losses from natural gas distribution), where percentages in parentheses represent the share of the total 2011 anthropogenic emission estimate of 178 Gg. Additionally, we also compiled a spatial inventory of the emissions from wastewater treatment plants as these act as strong local sources.

2.1.1 Agricultural sector

The largest agricultural source in the SGHGI is *4.A Enteric Fermentation* followed by *4.B Manure Management* (the headings and numbers correspond to the official nomenclature for reporting, see Table 2). Agricultural residue burning is only a small source in Switzerland and reported in the sector *6. Waste*, whereas emissions from agricultural soils, rice production, and burning of savannas are negligible.

The 57 600 registered farms manage about one third of Switzerland's area $(15\,000\,\mathrm{km}^2)$ including alpine pastures; FSO, 2013) and rear animals equivalent to 1316 600 livestock units (FSO, 2011).

Agricultural CH₄ emissions from livestock result from the microbial degradation of carbohydrates present in the rumen of ruminants, and to a lesser extent also in the hindgut of all herbivores (Jensen, 1996). Additionally, carbohydrates that are not digested and thus are excreted as volatile solids can subsequently be converted to CH₄ during manure management. Overall, the CH₄ production from enteric fermentation is primarily related to feed intake, standardized by using gross energy intake (GE) for inventory purposes. Intake differences quite reliably reflect variations in animal weight and performance (milk yield, growth, and pregnancy) and corresponding differences in CH₄ emissions (Soliva, 2006). However, variation in feed composition, i.e. in the sub-

15187

strates for the methanogenic archaea, is not accounted for. CH₄ production is assumed to decline when forage is partially replaced with concentrate in the ruminant diet (Beauchemin et al., 2008), but this reduction is often smaller than assumed, and about one third of this reduction may be subsequently compensated by correspondingly higher manure-derived CH₄ emissions (Hindrichsen et al., 2006). Since Swiss ruminant diet types are mostly forage-based, CH₄ conversion rates measured in Switzerland are higher than IPCC (2006) default values (Zeitz et al., 2012). On the other hand, experiments on CH₄ emissions from Swiss manure management result in lower emissions than currently estimated in the SGHGI using IPCC (2006) default values (Zeitz et al., 2012). In particular, emissions from liquid manure systems tend to be lower than those currently reported. The influence of animal genotype on the CH₄ emission potential is currently discussed at the global level, but Swiss studies do not indicate significant differences between dairy breeds (Münger and Kreuzer, 2006). In conclusion, preliminary analyses suggest no significant change in CH₄ emissions from livestock by applying Swiss-specific EFs (Zeitz et al., 2012), as different under- and overestimates compensate each other. However, this conclusion does not yet consider the potential to reduce GHG emissions using different feeding measures (addition of lipids, plant secondary compounds, etc.; see e.g., Beauchemin et al., 2008; Staerfl et al., 2012).

For our spatially-explicit inventory, emissions were calculated from livestock numbers in 2007, aggregated by farm (agricultural establishment census 2007; FSO, 2009), and multiplied with animal-specific EFs from the Swiss national air pollution database (EMIS, Federal Office for the Environment). Emissions for 2007 were then scaled to the 2011 value reported in the SGHGI. Following the Swiss husbandry practice, most emissions were assumed to be produced in the stall (80% for cattle, 20% for sheep, 100% for swine) and the remaining fraction on the pastures. The agricultural establishment census contains the location of the main farm building at one hectare resolution and was assumed identical to the stable and manure storage location (Kupper et al., 2010). Emissions on pastures were attributed to all grid cells covered by this land use type (Swiss land use statistics; FSO GEOSTAT, 2009) within the community of the re-

spective farm. As part of the Swiss farming practice, part of the livestock is moved to alpine pastures in summer. Consequently, the CH_4 emissions produced there were also allocated on those alpine pastures ($\approx 4\%$ of the agricultural emissions included in the spatially-explicit inventory).

5 2.1.2 Waste management

Within the waste management sector, CH₄ emissions originate mainly from *6.A Solid Waste Disposal on Land*, *6.B Wastewater Handling*, and *6.D Other* processes, including composting, digestion of organic waste, and biogas up-grading.

Landfills

Gas production by decomposition of organic material in the anoxic waste body (typically 50–70 % CH₄ (v/v), 30–50 % CO₂, and trace amounts of other gases; Farquhar and Rovers, 1973) leads to advective and diffusive gas transport within the landfill pore system and eventually to emissions to the atmosphere (e.g. Franzidis et al., 2008).

Recent research activities related to landfill-derived CH₄ in Switzerland are limited to the municipal waste landfill Lindenstock near Liestal. This 12 ha landfill received $\approx 3.2 \times 10^6 \, \text{m}^3$ of household, construction, and commercial waste between 1949 and 1994. Following closure, the waste was capped with a 2 to 2.5 m thick cover soil consisting primarily of silty loam, and a gas-collection system was installed constructed of vertical and horizontal, partially-screened, high density polyethylene pipes. However, gas collection has not been attempted in recent years, and gas outlets remain closed with screw-cap lids. This is a unique feature of this landfill as gas-collection systems on several other Swiss landfills are either in continuous operation or absent.

Experiments at Lindenstock compared CH_4 fluxes obtained by different methods (Gómez et al., 2009; Eugster and Plüss, 2010; Schroth et al., 2012) at or above the cover-soil surface, as well as below-ground fluxes. Results indicated that the studied section of the landfill was predominantly a net source of CH_4 , with highest emis-

15189

sions close to the gas-collection outlets (daily mean fluxes ranging between 0.05 and $1.5\,\mathrm{g\,CH_4\,m^{-2}\,d^{-1}}$) (Henneberger et al., 2012; Schroth et al., 2012). A net flux of up to $-0.002\,\mathrm{g\,CH_4\,m^{-2}\,d^{-1}}$ (uptake) was usually observed away from the gas-collection outlets. CH₄ efflux from the waste body was highly variable over short distances and time. CH₄ oxidation activity in the cover soil was generally high, mitigating most of the produced CH₄, but also exhibiting substantial spatial variability (estimated to -1.92 to $-64\,\mathrm{g\,CH_4\,m^{-2}\,d^{-1}}$ in 2010) being strongest where efflux from the waste body was highest. Mitigation of landfill-derived CH₄ in the Lindenstock cover soil is mediated by a highly diverse, abundant methanotrophic community (Henneberger et al., 2012, 2013). Similar experiments during winter indicated stronger net CH₄ emissions (up to $2.5\,\mathrm{g\,CH_4\,m^{-2}\,d^{-1}}$) from the studied landfill section (Ugolini et al., 2009). This was primarily attributed to a decrease in oxygen availability within the cover soil as a result of increased soil water content at shallow depths, but also to a decrease in temperature, which both adversely affected the CH₄ oxidation activity.

These results from Lindenstock are not sufficiently representative for estimating total landfill emissions in Switzerland, but they broadly agree with previous studies on landfills in Europe and the USA, reporting oxidation activities in a similar but higher range. Hence, cover soils in general provide an effective buffer for landfill-derived CH₄, mitigating emissions to the atmosphere as a result of the activity of methanotrophs (Whalen et al., 1990; Boeckx et al., 1996; Börjesson et al., 1998; Chanton et al., 2009; Gebert et al., 2009; Park et al., 2010).

Characteristics of the individual landfills, such as waste composition, dumping period, etc., were not available for Switzerland. Therefore, the national emissions of $8.6\,\mathrm{Gg\,CH_4\,yr^{-1}}$ as reported in the SGHGI FOEN (2013) were proportionally distributed to the hectares classified as landfills in the land use statistics (FSO GEOSTAT, 2009) for our spatially explicit inventory.

Wastewater treatment

CH₄ is produced in the sewage system as well as in the anoxic part of the wastewater treatment plant and the upgrading of sewage gas. To our knowledge, no direct wastewater CH₄ measurements exist for Switzerland; however, the CH₄ emissions can be estimated from the organic load in the wastewater. The chemical oxygen demand (COD) ranges from 100 to 110 gCOD person⁻¹ d⁻¹, with one third each being aerobically respired, converted to CH₄, and remaining in the sewage sludge. A large part of the CH₄ produced is used for power and heat supply of the wastewater plant, and only about 10 % is directly emitted to the environment. The resulting EF of 0.9 g CH₄ person⁻¹ day⁻¹ lies within the range of reported conversion rates by Dealman et al. (2012) of 0.08% to 1.2% of kg CH_4 (kg COD)⁻¹. The amount of released CH₄ also depends on the sewage system (higher with long pipes at low inclination) and the plant type (higher with uncovered anoxic post-digester). Using an average EF of 0.9 g CH₄ person⁻¹ day⁻¹ and a 12 million population equivalent (Swiss population plus industrial wastewater load converted to additional population), annual emissions from wastewater collection and treatment result in about 4 Gg CH₄ yr⁻¹. However, a recent publication proposes a higher EF of 1.5 g CH₄ person⁻¹ day⁻¹, arguing that CH₄ production in the sewage system was underestimated (Wunderlin et al., 2013). The resulting CH₄ emissions would increase by 50 % to about 6 Gg CH₄ yr⁻¹. In contrast, the SGHGI is based on a completely different method reporting only 0.48 Gg CH₄ yr⁻¹, because the emissions are estimated from loss rates within the individual plant units and the total CH₄ used for energy or biogas production. Hence, emissions from tanks that are not connected to the gas system and emissions in the sewage are not included. To be consistent with the SGHGI, we proportionally distributed the 0.48 Gg CH₄ yr⁻¹ to the 854 plants in Switzerland based (Foen, 2012) on their capacity expressed in population equivalents. However, emissions might turn out up to a factor twelve higher using alternative estimation approaches.

15191

2.1.3 Energy sector

Total CH₄ emissions in the energy sector are divided into the subcategories 1.A Fuel Combustion, where most emissions originate from road transportation and residential heating, and 1.B Fugitive Emissions from Fuels. The latter emissions largely occur during the transmission of natural gas in pipelines (Category 1.B.2 Oil and Natural Gas; FOEN, 2013).

In Switzerland, 12.2 % of the total energy consumption was covered by natural gas in 2011 (SFOE, 2012b). Gas distribution in Switzerland includes $\approx 19\,000\,\mathrm{km}$ of pipelines, from which 12 % are operated at pressures $> 5\,\mathrm{bar}$, 23 % between 1 and 5 bar, and $65\,\% < 1\,\mathrm{bar}$. Another $\approx 6000\,\mathrm{km}$ of pipes guarantee the final distribution to the end user (SGWA, 2012). A large proportion of the transported gas transits Switzerland on the way from the production sites in northern Europe to Italy (Xinmin, 2004).

In the SGHGI, fugitive emissions of natural gas are estimated based on the amount of transported gas as well as on the infrastructure, namely the length, type and pressure of the gas pipelines (FOEN, 2013). Most emissions are assumed to occur during final distribution and consumption, while emissions from welded high-pressure pipes are assumed to be low (Xinmin, 2004). Therefore, emissions reported in the SGHGI were distributed close to the gas consumers for our spatially-explicit inventory. Based on the national buildings and dwellings survey (FSO, 2010), the national emissions were proportionally distributed to those areas where natural gas is used for heating, i.e., to each 1 ha grid cell where at least two houses are heated with natural gas. The emissions were subsequently aggregated onto the $500\,\mathrm{m} \times 500\,\mathrm{m}$ grid.

2.2 Natural and semi-natural CH₄ sources and sinks

The SGHGI only reports anthropogenic CH₄ emissions while natural and semi-natural fluxes are omitted, except for wildfires in the Land Use, Land-Use Change and Forestry (LULUCF) sector. CH₄ flux estimates reported in the SAFEL report (1996) were up-

dated based on new EF and compiled into our spatially-explicit inventory as described below.

2.2.1 Lakes and reservoirs

Approximately 3.5% of Switzerland (1450 km²) is covered by lakes and reservoirs (FSO GEOSTAT, 2009), which can emit significant amounts of CH₄ (Bastviken et al., 2011). These CH₄ emissions can occur via four main pathways: (1) standard gas exchange at the air—water interface; (2) ebullition (bubbling) from aquatic sediments; (3) turnover of a stratified water column with storage of CH₄ in (anoxic) bottom water; and (4) transport by plants in the shallow littoral zones (Chanton and Whiting, 1995; Bastviken et al., 2004). Hydropower reservoirs have an additional fifth emission pathway as they release water for energy production. Often the turbine intakes of a hydropower dam are located in the CH₄-rich bottom water of a stratified reservoir, thus CH₄ can be emitted via degassing at the turbine or along the downstream river to which the water is released (Kemenes et al., 2007). The most important sink for CH₄ in aquatic environments is oxidation, which occurs mostly at oxic/anoxic boundaries in the sediment (e.g. Frenzel et al., 1990) or water column (e.g. Schubert et al., 2010) and can account for a significant reduction of total CH₄ produced by decomposition of organic material in a lake before the CH₄ reaches the atmosphere.

Measuring all of these CH₄ transport pathways and their spatiotemporal variability in a single lake requires immense effort. Thus, often only a subset of all possible pathways is directly measured while others are either neglected or estimated from literature data. Truly accurate and validated models for estimating CH₄ emissions via all these pathways do not exist. An approach that can be used when attempting to estimate CH₄ emissions from a large amount of lakes without direct measurements is to use the equations proposed by Bastviken et al. (2004), which estimate diffusion, ebullition, and storage emissions based on comprehensive measurements from a collection of North American and European lakes (see Supplement for details). Bastviken et al. (2004) found significant relationships between the CH₄ emission estimates and measurable

variables, such as lake area, dissolved organic carbon and phosphorus concentrations, water depth, and volume of the anoxic fraction of the water column.

Following Bastviken et al. (2004), we estimated diffusion, ebullition and storage emissions of CH₄ from the lake areas of all major Swiss water bodies, but made the following modifications. (1) We tripled CH₄ emissions from lakes and reservoirs shallower than 30 m based on direct measurements of emissions from a small, shallow lake in the low alpine region which indicated high rates of ebullition (Schubert et al., 2012). (2) For the hydroelectric reservoir Lake Wohlen on the Swiss Plateau, we directly used the emission estimate of DelSontro et al. (2010) that was based on a year-long measurement study and results in a value ten times higher than that obtained with the method of Bastviken et al. (2004). No adjustments to any other reservoirs were made as Lake Wohlen may not be a representative system within Switzerland. (3) We provided a rough temporal variability of ebullition emissions by assuming that ebullition occurs only during the warmest half of the year as DelSontro et al. (2010) found a strong correlation between emissions and seasonal water temperatures. (4) Finally, we assumed ebullition not to be a relevant process in high alpine lakes at altitudes above 1500 ma.s.l. since they receive only little organic input, have low water temperature, and quite low CH₄ concentrations in the water column (Diem et al., 2012). The resulting emission factors are summarized in Table S1. The above presented modifications suggest that other factors in addition to those proposed by Bastviken et al. (2004) may need to be considered for estimating CH₄ emissions from lakes and reservoirs in the future.

The locations and areas of Swiss lakes and reservoirs were taken from the primary surfaces of the digital version of the Swiss topographical map at 1:25000 scale in vector format (VECTOR25; Swisstopo, 2004), while the depths for lakes > 0.1 km² were obtained from FOEN (2007a). We included all lakes that are contained in the Swiss water bodies information system (GEWISS; FOWG, 2000). Water depth data could not be found for 652 out of 798 lakes. Therefore, we assumed that the depth of lakes < 0.2 km² (678 lakes) is less than 30 m. Lake altitude was taken from the digital ele-

vation model (FSO GEOSTAT, 2006). In total, we found that lakes $> 0.1 \, \text{km}^2$ are emitting 2.1 Gg CH₄ yr⁻¹, with a 21 % (0.4 Gg CH₄ yr⁻¹) share from hydroelectric reservoirs. Smaller water bodies contribute another 0.2 Gg CH₄ yr⁻¹.

2.2.2 Wetlands

Wetlands are the largest natural source of CH₄ globally, where it is produced by microbial decomposition of organic material under anoxic conditions. However, wetlands have become rare in Switzerland (0.5%, 200 km², of the land area today compared to 6% in 1800; FOEN, 2007b). In our study, we also considered wetland areas of a mixed ecosystem type and hence a ten times larger area (see Table S2). They are classified as wetland on the basis of their high biodiversity, protected by the Swiss legislation on the protection of mires, rather than by their hydrogeological properties that would better reflect their characteristics in terms of CH₄ fluxes.

Most information on wetland CH_4 fluxes originate from the arctic, boreal, and tropical zones, and it is not trivial to translate those results to Swiss wetlands. An important complication is the fact that even in moist environments the vegetated surface may act as a net sink for atmospheric CH_4 when water saturation in the soil is limited to deeper layers or when drainage ditches lower the average water table (e.g. Moore and Roulet, 1993). In most cases it can be expected that periods where wetlands are a sink for CH_4 are restricted to a few warm and dry weeks a year, which reduces the overall annual CH_4 emissions from such ecosystems compared to permanently waterlogged wetlands.

In Swiss fens, CH_4 emission rates ranging from 100 to 330 mg CH_4 m⁻² d⁻¹ have been reported for the summer months (alpine fen at Göschener Alp, Liebner et al., 2012). Constant emissions between 0.12 and 31 mg CH_4 m⁻² d⁻¹ were also found from glacier forefields with calcareous bedrock (Nauer et al., 2012), while mires on siliceous bedrock were either a weak source of CH_4 (38 % of all cases), neutral (31 %), or a CH_4 sink (31 %; -0.14 to -1.1 mg CH_4 m⁻² d⁻¹; Nauer et al., 2012). Even in the case of

15195

large emissions from calcareous glacier forefields, Nauer et al. (2012) observed that roughly 90 % of the CH₄ produced in the deeper soil was oxidized before it reached the soil surface and the atmosphere. This agrees with other studies which indicate that in the top centimeters of the soil above the water table, where oxygen is abundant, most of the CH₄ produced by methanogenic archaea is oxidized and hence the flux of CH₄ to the atmosphere is substantially lower than what microorganisms produce (e.g. King et al., 1998).

For our spatially-explicit inventory, CH_4 emissions from Swiss wetlands were estimated from the wetland areas in Switzerland and literature-based EFs available for different wetland types as summarized in Table S2. Different types of wetland areas were determined from the national inventories of raised bogs, fens and mires (FOEN, 2008b, 2010) as well as of riparian landscapes (FOEN, 2008a). Additionally, the wetland core and sprawl areas reported in the national ecological network (FOEN, 2011b) were included in the analysis since these contain additional wetlands of regional and local importance. For the emission estimate, polygons were mapped to a $100\,\mathrm{m} \times 100\,\mathrm{m}$ raster. Grid cells classified by one of the different types of wetlands were subsequently multiplied with the corresponding EF. If a grid cell belonged to more than one wetland type, the one with highest priority was selected. The priority refers to the level of detail of the data set (e.g. specification of different zones within a wetland) and the importance of a wetland type for CH_4 emissions. As a final step, the data were averaged to the $500\,\mathrm{m} \times 500\,\mathrm{m}$ grid. In total, Swiss wetlands are estimated to emit approximately $2.3\,\mathrm{Gg}\,CH_4\,\mathrm{yr}^{-1}$.

2.2.3 Wild animals

Red and roe deer, alpine chamois and alpine ibex are the most abundant wild living ruminants in Switzerland. CH₄ emissions from these wild animals were estimated from the animal population estimates at cantonal (state) level in 2011 (except for Canton of Jura: 2006 and Canton of Vaud: 2009) (FOEN, 2011a). We multiplied these animal populations by the respective species dependent EF in SAEFL (1996) (see Table S3). The

spatial distribution depends on the habitat of the animals. While red deer prefer dense and open forest, row deer prefer dense forest. Alpine chamois prefer unproductive vegetation as well as rocks and scree, while Alpine ibex mainly thrive on rocks and scree. The respective land cover types were selected from the Swiss land-use statistic (FSO GEOSTAT, 2009). Additionally, the locations of these alpine habitats were restricted to altitudes above 1500 m a.s.l. (FSO GEOSTAT, 2006).

The number of large wild animals (260 000 red and roe dear, alpine chamois and alpine ibex) in Switzerland (FOEN, 2011a) is substantially less than the 1 580 000 cattle (FSO, 2011) in the agricultural sector. Moreover, wild animals are smaller in size and show a smaller energy uptake than cattle. This results in a comparatively low emission estimate of $1.1 \, \text{Gg CH}_4 \, \text{yr}^{-1}$.

SAFEL (1996) also reported substantial emissions of 2.8 Gg ${\rm CH_4\,yr^{-1}}$ from rodents. Radar measurements of the mice density on Swiss fields resulted in an average of 9000 mice km⁻² (AGFF, 2012), while the rabbit density was estimated as 2.7 rabbits km⁻² (Zellweger-Fischer, 2012). Scaled to the 10 500 km² agricultural area in Switzerland (FSO, 2011), this translates to \approx 94.5 mio. mice and 28 350 rabbits. Multiplied with the EFs of 0.26 g ${\rm CH_4\,mouse^{-1}\,yr^{-1}}$ (Jensen, 1996) and 80 g ${\rm CH_4\,rabbit^{-1}\,yr^{-1}}$ (IPCC, 2006), the annual emissions result in 0.027 Gg ${\rm CH_4\,yr^{-1}}$, which is far less than previously assumed and does not represent a significant contribution to the emissions from wild animals. Hence, rodents were not included in our spatially-explicit inventory.

2.2.4 Agricultural soils

Two counteracting processes – methanogenesis and methanotrophy – drive the net exchange of CH₄ between agricultural soils and the atmosphere. In Switzerland, the agricultural sector comprises typical crop production on arable land (18%) and comparatively large areas of grasslands (49%) and alpine summer pastures (33%), adding up to 15 000 km², corresponding to more than one third of the total area of Switzerland (FSO GEOSTAT, 2009; FSO, 2011). Several studies conducted at managed grasslands

15197

and alpine pastures in Switzerland have reported small CH4 uptake rates by soils (Hartmann et al., 2010; Stiehl-Braun et al., 2011; Imer et al., 2013; Merbold et al., 2013), which is also supported by other studies (Mosier et al., 1991; Flessa et al., 1998; Ineson et al., 1998; van den Pol-van Dasselaar et al., 1999; Kammann et al., 2001). The CH_4 fluxes depend on multiple drivers such as water filled pore space, soil and air temperatures, nutrient availability, management activity such as fertilizer application or tilling, and soil texture. These drivers are site-specific, but also change temporally at a single site. Recent results from three grassland sites in Switzerland reveal large temporal and spatial variations in CH₄ fluxes from managed ecosystems (Imer et al., 2013) ranging from a small sink $(-1.37 \text{ mg CH}_4 \text{ m}^{-2} \text{d}^{-1})$ to a slight source $(0.59 \text{ mg CH}_4 \text{ m}^{-2} \text{d}^{-1})$ on a daily timescale, and averaging to an annual mean flux of $-0.21\,\text{mg}\,\text{CH}_{\!_4}\,\text{m}^{-2}\,\text{d}^{-1}$ and $-0.30\,\text{mg}\,\text{CH}_4\,\text{m}^{-2}\,\text{d}^{-1}$ for two sites with almost year-round measurements (Imer et al., 2013). To the best of our knowledge, these are the only two year-round data sets that exist in Switzerland, leading to large uncertainties when up-scaling to the total area of managed agroecosystems. We expect the annual net CH₄ flux for Switzerland to range between 0 and $-1.5 \,\text{Gg} \,\text{CH}_4 \,\text{yr}^{-1}$ (EF: $-0.14 \pm 0.14 \,\text{mg} \,\text{CH}_4 \,\text{m}^{-2} \,\text{d}^{-1}$; Freibauer, 2003) for the 10 500 km² agricultural land excluding Alpine pastures, being a small sink. This is comparable in magnitude to other natural fluxes, but does not significantly contribute to the total CH₄ budget of Switzerland. Since CH₄ uptake across the agricultural areas is highly spatially variable, we did not attempt to spatially distribute this small CH₄ sink across Switzerland in our study.

2.2.5 Forest soils

The net CH₄ flux of forest soils is again dominated by the two counteracting processes, methanogenesis and methanotrophy. The available literature suggests that forests soils generally are a larger CH₄ sink than agricultural soils due to higher soil gas diffusivity in these systems (Smith et al., 2000). CH₄ fluxes over Swiss forest soils have been investigated only very recently (Frey et al., 2011; Gundersen et al., 2012; Hiltbrunner

et al., 2012). Interestingly, uptake rates of $-1.5\,\mathrm{mg}\,\mathrm{CH_4}\,\mathrm{m^{-2}}\,\mathrm{d^{-1}}$ for forest soils were found, which changed to a $\mathrm{CH_4}$ source of up to $2\,\mathrm{mg}\,\mathrm{CH_4}\,\mathrm{m^{-2}}\,\mathrm{d^{-1}}$ when soils were compacted by forestry machinery (Frey et al., 2011). These soil emissions persisted for several years (S. Zimmermann, personal communication, 2012), but were limited to relatively small areas compared to the total forest extent. Effects of soil compaction were therefore not considered in our spatially-explicit inventory.

To estimate the CH $_4$ uptake by Swiss forests, we followed a method developed by Hobi et al. (2011). Forest cover was derived from the land-use statistics (FSO GEO-STAT, 2009), and forest type information was taken from the $25\,\mathrm{m}\times25\,\mathrm{m}$ forest mixture data set (FSO GEOSTAT, 2004) and thereafter aggregated to $100\,\mathrm{m}\times100\,\mathrm{m}$. CH $_4$ uptake rates differ significantly between evergreen ($-0.46\pm0.27\,\mathrm{mg}$ CH $_4\,\mathrm{m}^{-2}\,\mathrm{d}^{-1}$) and deciduous forest soils ($-1.12\pm68\,\mathrm{mg}$ CH $_4\,\mathrm{m}^{-2}\,\mathrm{d}^{-1}$), according to the literature reviewed by Hobi et al. (2011). Forest areas were therefore multiplied with the uptake rate appropriate for the type of forest at a 1 ha resolution. For mixed forests an average rate was used. Finally, the data were averaged to a $500\,\mathrm{m}\times500\,\mathrm{m}$ grid. Overall, our estimate of CH $_4$ net flux of forest soils is $-2.8\,\mathrm{Gg}$ CH $_4\,\mathrm{yr}^{-1}$ for 2011.

3 Results and discussion

3.1 Spatially-explicit CH₄ inventory

Anthropogenic emissions are strongly dominating total Swiss CH₄ emissions and mostly originate from agriculture (see Table 2). Hence, the highest emissions are observed in the southern part of the Swiss Plateau, an area dominated by livestock farming between the pre-Alps to the south and the Jura mountains to the north, covering approx. 30% of Switzerland (Figs. 1 and 2a). Due to the proximity to the Alps, this region receives more precipitation than the rest of the Swiss Plateau and is therefore less suited for production of vegetable and cereal, which are mainly cultivated in the northern and western parts of the Swiss Plateau. The central and northern parts of

the Swiss Plateau are densely populated and consequently less land is dedicated to agriculture, which corresponds to relatively low emissions in this region. In the Alps, agricultural activity is concentrated on the valley floors. During the summer months, part of the livestock is moved to Alpine pastures for grazing to save the resources in the valley for the winter. This practice is part of the traditional Swiss three-stage farming system (Bätzing, 2003) and therefore CH_4 emissions can also be found in relatively remote areas of the Alps.

 ${\rm CH_4}$ emissions from waste management (Fig. 2b) are more abundant in regions with high population density. This also applies to the energy sector (Fig. 2c), where highest ${\rm CH_4}$ emissions occur in urban areas because natural gas is distributed to private households for cooking and heating.

Natural and semi-natural CH₄ emissions from lakes, wetlands, and wild animals (Fig. 2d-f) as well as the uptake by forest soils (Fig. 2f) are considerably lower than anthropogenic emissions (Table 2). Natural lakes in Switzerland are remnants from previous glaciations. The largest lakes are located in the lowlands, while many small lakes are found throughout the country. Reservoirs are mainly situated in Alpine areas to exploit the descent for hydropower generation (Fig. 2f). Since the large wetlands in the floodplains were drained for agricultural use in the 19th and 20th centuries, highest emissions from this ecosystem type are limited today to shore areas and to hilly landscapes where agriculture is less favorable (Fig. 2d). Wild animals are more abundant in rural areas with continuous forests, the preferred habitat for many species. Alpine ibex and chamois also populate remote and sparsely vegetated mountainous areas (Fig. 2e). Forests cover mountain slopes up to the timberline, protecting from natural hazards. At lower elevations, forests were often converted into agricultural land during the last centuries, but some remained and are protected today by law. While wild animals living in the forest are a source of CH₄, the forest soil acts as a sink. Deciduous forests are limited to lower elevations whereas evergreen forests dominate in higher elevations. Due to the lower uptake rate of evergreen forests, CH₄ uptake by forest soil tends to decrease with elevation.

3.2 Comparison with other inventories

The EDGAR v4.2 inventory and the TNO/MACC inventory in Fig. 3 show spatial distributions of total anthropogenic CH_4 emissions over Switzerland for the latest available years of 2008 and 2009, respectively. These maps can be qualitatively compared with the total emissions of our inventory presented in Fig. 1, where anthropogenic emissions make up more than 95 %.

Total emission of EDGAR v4.2 clipped to the domain of Switzerland amount to 233 Gg for 2008 consistent with the country total of 236 Gg reported by EDGAR v4.2 for Switzerland. This total is almost 30 % higher than the 183 Gg reported in the SGHGI for the same year. The TNO/MACC inventory adds up to 189 Gg over the domain of Switzerland in 2009, which is very close to the 180 Gg in the SGHGI for 2009 (FOEN, 2013). The difference between EDGAR and TNO/MACC likely reflects the fact that EDGAR is an independent inventory applying its own methodologies for the collection of activity data, application of emission factors, and spatial allocation. The TNO/MACC inventory, in contrast, is scaled to total emissions reported by the individual countries. In both inventories, the spatial allocation of the emissions is based on different and less detailed geostatistical information than available in our study. Emissions in the EDGAR inventory are higher in densely populated regions but lower in agriculturallydominated regions compared to our inventory (Fig. 3c), suggesting that the EDGAR inventory is too dependent on population density. Differences are less pronounced between the TNO/MACC inventory and our inventory (Fig. 3d). The TNO/MACC inventory correctly identifies the regions of farming in the southern parts of the Swiss Plateau but the emissions tend to be higher in these areas and lower in the mountains compared to our inventory. The spatial differences are further assessed in Sect. 3.3.1 to obtain a rough estimate of the uncertainty associated with the spatial disaggregation.

For natural CH_4 emissions, we only compare our country totals with numbers reported in an earlier study for Switzerland (SAEFL, 1996). Compared to that study, our estimates are considerably lower. Forests were considered a significant CH_4 source

15201

(50 Gg CH $_4$ yr $^{-1}$) in the former study, which was based on much more limited information. However, in the past two decades, no evidence for such strong CH $_4$ emissions could be found in Switzerland, and hence our updated estimate suggests that forests are a net CH $_4$ sink instead (net flux of -2.3 to -3.2 Gg CH $_4$ yr $^{-1}$) (Hobi, 2011). Moreover, contributions from small wild animals, namely rodents, are estimated to be much lower (0.027 Gg CH $_4$ yr $^{-1}$) than previously (2.8 Gg CH $_4$ yr $^{-1}$). Our findings indicate that agricultural soils may act as a small net sink (net flux of -1.5 Gg to 0 CH $_4$ yr $^{-1}$), while emissions of up to 2.1 Gg CH $_4$ yr $^{-1}$ were previously attributed to this type of ecosystem. In contrast, lakes had been estimated to be CH $_4$ neutral, whereas our findings suggest that they are a source of 2.3 Gg CH $_4$ yr $^{-1}$. Only the previous estimates for large wild animals (0.9 Gg CH $_4$ yr $^{-1}$) and wetlands (1.2 Gg CH $_4$ yr $^{-1}$) compare well with our study (1.1 Gg CH $_4$ yr $^{-1}$ and 2.3 Gg CH $_4$ yr $^{-1}$, respectively). Overall, the natural and semi-natural CH $_4$ emissions estimated in our study (5.7 Gg CH $_4$ yr $^{-1}$) are only about 10% of those reported by SAEFL (1996), but equates to 3% of the total CH $_4$ emissions in Switzerland.

3.3 Uncertainties of the inventory

For many purposes, and in particular for inverse modeling studies in which emission inventories are used as a priori estimates, it is important to quantify not only the distribution of the emissions but also its uncertainty. In the SGHGI (FOEN, 2013), an uncertainty is determined for each emission category based on errors associated with the activity data and the EFs. The combined uncertainties are listed in Table 2 together with the mean emissions for 2011. The uncertainty of the annual total emissions can then be computed as the square root of the sum of squares of the individual uncertainties, assuming uncorrelated errors. The uncertainty of the total Swiss anthropogenic CH₄ emissions is estimated to only 16 % (see Table 2), which is largely due to the low uncertainty of 18 % assigned by the SGHGI to the main emission source 4.A Enteric

Fermentation. It is interesting to note that this uncertainty is smaller than the difference between the SGHGI and the EDGAR v4.2 inventory.

For the uncertainty of emissions of a given grid cell at a given time, additional errors need to be considered, including errors associated with the spatial disaggregation and with the temporal variability as described in the following.

3.3.1 Spatial uncertainty

Uncertainties associated with the spatial disaggregation are difficult to assess. They depend on the accuracy of the spatial data sets, on quantization errors due to the use of discrete classes, and on the often crude assumptions made for spatial disaggregation. Therefore, we adopted a pragmatic approach by comparing the spatial distribution in our inventory with those of the EDGAR v4.2 and TNO/MACC inventories shown in Fig. 3 (see also Table 1). All inventories were first linearly scaled to the same country total. To determine a representative error correlation length scale, we analyzed the variogram of the residuals R, where R = E (this study) -E (REF), the difference between emissions in our spatially-explicit inventory E(this study) and emissions in a reference inventory E(REF) (EDGAR or TNO/MACC) (Fig. 4). A variogram describes the variance of the difference of a spatial variable R, i.e. var(R(x) - R(x + h)) as a function of the distance h (Cressie, 1993). The standard deviation of the residuals is larger for EDGAR than for TNO/MACC, which also results in a higher sill (see Fig. 4). As described in Lin and Gerbig (2005), a correlation length scale L can then be derived by fitting an exponential variogram model to the raw variogram. The length scale L obtained in this way was 13.0 km for EDGAR v4.2 and 8.0 km for TNO/MACC, which is close to the grid sizes of the two inventories, suggesting that their limited resolution is a constraining factor and that the true correlation length may be even smaller.

For each grid cell, the uncertainty was assumed to be a fraction f of the absolute emission in that cell. The fraction f was then determined based on the requirement that the uncertainties add up, following Gaussian error propagation, to the 16% uncertainty of the total country emissions. Thereby, the correlation length scale L was

used to compute the error covariances. Using this approach, the uncertainty of the individual $500\,\text{m}\times500\,\text{m}$ grid cells in our inventory was estimated as $110\,\%$ (mean of $85\,\%$ and $130\,\%$ determined for the two different length scales derived for EDGAR and TNO/MACC). Emissions in individual grid cells thus have a large uncertainty and could well be double or half as large as estimated.

3.3.2 Temporal variability

Our spatially-explicit inventory only includes annual mean emissions, but no seasonal and diurnal cycles due to a lack of suitable data. Nevertheless, we will briefly discuss the available temporal information relevant to our inventory to estimate the importance of temporal variability.

In the agricultural sector, livestock numbers are reported once a year in April, and seasonal fluctuations are only on the order of $\pm 3\,\%$, with census data slightly above the annual mean (Bretscher, 2010). Within the traditional Swiss three-stage farming system, cattle is moved to Alpine meadows in summer to save the fertile valley floor for crop and winter fodder production. Hence, the spatial allocation of CH₄ emissions from ruminants changes between summer and winter. In addition, CH₄ emissions from ruminants depend on animal metabolism; thus, emissions peak following feed intake with a delay of a few hours and therefore display a diurnal pattern. Kinsman et al. (1995), for example, reported an average 20 % higher emission during the day than during the night, while Gao et al. (2011) observed emissions peaks following the feeding rhythm.

Emissions from manure are lowest at low temperatures and increase with longer storage duration, peaking only after about two months (Hindrichsen et al., 2005, 2006; Klevenhusen et al., 2010). The storage period before application is typically longer in winter, but lower storage temperatures likely dominate the influence on CH₄ production. Manure storage practice further influences CH₄ emissions (Külling et al., 2001, 2002, 2003). Higher than average emissions from farmyard manure are compensated by lower emissions from urine-rich slurry, and on average do not differ significantly

compared to complete slurry. Hence, these differences are of no relevance compared to the effects of storage period and temperature.

Landfills in Switzerland are covered by a soil layer; therefore, no large seasonal temperature fluctuations are expected within the deposited waste. However, the cover soil, where CH_4 is oxidized by methanotrophs, undergoes seasonal temperature fluctuations. More importantly, moisture positively influences CH_4 production in the waste body and inhibits CH_4 uptake in the cover soil (Chanton and Liptay, 2000). Both factors are expected to lead to higher CH_4 emissions in winter than in summer (Klusman and Dick, 2000). Nevertheless, the available information is insufficient to quantify seasonal fluctuations of CH_4 emissions from Swiss landfills in general.

A large proportion of natural gas is used for heating and therefore consumption is more than four times higher in January than in July (VSG, 2012). $\mathrm{CH_4}$ emissions from leaking pipelines are therefore expected to be higher in winter than in summer, but no reliable data are available for proposing a seasonal cycle of these emissions.

Lake CH₄ emissions may exhibit a strong seasonal cycle similar to that found in a Swiss reservoir where emissions were positively correlated with water temperature (DelSontro et al., 2010). In addition, turnover of a seasonally stratified water column can also significantly contribute to the annual CH₄ emissions from lakes (Schubert et al., 2010), a quite common process in Swiss lakes. Thus, both processes lead to a pronounced seasonal cycle in CH₄ emissions from water bodies in temperate zones with higher emissions during summer than during winter (Sect. 2.2.1).

The above listed diurnal and seasonal cycles indicate that observed CH_4 fluxes on a single day at a given time may significantly differ from the annual mean fluxes reported in our spatially explicit inventory, but at present the available information is not sufficient to provide source-category specific time functions.

15205

4 Conclusions

A spatially-explicit high resolution CH₄ inventory was developed for Switzerland for the year 2011. This is the first comprehensive inventory at national level synthesizing most of the available Swiss datasets on anthropogenic as well as on natural and semi-natural fluxes. Anthropogenic emissions of 177 Ggyr⁻¹ in 2011 are by far larger than the emissions from all natural and semi-natural sources, which were estimated to only 5.7 Gg yr⁻¹, an order of magnitude less than an estimate reported in an earlier study on natural sources in Switzerland (SAEFL, 1996). Forest soils are estimated to be a net sink with a net flux of -2.8 Ggyr⁻¹ and agricultural soils are estimated to be CH₄ neutral or a small sink with a net flux between -1.5 and 0 Gg yr⁻¹ for agricultural soils, partially offsetting the natural emissions. In total, Switzerland acted as a net CH₄ source of 180 Gg CH₄ yr⁻¹ in 2011. With a share of nearly 85 %, agricultural emissions are by far the most important anthropogenic source in Switzerland, followed by the waste and energy sectors. The uncertainty of the total anthropogenic emissions is estimated to be only 16%, which is largely a result of the low uncertainty assigned to the largest single CH₄ source – enteric fermentation of ruminants. Detailed geospatial information is available for Switzerland, thereby allowing the spatial allocation of the individual emission sources. Information on temporal variability of CH₄ emissions, however, is very sparse and currently insufficient for prescribing diurnal and seasonal variations, an aspect that should be better addressed in future studies.

This inventory will provide invaluable input for regional-scale atmospheric modelling and inverse source estimation, which are urgently needed for independent validation of inventories based on atmospheric measurements. The spatial disaggregation of other ${\rm CH_4}$ sources currently not covered by this inventory, especially from biogas production and composting, might become more critical in the future with the expected increase of the relative importance of these sources.

Supplementary material related to this article is available online at http://www.biogeosciences-discuss.net/10/15181/2013/bgd-10-15181-2013-supplement.pdf.

Acknowledgements. We thank Martina Alig and Mireille Faist for their input on CH₄ emissions from biogas production and composting as well as Christoph Ort, Ivo Strahm, and Pascal Wunderlin on emissions from wastewater treatment. The many CH₄ flux measurements on lakes would not have been possible without the help of Beat Müller, Oliver Scheidegger, Gijs Nobbe, Zwyssig Alois, Michael Schurter, Daniel McGinnis, Sebastian Sobek, and Peter Plüss and were supported by the Swiss National Science Fondation grants no. 200020-112274 and 200021-120112. The contribution of Rurth Henneberger and Martin Schroth on land-fills was supported by the European Science Foundation EUROCORES Program EuroEEFG, project MECOMECON, with funds from the Swiss National Science Foundation under grant no. 31EE30-131170. Soil CH₄ emissions were carried out with the project GHG Europe funded by the European Union Seventh Framework Program (FP7/2007-2013) under grant agreement no. 244122 (GHG-Europe). This synthesis project as well as the joint project MAIOLICA were funded by the Competence Center Environment and Sustainability (CCES) of ETH Zurich.

References

- AGFF: Mäuse Radar: Übersicht Erhebungen 2012, Arbeitsgemeinschaft zur Förderung des Futterbaues (AGFF)/Agroscope Reckenholz Tänikon Research Station (ART), available at: http://www.agff.ch/deutsch/publikationen/maeusebekaempfung/maeuse-radar-2012.html (last access: 13 March 2013), 2012.
 - Bastviken, D., Cole, J., Pace, M., and Tranvik, L.: Methane emissions from lakes: dependence of lake characteristics, two regional assessments, and a global estimate, Global Biogeochem. Cy., 18, GB4009, doi:10.1029/2004GB002238, 2004.
- Bastviken, D., Tranvik, L. J., Downing, J. A., Crill, P. M., and Enrich-Prast, A.: Freshwater methane emissions offset the continental carbon sink, Science, 331, 593–596, doi:10.1038/ngeo1211, 2011.

- Bätzing, W.: Die Alpen: Geschichte und Zukunft einer Europäischen Kulturlandschaft, 3rd edn., C. H. Beck oHG, München, 431 pp., 2003.
- Beauchemin, K. A., Kreuzer, M., O'Mara, F., and McAllister, T. A.: Nutritional management for enteric methane abatement: a review, Aust. J. Exp. Agr., 48, 21–27, 2008.
- Bergamaschi, P., Krol, M., Dentener, F., Vermeulen, A., Meinhardt, F., Graul, R., Ramonet, M., Peters, W., and Dlugokencky, E. J.: Inverse modelling of national and European CH₄ emissions using the atmospheric zoom model TM5, Atmos. Chem. Phys., 5, 2431–2460, doi:10.5194/acp-5-2431-2005, 2005.
- Beswick, K. M., Simpson, T. W., Fowler, D., Choularton, T. W., Gallagher, M. W., Hargreaves, K. J., Sutton, M. A., and Kaye, A.: Methane emissions on large scales, Atmos. Environ., 32, 3283–3291, 1998.
 - Boeckx, P., Van Cleemput, O., and Villaralvo, I.: Methane emission from a landfill and the methane oxidising capacity of its covering soil, Soil Biol. Biochem., 28, 1397–1405, doi:10.1016/S0038-0717(96)00147-2, 1996.
- Börjesson, G., Sundh, I., Tunlid, A., Frostegard, A., and Svensson, B. H.: Microbial oxidation of CH₄ at high partial pressures in an organic landfill cover soil under different moisture regimes, FEMS Microbiol. Ecol., 26, 207–217, doi:10.1111/j.1574-6941.1998.tb00506.x, 1998.
- Bretscher, D.: Agricultural CH₄ and N₂O emissions in Switzerland: QA/QC, Agroscope Reckenholz Tänikon Research Station (ART), 56, available at: http://www.bafu.admin.ch/climatereporting/00545/01913/index.html?lang=en&download=NHzLpZeg7t, lnp6I0NTU042l2Z6ln1ad1IZn4Z2qZpnO2Yuq2Z6gpJCGd4N6g2ym162epYbg2c_ JjKbNoKSn6A-- (last access: 13 March 2013), 2010.
- Bun, R., Hamal, K., Gusti, M., and Bun, A.: Spatial GHG inventory at the regional level: accounting for uncertainty, Climatic Change, 103, 227–244, doi:10.1007/s10584-010-9907-5, 2010
- Chanton, J. and Liptay, K.: Seasonal variation in methane oxidation in a landfill cover soil as determined by an in situ stable isotope technique, Global Biogeochem. Cy., 14, 51–60, 2000.
- Chanton, J. P. and Whiting, G. J.: Trace gas exchange in freshwater and coastal marine environments: ebullition and transport by plants, in: Biogenic Trace Gases: Measuring Emissions from Soil and Water, edited by: Matson, P. A. and Harriss, R. C., Blackwell Science, 98–125, 1995.
- Chanton, J. P., Powelson, D. K., and Green, R. B.: Methane oxidation in landfill cover soils, is a 10 % default value reasonable?, J. Environ. Qual., 38, 654–663, 2009.

- Choularton, T. W., Gallagher, M. W., Bower, K. N., Fowler, D., Zahniser, M., Kaye, A., Monteith, J. L., and Harding, R. J.: Trace gas flux measurements at the landscape scale using boundary-layer budgets, Philos. T. Roy. Soc. A, 351, 357–369, doi:10.1098/rsta.1995.0039, 1995.
- Ciais, P., Paris, J. D., Marland, G., Peylin, P., Piao, S. L., Levin, I., Pregger, T., Scholz, Y., Friedrich, R., Rivier, L., Houwelling, S., and Schulze, E. D.: The European carbon balance. Part 1: fossil fuel emissions, Glob. Change Biol., 16, 1395–1408, doi:10.1111/j.1365-2486.2009.02098.x, 2010.
 - Cressie, N. A. C.: Statistics for Spatial Data, John Wiley and Sons, New York, 900 pp., 1993.
- Daelman, M. R. J., Van Voorthuizen, E. M., Van Dongen, U. G. J. M., Volcke, E. I. P., and Van Loosdrecht, M. C. M.: Methane emission during municipal wastewater treatment, Water Res., 46, 3657–3670, doi:10.1016/j.watres.2012.04.024, 2012.
 - DelSontro, T., McGinnis, D. F., Sobek, S., Ostrovsky, I., and Wehrli, B.: Extreme methane emissions from a Swiss hydropower reservoir: contribution from bubbling sediments, Environ. Sci. Technol., 44, 2419–2425, doi:10.1021/es9031369, 2010.
 - Diem, T., Koch, S., Schwarzenbach, S., Wehrli, B., and Schubert, C. J.: Greenhouse gas emissions (CO₂, CH₄, and N₂O) from several perialpine and alpine hydropower reservoirs by diffusion and loss in turbines, Aquat. Sci., 74, 619–635, doi:10.1007/s00027-012-0256-5, 2012.
- Eugster, W. and Plüss, P.: A fault-tolerant eddy covariance system for measuring CH₄ fluxes, Agr. Forest Meteorol., 150, 841–851, doi:10.1016/j.agrformet.2009.12.008, 2010.
 - Farquhar, G. J. and Rovers, F. A.: Gas production during refuse decomposition, Water Air Soil Poll., 2, 483–495, doi:10.1007/BF00585092, 1973.
 - Flessa, H., Wild, U., Klemisch, M., and Pfadenhauer, J.: Nitrous oxide and methane fluxes from organic soils under agriculture, Eur. J. Soil Sci., 49, 327–335, doi:10.1046/j.1365-2389.1998.00156.x, 1998.
 - FOEN: Seen in der Schweiz, Federal Office for the Environment (FOEN), available at: http://www.bafu.admin.ch/hydrologie/01835/02118/index.html?lang=de&download=NHzLpZeg7t, lnp6l0NTU042l2Z6ln1acy4Zn4Z2qZpnO2Yuq2Z6gpJCEdoF_gmym162epYbg2c_
- JjKbNoKSn6A-- (last access: 13 March 2013), 2007a.
 - FOEN: Zustand und Entwicklung der Moore in der Schweiz, in Umwelt-Zustand, vol. UZ-0730-D, Federal Office for the Environment (FOEN), 97 pp., 2007b.

- FOEN: Bundesinventar der Auengebiete von nationaler Bedeutung, Federal Office for the Environment (FOEN), available at: http://www.bafu.admin.ch/gis/02911/07403/index.html?lang=de (last access: 28 March 2013), 2008a.
- FOEN: Bundesinventar der Hoch- und Übergangsmoore von nationaler Bedeutung, Federal Office for the Environment (FOEN), available at: http://www.bafu.admin.ch/gis/02911/07403/index.html?lang=de (last access: 28 March 2013), 2008b.
 - FOEN: Bundesinventar der Flachmoore von nationaler Bedeutung, Federal Office for the Environment (FOEN), available at: http://www.bafu.admin.ch/gis/02911/07403/index.html?lang=de (last access: 28 March 2013), 2010.
- FOEN: Eidgenössische Jagdstatistik, Federal Office for the Environment (FOEN) available at: http://www.wild.uzh.ch/jagdst/ (last access: 13 March 2013), 2011a.
 - FOEN: Nationales ökologisches Netzwerk (REN: Lebensraum Feuchtgebiet), Federal Office for the Environment (FOEN), available at: http://www.bafu.admin.ch/gis/02911/07403/index. html?lang=de (last access: 28 March 2013), 2011b.
- FOEN: Kläranlagen-Datenbank (wastewater treatment plant database), Federal Office for the Environment (FOEN), 2012.
 - FOEN: Switzerland's greenhouse gas inventory 1990–2011, Submission of 15 April 2013 under the United Nations Framework Convention on Climate Change and under the Kyoto Protocol, Federal Office for the Environment (FOEN), available at: http://www.bafu.admin.ch/climatereporting/00545/12558/index.html?lang=en, last access: 15 April 2013, 2013.
- FOWG: Gewässerinformationssystem Schweiz GEWISS: Struktur und Adressierung digitaler Gewässernetze, Federal Office for Water and Geology (FOWG), available at: http://www.bafu.admin.ch/hydrologie/01835/02114/02116/index.html?lang=en&download=NHzLpZeg7t,lnp6l0NTU042l2Z6ln1ad1lZn4Z2qZpnO2Yuq2Z6gpJCEdoF_hGym162epYbq2c_JjKbNoKSn6A (last access: 2 June 2013), 21 pp., 2000.
- Fowler, D., Hargreaves, K. J., Choularton, T. W., Gallagher, M. W., Simpson, T., and Kaye, A.: Measurements of regional CH₄ emissions in the UK using boundary layer budget methods, Energ. Convers. Manage., 37, 769–775, 1996.
- Franzidis, J.-P., Héroux, M., Nastev, M., and Guy, C.: Lateral migration and offsite surface emission of landfill gas at City of Montreal landfill site, Waste Manage. Res., 26, 121–131, doi:10.1177/0734242X07085752, 2008.
- Freibauer, A.: Regionalised inventory of biogenic greenhouse gas emissions from European agriculture, Eur. J. Agron., 19, 135–160, doi:10.1016/S1161-0301(02)00020-5, 2003.

- Frenzel, P., Thebrath, B., and Conrad, R.: Oxidation of methane in the oxic surface layer of a deep lake sediment (Lake Constance), FEMS Microbiol. Lett., 73, 149–158, doi:10.1016/0378-1097(90)90661-9, 1990.
- Frey, B., Niklaus, P. A., Kremer, J., Lüscher, P., and Zimmermann, S.: Heavy-machinery traffic impacts methane emissions as well as methanogen abundance and community structure in oxic forest soils, Appl. Environ. Microb., 77, 6060–6068, doi:10.1128/AEM.05206-11, 2011.
- Friedrich, R.: NATAIR: Improving and applying methods for the calculation of natural and biogenic emissions and assessment of impacts to the air quality, available at: http://natair.ier.uni-stuttgart.de/NatAir_Final_Activity_Report.pdf (last access: 13 March 2013), 193 pp., 2007
- FSO: Landwirtschaftliche Betriebszählung (agricultural establishment census) 2007, Federal Statistical Office (FSO), 2009.
- FSO: Gebäude- und Wohnungserhebung (buildings and dwellings survey) 2000, ha-grid, Federal Statistical Office (FSO), 2010.
- FSO: Landwirtschaftliche Betriebszählungen und landwirtschaftliche Betriebsstrukturerhebungen, Federal Statistical Office (FSO), available at: http://www.sbv-usp.ch/de/statistik/ (last access: 13 March 2013), 2011.
 - FSO: Schweizer Landwirtschaft Taschenstatistik 2013, Federal Statistical Office (FSO), available at: http://www.bfs.admin.ch/bfs/portal/de/index/news/publikationen.Document.167626. pdf (last access: 31 May 2013), 35 pp., 2013.
 - FSO GEOSTAT: Waldmischungsgrad der Schweiz 1992/97, Federal Statistical Office (FSO), 2004
 - FSO GEOSTAT: Geländedaten (digital elevation model), Federal Statistical Office (FSO), available at: http://www.bfs.admin.ch/bfs/portal/de/index/dienstleistungen/geostat/datenbeschreibung/gelaendedaten.html (last access: 2 June 2013), 2006.
 - FSO GEOSTAT: Land use statistics, (Arealstatistik) 1992/97, ha-grid, Federal Statistical Office (FSO), 2009.
 - Gallagher, M. W., Choularton, T. W., Bower, K. N., Stromberg, I. M., Beswick, K. M., Fowler, D., and Hargreaves, K. J.: Measurements of methane fluxes on the landscape scale from a wetland area in North Scotland, Atmos. Environ., 28, 2421–2430, doi:10.1016/1352-2310(94)90394-8, 1994.

- Gao, Z., Yuan, H., Ma, W., Liu, X., and Desjardins, R. L.: Methane emissions from a dairy feedlot during the fall and winter seasons in Northern China, Environ. Pollut., 159, 1183– 1189, 2011
- Gebert, J., Singh, B. K., Pan, Y., and Bodrossy, L.: Activity and structure of methanotrophic communities in landfill cover soils, Environ. Microbiol. Rep., 1, 414–423, doi:10.1111/j.1758-2229.2009.00061.x, 2009.
- Gómez, K. E., Gonzalez-Gil, G., Lazzaro, A., and Schroth, M. H.: Quantifying methane oxidation in a landfill-cover soil by gas push-pull tests, Waste Manage., 29, 2518–2526, doi:10.1016/j.wasman.2009.05.011, 2009.
- Gundersen, P., Christiansen, J. R., Alberti, G., Brüggemann, N., Castaldi, S., Gasche, R., Kitzler, B., Klemedtsson, L., Lobo-do-Vale, R., Moldan, F., Rütting, T., Schleppi, P., Weslien, P., and Zechmeister-Boltenstern, S.: The response of methane and nitrous oxide fluxes to forest change in Europe, Biogeosciences, 9, 3999–4012, doi:10.5194/bg-9-3999-2012, 2012.
- Hartmann, A. A., Buchmann, N., and Niklaus, P. A.: A study of soil methane sink regulation in two grasslands exposed to drought and N fertilization, Plant Soil, 342, 265–275, doi:10.1007/s11104-010-0690-x, 2010.
 - Henneberger, R., Lüke, C., Mosberger, L., and Schroth, M. H.: Structure and function of methanotrophic communities in a landfill-cover soil, FEMS Microbiol. Ecol., 81, 52–65, doi:10.1111/j.1574-6941.2011.01278.x, 2012.
 - Henneberger, R., Chiri, E., Blees, J., Niemann, H., Lehmann, M. F., and Schroth, M. H.: Field-scale labelling and activity quantification of methane-oxidizing bacteria in a landfill-cover soil, FEMS Microbiol. Ecol., 83, 392–401, doi:10.1111/j.1574-6941.2012.01477.x, 2013.
- Hiller, R. V.: Greenhouse Gases From the Ecosystem Scale to a Regional Integration, available at: http://e-collection.library.ethz.ch/view/eth:5927 (last access: 28 February 2013), ETH Zurich, 179 pp., 2012.
 - Hiltbrunner, D., Zimmermann, S., Karbin, S., Hagedorn, F., and Niklaus, P. A.: Increasing soil methane sink along a 120-year afforestation chronosequence is driven by soil moisture, Glob. Change Biol., 18, 3664–3671, doi:10.1111/j.1365-2486.2012.02798.x, 2012.
- Hindrichsen, I. K., Wettstein, H. R., Machmüller, A., Jörg, B., and Kreuzer, M.: Effect of the carbohydrate composition of feed concentratates on methane emission from dairy cows and their slurry, Environ. Monit. Assess., 107, 329–350, doi:10.1007/s10661-005-3008-3, 2005.

- Hindrichsen, I. K., Wettstein, H. R., Machmüller, A., and Kreuzer, M.: Methane emission, nutrient degradation and nitrogen turnover in dairy cows and their slurry at different milk production scenarios with and without concentrate supplementation, Agr. Ecosyst. Environ., 113, 150–161, 2006.
- Hobi, S.: Spatial allocation of methane sources and sinks in Switzerland, ETH Zurich, 76 pp., 2011.
 - Imer, D., Merbold, L., Eugster, W., and Buchmann, N.: Temporal and spatial variations of CO₂, CH₄ and N₂O fluxes at three differently managed grasslands, Biogeosciences Discuss., 10, 2635–2673, doi:10.5194/bgd-10-2635-2013, 2013.
- Ineson, P., Coward, P. A., and Hartwig, U. A.: Soil gas fluxes of N₂O, CH₄ and CO₂ beneath Lolium perenne under elevated CO₂: the Swiss free air carbon dioxide enrichment experiment, Plant Soil, 198, 89–95, doi:10.1023/A:1004298309606, 1998.
 - IPCC: Greenhouse Gas Inventory: Reference Manual revised 1996, IPCC Guidelines for National Greenhouse Gas Inventories, IGES, Japan, available at: http://www.ipcc-nggip.iges.or.jp/public/gl/invs1.html (last access: 13 March 2013), 1997.
 - IPCC: Good Practice Guidance and Uncertainty Management in National Greenhouse Gas Inventories (IPCC GPG), Institute for Global Environmental Strategies (IGES), Japan, available at: http://www.ipcc-nggip.iges.or.jp/public/gp/english/ (last access: 13 March 2013), 2000.
- IPCC: Good Practice Guidance for Land Use, Land-Use Change and Forestry (IPCC GPG LULUCF), edited by: Penman, J., Gytarsky, M., Hiraishi, T., Krug, T., Kruger, D., Pipatti, R., Buendia, L., Miwa, K., Ngara, T., Tanabe, K., and Wagner, F., Institute for Global Environmental Strategies (IGES), Japan, available at: http://www.ipcc-nggip.iges.or.jp/public/gpglulucf/gpglulucf.html (last access: 15 March 2013), 2003.
- IPCC: 2006 IPCC Guidelines for National Greenhouse Gas Inventories, Institute for Global Environmental Strategies (IGES), Japan, available at: http://www.ipcc-nggip.iges.or.jp/public/2006gl/index.html (last access: 13 March 2013), 2006.
- Janssens-Maenhout, G., Dentener, F., Van Aardenne, J., Monni, S., Pagliari, V., Orlandini, L., Klimont, Z., Kurokawa, J., Akimoto, H., Ohara, T., Wankmueller, R., Battye, B., Grano, D., Zuber, A., and Keating, T.: EDGAR-HTAP: a harmonized gridded air pollution emission dataset based on national inventories, European Commission Publications Office, Ispra (Italy), 41 pp., 2012.
- Jensen, B.: Methanogenesis in monogastric animals, Environ. Monit. Assess., 42, 99–112, doi:10.1007/BF00394044, 1996.

- Kammann, C., Grünhage, L., Jäger, H.-J., and Wachinger, G.: Methane fluxes from differentially managed grassland study plots: the important role of CH₄ oxidation in grassland with a high potential for CH₄ production, Environ. Poll., 115, 261–273, doi:10.1016/S0269-7491(01)00103-8, 2001.
- Kemenes, A., Forsberg, B. R., and Melack, J. M.: Methane release below a tropical hydroelectric dam, Geophys. Res. Lett., 34, doi:10.1029/2007GL029479, 2007.
 - King, J. Y., Reeburgh, W. S., and Regli, S. K.: Methane emission and transport by arctic sedges in Alaska: results of a vegetation removal experiment, J. Geophys. Res.-Atmos., 103, 29083–29092, 1998.
- Kinsman, R., Sauer, F. D., Jackson, H. A., and Wolynetz, M. S.: Methane and carbon dioxide emissions from dairy cows in full lactation monitored over a six-month period, J. Dairy Sci., 78, 2760–2766, doi:10.3168/jds.S0022-0302(95)76907-7, 1995.
 - Klevenhusen, F., Kreuzer, M., and Soliva, C. R.: Enteric and manure-derived methane and nitrogen emissions as well as metabolic energy losses in cows fed balanced diets based on maize, barley or grass hay, Animal, 5, 450–461, 2010.
 - Klusman, R. W. and Dick, C. J.: Seasonal variability in CH₄ emissions from a landfill in a cool, semiarid climate., J. Air Waste Manage.1995, 1632–1636, 2000.
 - Külling, D. R., Menzi, H., Krober, T. F., Neftel, A., Sutter, F., Lischer, P., and Kreuzer, M.: Emissions of ammonia, nitrous oxide and methane from different types of dairy manure during storage as affected by dietary protein content, J. Agr. Sci., 137, 235–250, 2001.
 - Külling, D. R., Dohme, F., Menz, H., Sutter, F., Lischer, P., and Kreuzer, M.: Methane emissions of differently fed dairy cows and corresponding methane and nitrogen emissions from their manure during storage, Environ. Monit. Assess., 79, 129–150, 2002.
- Külling, D. R., Menzi, H., Sutter, F., Lischer, P., and Kreuzer, M.: Ammonia, nitrous oxide and methane emissions from differently stored dairy manure derived from grass- and hay-based rations, Nutr. Cycl. Agroecosys., 65, 13–22, doi:10.1023/A:1021857122265, 2003.
- Kupper, T., Bonjour, C., Achermann, B., Zaucker, F., Rihm, B., Nyfeler-Brunner, A., Leuenberger, C., and Menzi, H.: Ammoniakemissionen in der Schweiz: Neuberechnung 1990–2007 Prognose bis 2020, available at: http://www.bafu.
- admin.ch/luft/11017/11023/11205/index.html?lang=de&download=NHzLpZeg7t, lnp6l0NTU042l2Z6ln1acy4Zn4Z2qZpnO2Yuq2Z6gpJCGe3t5f2ym162epYbg2c_ JjKbNoKSn6A-- (last access: 15 March 2013), 79 pp., 2010

- Levin, I., Glatzel-Mattheier, H., Marik, T., Cuntz, M., Schmidt, M., and Worthy, D. E.: Verification of German methane emission inventories and their recent changes based on atmospheric observations, J. Geophys. Res., 104, 3447–3456, doi:10.1029/1998JD100064, 1999.
- Liebner, S., Schwarzenbach, S., and Zeyer, J.: Methane emissions from an alpine fen in central Switzerland, Biogeochemistry, 109, 287–299, doi:10.1007/s10533-011-9629-4, 2012.
- Lin, J. C., and Gerbig, C.: Accounting for the effect of transport errors on tracer inversions, Geophys. Res. Lett., 32, L01802, doi:10.1029/2004GL021127, 2005.
- Lowry, D., Holmes, C. W., Rata, N. D., O'Brien, P., and Nisbet, E. G.: London methane emissions: use of diurnal changes in concentration and δ^{13} C to identify urban sources and verify inventories, J. Geophys. Res., 106, 7427–7448, doi:10.1029/2000JD900601, 2001.
- Manning, A. J., O'Doherty, S., Jones, A. R., Simmonds, P. G., and Derwent, R. G.: Estimating UK methane and nitrous oxide emissions from 1990 to 2007 using an inversion modeling approach, J. Geophys. Res., 116, D02305, doi:10.1029/2010JD014763, 2011.
- Merbold, L., Steinlin, C., and Hagedorn, F.: Winter greenhouse gas fluxes (CO₂, CH₄ and N₂O) from a subalpine grassland, Biogeosciences, 10, 3185–3203, doi:10.5194/bg-10-3185-2013, 2013.
 - Miller, J. B.: The carbon isotopic composition of atmospheric methane and its constraint on the global methane budget, in: Stable Isotopes and Biosphere–Atmosphere Interactions, edited by: Flanagan, L. B., Ehleringer, J. R., and Pataki, D. E., Academic Press, San Diego, 288– 310, 2005.
 - Moore, T. R. and Roulet, N. T.: Methane flux—water-table relations in northern wetlands, Geophys. Res. Lett., 20, 587–590, 1993.
 - Mosier, A., Schimel, D., Valentine, D., Bronson, K., and Parton, W.: Methane and nitrous oxide fluxes in native, fertilized and cultivated grasslands, Nature, 350, 330–332, doi:10.1038/350330a0, 1991.
 - Münger, A. and Kreuzer, M.: Methane emission as determined in contrasting dairy cattle breeds over the reproduction cycle, Int. Congr. Ser., 1293, 119–122, doi:10.1016/j.ics.2006.01.072, 2006.
- Nauer, P. A., Dam, B., Liesack, W., Zeyer, J., and Schroth, M. H.: Activity and diversity of methane-oxidizing bacteria in glacier forefields on siliceous and calcareous bedrock, Biogeosciences, 9, 2259–2274, doi:10.5194/bg-9-2259-2012, 2012.

- Park, S., Brown, K. W., Thomas, J. C., Lee, I., and Sung, K.: Comparison study of methane emissions from landfills with different landfill covers, Environ. Earth Sci., 60, 933–941, doi:10.1007/s12665-009-0229-8, 2010.
- Polson, D., Fowler, D., Nemitz, E., Skiba, U., McDonald, A., Famulari, D., Marco, C. Di, Simmons, I., Weston, K., Purvis, R., Coe, H., Manning, A. J., Webster, H., Harrison, M., O'Sullivan, D., Reeves, C., and Oram, D.: Estimation of spatial apportionment of greenhouse gas emissions for the UK using boundary layer measurements and inverse modelling technique, Atmos. Environ., 45, 1042–1049, doi:10.1016/j.atmosenv.2010.10.011, 2011.
- Pouliot, G., Pierce, T., Van der Gon, H. D., Schaap, M., Moran, M., and Nopmong-col, U.: Comparing emission inventories and model-ready emission datasets between Europe and North America for the AQMEII project, Atmos. Environ., 53, 4–14, doi:10.1016/j.atmosenv.2011.12.041, 2012.
 - SAEFL: Luftschadstoff-Emissionen aus natürlichen Quellen in der Schweiz, in Schriftenreihe Umwelt–Luft, vol. 257, Swiss Agency for the Environment, Forests and Landscape (SAEFL), 1996.

- Schroth, M. H., Eugster, W., Gómez, K. E., Gonzalez-Gil, G., Niklaus, P. A., and Oester, P.: Above- and below-ground methane fluxes and methanotrophic activity in a landfill-cover soil, Waste Manage., 32, 879–889, doi:10.1016/j.wasman.2011.11.003, 2012.
- Schubert, C. J., Lucas, F. S., Durisch-Kaiser, E., Stierli, R., Diem, T., Scheidegger, O., Vazquez, F., and Müller, B.: Oxidation and emission of methane in a monomictic lake (Rotsee, Switzerland), Aquat. Sci., 72, 455–466, doi:10.1007/s00027-010-0148-5, 2010.
- Schubert, C. J., Diem, T., and Eugster, W.: Methane emissions from a small wind shielded lake determined by eddy covariance, flux chambers, anchored funnels, and boundary model calculations: a comparison, Environ. Sci. Technol., 46, 4515–4522, doi:10.1021/es203465x, 2012.
- SFOE: Erläuternder Bericht zur Energiestrategie 2050, Swiss Federal Office of Energy SFOE, available at: http://www.bfe.admin.ch/php/modules/publikationen/stream.php?extlang=de&name=de_566812305.pdf&endung=ErläuternderBerichtzurEnergiestrategie2050 (last access: 18 April 2013), 138 pp., 2012a.
- SFOE: Schweizerische Gesamtenergiestatistik 2011, Swiss Federal Office of Energy SFOE, available at: http://www.bfe.admin.ch/php/modules/publikationen/stream.php?extlang=de&name=de_872595201.pdf&endung=SchweizerischeGesamtenergiestatistik2011 (last access: 13 March 2013), 61 pp., 2012b.

- SGWA: Technische Jahresstatistik Gas 2011, Swiss Gas and Water Industry Association (SGWA), available at: http://www.svgw.ch/fileadmin/resources/svgw/web/Shop-Boutique/download/05_G-Fachinformationen/SVGW_Shop_G15001_d_2012_NEU.pdf (last access: 30 June 2013), 2012.
- Smith, K. A., Dobbie, K. E., Ball, B. C., Bakken, L. R., Sitaula, B. K., Hansen, S., Brumme, R., Borken, W., Christensen, S., Priemé, A., Fowler, D., Macdonald, J. A., Skiba, U., Klemedtsson, L., Kasimir-Klemedtsson, A., Degórska, A., and Orlanski, P.: Oxidation of atmospheric methane in Northern European soils, comparison with other ecosystems, and uncertainties in the global terrestrial sink, Glob. Change Biol., 6, 791–803, doi:10.1046/j.1365-2486.2000.00356.x, 2000.
 - Soliva, C. R.: Report to the attention of IPCC about the data set and calculation method used to estimate methane formation from enteric fermentation of agricultural livestock population and manure management in Swiss agriculture, available at: http://www.bafu.admin.ch/climatereporting/00545/01913/index.html?lang=en&download=NHzLpZeg7t,lnp6I0NTU042I2Z6In1ad1IZn4Z2qZpnO2Yuq2Z6gpJCEd31, gGym162epYbg2c_JjKbNoKSn6A-- (last access: 15 March 2013), 2006.
 - Staerfl, S. M., Zeitz, J. O., Kreuzer, M., and Soliva, C. R.: Methane conversion rate of bulls fattened on grass or maize silage as compared with the IPCC default values, and the long-term methane mitigation efficiency of adding acacia tannin, garlic, maca and lupine, Agr. Ecosyst. Environ., 148, 111–120, doi:10.1016/j.agee.2011.11.003, 2012.
 - Stiehl-Braun, P. A., Powlson, D. S., Poulton, P. R., and Niklaus, P. A.: Effects of N fertilizers and liming on the micro-scale distribution of soil methane assimilation in the long-term Park Grass experiment at Rothamsted, Soil Biol. Biochem., 43, 1034–1041, doi:10.1016/j.soilbio.2011.01.020, 2011.
- Swisstopo: VECTOR25: Das digitale Landschaftsmodell der Schweiz, Federal Office of Topography (swisstopo), 2004.
 - Ugolini, F., Gómez, K., Schroth, M. H., Eugster, W., Niklaus, P., Oester, P., and Zeyer, J.: Seasonal changes in the fate of methane in a landfill-cover soil, in: Annual Meeting of the Swiss Society for Microbiology, June 4–5, Lausanne, Switzerland, 2009.
- Van den Pol-van Dasselaar, A., Van Beusichem, M. L., and Oenema, O.: Effects of nitrogen input and grazing on methane fluxes of extensively and intensively managed grasslands in the Netherlands, Biol. Fert. Soils, 29, 24–30, doi:10.1007/s003740050520, 1999.

- Vermeulen, A. T., Eisma, R., Hensen, A., and Slanina, J.: Transport model calculations of NW-European methane emissions, Environ. Sci. Policy, 2, 315–324, doi:10.1016/S1462-9011(99)00021-0, 1999.
- VSG: Erdgas in der Schweiz VSG-Jahresstatistik, Verband der Schweizerischen Gasindustrie (VSG), available at: http://www.erdgas.ch/fileadmin/customer/erdgasch/Data/Broschueren/Jahresstatistik/VSG-Jahresstatistik_2012.pdf (last access: 15 March 2013), 26 pp., 2012.
- Wennberg, P. O., Mui, W., Wunch, D., Kort, E. A., Blake, D. R., Atlas, E. L., Santoni, G. W., Wofsy, S. C., Diskin, G. S., Jeong, S., and Fischer, M. L.: On the sources of methane to the Los Angeles atmosphere, Environ. Sci. Technol., 46, 9282–9289, doi:10.1021/es301138y, 2012
- Whalen, S. C., Reeburgh, W. S., and Sandbeck, K. A.: Rapid methane oxidation in a landfill cover soil, Appl. Environ. Microb., 56, 3405–3411, 1990.
- Wratt, D. S., Gimson, N. R., Brailsford, G. W., Lassey, K. R., Bromley, A. M., and Bell, M. J.: Estimating regional methane emissions from agriculture using aircraft measurements of concentration profiles, Atmos. Environ., 35, 497–508, 2001.
- Wunderlin, P., Mohn, J., Joss, A., Emmenegger, L., and Siegrist, H.: Lachgas (N₂O) Emissionen aus Abwasserreinigungsanlagen (ARA), Aqua & Gas, 2, 54–59, 2013.
- Xinmin, J.: Die Methanemissionen der Schweizer Gasindustrie, Gas, Wasser, Abwasser, 5, 337–345, 2004
- Zeitz, J. O., Soliva, C. R., and Kreuzer, M.: Swiss diet types for cattle: how accurately are they reflected by the Intergovernmental Panel on Climate Change default values?, J. Integr. Environ. Sci., 9, 199–216, doi:10.1080/1943815X.2012.709253, 2012.
 - Zellweger-Fischer, J.: Schweizer Feldhasenmonitoring 2012/Suivi des populations de lièvres en Suisse en 2012, Schweizerische Vogelwarte Sempach, 28 pp., 2012.

Table 1. Existing high resolution CH₄ inventories that include Switzerland.

	EDGARv4.2	EDGAR-HTAP	TNO-MACC 2009	NatAir	
Aim	Emission database for global atmospheric research	Emission database for global atmospheric research	Monitoring Atmospheric Composition and Cli- mate (FP7)	Improving and Applying Methods for the Calculation of Natural and Biogenic Emissions and Assessment of Impacts on Air Quality (FP6)	
Spatial resolution	0.1° × 0.1°	0.1° × 0.1°	1/8° × 1/16°	10km × 10km	
Spatial coverage	Global	Global	Europe	Europe	
Temporal coverage	1970–2008	2000–2005	2003–2007 and 2009	1997, 2000, 2001 and 2003 at hourly to an- nual time resolution	
Included emissions	Anthropogenic emissions	Anthropogenic emissions	Anthropogenic emissions	Natural and biogenic emissions	
Approach	Bottom-up inventory of internationally reported emissions	Official regional inventories like EMEP, gap filled with EDGAR v4.1	EMEP country totals checked for consis- tency, distributed ac- cording to geostatisti- cal proxies	Bottom-up estimate	
Reference	http://edgar.jrc.ec. europa.eu/index.php (last access: 1 Nov 2012)	Janssens-Maenhout et al. (2012)	Pouliot et al. (2012)	http://natair.ier. uni-stuttgart.de/ (last access: 1 Nov 2011), Friedrich (2007)	

Table 2. Swiss CH_4 emissions in 2011, uncertainty estimate, and changes from 1990 to 2011 for the major source categories listed by the official Nomenclature for Reporting (NFR) codes. The provided uncertainty estimates follow the Tier 1 methodology (IPCC, 2000), represent half of the 95 % confidence interval expressed in percent (IPCC, 1997), and accounts for uncertainties in emission factors (EFs) and activity data for the individual level or category. Total national emissions exclude the Land Use, Land-Use Change and Forestry sector (LULUCF in italics) as well as International Bunkers (not shown) in accordance with the reporting requirements under the UNFCCC. Methods applied and EFs used are indicated (D = IPCC Default, T1 = IPCC Tier 1, T2 = IPCC Tier 2, T3 = IPCC Tier 3, CR = CORINAIR, CS = Country-specific). All data for the anthropogenic sources are taken from the national Greenhouse Gas Inventory (FOEN, 2013), while CH_4 fluxes from the natural categories base on estimates presented in this study. The categories indicated with an asterisk are included in our spatially explicit inventory.

CH ₄ Source and Sink Categories	2011	Uncertainty	Change since	Methods	EFs
	[Ggyr ⁻¹]	[%]	1990 [%]		
Anthropogenic	177.73	16	-20.2		
1. Energy	12.14	35	-58.9		
A. Fuel Combustion	3.89	35	-65.9	CS, T2, T3	CR, CS
3.b Transport; Road Transportation – Gasoline	1.00	35	-79.3		
4.b Other Sectors; Residential – Biomass	1.43	48	-68.7		
B. 2 Fugitive Emissions from Fuels; Oil and Natural Gas*	8.25	50	-54.4	T3, CS	CS
Industrial Processes (Chemical Industry	0.41	30	-10.5	CS, T2	CS, D
3. Solvent and Other Product Use	NO				
4. Agriculture	150.43	18	-4.5		
A Enteric Fermentation*	119.48	18	-4.8	T2	CS
B Manure Management*	30.94	54	-3.2	T2	CS, D
5. Land Use, Land-Use Change and Forestry (Wildfires in Forest Land)	0.06	70	-84.9	T1	CS
6. Waste	14.72	48	-58.0		
A Solid Waste Disposal on Land*	8.61	58	-73.7	CS, D	CS, D
B Wastewater Handling*	0.48	30	115.6	D	CS,D
D Other	5.04	100	253.2	CS	CS
7. Other (Fire Damage in Buildings and Motor Vehicles)	0.03	30	3.9	T1	CS
Natural and semi-natural	5.7/-2.8	NA	NA		
Lakes and reservoirs*	2.3	NA	NA	See Sect	. 2.2.1
Wetlands*	2.3	NA	NA	See Sect	. 2.2.2
Wild animals*	1.1	NA	NA	See Sect	. 2.2.3
Agricultural soils	-1.5 to 0	NA	NA	See Sect	. 2.2.4
Forest soils*	-2.8	NA	NA	See Sect	. 2.2.5

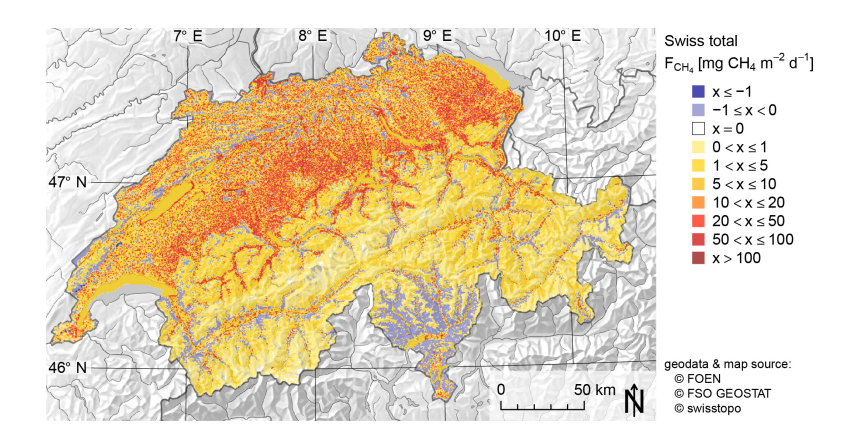


Fig. 1. Our spatially-explicit Swiss ${\rm CH_4}$ emission inventory including both anthropogenic and natural ${\rm CH_4}$ sources.

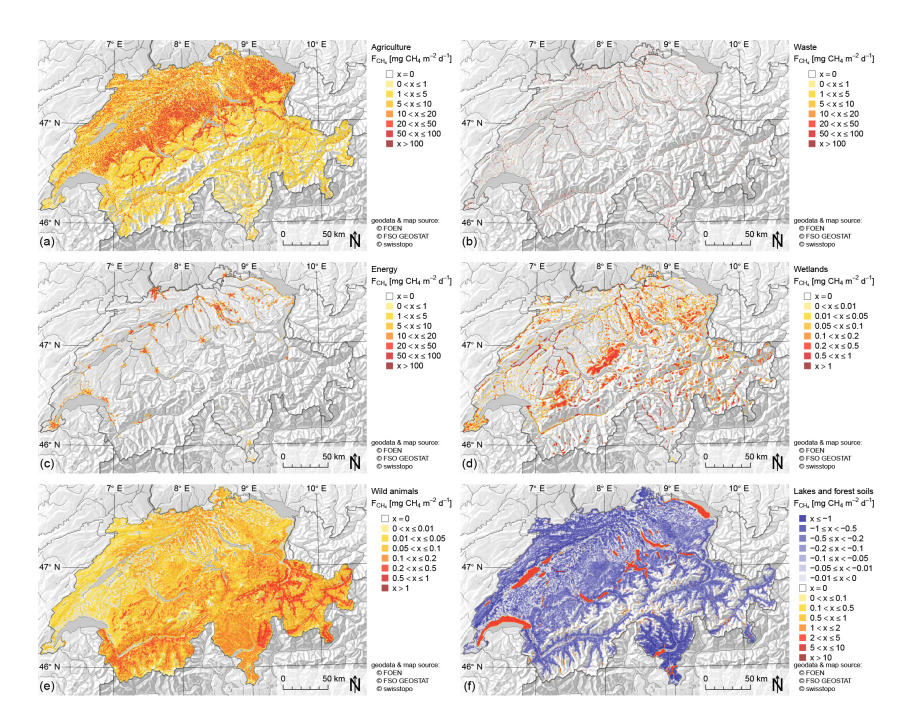


Fig. 2. Individual layers of the inventory presented in Fig. 1. Note that the scale for anthropogenic fluxes of the agricultural sector **(a)**, the waste sector **(b)** and the energy sector **(c)** are a factor 10 to 100 larger than that for natural and semi-natural fluxes from wetlands **(d)**, wild animals **(e)**, and forest soil and lakes **(f)**.

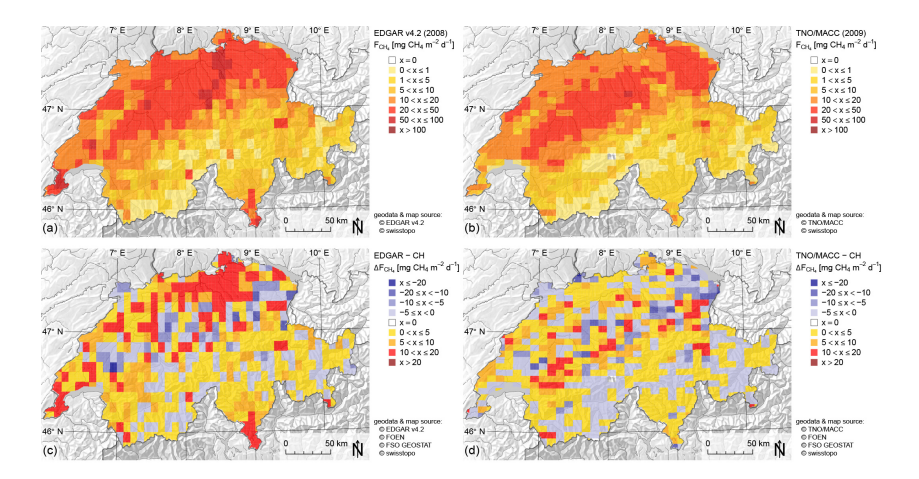


Fig. 3. Total anthropogenic CH_4 emissions over Switzerland according to the EDGAR v4.2 inventory for the year 2008 **(a)** and the TNO/MACC inventory for the year 2009 **(b)**. Panels **(c)** and **(d)** are absolute differences from the total anthropogenic emissions in our inventory (Fig. 1).

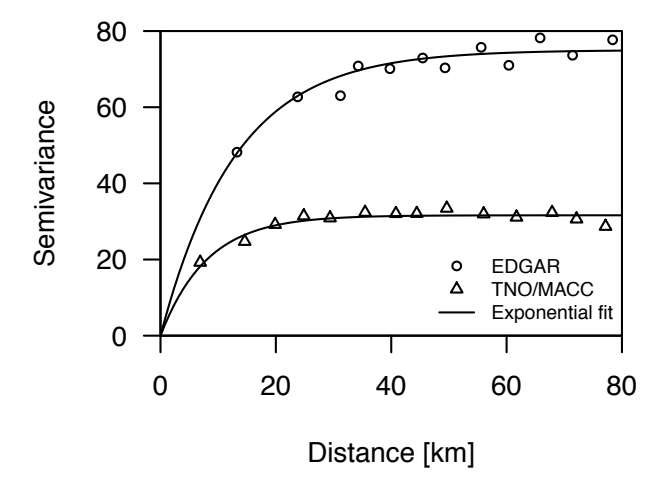


Fig. 4. Semivariogram of the differences between the EDGAR v4.2 and TNO/MACC inventories and our inventory. Also shown are exponential fits to the data (see text for further details).

Appendix B

Contrasting response of grassland versus forest carbon and water fluxes to spring drought in Switzerland

Sebastian Wolf^{1,2}, Werner Eugster², Christof Ammann³, Matthias Häni², Sebastian Zielis², Rebecca Hiller⁴, Jacqueline Stieger², Dennis Imer², Lutz Merbold², Nina Buchmann¹

¹Department of Environmental Science, Policy and Management, University of California, Berkeley, CA, USA
²Institute of Agricultural Sciences, ETH Zurich, Zurich, Switzerland
³Agroscope Reckenholz-Tänikon Research Station ART, Zurich, Switzerland
⁴Empa, Swiss Federal Laboratories for Materials Science and Technology, Duebendorf, Switzerland

This manuscript was published in: Environmental Research Letters, 2013, 8, 3, 035007



IOP PUBLISHING

Environ. Res. Lett. 8 (2013) 035007 (12pp)

ENVIRONMENTAL RESEARCH LETTERS

doi:10.1088/1748-9326/8/3/035007

Contrasting response of grassland versus forest carbon and water fluxes to spring drought in Switzerland

Sebastian Wolf^{1,2}, Werner Eugster², Christof Ammann³, Matthias Häni², Sebastian Zielis², Rebecca Hiller⁴, Jacqueline Stieger², Dennis Imer², Lutz Merbold² and Nina Buchmann²

- Department of Environmental Science, Policy and Management, University of California, Berkeley, 130 Mulford Hall, Berkeley, CA 94720, USA
- ² Institute of Agricultural Sciences, ETH Zurich, Universitaetsstrasse 2, 8092 Zurich, Switzerland
- ³ Research Station Agroscope Reckenholz-Tänikon ART, Reckenholzstrasse 191, 8046 Zurich, Switzerland
- ⁴ Swiss Federal Laboratories for Materials Science and Technology (EMPA), Ueberlandstrasse 129, 8600 Duebendorf, Switzerland

E-mail: sewolf@berkeley.edu

Received 11 March 2013 Accepted for publication 3 June 2013 Published 3 July 2013 Online at stacks.iop.org/ERL/8/035007

Abstract

Since the European summer heat wave of 2003, considerable attention has been paid to the impacts of exceptional weather events on terrestrial ecosystems. While our understanding of the effects of summer drought on ecosystem carbon and water vapour fluxes has recently advanced, the effects of spring drought remain unclear. In Switzerland, spring 2011 (March–May) was the warmest and among the driest since the beginning of meteorological measurements. This study synthesizes Swiss FluxNet data from three grassland and two forest ecosystems to investigate the effects of this spring drought. Across all sites, spring phenological development was 11 days earlier in 2011 compared to the mean of 2000–2011. Soil moisture related reductions of gross primary productivity (GPP) were found at the lowland grassland sites, where productivity did not recover following grass cuts. In contrast, spring GPP was enhanced at the montane grassland and both forests (mixed deciduous and evergreen). Evapotranspiration (ET) was reduced in forests, which also substantially increased their water-use efficiency (WUE) during spring drought, but not in grasslands. These contrasting responses to spring drought of grasslands compared to forests reflect different adaptive strategies between vegetation types, highly relevant to biosphere–atmosphere feedbacks in the climate system.

Keywords: Swiss FluxNet, drought response, eddy covariance, carbon dioxide fluxes, water vapour fluxes, water deficit, evapotranspiration, water-use efficiency

1. Introduction

Europe has experienced a number of exceptional weather events during the past decades that have attracted the interest

Content from this work may be used under the terms of the Creative Commons Attribution 3.0 licence. Any further distribution of this work must maintain attribution to the author(s) and the title of the work, journal citation and DOI.

of ecologists, such as severe droughts and heatwaves in summer 2003 (Ciais *et al* 2005) and 2010 (Barriopedro *et al* 2011), flood events in 2002 (Christensen and Christensen 2003) and 2005 (Schmocker-Fackel and Naef 2010), and severe storms—such as 'Lothar' in 1999 and 'Gudrun' in 2005 (Lindroth *et al* 2009). These events have claimed lives, caused substantial economic damage in agriculture, forestry and infrastructure, and heavily disturbed the carbon and water balances of terrestrial ecosystems in Europe (Ciais *et al*

1748-9326/13/035007+12\$33.00

© 2013 IOP Publishing Ltd Printed in the UK

S Wolf et al

Environ. Res. Lett. 8 (2013) 035007

2005, Reichstein et al 2007). With increasing atmospheric greenhouse gas concentrations, regional climate scenarios have predicted more intense and frequent extreme events in Europe for the future (Schär et al 2004, Frei et al 2006). In addition, soil moisture feedbacks to the atmosphere might further enhance extreme temperatures on local and regional scales due to reduced evaporative cooling (Granier et al 2007, Seneviratne et al 2010). However, our knowledge about the changes in ecosystem carbon and water fluxes in response to such extreme events is still limited, in particular during the transitional seasons of spring and autumn (Richardson et al 2010, Zhang et al 2012).

Research has recently focused on summer droughts and heatwaves, e.g. 2003 (Ciais et al 2005) and 2010 (Barriopedro et al 2011) in Europe. However, drought events have also occurred during spring, such as in France and south-eastern UK in 2006, in Germany, The Netherlands and Austria in April 2007, and more recently throughout most of central and north-western Europe in spring 2011 (Vogt 2012, Quesada et al 2012, Sepulcre-Canto et al 2012), when historic records of high temperatures were observed (European Drought Observatory 2011).

In Switzerland, spring 2011 was the warmest (+3.4 °C above average) and the third driest (-47% below average seasonal precipitation) since the beginning of meteorological measurements in 1864 (MeteoSwiss 2012), following an exceptionally dry winter with below average precipitation and snow accumulation (Pielmeier 2011). This combination resulted in a pronounced spring drought that affected plant phenology, agricultural production and water supply. Reservoir levels reached record lows, and irrigation measures were required to preserve agricultural production in parts of Switzerland (BAFU 2011).

The current understanding of drought effects suggests that plant water limitations are less likely in spring than in summer as soil reservoirs should have been recharged by winter precipitation. However, extreme weather events during early season growth could have severe effects on carbon and water fluxes of terrestrial ecosystems.

Only a few studies have investigated the effects of spring drought on ecosystem carbon and water fluxes so far. These studies reported overall reductions in carbon uptake (Zhang et al 2012, Dong et al 2011, Kwon et al 2008, Parton et al 2012), a small suppression in evapotranspiration (ET; Dong et al 2011), and a shift in the environmental controls of net ecosystem exchange (NEE) from vapour pressure deficit (VPD) to soil moisture with progressing drought (Kwon et al 2008). While the temperature effects are well understood, the effects of moisture limitation during spring on phenology, carbon uptake and water vapour fluxes remain unknown.

The objectives of our study are (1) to synthesize ecosystem carbon dioxide and water vapour fluxes from the national eddy covariance network, Swiss FluxNet, (2) to evaluate the phenological development of vegetation, (3) to investigate carbon—water interactions, and (4) to compare the response of grasslands and forests to the 2011 spring drought in Switzerland.

2. Material and methods

2.1. Swiss FluxNet

We synthesized data from the Swiss FluxNet national eddy covariance network (www.swissfluxnet.ch). Swiss FluxNet includes the major land-use types of deciduous and evergreen forests, grassland and cropland along an elevational gradient in Switzerland and currently encompasses eight long-term ecosystem sites. Our synthesis study included five of these sites that provided data for spring 2010 and 2011: Chamau, Oensingen1, Früebüel (managed grasslands, elevation range from 393 to 982 m a.s.l.), Laegeren (lowland mixed deciduous forest), and Davos (subalpine evergreen forest, table 1). All sites have a temperate climate with elevation as a confounding factor, particularly the montane grassland in Früebüel and the subalpine evergreen forest in Davos. Management varied across sites and included 4-6 grass cuts per year with subsequent manure or synthetic fertilizer applications in the intensively managed Oensingen1 and Chamau grasslands. At the moderately managed grassland Früebüel, only solid manure was applied once per year and grass cuts were occasionally replaced by cattle grazing. The Laegeren and Davos forest sites had no management events during the time of observations.

2.2. Flux measurements and data processing

Flux densities of carbon dioxide, water vapour and energy were measured during 2010 and 2011 using the eddy covariance (EC) method. The micrometeorological measurement setup consisted of open-path infrared gas analysers (Li-7500, LI-COR, Lincoln, USA) and threedimensional sonic anemometers (models Solent R3-50 and HS. Gill Instruments, Lymington, UK), Raw data were recorded at 10 or 20 Hz and processed to half-hourly averages using the eth-flux EC software (Mauder et al 2008) or a comparable custom-made EC software for Oensingen1 (Ammann et al 2007). Post-processing included corrections for damping losses (Eugster and Senn 1995), air density fluctuations (Webb et al 1980), and data screening for optical sensor contamination, stationarity (Foken and Wichura 1996), low turbulence conditions (see table 1 for site-specific u_* -thresholds) and statistical outliers (14 day running mean with ± 3 SD range). In addition, negative nighttime fluxes (unreasonable as no photosynthesis occurs at night) and a corresponding amount of positive nighttime fluxes were removed using a trimmed mean approach to avoid a systematic bias of cumulative sums. Standardized gap filling and partitioning of carbon dioxide fluxes was performed using the methodology by Reichstein et al (2005), i.e., with the marginal distribution sampling (MDS) gap filling algorithm and flux partitioning based on a temperature regression with nighttime fluxes $(GPP = -NEE_{daytime} + TER)$. In addition, we corrected for physiologically unrealistic, negative values of gross primary productivity (GPP) when net ecosystem exchange (NEE) exceeded nighttime derived total ecosystem respiration (TER; e.g., with onset of turbulent mixing or following rainfall),

Environ. Res. Lett. 8 (2013) 035007 S Wolf et al.

Table 1. Swiss FluxNet sites used in this synthesis study. Abbreviations denote the International Geosphere–Biosphere Programme (IGBP), mean annual temperature (MAT), mean annual precipitation (MAP), and friction velocity (u_*)—a measure for turbulence conditions. Data were compiled from published literature except MAP, which was derived from long-term data provided by MeteoSwiss (see table 2).

Site	Chamau	Oensingen1	Früebüel	Laegeren	Davos
IGBP land use, Abbreviation	Grasslands, GRA (intensively managed)	Grasslands, GRA (intensively managed)	Grasslands, GRA (moderately managed)	Mixed Forest, MF (deciduous dominated)	Evergreen Needleleaf Forest, ENF
Dominant species	Italian ryegrass (Lolium multifl.) White clover (Trifolium repens)	English ryegrass (Lolium perenne) Meadow foxtail (Alopecurus prat.) White clover (Trifolium repens)	Meadow foxtail (Alopecurus prat.) Cocksfoot grass (Dactylis glomerata) Dandelion (Taraxacum offic.) Buttercup (Ranunculus sp.) White clover (Trifolium repens)	European beech (Fagus sylvatica) Norway spruce (Picea abies) European ash (Fraxinus excelsior) Sycamore maple (Acer pseudopl.)	Norway spruce (Picea abies)
Latitude	47°12′36.8″N 8°24′37.6″E	47°17′08.1″N 7°43′55.9″E	47°06′57.0″N 8°32′16.0″E	47°28′42.0″N 8°21′51.8″E	46°48′55.2″N 9°51′21.3″E
Longitude Elevation (a.s.l.)	393 m	452 m	982 m	682 m	1639 m
MAT	9.8 °Ca	9.5 °C	7.5 °Ca	7.4 °C	3.4 °C
MAP	1125 mm	1184 mm	1516 mm	1070 mm	992 mm
u_* -threshold (m s ⁻¹)	0.08	0.10	0.08	0.30	0.20
References	Zeeman <i>et al</i> (2009) Zeeman <i>et al</i> (2010)	Ammann <i>et al</i> (2007) Ammann <i>et al</i> (2009)	Zeeman et al (2009) Zeeman et al (2010)	Ahrends <i>et al</i> (2009) Zweifel <i>et al</i> (2010) Etzold <i>et al</i> (2010) Etzold <i>et al</i> (2011)	Zweifel et al (2010) Etzold et al (2011)

^a Mean from 2006 to 2007 (Zeeman et al 2010).

by replacing TER with NEE and setting GPP to zero (Wolf et al 2011).

Besides flux densities, meteorological variables such as air temperature, relative humidity, precipitation, incoming shortwave radiation ($R_{\rm G}$), soil temperature and volumetric soil water content (SWC, in %, 5 cm depth; except at Oensingen1: 10 cm) were measured continuously (half-hourly averages, sums for precipitation) at all sites. SWC was also measured at 15–30 cm depth but showed similar results as for 5 cm depth (not shown). Long-term precipitation data for nearby reference stations (see table 2) were provided by MeteoSwiss.

2.3. Phenology

Phenological development of vegetation was analysed from species-specific observational data (i.e., dates of phenological phases) provided by MeteoSwiss from the national phenological monitoring network. We used the following nearby stations from this network (including distance and direction from the respective tower site): Chamau-Muri (9.0 km, 317°NW), Oensingen-Wynau (6.6 km, 115°SE), Früebüel-Edlibach (7.5 km, 18°N), Laegeren-Oberehrendingen (5.7 km, 274°W), and Davos-Davos-Dorf (1.4 km, 244°SW). According to the composition of the dominant vegetation at each site (see table 1), we used the date of needle emergence of Norway spruce (Picea abies) for the Davos site, and averaged the dates of leaf unfolding of European beech (Fagus sylvatica) and needle emergence for Norway spruce (Picea abies) at the Laegeren site. For all grassland sites, we consistently used the same plant species

and averaged the dates of full flowering from cocksfoot grass (*Dactylis glomerata*) and dandelion (*Taraxacum officinale*).

2.4. General conventions

We used the R statistics software package, version 2.13.2 (R Development Core Team 2009, www.r-project.org) for data analyses. Daytime data were defined by $R_{\rm G}$ exceeding 10 W m $^{-2}$. The term 'spring' refers to the meteorological definition (March, April and May). We use the term 'drought' related to precipitation deficits, which can impose (1) plant physiological stress due to soil moisture deficiency and (2) stomatal adjustments in response to high VPD. We compare our data of 2011 relative to 2010, with 2011 being closer to the long-term average precipitation regime for most sites (see table 2).

3. Results

3.1. Weather conditions during spring 2011

The weather anomaly during spring 2011 resulted in record high temperatures (+3.4 °C above average) and substantial below average precipitation (-47%) in Switzerland (MeteoSwiss 2012). March and April were particularly dry and all sites received below average precipitation, ranging from -35 to -85% in March and -42 to -79% in April. The Früebüel montane grassland had the lowest deviations from the long-term mean (-35% and -42%), because of its topographic exposure. Most sites also received below

Environ. Res. Lett. 8 (2013) 035007 S Wolf et al

Table 2. Precipitation sums and relative deviations from the long-term means (1981–2010) for the year 2011. Deviations for 2010 are reported for comparison. Long-term data were derived from nearby reference stations by MeteoSwiss while data for 2010 and 2011 were measured directly at the sites.

Site	Chamau	Oensingen	Früebüel	Laegeren	Davos
Reference station	Cham	Wynau	Zugerberg	Dietikon	Davos
Mean ± SD (mm) Winter (DJF) Spring (MAM) Annual	180 ± 70 274 ± 85 1112 ± 162	251 ± 82 264 ± 100 1129 ± 201	215 ± 100 353 ± 111 1457 ± 272	238 ± 71 279 ± 102 1110 ± 164	185 ± 82 204 ± 56 1035 ± 156
2011 (mm) Winter (DJF) Spring (MAM) Annual	165 182 1084	173 93 995	245 353 869	132 89 624	66 133 776
Deviation 2011 (%) Winter (DJF) Spring (MAM) Annual	-8 -34 -3	-31 -65 -12	+14 0 -40	-45 -68 -44	-64 -35 -25
Deviation 2010 (%) Winter (DJF) Spring (MAM) Annual	-5 0 +3	-24 -34 -20	+23 +43 +58	-43 -29 -20	-56 -14 -28

average precipitation during early May 2011, but heavy precipitation events after DOY 131 (May 11) resulted in a substantial monthly surplus at Davos and Früebüel, and a small surplus in Chamau. During spring 2011, all sites except Früebüel had a cumulative precipitation deficit of 34–68% (mean 51%, Früebüel excluded), which was larger than the small deficit of 7% across all sites during spring 2010 (table 2). In both years, spring was preceded by similarly dry winters across sites, except at Früebüel (2010: –32%, 2011: –37%).

This precipitation anomaly during spring 2011 was also reflected in the temporal patterns of SWC (figure 1), with a substantial decrease from a maximum of 52% (overall mean) on DOY 95 (April 5) to a minimum of 30% on DOY 131 (May 11), which confined the spring drought across all sites between DOY 102-132 (April 12-May 12). Low and increasing SWC at the subalpine Davos site (1639 m) during March was related to frozen soil and associated measurement limitations. During spring 2011, all sites received higher amounts of daily R_G compared to 2010, in the range of +17% (Davos) to +36% (Früebüel), with a mean of +27% (data not shown). Daily VPD was substantially higher at all sites (overall mean +85%) during spring 2011, particularly at the forest sites (+228% versus +45% at grasslands). Spring was also substantially warmer in 2011 compared to 2010 (see figure 5), with mean air temperatures differences of +2.1 to +3.4°C at our sites (overall mean +2.8°C) and the largest increase found at the forest sites (+3.3 °C).

3.2. Phenological development

Phenological observations showed that vegetation development started 8–17 days earlier (overall mean -11 days) in 2011 compared to the mean of 2000–2011 (figure 2). The opposite pattern was observed in 2010, when vegetation

started later at all sites (overall mean +7 days). While sites differed considerably between 2000 and 2009, the late vegetation developments in 2010 and the early vegetation development in 2011 were more consistent across all sites. Compared to 2010, spring phenology developed on average 18 days earlier during spring 2011 at our sites.

${\it 3.3. Range and magnitude of carbon and water vapour fluxes}$

We observed large differences in GPP and TER among sites during spring 2011 (figure 3, table 3). GPP was highest for the grassland sites Chamau (10.2 \pm 4.5 g C m⁻² d⁻¹, mean \pm standard deviation) and Früebüel (8.8 \pm 5.3 g C m⁻² d⁻¹), while lowest GPP was found at the evergreen forest site in Davos (3.4 \pm 1.9 g C m⁻² d⁻¹). During the drought period 2011 (DOY 102-132), GPP decreased substantially at Chamau (figure 3(a)). Smaller reductions in GPP were observed for the two other grassland sites Oensingen1 and Früebüel at the beginning and towards the end of the drought period (figures 3(b) and (c)). We did not find drought related GPP reductions of the forests. However, GPP of the two forest sites was substantially higher in 2011 compared to 2010 (LAE: +54%, DAV: +19%), while the grassland sites did not show a consistent pattern and substantially higher GPP was only found at Früebüel (+38%, table 3).

Range and magnitude of TER largely followed the GPP pattern, except for the forest sites Laegeren $(3.4 \pm 1.2 \text{ g C m}^{-2} \text{ d}^{-1})$ and Davos $(1.5 \pm 0.5 \text{ g C m}^{-2} \text{ d}^{-1})$, where TER remained low, remarkably stable and decoupled from GPP following the onset of drought conditions in April (figure 3). Management of the grassland sites (grass cuts and grazing) resulted in a short-term decoupling of TER from GPP, i.e., reduced GPP along with increased TER (figures 3(a)–(c)). Compared to 2010, we observed higher respiratory fluxes for the forest sites (LAE: $\pm 23\%$.

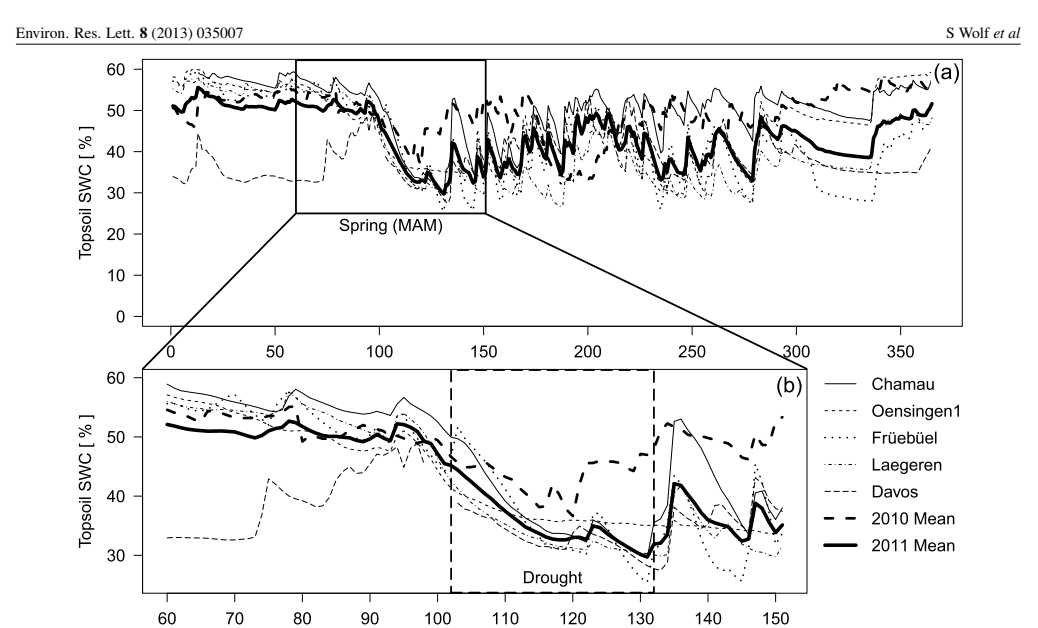


Figure 1. Daily mean volumetric soil water content (SWC) at 5 cm depth (Oensingen1: 10 cm depth) at five Swiss FluxNet sites for the full year (a) and for spring 2011 (b). For comparison, the overall mean SWC across all sites is also shown for 2010. The dashed box in (b) confines the period of spring drought across all sites (DOY 102–132).

Day of Year

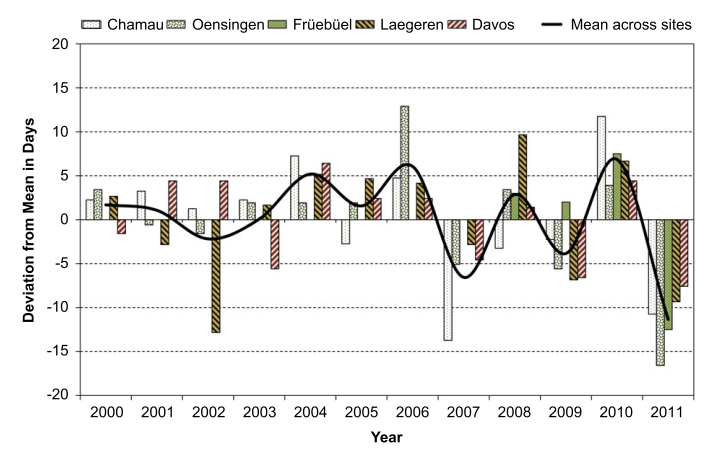


Figure 2. Site-specific phenological development compared to 2000–2011 mean of each site. Grasslands are denoted by dotted and forests by striped fill patterns. Sites are ordered according to land-use type (grassland, forest) and their respective elevational gradient from left (lowest) to right (highest). The bold black line shows the mean across all sites. Negative deviations indicate earlier, positive deviations later than average phenological development in spring. Species-specific observational data were provided by MeteoSwiss for nearby sites from the national phenological monitoring network: Davos–Norway spruce (needle emergence), Laegeren–European beech and Norway spruce (leaf unfolding/needle emergence), Früebüel, Chamau, Oensingen–Cocksfoot grass and Dandelion (full flowering). Data availability for Früebüel was limited to the years 2008–2011.

DAV: +93%) in spring 2011 (table 3). The relative change in GPP *versus* TER between these years was generally similar or larger for GPP, except at the subalpine site Davos, where

higher soil temperatures in 2011 (i.e., $T_{Soil} > 0$ °C about three weeks earlier) resulted in enhanced TER and substantially larger changes in TER compared to GPP.

Environ. Res. Lett. 8 (2013) 035007 S Wolf et al

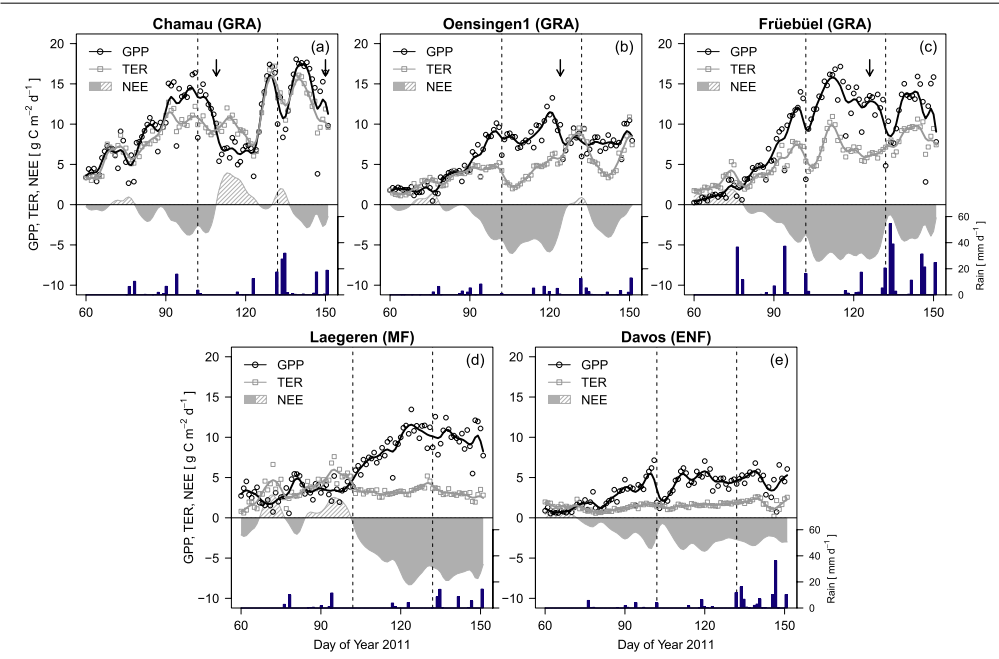


Figure 3. Daily total gross primary productivity (GPP), total ecosystem respiration (TER) and net ecosystem exchange (NEE; full shading indicates periods of carbon sink, striped shading of carbon sources) during spring 2011. Lines and shading are 7 day running means. The bars at the bottom of each panel show daily precipitation totals. Arrows indicate management at grassland sites, i.e. grass cuts (a), (b) and begin of grazing (c). The dashed lines confine the period of spring drought across all sites (DOY 102–132). Abbreviations in titles indicate the IGBP land-use class with grasslands (GRA), mixed forest (MF) and evergreen needleleaf forest (ENF). The grassland sites in the top panels are ordered according to their elevational gradient from left (lowest) to right (highest), and similarly the forest sites in the bottom panels.

Table 3. Cumulative gross primary productivity (GPP), total ecosystem respiration (TER), net ecosystem exchange (NEE), and evapotranspiration (ET) during spring (MAM) 2011. Relative deviations are reported for spring 2011 compared to 2010.

Site	Chamau	Oensingen1	Früebüel	Laegeren	Davos
GPP (g C m ⁻²)	940	586	809	598	324
TER (g C m ⁻²)	891	401	536	316	137
NEE (g C m ⁻²)	-49	-185	-273	-282	-187
ET (mm)	181	196	233	198	125
Deviation 2011 versus 2010 (%)					
GPP	3	-20	38	54	19
TER	4	-20	15	23	93
NEE	-14	-21	123	114	-7
ET	-4	1	49	-21	-32

Ecosystem ET (i.e., soil and canopy evaporation plus plant transpiration) was highest at the grassland site Früebüel $(2.5\pm1.4~\mathrm{mm~m^{-2}~d^{-1}})$ and lowest at the evergreen forest in Davos $(1.4\pm0.8~\mathrm{mm~m^{-2}~d^{-1}})$, figure 4). ET was higher in 2011 than 2010 at the Früebüel grassland site (+49%) and lower at the forest sites (LAE: -21%, DAV: -32%; table 3).

3.4. Environmental controls of spring fluxes

In 2011, the main environmental controls of daily spring GPP were R_G for Chamau ($R^2 = 0.48$) and Früebüel ($R^2 = 0.67$),

soil temperature for Davos ($R^2=0.38$), and soil moisture for Oensingen1 ($R^2=0.66$) and Laegeren ($R^2=0.76$, all p<0.001, linear regression analysis). For Früebüel, soil moisture was a strong residual control of GPP ($R^2=0.31$, p<0.001) while no significant control of moisture was detected for Chamau and Davos. Soil temperature and soil moisture were together the main environmental controls of daily spring TER for all sites, but explained a higher variability in TER for the grasslands ($R^2=0.54-0.84$, p<0.001) compared to the forest sites ($R^2=0.23-0.47$, p<0.001). $R_{\rm G}$ was the main environmental control for daily

S Wolf et al

Environ. Res. Lett. 8 (2013) 035007

Chamau (GRA) Oensingen1 (GRA) Früebüel (GRA) 2010: 188 mm 2010: 194 mm (b) 2010: 156 mm (a) (c) 2011: 181 mm 2011: 196 mm 2011: 233 mm ET [mm d⁻¹] 120 150 60 120 150 120 150 Davos (ENF) Laegeren (MF) 2010: 184 mm 2011: 125 mm 2010: 251 mm (e) 2011: 198 mm 6 6 5 ET [mm d-1] 3 2 Day of Yea Day of Year

Figure 4. Daily total ecosystem evapotranspiration (ET) during spring 2010 and 2011. Lines are 7 day running means and numbers following years show total spring ET. Arrows indicate management at grassland sites, i.e. grass cuts (a), (b) and start of grazing (c). The dashed lines confine the period of spring drought across all sites (DOY 102-132). Abbreviations in titles indicate the IGBP land-use class with grasslands (GRA), mixed forest (MF) and evergreen needleleaf forest (ENF).

NEE for all grassland sites ($R^2 = 0.19-0.67$, all p < 0.001). In addition, spring NEE of the forest sites was driven by soil moisture at Laegeren ($R^2 = 0.66$) and air temperature at Davos ($R^2 = 0.32$, both p < 0.001). Low explanatory power of R_G for NEE of the grasslands Chamau (R^2 = 0.19) and Oensingen1 ($R^2 = 0.30$) seemed largely related to management effects (grass cuts), while grazing at Früebüel $(R^2 = 0.67, \text{ all } p < 0.001)$ had smaller effects on NEE than meteorological variables (figure 3(c)). The main driver of ET at the grassland sites was R_G , while temperature was the main control at the forest sites ($R^2 = 0.65 - 0.77$, all p < 0.001). VPD was the secondary environmental control of ET at all

3.5. Carbon uptake and water deficits

We observed net carbon uptake at all sites during spring 2011, ranging from 49 g C m $^{-2}$ for Chamau to 282 g C m $^{-2}$ for Laegeren (figure 5, table 3). Unlike the previous year, net carbon uptake (cumulative NEE < 0) in spring 2011 generally started earlier, except for the Oensingen1 grassland. No considerable differences in NEE were found at Chamau, Oensingen1 and Davos between spring 2010 and 2011. Compared to the previous spring, substantially higher net carbon uptake was observed at the sites Früebüel (+123%) and Laegeren (+114%) in 2011.

Spring ET ranged from 125 mm at Davos to 233 mm at Früebüel (mean 187 mm; figure 4, table 3) during 2011. The difference of precipitation minus ET showed cumulative spring water deficits of -104 and -109 mm for the sites Oensingen1 and Laegeren, respectively (figure 6). Only the sites Chamau and Davos recovered from the water deficits accumulated during the drought, mainly due to substantial precipitation in the second half of May 2011. The Früebüel montane grassland had a water surplus of 120 mm at the end of spring 2011. Compared to an overall surplus of 70 mm in spring 2010, the mean water deficit was 17 mm across all sites for spring 2011.

3.6. Water-use efficiency

During spring 2011, the highest water-use efficiency (WUE, gross carbon uptake per unit water lost) was observed at the Chamau grassland (4.6 g C (kg H_2O)⁻¹), while the forest sites Laegeren (2.3 g C (kg H₂O)⁻¹) and Davos (1.9 g C (kg H₂O)⁻¹) showed overall much lower WUE (figure 7). Differences between spring 2011 and 2010 were insignificant at the grassland sites (p > 0.05), whereas WUE of the forest Environ. Res. Lett. 8 (2013) 035007 S Wolf et al

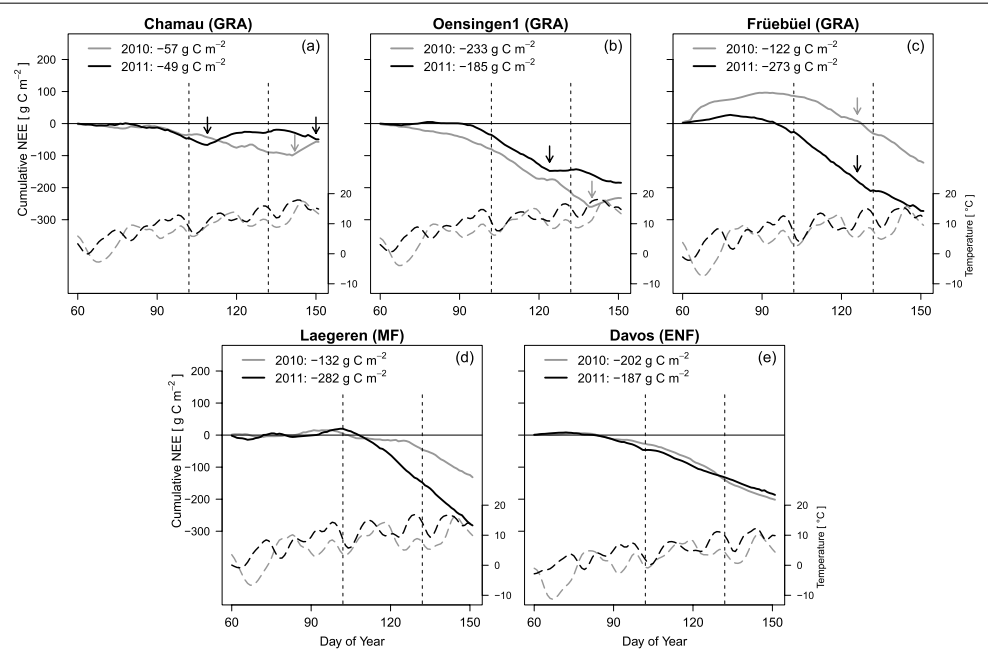


Figure 5. Cumulative net ecosystem exchange (NEE, solid lines) and air temperature (dashed lines, 7 day running mean) during spring 2010 (grey) and 2011 (black). The numbers following the years show total spring NEE. Arrows indicate management at grassland sites, i.e. grass cuts (a), (b) and start of grazing (c). The vertical dashed lines confine the period of spring drought across all sites (DOY 102–132). Abbreviations in titles indicate the IGBP land-use class with grasslands (GRA), mixed forest (MF) and evergreen needleleaf forest (ENF).

sites significantly increased (Laegeren +109%, Davos +58%, both p < 0.001). A combination of increased GPP along with decreased ET caused the higher WUE of the two forest sites in 2011 (table 3).

4. Discussion

Precipitation deficits during spring 2011 resulted in soil moisture deficiencies similar to those typical during summer months, persisting for an extended period (4–6 weeks) at high temperatures. While a consistently earlier phenological development was found at all sites independent of land-use type or elevation, the response of ecosystem carbon dioxide and water vapour fluxes to these spring drought conditions differed strongly among sites, in particular for water-use efficiency between forests and grasslands. Forests adapted to spring drought conditions by increasing water-use efficiency (i.e., reducing transpiration). In contrast, grasslands did not adapt and reductions in productivity of grasslands indicated soil moisture limitations inhibiting regrowth of vegetation after grass cuts during drought conditions in spring.

4.1. Phenology

The phenological development in 2011 was the second earliest since 1950 (MeteoSwiss 2011). It was largely

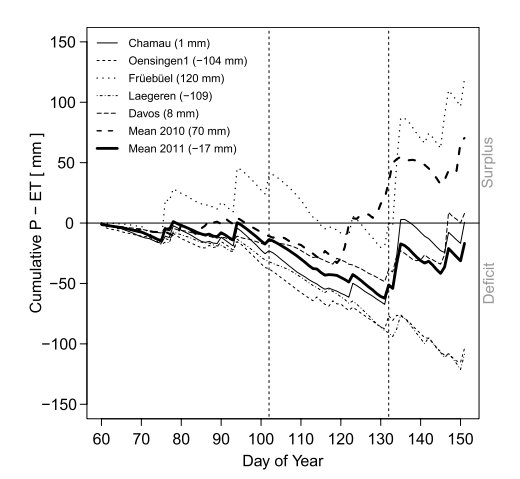


Figure 6. Cumulative daily precipitation (P) minus evapotranspiration (ET) during spring 2011. For comparison, the ensemble mean of all sites is also shown for 2010. The numbers in brackets show spring totals. The vertical dashed lines confine the period of spring drought across all sites (DOY 102–132).

Chamau (GRA) Oensingen1 (GRA) Früebüel (GRA) 2010: WUE = 3.7 g C (kg H₂O)⁻¹, R²=0.56 2010: WUE = 2.8 g C (kg H₂O)⁻¹, R²=0.44 2010: WUE = 3.3 g C (kg H₂O)⁻¹, R²=0.51 2011: WUE = $3.3 \text{ g C (kg H}_2\text{O})^{-1}$, R²=0.71 2011: WUE = 4.6 g C (kg H_2O)⁻¹, R^2 =0.72 2011: WUE = 2.7 g C (kg H_2O)⁻¹, R^2 =0.63 20 20 GPP[gCm⁻²d⁻¹; 15 15 10 10 (a) (b) (c) 8 Laegeren (MF) Davos (ENF) 2010: WUE = 1.1 g C (kg H_2O)⁻¹, R^2 =0.42 2010: WUE = 1.2 g C (kg H_2O)⁻¹, R^2 =0.54 2011: WUE = 2.3 g C (kg H₂O)⁻¹, R²=0.53 2011: WUE = 1.9 g C (kg H₂O)⁻¹, R²=0.61 20 20 GPP [g C m⁻² d⁻¹] 15 15 10 10 (d) (e) ET [kg H₂O m⁻² d⁻¹] ET [kg H₂O m⁻² d⁻¹]

Environ. Res. Lett. **8** (2013) 035007 S Wolf *et al*

Figure 7. Water-use efficiency (WUE), i.e. the ratio of gross primary productivity (GPP) and ecosystem evapotranspiration (ET), in spring 2011 compared to 2010. Significant differences in WUE (slopes) were detected at the forest sites Laegeren (d) and Davos (e), both p < 0.001. Abbreviations in titles indicate the IGBP land-use class with grasslands (GRA), mixed forest (MF) and evergreen needleleaf forest (ENF).

related to temperature and none of our sites showed a delayed development related to drought. While below average precipitation was also observed during early spring 2010 (table 2), temperatures were considerably lower in 2010 ($-2.7\,^{\circ}\mathrm{C}$), and closer to the long-term average as compared to 2011 (MeteoSwiss 2012). These differences and regression analysis (phenological development *versus* temperature) showed that temperature was the main control for spring phenology at our sites during both years ($R^2=0.74$, p<0.001), along with photoperiod and chilling (Körner and Basler 2010), and that soil moisture limitations during spring did not inhibit the onset of leaf activity, despite strong effects on ecosystem fluxes.

4.2. Carbon uptake and gross primary productivity

In contrast to other studies that found largely reduced carbon uptake during spring drought in steppe ecosystems (Dong et al 2011, Parton et al 2012, Kwon et al 2008), we observed only small reductions in net carbon uptake (NEE) for some of our sites. Instead, we found substantially increased net carbon uptake of a montane grassland (Früebüel), similar to Gilgen and Buchmann (2009), and lowland mixed deciduous forest (Laegeren) in response to drought—similar to findings

by Black *et al* (2000) for boreal deciduous forest in years with a warm spring. Overall, these results indicated that spring drought resulted in smaller carbon losses, which are in contrast to the substantial carbon losses that were observed during the severe summer drought in 2003 (Ciais *et al* 2005).

GPP reductions for most sites at the beginning of the drought period (DOY 102–107) were related to incoming cold air masses from the arctic (MeteoSwiss 2011) that affected in particular the higher elevation sites Früebiel and Davos, where mean temperatures dropped below 5 °C and close to freezing, respectively (figure 5). This temperature drop also reduced TER at all sites, with larger reductions observed for the grassland compared to the forest sites (figure 3).

Soil moisture related reductions in GPP were found at the lowland grassland sites, where productivity did not recover following grass cuts in Chamau mid-April (DOY 109, figure 3(a)) and Oensingen1 in early May (DOY 124, figure 3(b)). At Chamau, GPP only recovered following the next major rainfall (DOY 123). Similar reductions in grassland productivity in response to drought were found by Gilgen and Buchmann (2009) for the Chamau grassland, and by Craine *et al* (2012) for grasslands in north-eastern Kansas. In addition, the smaller net carbon uptake of Chamau seemed related to higher manure inputs compared to the Oensingen1

Environ. Res. Lett. 8 (2013) 035007

S Wolf et al

grassland (Zeeman *et al* 2010), which resulted in higher TER relative to GPP (ratio of 0.95 *versus* 0.68, table 3).

For both forest sites, cumulative annual net carbon uptake (not shown) started earlier in 2011 compared to 2010, 16 days at Laegeren and 13 days at Davos. These differences were similar to the results from phenological observations, which showed differences of 16 and 12 days for both forest sites between years (figure 2). The findings for Laegeren confirmed Ahrends et al (2009) and Etzold et al (2011), who reported enhanced productivity and net carbon uptake in a year (2007), when bud break at Laegeren occurred 10 days earlier compared to the two previous years (Ahrends et al 2009). In contrast to our two forests, we could not find a similar relation of phenological observations and NEE for the grasslands due to management at these sites, i.e., grass cuts being performed before flowering to prevent reduced biomass production after flowering.

GPP increases from 2010 to 2011 were smaller in Davos compared to Laegeren (table 3), suggesting that productivity in evergreen needleleaf forest is less sensitive to seasonal climate anomalies compared to deciduous broadleaf forest (Richardson et al 2010). In contrast, the opposite pattern was found for TER between both years: during spring 2011, TER was increased only marginally in Laegeren but largely enhanced in Davos (related to higher temperatures), where TER substantially exceeded the increase in GPP (table 3). This indicated limitations for higher net carbon uptake in subalpine forest ecosystems during years with above average spring temperatures—an important implication when considering the projected temperature increases for Switzerland for all seasons (CH2011 2011).

4.3. Evapotranspiration and water-use efficiency

Evapotranspiration of both forests was substantially reduced in spring 2011 compared to 2010, a clear signal of stomatal regulation (i.e., reduction of leaf transpiration) as an early response to drought (see also Jarvis and McNaughton 1986). Such regulation in forests was also shown by Teuling et al (2010) during a summer heatwave that was enhanced by drought: unlike grasslands, forests employ water saving strategies and reduce their ET early on, thereby reducing evaporative cooling of the atmosphere. In contrast, grasslands maintain their ET as long as soil moisture is available. In our study, grasslands did not reduce ET during spring drought either, suggesting a consistent behaviour of grassland vegetation to spring and summer droughts. The Früebüel grassland even increased ET, probably due to more available energy from clear skies during spring 2011.

In addition, both our forest sites significantly increased their WUE in response to spring drought, while no such effect was observed for the grassland sites in Switzerland. This increase in WUE is in accordance with the expected response of WUE at the leaf level, to reduce water stress while keeping foliar assimilation high (see Bacon 2004; Schulze *et al* 2005). However, such response at the leaf level does not necessarily translate to the ecosystem scale (Jarvis and McNaughton 1986), which additionally includes soil evaporation, and in

fact, only few ecosystem-scale studies reported increased WUE during drought (e.g. Krishnan *et al* 2006). Nonetheless, Beer *et al* (2009) concluded from a global synthesis study of 43 flux tower sites that changes in WUE (or inherent WUE) indicate the adjustment of ecophysiology at stand level and thus enable the transfer of the WUE concept from the leaf to the ecosystem level.

The stronger increase of WUE at Laegeren (broadleaved) compared to Davos (coniferous) can be explained by stronger stomatal regulation of leaves *versus* needles (Schulze *et al* 2005), supporting results from Granier *et al* (2007) in response to the 2003 summer drought in Europe. For the same drought event, however, decreased WUE was also reported by Reichstein *et al* (2017) for mostly forest ecosystems and Hussain *et al* (2011) for a grassland. Ponce Campos *et al* (2013) recently added further evidence for higher WUE across biomes during drier years that increased with drought intensity. Therefore, further research with large observational datasets (e.g. FLUXNET) is needed to comprehensively distinguish the WUE response to drought between forests and grasslands—in general and also evaluating potential differences between spring and summer drought.

The observed water deficits (negative P-ET) or minor surplus at the end of spring could have important implications for the vegetation during summer, as spring is typically a period of water recharge for soil and groundwater reservoirs. A combination of spring and summer droughts in the same year could substantially increase the impact of summer drought, e.g. with larger reductions in productivity, enhanced temperature feedbacks amplifying heatwaves, and severe deficits in water supply for agriculture and society. In 2011, however, carry-over effects into the following season were prevented by heavy precipitation during early summer that counteracted the potential risk of extreme summer temperatures (Ouesada et al 2012).

Overall, we conclude that forests adapt to spring drought by increasing WUE much stronger than grasslands, which could be due to an evolutionary strategy to secure carbon investments during harsh conditions (Schulze *et al* 2005).

5. Conclusions

Grasslands and forests responded very differently to spring drought in terms of ecosystem carbon dioxide and water vapour fluxes: while forests adapted and reduced their WUE significantly, grasslands did not show this behaviour, or maybe would only after a prolonged drought. These contrasting responses to drought will not only affect the feedback to the atmosphere via ET, but also indicate different susceptibilities of grasslands versus forests to future drought events, predicted to increase in frequency and severity. Our results further suggest that understanding the response of different land-use types to drought is highly relevant to predict impacts of climate change on biosphere–atmosphere fluxes of terrestrial ecosystems.

Acknowledgments

Funding was received from the Swiss National Science Foundation (SW, Fellowship for Prospective Researchers), the

Environ. Res. Lett. 8 (2013) 035007 S Wolf et al

European Commission's FP7 (SW, Marie Curie International Outgoing Fellowship, grant no. 300083; NB, GHG-Europe, grant no. 244122; NB, CARBO-Extreme, grant no. 226701), and ETH Zurich (NB, ETH Research Grant CH2-01 11-1). Meteorological data were provided by MeteoSwiss, the Swiss Federal Office of Meteorology and Climatology, and the Swiss Federal Office for the Environment (FOEN). MeteoSwiss also provided phenological data. We thank Sabina Keller for database management, Peter Plüss and Thomas Baur for technical support, and Matthias Barthel, Eugénie Paul-Limoges and Dennis Baldocchi for critical comments that helped to improve this manuscript.

Author contributions

SW conceived the study with inspiration from NB. WE, CA, MH, SZ, RH, JS and DI provided data. SW, WE and CA post-processed the data. SW performed the analyses and wrote the first draft of the manuscript. All authors contributed to data interpretation and the final manuscript.

References

- Ahrends H E, Etzold S, Kutsch W L, Stoeckli R, Bruegger R, Jeanneret F, Wanner H, Buchmann N and Eugster W 2009 Tree phenology and carbon dioxide fluxes: use of digital photography at for process-based interpretation the ecosystem scale Clim. Res. 39 261-74
- Ammann C, Flechard C R, Leifeld J, Neftel A and Fuhrer J 2007 The carbon budget of newly established temperate grassland depends on management intensity Agric. Ecosyst. Environ.
- Ammann C, Spirig C, Leifeld J and Neftel A 2009 Assessment of the nitrogen and carbon budget of two managed temperate grassland fields *Agric. Ecosyst. Environ.* **133** 150–62
- Bacon M A 2004 Water Use Efficiency in Plant Biology (Oxford: Blackwell)
- BAFU 2011 Trockenheit Frühling 2011: Auswirkungen der
- Trockenheit auf Natur und Umwelt (Bern: BAFU)
 Barriopedro D, Fischer E M, Luterbacher J, Trigo R M and García-Herrera R 2011 The hot summer of 2010: redrawing
- the temperature record map of Europe Science 332 220-4

 Beer C et al 2009 Temporal and among-site variability of inherent water use efficiency at the ecosystem level Glob. Biogeochem. Cycles 23 GB2018
- Black T A, Chen W J, Barr A G, Arain M A, Chen Z, Nesic Z, Hogg E H, Neumann H H and Yang P C 2000 Increased carbon sequestration by a boreal deciduous forest in years with a warm spring *Geophys. Res. Lett.* **27** 1271–4
- CH2011 2011 Swiss Climate Change Scenarios CH2011 (Zurich: C2SM, MeteoSwiss, ETH Zurich, NCCR Climate and OcCC)
- Christensen J H and Christensen O B 2003 Climate modelling: severe summertime flooding in Europe *Nature* **421** 805–6 Ciais P *et al* 2005 Europe-wide reduction in primary productivity
- caused by the heat and drought in 2003 Nature
- Craine J M, Nippert J B, Elmore A J, Skibbe A M, Hutchinson S L and Brunsell N A 2012 Timing of climate variability and grassland productivity *Proc. Natl Acad. Sci.* **109** 3401–5 Dong G, Guo J X, Chen J Q, Sun G, Gao S, Hu L J and Wang Y L
- 2011 Effects of spring drought on carbon sequestration, evapotranspiration and water use efficiency in the songnen meadow steppe in northeast China *Ecohydrology* 4 211–24 Etzold S, Buchmann N and Eugster W 2010 Contribution of
- advection to the carbon budget measured by eddy covariance at a steep mountain slope forest in Switzerland Biogeosciences

- Etzold S, Ruehr N, Zweifel R, Dobbertin M, Zingg A, Pluess P, Häsler R, Eugster W and Buchmann N 2011 The carbon balance of two contrasting mountain forest ecosystems in Switzerland: similar annual trends, but seasonal differences Ecosystems 14 1289-309
- Eugster W and Senn W 1995 A cospectral correction model for measurement of turbulent NO2 flux Bound.-Layer Meteorol.
- European Drought Observatory 2011 Drought News in Europe. Situation in May 2011 (Ispra: European Commission—Joint Research Centre)
- Foken T and Wichura B 1996 Tools for quality assessment of surface-based flux measurements *Agric. Forest Meteorol.* **78** 83–105
- Frei C, Schöll R, Fukutome S, Schmidli J and Vidale P L 2006 Future change of precipitation extremes in Europe: intercomparison of scenarios from regional climate models J. Geophys. Res. 111 D06105
- Gilgen A K and Buchmann N 2009 Response of temperate grasslands at different altitudes to simulated summer drought differed but scaled with annual precipitation Biogeosciences
- Granier A et al 2007 Evidence for soil water control on carbon and water dynamics in European forests during the extremely dry year: 2003 Agric. Forest Meteorol. 143 123-45
- Hussain M Z et al 2011 Summer drought influence on CO2 and water fluxes of extensively managed grassland in Germany Agric. Ecosyst. Environ. 141 67–76
- Jarvis P G and McNaughton K G 1986 Stomatal control of transpiration: scaling up from leaf to region Adv. Ecol. Res.
- Körner C and Basler D 2010 Phenology under global warming Science 327 1461-
- Krishnan P, Black T A, Grant N J, Barr A G, Hogg E H, Jassal R S and Morgenstern K 2006 Impact of changing soil moisture distribution on net ecosystem productivity of a boreal aspen forest during and following drought Agric. Forest Meteorol.
- Kwon H, Pendall E, Ewers B E, Cleary M and Naithani K 2008 Spring drought regulates summer net ecosystem CO2 exchange in a sagebrush-steppe ecosystem Agric. Forest Meteorol. **148** 381-91
- Lindroth A, Lagergren F, Grelle A, Klemedtsson L, Langvall O, Weslien P and Tuulik J 2009 Storms can cause Europe-wide reduction in forest carbon sink Glob. Change Biol. 15 346-55
- Mauder M, Foken T, Clement R, Elbers J A, Eugster W Grunwald T, Heusinkveld B and Kolle O 2008 Quality control of CarboEurope flux data—Part 2: inter-comparison of eddy-covariance software Biogeosciences 5 451-62
- MeteoSwiss 2011 Witterungsbericht 2011 (Zurich: MeteoSwiss) MeteoSwiss 2012 Klimakarten Schweiz, Trends (Zurich: MeteoSwiss)
- Parton W, Morgan J, Smith D, Del Grosso S, Prihodko L, LeCain D, Kelly R and Lutz S 2012 Impact of precipitation dynamics on net ecosystem productivity Glob. Change Biol. 18 915–27 Pielmeier C 2011 Wetter, Schneedecke und Lawinengefahr.
- Hydrologisches Jahr 2010/11 (Davos: WSL-Institut für Schnee-und Lawinenforschung SLF) p 23 Ponce Campos G E et al 2013 Ecosystem resilience despite
- large-scale altered hydroclimatic conditions Nature
- Quesada B, Vautard R, Yiou P, Hirschi M and Seneviratne S I 2012 Asymmetric European summer heat predictability from wet and dry southern winters and springs Nature Clim. Change
- Reichstein M et al 2007 Reduction of ecosystem productivity and respiration during the European summer 2003 climate anomaly: a joint flux tower, remote sensing and modelling analysis Glob. Change Biol. 13 634-51

S Wolf et al

Environ. Res. Lett. 8 (2013) 035007

Reichstein M et al 2005 On the separation of net ecosystem exchange into assimilation and ecosystem respiration: review and improved algorithm *Glob. Change Biol.* 11 1424–39 Richardson A D *et al* 2010 Influence of spring and autumn

- phenological transitions on forest ecosystem productivity Phil.
- Trans. R. Soc. B 365 3227–46 Schär C, Vidale P L, Luthi D, Frei C, Haberli C, Liniger M A and Appenzeller C 2004 The role of increasing temperature variability in European summer heatwaves *Nature* **427** 332–6 Schmocker-Fackel P and Naef F 2010 More frequent flooding?
- changes in flood frequency in Switzerland since 1850 J. Hydrol. 381 1-8
- Schulze E D, Beck E and Müller-Hohenstein K 2005 Plant Ecology
- (Heidelberg: Springer)
 Seneviratne S I, Corti T, Davin E L, Hirschi M, Jaeger E B,
 Lehner I, Orlowsky B and Teuling A J 2010 Investigating soil moisture-climate interactions in a changing climate: a review *Earth-Sci. Rev.* **99** 125–61
- Sepulcre-Canto G, Horion S, Singleton A, Carrao H and Vogt J 2012 Development of a combined drought indicator to detect agricultural drought in Europe Nat. Hazards Earth Syst. Sci.
- Teuling A J et al 2010 Contrasting response of European forest and grassland energy exchange to heatwaves *Nature Geosci.* 3 722–7

- Vogt J 2012 Drought Monitoring, Assessment and Forecasting (Ispra: European Commission—Joint Research Centre)
- Webb E K, Pearman G I and Leuning R 1980 Correction of flux measurements for density effects due to heat and water-vapor transfer O. J. R. Meteorol. Soc. 106 85–100
- Wolf S, Eugster W, Potvin C, Turner B L and Buchmann N 2011 Carbon sequestration potential of tropical pasture compared
- with afforestation in Panama *Glob. Change Biol.* **17** 2763–80 Zeeman M J, Hiller R, Gilgen A K, Michna P, Pluss P, Buchmann N and Eugster W 2010 Management and climate impacts on net CO2 fluxes and carbon budgets of three grasslands along an elevational gradient in Switzerland Agric. Forest Meteorol. 150 519–30
- Zeeman M J, Tuzson L, Emmenegger L, Knohl A, Buchmann N and Eugster W 2009 Conditional CO₂ flux analysis of a managed grassland with the aid of stable isotopes Biogeosci. Discuss. 6 3481-510
- Zhang L, Xiao J F, Li J, Wang K, Lei L P and Guo H D 2012 The 2010 spring drought reduced primary productivity in southwestern China Environ. Res. Lett. 7 045706
- Zweifel R, Eugster W, Etzold S, Dobbertin M, Buchmann N and Häsler R 2010 Link between continuous stem radius changes and net ecosystem productivity of a subalpine Norway spruce forest in the Swiss Alps New Phytol. 187 819-30

Appendix C

Large peaks of N_2O emissions following grassland restoration

Lutz Merbold¹, Werner Eugster¹, Jacqueline Stieger¹, Mark Zahniser²,
David Nelson², Nina Buchmann¹

 $^1{\rm Department}$ of Environmental Systems Science, ETH Zurich, Zurich, Switzerland $^2{\rm Aerodyne}$ Research Inc., Massachusetts, Billerica, USA

This manuscript was submitted to: Global Change Biology, GCB-13-1126

Large peaks of N₂O emissions following grassland restoration

Lutz Merbold^{1*}, Werner Eugster¹, Jacqueline Stieger¹, Mark Zahniser², David Nelson² and Nina Buchmann¹

¹Department of Environmental Systems Science, ETH Zurich, Universitaetsstr. 2, 8092, Zurich, Switzerland ²Aerodyne Research Inc., 45 Manning Rd, MA 01821, Massachusetts, Billerica.USA

Abstract

The first full greenhouse gas (GHG) flux budget of an intensively managed grassland in Switzerland (Chamau, CHA) is presented. The three major trace gases, carbon dioxide (CO₂), methane (CH₄) and nitrous oxide (N₂O) were measured with the eddy covariance (EC) technique. For CO₂ concentrations, an open-path infrared gas analyzer was used, while N₂O and CH₄ concentrations were measured with a recently developed continuous-wave quantum cascade laser absorption spectrometer (QCLAS). We investigated the magnitude of these trace gas emissions after grassland restoration, including ploughing, harrowing, sowing and fertilization with inorganic and organic fertilizers over a period of one year (January to December 2012). Large peaks of N₂O fluxes (20 – 50 nmol m⁻² s⁻¹ compared to a < 5 nmol m⁻² s⁻¹ ¹ background flux) were observed during thawing of the soil after the winter period and after mineral fertilizer application followed by re-sowing in the beginning of the summer season. N₂O fluxes were controlled by nitrogen input, plant productivity, soil water content and temperature. Management activities led to increased variations of N2O fluxes up to 14 days after the management event as compared to background fluxes measured during periods without management (< 5nmol m⁻² s⁻¹). The annual GHG flux budget was dominated by N₂O (48 % contribution) and CO₂ emissions (44 %). CH₄ flux contribution to the annual budget was only minor (8 %).

We conclude that recently developed multi-species QCLAS in an EC system open new opportunities to determine the temporal variation of N_2O fluxes, which further allow to thoroughly quantify annual emissions including management events. With respect to grassland restoration, our study emphasizes the key role of N_2O and CO_2 losses after ploughing, changing a permanent grassland from a carbon sink to a significant carbon source.

1. Introduction

Grassland ecosystems are commonly known for their greenhouse gas (GHG) mitigation potential (Lal, 2010). At the same time emissions of N_2O after management activities such as fertilization and ploughing have been shown to reduce this mitigation potential in agricultural systems (Baggs *et al.*, 2000, Sarkodie-Addo *et al.*, 2003). However, up to date the magnitude of N_2O emissions after ploughing and their effect on the full GHG budget of a permanent grassland has not been quantified with continuous N_2O flux measurements. Here, we investigated how restoration and management of an intensively managed grassland in Switzerland affects GHG emissions (CO_2 , CH_4 and N_2O). Prior to our measurements we hypothesized large variations in CO_2 uptake rates caused by harvest and fertilization events, minor release and uptake of CH_4 , and peaks of N_2O emissions after fertilization events.

Greenhouse gas emissions (CO₂, CH₄ and N₂O) from managed ecosystems, including grasslands have been identified to be of major relevance for the global climate system (Dalal & Allen, 2008). Up to date, available knowledge suggests that agricultural production systems are often GHG neutral, with N₂O and CH₄ offsetting potential CO₂ sequestration (Schulze et al., 2009). While most research so far has been focusing on the exchange of the most important greenhouse gas - carbon dioxide - less research has been undertaken on CH₄ and N₂O fluxes. Few exceptions are the so-called highflux ecosystems, e.g. livestock production systems and wetlands in terms of CH₄ emissions (e.g. Dengel et al., 2011) and agricultural systems with large N₂O emissions (e.g. Skiba et al., 2009, Soussana et al., 2007, Zona et al., 2013). Particularly the lack of high temporal resolution continuous flux datasets is one of the major reasons for limited knowledge on N₂O and CH₄ exchange and there are three major reasons for this shortage in data: (1) the GHG balance of an ecosystem is often dominated by the net exchange of CO₂ (> 60-80%) with the additional gases being less important for annual balances of many ecosystems (e.g. Chen et al., 2011, Schulze et al., 2009). Moreover CH₄ and N₂O fluxes have often been ignored due to more complex processes (nitrification, de-nitrification, methanogenesis, methantrophy a.o.) underlying the net exchange of both GHGs compared to CO₂ exchange (e.g. Palm et al., 2002, Schaufler et al., 2010); (2) the application of the until recently available measurements devices, primarily manual or automatic chambers in combination with a gas chromatograph are both labor intensive and provide only a spatial snapshot of the GHG exchange of a fraction of an ecosystem (e.g. Flechard et al., 2005, Skiba et al., 2009). While chambers allow to measure various hot spots, chamber measurements further result in weekly to monthly measurements only (e.g. Imer et al., 2013, Mishurov & Kiely, 2011). The occurring data gaps must be gap-filled and are often biased by missing possible peak emissions during natural events such as heavy rainfalls or anthropogenic management activities such as fertilization and ploughing;(3) analyzers such as fast response laser absorption spectrometers which can be easily deployed in the field have became commercially available for CH_4 and N_2O only recently (Kroon et al., 2010).

Most of these drawbacks can be overcome by the use of such laser absorption spectrometers (Neftel et~al., 2010, Tuzson et~al., 2010). With these instruments researches are enabled to measure single or multiple GHGs at a high temporal resolution with a previously unavailable precision of < 0.05 ppb Hz^{-1/2} for N₂O (McManus et~al., 2010). If these QCLAS are combined with high frequency wind measurements such as done in the eddy covariance approach, full GHG flux datasets covering annual timescales and whole ecosystems become available providing the essential datasets to close the still occurring knowledge gaps. Therefore we upgraded an already existing EC system measuring CO_2/H_2O in intensively managed grassland in Switzerland with a QCLAS to additional measure the concentrations of N₂O and CH_4 .

Our specific objectives were, (i) to investigate the full GHG budget of a recently restored permanent grassland, (ii) to study the temporal behavior of GHG emissions in relation to management activities, and (iii) to test a recently developed continuous quantum cascade laser absorption spectrometer (QCLAS) to measure the concentrations of CH_4 and N_2O within an eddy covariance setup.

2. Material & Methods

2.1 Study site

The intensively managed grassland under investigation (Chamau, CHA, Zeeman et al. 2010) is located in the pre-alpine lowlands of Switzerland at an altitude of 400 m a.s.l. (47° 12' 37" N, 8° 24' 38" E). Mean annual temperature is 9.1°C and mean annual precipitation is 1151 mm (Sieber et al., 2011). The soil type is a Cambisol (Roth, 2006) with a pH of 5, a bulk density ranging between 0.9 and 1.3 kg m⁻³ and a carbon stock of 55.5 – 69.4 t C ha-1 in the upper 20 cm of the soil (Zeeman et al., 2010). The common species composition consists of Italian ryegrass (Lolium multiflorum) and white clover (Trifolium repens L.). Typical management for forage production consists of up to six harvest events and subsequent slurry application (Zeeman et al., 2010). However, the grassland is restored approximately every ten years (pers. communication Hans-Rudolf Wettstein) in order to eliminate mice populations and therefore to maintain a high quality sward for fodder production. Restoration as done in 2012, the year of observation, included ploughing, sowing, application of mineral and organic fertilizer, pesticide application if needed and regular harvests. Representative fertilizer samples applied to the plot were collected at the day of management and sent to a central lab for nutrient content analysis (Table 1, Labor fuer Bodenund Umweltanalytik, Eric Schweizer AG, Thun, Switzerland).

2.2 Environmental data

Environmental variables were measured every 10 s and stored as 30 min averages within a datalogger (CR10X, Campbell Scienctific, Logan, USA). These variables included measurements of air temperature and relative humidity (2 m height, Hydroclip S3 sensor, Rotronic AG, Switzerland), soil temperature (depths of 0.01, 0.02, 0.05, 0.10 and 0.15 m, TL107 sensors, Markasub AG, Olten, Switzerland), volumetric soil water content (depths of 0.02 and 0.15 m, ML2x sensors, Delta-T Devices Ltd., Cambridge, UK), and photosynthetic active radiation (2 m height, PARlite sensor, Kipp and Zonen, Delft, The Netherlands).

2.3 Greenhouse gas flux measurements

Flux measurements of CO_2 , CH_4 and N_2O with the eddy covariance technique were undertaken from January until December 2012 (Baldocchi & Meyers, 1998).

The eddy covariance setup consisted of a three-dimensional sonic anemometer (2m height, Solent R3, Gill Instruments, Lymington, UK), an open-path infrared gas analyzer (LI-7500, LiCor Biosciences, Lincoln, Nebraska, USA) to measure the concentrations of CO₂ and H₂O_{vapor}, and a recently developed continuous-wave quantum cascade laser absorption spectrometer (mini-QCLAS, Aerodyne Research Inc., Billerica. Massachusetts, USA) to measure the concentrations of CH₄, N₂O and H₂O_{vapor} at 10Hz. The QCLAS provided the dry mole fraction for both trace gases (CH₄ and N₂O) and data were transferred to the data acquisition system (MOXA embedded Linux computer) via an RS-232 serial data link and merged with other data streams in near-real time (Eugster & Pluss, 2010). Flux calculation followed the CarboEurope-IP standards (Aubinet et al., 2012), where the vertical turbulent flux (F_{GHG}) is calculated as covariance of the fluctuation of the vertical wind velocity (w') and the GHG concentration (c_{GHG}) , averaged over 30 minutes (Eq. 1).

$$F_{GHG} = \overline{w'c_{GHG}'} \times V_{air} \tag{1}$$

The overbar denotes time averages, c_{GHG} ' the half-hourly concentration of the respective greenhouse gas (ppm CO_2 , ppb CH_4 or ppb N_2O) after having subtracted the linear trend, w' the vertical wind speed (m s⁻¹), V_{air} the molar volume of air ($\approx 22.4 \times 10^{-3}$ m³ mol⁻¹), computed as $V_{air} = M_{air}/\rho_{air}$, where M_{air} is the molar mass of air (≈ 0.286 kg mol⁻¹), and ρ_{air} is the measured density of air (kg m⁻³). Greenhouse gas flux calculations included the necessary corrections for high-frequency dampening losses (Eugster & Senn, 1995) and density fluctuations according to Webb et al. (1980) for CO_2 .

Throughout this manuscript, we use the micrometeorological convention of the flux direction, with positive fluxes indicating a loss of the respective GHG from the surface to the atmosphere, and a negative fluxes indicating uptake of the respective GHG.

2.4 Flux data post-processing

All 30 min averages were screened for obvious out-of-range values (\pm 50 µmol m⁻² s⁻¹ for CO₂, \pm 500, \pm 100 nmol m⁻² s⁻¹ for N₂O and CH₄ respectively), and periods of low mechanical turbulence indicated by a friction velocity u* < 0.08 m s⁻¹ (Zeeman et al. 2010). In addition, CO₂ fluxes were further filtered for periods of window dirtiness of the infrared gas analyzer (Automatic Gain Control, AGC > 70%) and spikes in the 30 min flux data according to Papale et al. (2006). The analysis of CO₂ fluxes was based on the 30 min flux averages, while N₂O and CH₄ fluxes were further aggregated to daily means due to the large variations in the 30 min fluxes. Daily averages were only calculated for days where more than 30 half-hour records were available. The remaining high-quality fluxes were separated by management activity before further analysis (Table 1).

2.5 Annual sums of CO₂, CH₄ and N₂O and flux partitioning

In order to calculate the annual exchange of each GHG, missing flux data of CO_2 , CH_4 and N_2O were gap-filled using data from time-periods with comparable environmental conditions – so called look-up tables (Reichstein et al., 2005). These look-up tables were adapted for periods of similar management events to avoid filling of data gaps within a specific management (e.g. ploughing) with data from a time period of different management (e.g. harvest).

Net ecosystem exchange of CO_2 (NEE_{CO2}) was partitioned into ecosystem respiration (R_{eco}) and gross primary production (GPP) via separation of night-and daytime data assuming that the plant canopy is photosynthetically inactive during night. If photosynthetic active radiation (PAR) was smaller than 10 µmol m⁻² s⁻¹, data were classified as night, if values were above 10 µmol m⁻² s⁻¹, data were marked as daytime data. The resulting nighttime data were then correlated to common driver variables, e.g. air and soil temperature as well as soil water content in different depths. Partitioning of CH_4 and N_2O fluxes could not be performed due to interacting processes occurring simultaneously in the soil during the whole day.

Calculation of the global warming potential (GWP) followed the recommendations given by the IPCC, with CH_4 having a 25 and N_2O a 298 times greater GWP than CO_2 on a per mass basis over a time horizon of 100 years (IPCC, 2007).

3. Results

3.1 Dynamics of N₂O, CO₂ and CH₄ fluxes

The overall environmental conditions in 2012 (mean annual temperature, $MAT_{2012} = 9.56$ °C; mean annual precipitation, $MAP_{2012} = 1023.5$ mm) were slightly warmer and slightly less rainy in comparison to interpolated long-term measurements of nearby MeteoSwiss stations (MAT = 9.1°C, MAP = 1151mm, Sieber et al., 2011). Between January and mid-April environmental

conditions remained unfavorable for plant growth including low temperatures (< 10 °C) and less precipitation in comparison to the following months (Fig. 1a - d).

Background N₂O emissions were estimated to be smaller than 5 nmol N₂O m⁻ ² s⁻¹ as seen towards the end of the growing season (Oct. - Dec.) and during the dormant winter season (Figs. 2a, b). In contrast peak emissions of N₂O could be as large 70 nmol N_2O m⁻² s⁻¹ on the half-hourly basis (Fig. 2a) and as large as 30 nmol N₂O m⁻² s⁻¹ as a daily average emission value (Fig. 2b). We observed distinct peaks of nitrous oxide in relation to abrupt changes in environmental conditions (e.g. thawing of the soil in spring) and specific management activities, e.g. after molluscicide application and slurry applications (Fig. 2b; M1, M4 and M5). Daily losses of N₂O were largest in the first half of 2012, before considerable plant canopy development highlighted by considerable CO₂ losses during the same period (Figs. 2b and 5b, Tab. 2). Environmental factors driving N₂O emissions varied for periods of different management activity (Fig. 3a-c, Tab. 3). For instance, manure application prior to ploughing in the beginning of January did not result in a clearly detectable N₂O flux peak (Fig. 3a; M0). The first peaks of N₂O fluxes occurred shortly after ploughing of the field (M1) and were most likely connected to rising air temperatures (> 0°C) and soil thawing in February 2012 (Figs 3a, M2). Slightly larger emissions of N₂O were found for the time after reinstallation of the QCLAS in mid-March and after harrowing, rolling and sowing of the field (M2, M3). These larger fluxes were mostly controlled by soil water content ($r^2 = 0.13$, p < 0.05, Fig. 3a, M2 and M3, Tab. 3). Among the largest peaks were the fluxes observed at the end of April shortly after the application of mineral fertilizer (M4) and both soil temperature and soil water content seemed to have strong influence on the field-scale N2O emissions ($r^2 = 0.22$ and 0.19, p < 0.05; Fig. 3a, M4). Largest emissions of N₂O were observed after re-sowing the field in mid May (M5) and following the first harvest (M6) of the biomass in June 2012, where the plant residues were left on the field (Fig. 3b, M5 and M6). From this point onwards, fluxes of N₂O decreased continuously towards the background values of < 5 nmol N₂O m⁻² s⁻¹ with only a few exceptions shortly after slurry (Fig. 3c, M11 and M13). Background flux values could not sufficiently be explained by environmental variables. Smaller fluxes, in the same order of magnitude as measured during January 2012, were observed between September and December 2012 (Fig. 3, M14; Tab. 3).

 N_2O emissions after fertilizer application were strongly related to plant productivity ($r^2=0.78;\ \mbox{Fig. 4}).$ Given that net ecosystems exchange of CO_2 (NEE $_{CO2}$) can be seen as a proxy of plant activity (more negative values indicate higher uptake rates, NEE = GPP + $R_{\rm eco}$) we correlated the ratio of the average loss of nitrogen (N) via N_2O emission and N input per fertilizer event to the average CO_2 flux during the same period. Our results clearly showed larger losses of nitrogen via N_2O emission with larger net emissions of CO_2 and vice versa. This result indicates that during periods of reduced net uptake rates of CO_2 , nitrogen is more likely to be released as N_2O to the atmosphere than taken up by the plant community (Fig. 4).

NEE_{CO2} was dominated by respiration with little photosynthetic activity until mid April due to little plant development after ploughing (M1) and sowing (M3) in February and March 2012, respectively (Figs. 5a, b). Net uptake rates of CO₂ exceeding 10 µmol m⁻² s⁻¹ were only found from the beginning of June onwards (Fig. 5a), following re-sowing (M5) and continuously favorable environmental conditions (Fig. 1). Net CO₂ fluxes decreased towards the end of the growing season (Oct.) and daily net fluxes switched between net release and net uptake during the following months (Fig. 5b). This pattern was mainly caused by still active vegetation but unstable environmental conditions, such as fluctuating air temperatures (< 0°C but also > 15°C), and decreasing photosynthetic radiation (not shown) until mid December (Figs. 1, 5; Tab. 2). During the peak growing season (May-Sep.) net CO₂ exchange showed increases in both, Reco and GPP indicated by clear drops in net uptake rates and less pronounced decreases in CO2 emissions following harvest events (Fig. 5a, b). Increasing values of net uptake and net release of CO2 were observed with plant growth after each harvest and subsequent fertilizer (slurry) application (Fig. 5b, M7-M13).

Ecosystem respiration ($R_{\rm eco}$) showed a strong exponential correlation with air temperature (Fig. 6a), while GPP was driven by light (Fig. 6b). Furthermore, light saturated GPP (PAR > 1000 µmol m⁻² s⁻¹) became less negative if values of vapor pressure deficit (VPD) exceeded 2.5 kPa (Fig. 6c). A strong influence of air temperature on light saturated GPP was recognized for values with VPD lower than 2.5 kPa (Fig. 6d). Detailed driver analysis per management period could not be performed due to the limited amounts of high quality 30min CO_2 flux data.

Methane fluxes were highly variable across the year 2012, with values fluctuating around zero during freezing (Jan./Feb.) and during dry periods in summer (Jun.-Aug.; Fig. 7a, b). Slightly larger methane release was found with temperatures continuously rising above 0 °C in mid February (Figs. 1, 7; Tab. 2). CH₄ flux magnitude and variation could neither be determined by management activities nor related to single environmental variables (Fig. 7b). However, with larger values of soil water content, both CH₄ uptake and release showed much larger variation (Fig. 8).

3.2 Total GHG budget and global warming potential (GWP)

Annual emissions of N_2O , CO_2 and CH_4 totaled 2.91 g N_2O -N m^{-2} , 339 g CO_2 -C m^{-2} , 2.65 g CH_4 -C m^{-2} , indicating a considerable carbon and nitrogen loss from this permanent grassland after restoration in 2012 (Tab. 4). The GWP of these emissions accumulated to 2851 g CO_2 -eq. m^{-2} , with N_2O contributing 48 % (1363 g CO_2 -eq. m^{-2}), CO_2 contributing 44 % (1245 g CO_2 -eq. m^{-2}) and CH_4 contributing 8 % (243 g CO_2 eq. m^{-2}) to the annual budget (Tab. 4).

4. Discussion

Increased emissions of N₂O after fertilization and ploughing of grassland soils have been shown previously in laboratory and in-situ experiments (Hansen et al., 1993. MacDonald et al., 2011. Mori & Hoiito, 2007. Necpalova et al., 2013). However, in contrast to these previous studies, that were primarily based on GHG chambers and carried out during few campaigns while focusing on N₂O only, our study investigated the emissions of all three GHGs (N_2O, CO_2) and CH_4 , continuously and at the ecosystem-scale using the eddy covariance technique. This approach enabled us to identify N₂O peaks varying in magnitude following similar management events (e.g. slurry applications, Figs. 2, 3) suggesting the influence of a range of variables on N₂O fluxes besides nitrogen input from fertilization. Up to date several drivers have been identified to drive N₂O emissions from grassland soils. These drivers include N inputs (Mori & Hojito, 2012), N mineralization after ploughing (Vellinga et al., 2004), nitrate content of the soil (Abdalla et al., 2010), soil water content (Hartmann & Niklaus, 2012), the fraction of waterfilled pore space (Flechard et al., 2005) and compaction of the soil (Hansen et al., 1993). Ball (2013) synthesized the environmental variables, including temperature as a crucial variable, influencing N₂O emissions recently. Our data clearly identified a set of variables driving N₂O fluxes, including N inputs besides soil water content and air temperature. Furthermore the response to the environmental variables was not uniform (Fig. 3a-c) which goes along with results presented by Hartmann et al. (2013). In addition we further identified plant activity as a major determinant of N₂O emissions. Our results suggest a fast turnover of mineral nitrogen either leading to increased productivity, indicated by larger net CO₂ uptake rates, and less N₂O emissions (Fig. 4) or vice versa. In particular the large emissions of N₂O compared to larger net release of CO₂ directly after the application of mineral fertilizer (M4) and smaller emissions during the course of the summer after slurry application (M7-M13) coinciding with larger net uptakes of CO₂ prove this hypothesis. Daily N₂O emissions from our grassland observed in 2012 (> 2 and < 40 nmol N₂O m⁻² s⁻¹) were orders of magnitude larger than emissions reported for an intensively managed pasture in France (Klumpp et al., 2011) and comparable to values presented by Mori & Hojito (2007) for a permanent grassland in Japan.

Net $\rm CO_2$ fluxes in 2012 showed similar patterns (daily net uptake rates > 5µmol $\rm CO_2$ m⁻² d⁻¹, excluding time periods of ploughing and re-sowing) when compared to periods of similar management during previous years (2006 – 2011). However, when comparing NEE_{CO2} in spring 2010 (a year with similar environmental conditions as those observed in 2012) to spring 2012, the loss of C was almost fourfold in the year of restoration (+ 121 g $\rm CO_2$ -C Jan.-May. 2010 compared to + 423 g $\rm CO_2$ -C Jan.-May 2012). Such increased emissions of $\rm CO_2$ after ploughing have been observed by Willems et al. (2011) in an Irish grassland and have further been highlighted in a modeling study for Dutch grasslands (Vellinga *et al.*, 2004). While the increase in NEE_{CO2} after ploughing most likely occurred from reduced photosynthetic activity, but not from

increased soil respiration at the Irish site, our results suggest both, limited photosynthetis caused by the absence of active vegetation after ploughing in spring 2012 and enhanced ecosystem respiration due to larger nutrient availability. Furthermore, the increases in ecosystem respiration were likely a result of (1) the application of manure prior to ploughing (in mid-Jan. 2012, Tab. 1) and (2) the organic rich soils at the Chamau grassland (SOC 55.5 -69.4 t C ha until 20 cm depth, Zeeman et al. 2010). In contrast, ploughing of a drained grassland in Canada lead to reduced soil respiration rates due to the strong decline in microbial biomass (MacDonald et al., 2010), while Eugster et al. (2010) found increased respiration rates for a ploughed cropland in France, presumably caused by larger soil temperatures in the field when compared to pre-ploughing conditions. Still, large emissions after ploughing have also been shown for a pasture in California (Teh et al., 2011), as well as for a permanent grassland in Ireland (Willems et al., 2011). The effects of harvest and fertilizer application on CO2 exchange (reduced net CO₂ uptake) as found in 2012, has previously been shown by Zeeman et al. (2010) for the same grassland and for a moderately managed mountain grassland in Austria by Wohlfahrt et al. (2008).

Restoration clearly led to a substantial loss of carbon during the year of restoration (339 g C m⁻² yr⁻¹, this study). Assuming that grassland restoration including ploughing carried out approximately every 10 years and between such events an average net uptake of 60 - 70 g CO₂-C m⁻² yr⁻¹ is observed (based on CO₂ flux measurements in 2006 and 2007, Zeeman et al. 2010), then such a 10 year interval would be to short to even compensate 50 % of the carbon losses caused by restoration. It should however be noted that such a calculation only includes the emissions of CO₂ but does not consider any lateral inputs/outputs via harvest and fertilization nor losses/gains of C via methane release/uptake.

Most studies investigating methane exchange in grasslands are commonly based on chamber techniques and report a small to intermediate methane sink of such ecosystems (Blankinship et al., 2008, Dalal & Allen, 2008, Ojima et al., 1993). However, Baldocchi et al. (2012) reported methane emissions measured by EC on a peatland pasture in California, which were in the same order of magnitude as our results. Furthermore, Dengel et al. (2011) reported EC based methane emissions exceeding several 100 nmol CH₄ m⁻² s⁻¹ from a sheep pasture in Scotland, where methane fluxes increased with animal stocking rate. Even though EC based methane fluxes still include large uncertainties, mainly due to the fact that one tries to determine a very small flux at the ecosystem scale, our data shows a small methane source in 2012. Up to date available continuous flux datasets state a net source methane from grasslands (Baldocchi et al., 2012, Dengel et al., 2011) indicating a potential overestimation of the postulated methane sink originating from chamber based and modeling studies in the past (Dalal & Allen, 2008). Therefore one of the future challenges in GHG research is to better constrain currently available and future methane flux data particularly from so-called low CH₄ flux ecosystems such as grasslands.

4.1 Uncertainty related to methodology

Net ecosystem exchange of N₂O, CO₂ and CH₄ presented in this study were gained by an easily applicable and recently developed fast-response continuous wave quantum cascade laser absorption spectrometer (QCLAS, mini QCL Aerodyne Research Inc., Billerica MA, USA). To our best knowledge this study is amongst the first who used such a recently developed instrument above a grassland combining eddy covariance measurements of all three GHGs. A previous version of this laser absorption spectrometer (model QCL-TILDAS-76, Aerodyne Research Inc., Billerica MA, USA) has been used by other researchers in a fen in the Netherlands focusing on N₂O and CH₄ fluxes but not CO₂ (Kroon et al., 2007) and only few additional approaches to measure N2O fluxes with micrometeorological methods have been undertaken in the past (e.g. Skiba et al., 1996). The eddy covariance (EC) technique has become a widely used tool to estimate the exchange of carbon dioxide above ecosystems (Baldocchi et al., 2001). Still, this technique has only rarely been used for other GHGs including CH₄ and N₂O. With the development of fast response QCLAS such measurements are likely to become available more regularly. Few studies focused on the methane exchange of grasslands and pastoral ecosystems (Baldocchi et al., 2012, Dengel et al., 2011, Hatala et al., 2012, Kroon et al., 2010) and none of these studies investigated N₂O emissions over a grassland nor the specific event of grassland restoration including multiple management types. Therefore our setup of measuring the three major GHGs (CO₂, CH₄ and N₂O) above a managed and restored grassland using the EC approach is unique and was shown to deliver reliable results. This included small in magnitude background emissions of N₂O but also larger peaks of N₂O after specific management activities (Figs. 2, 3). Besides N₂O, measurements of CH₄ fluxes, commonly known to be very small above permanent grassland (Blankinship et al., 2008) showed a much larger noise when compared to the N₂O flux measurements, indicating the need for further corrections in order to being able to separate noise from signal (Fig. 8).

Currently available GHG flux budgets commonly use gap-filled flux data with gaps in CO₂ data are often filled via look-up tables (Falge et al., 2001) or flux partitioning of NEE of CO₂ into gross primary production (GPP) and ecosystem respiration (R_{eco}), which are both quantified via functional relations using environmental variables (Gilmanov et al., 2007, Reichstein et al., 2005). Such general gap-filling procedures however are currently neither available for N₂O nor CH₄ fluxes due to two major reasons. First, the complexity of the underlying processes, e.g. methanotrophy and methanogenesis concerning CH₄ and nitrification, denitrification and nitrifier denitrification besides others concerning N₂O, occur 24 hours per day without the clear distinction of either process during night and day as known for processes driving CO₂ exchange. This drawback does neither allow for partitioning nor quantifying the contribution of single flux components to the net flux. Secondly, the lack of continuous datasets to successfully use look-up tables (Mishurov & Kiely, 2011) or identify possible functional relations are still lacking with only few exceptions (Dengel et al., 2011). In this study we used a modification of the look-up tables suggested by Falge et al. (2001) where gaps in data were filled with data available from similar environmental conditions, e.g. radiation, temperature or moisture. While look-up tables may be easily applied for non-managed ecosystems, filling of gaps in flux data for managed ecosystem has been shown to be more complex (Ammann et al., 2009). In order to avoid filling of gaps within one management type only we split the data set into subsets by management type (see also the Material & Methods section). This approach led to more reasonable results than the conservative approach of using whole-year datasets. For instance, cumulative CO₂ emissions accounted for 1245 g CO₂-eq. m⁻² with our approach, whereas the conservative approach resulted in much higher losses of 4115 g CO₂-eq. m⁻² for the year 2012. This large overestimation (compared to a net uptake of CO₂ of about 65 g in 2006 and 2007 at this site, Zeeman et al. 2010) of the net emissions of CO₂ was primarily caused by an overestimation of nighttime emissions in spring 2012 (not shown).

Alternatively, emission factors (EF) can be used in place of gap-filling strategies to estimate N2O emissions from managed ecosystems if measurements are unavailable. Emission factors can either be taken from a national GHG inventory or from the IPCC guidelines for national greenhouse gas inventories (IPCC 2007), 1.1 % and 1.25 % of the applied nitrogen are released as N₂O, respectively. In our study a total of 197.8 kg N ha⁻¹ were applied in form of mineral and organic fertilizer in 2012. During the same period the ecosystem lost 29.1 kg N ha⁻¹ via N₂O emissions. That means that almost 15 % (14.71 %) of the applied N were lost via N₂O emissions and hence currently used EFs need to be modified for years of restoration of an ecosystem in future studies. Even if one includes additional available (>100 kg N ha⁻¹, Erikson & Jensen 2001) caused by increased mineralization of nutrients after ploughing, the systems looses considerable amounts of N2O, which is among the strongest greenhouse gases. The magnitude of annual N₂O-N losses of the Chamau grassland exceeded by far (factor of 10) the emissions calculated using IPCC emission factors, suggesting that an adjustment of these factors for specific cases such a grassland restoration may be necessary. These findings can contribute to improve the nutrient use efficiency of agricultural systems (Snyder et al., 2009) by adjusting the timing of certain management activities and therefore having a potential of reducing GHG emissions from permanent grasslands.

Acknowledgements

Funding for this study by GHG-Europe (FP7, EU contract No. 244122) and COST-ES0804 ABBA is gratefully acknowledged. We are thankful to Hans-Ruedi Wettstein and Ivo Widmer for providing crucial management data and support in the field. Further, this project would not have been accomplished without the help from our technical team, specifically Peter Pluess, Thomas Baur and Patrick Fluetsch. We acknowledge their help during the planning stage and the endurance during the setup of the new laser and regular maintenance.

5. Figures and tables

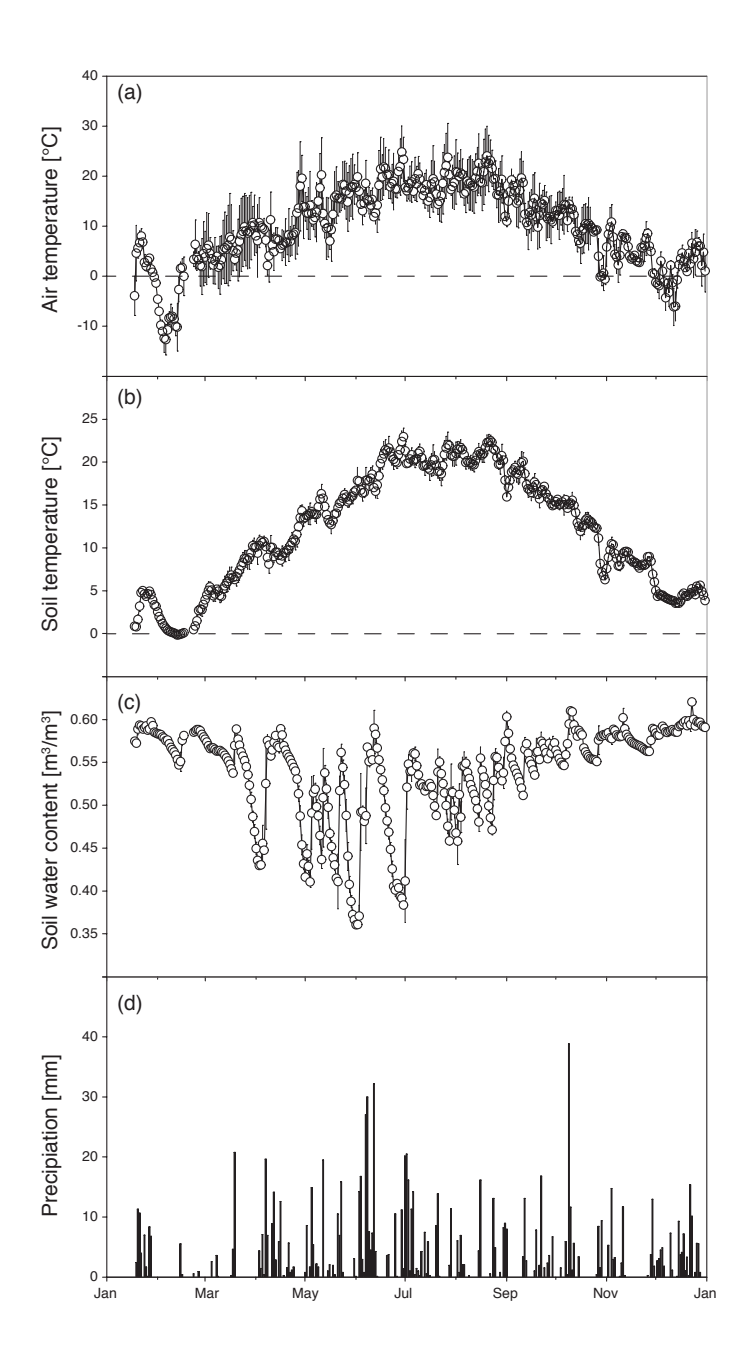


Figure 1: Summary of important environmental variables measured at the grassland site Chamau (CHA) in 2012. The variables shown are daily averages \pm SD of (a) air temperature at 2 m height, (b) soil temperature at 0.02 m depth, (c) soil water content at 0.05m depth, and (d) precipitation (daily sums). Sudden increases in soil water content coincide with precipitation events.

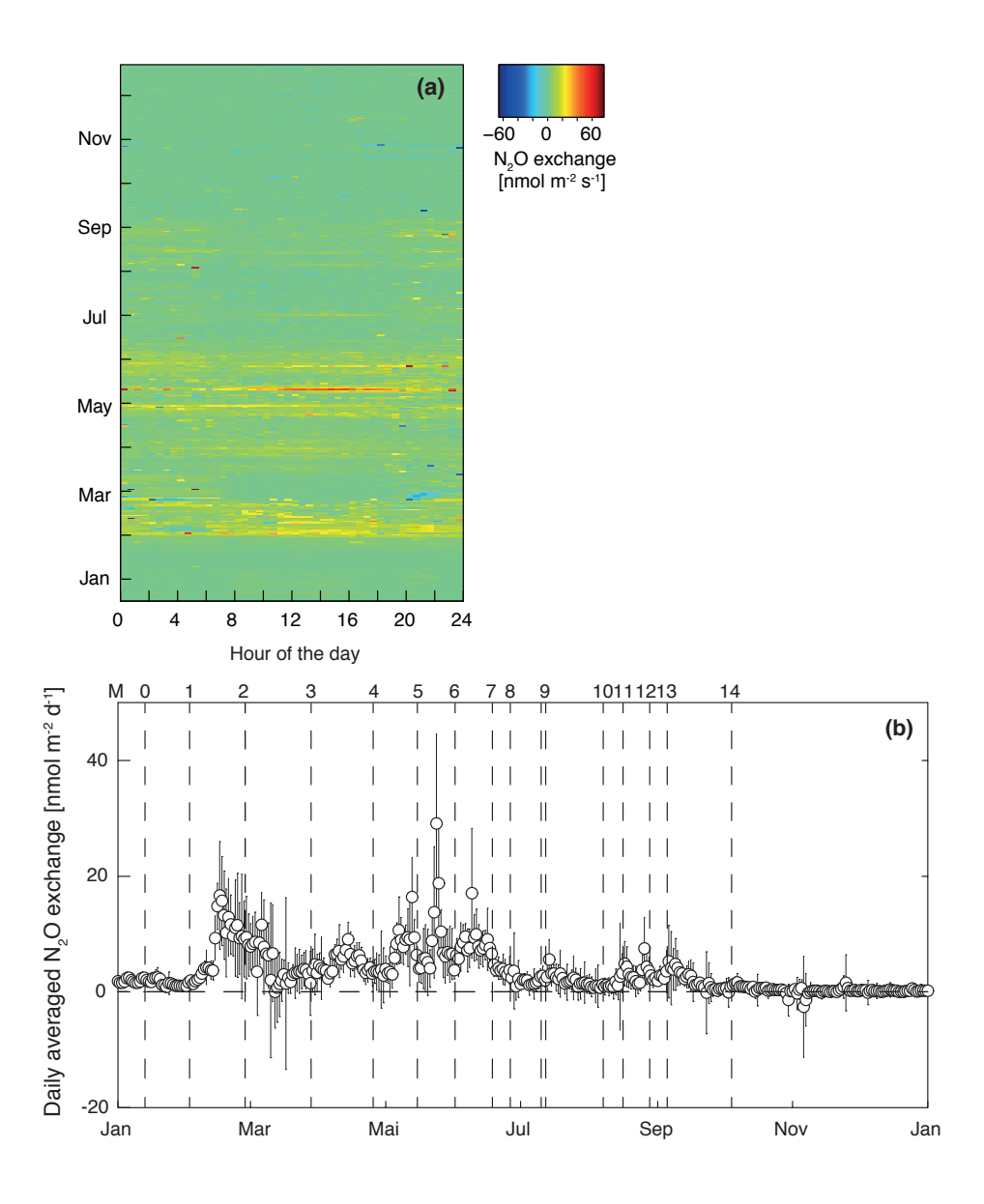


Figure 2: Net ecosystem exchange of nitrous oxide: **(a)** flux fingerprint visualizing gap-filled 30min averaged N_2O exchange across each day in 2012 in nmol m^{-2} s⁻¹, **(b)** daily averaged gap-filled N_2O exchange (\pm SD). The vertical dashed lines represent the specific management activities (M0 - M14, see also Tab. 1). Negative fluxes indicated net uptake of N_2O and positive values indicate net release of N_2O .

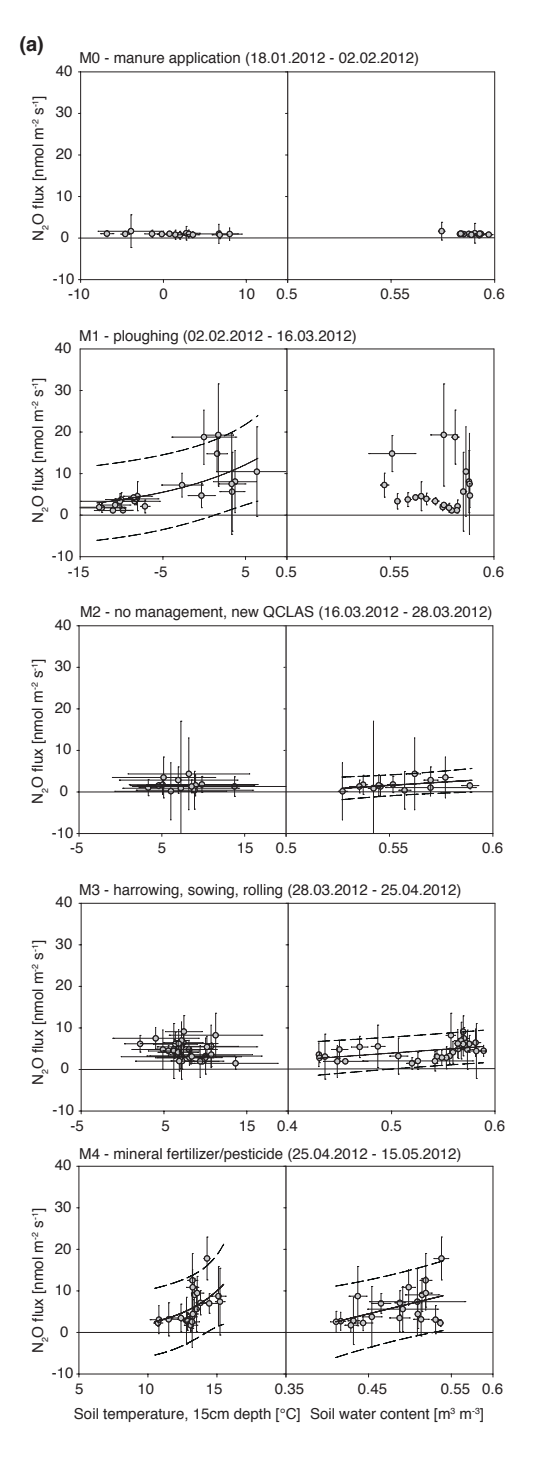


Figure 3a: Responses of measured N_2O flux data to temperature and soil water content shown for management periods MO-M4. Solid lines indicate fitted curves and dashed lines represent the 95% prediction bands. Scaling for air-, soil temperature soil water content varies. Larger flux magnitudes were observed during management activities with limited plant growth (M0-M6, Jan. 2012 - mid Jun. 2012). Soil moisture sensors were placed in 0.05 m depth. Statistics are given in Tab. 3.

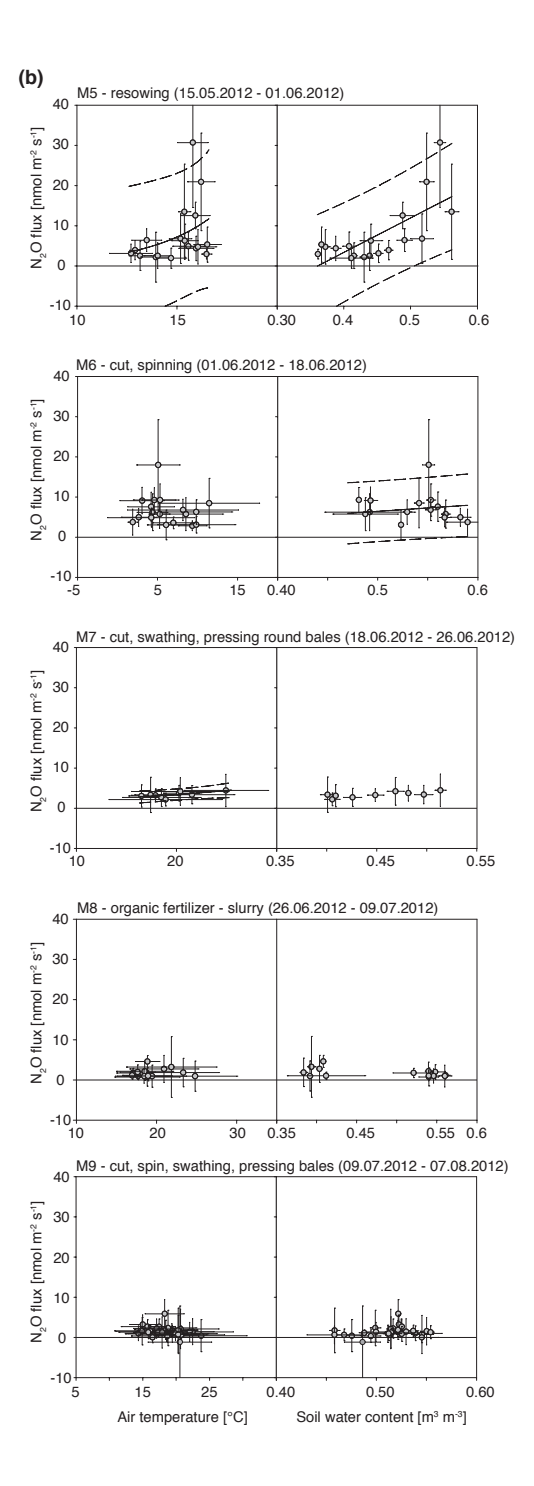


Figure 3a: Responses of measured N_2O flux data to temperature and soil water content shown for management periods M5 – M9. Solid lines indicate fitted curves and dashed lines represent the 95% prediction bands. Scaling for air-, soil temperature soil water content varies. Larger flux magnitudes were observed during management activities with limited plant growth (M0-M6, Jan. 2012 - mid Jun. 2012). Soil moisture sensors were placed in 0.05 m depth. Statistics are given in Tab. 3.

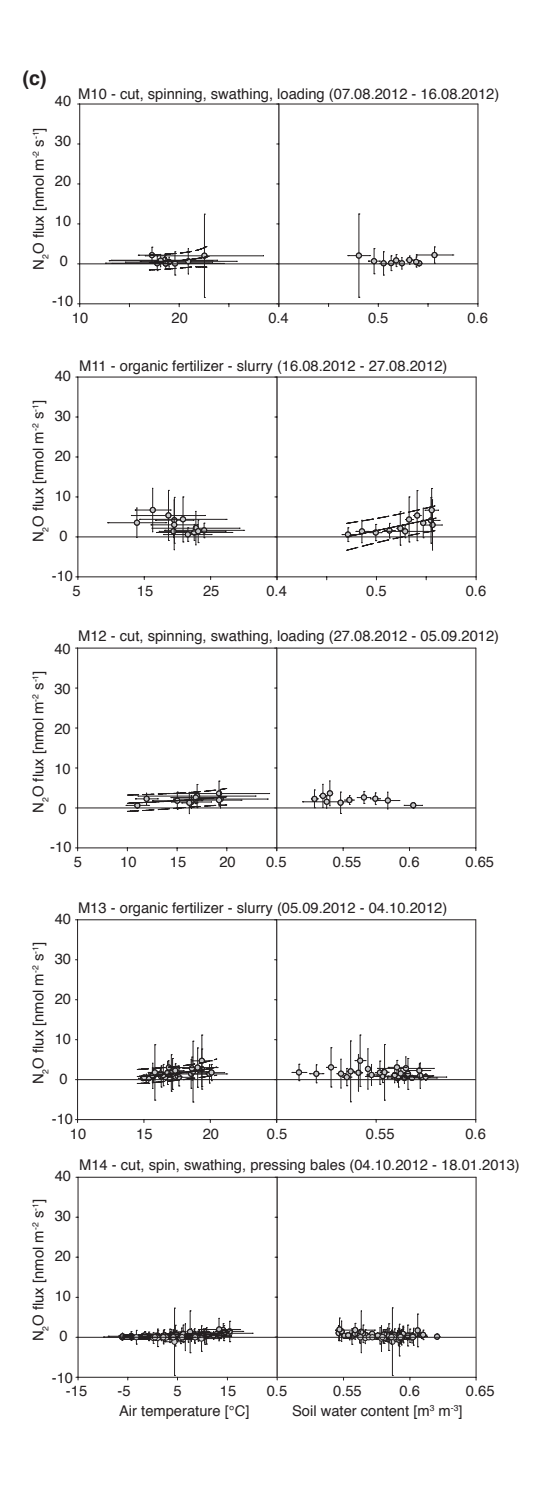


Figure 3a: Responses of measured N_2O flux data to temperature and soil water content shown for management periods M10 – M14. Solid lines indicate fitted curves and dashed lines represent the 95% prediction bands. Scaling for air-, soil temperature soil water content varies. Larger flux magnitudes were observed during management activities with limited plant growth (M0-M6, Jan. 2012 - mid Jun. 2012). Soil moisture sensors were placed in 0.05 m depth. Statistics are given in Tab. 3.

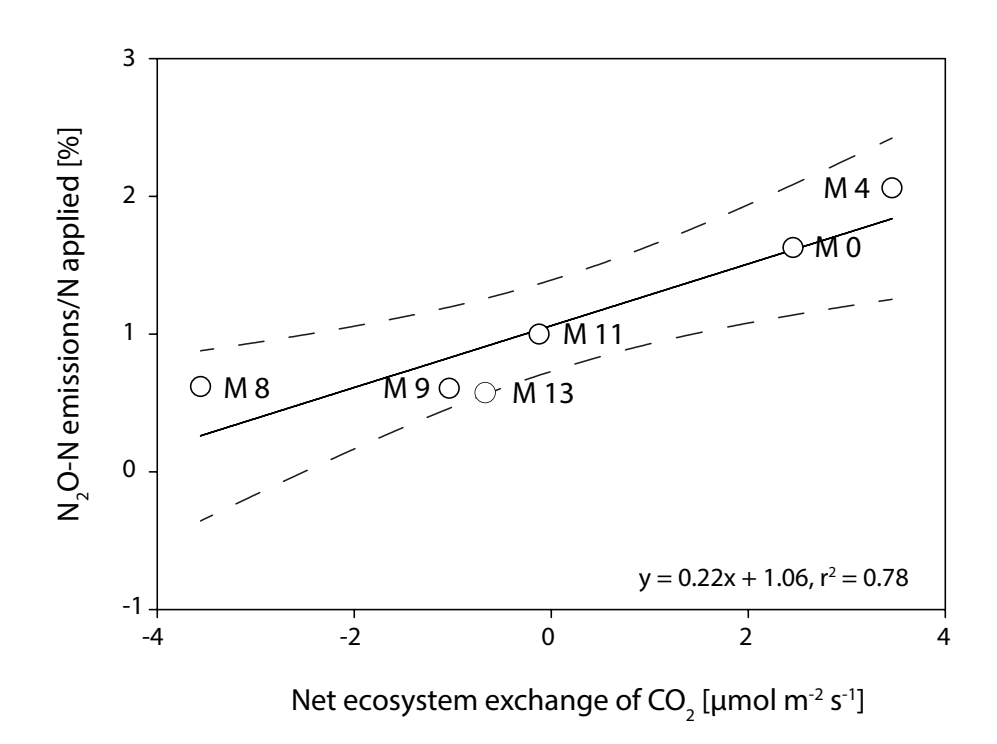


Figure 4: Relationship between the ratio of N emissions (N_2O-N) and N input versus net ecosystem exchange (NEE) of CO_2 of the grassland for management increments that included fertilization. NEE was used as proxy for plant productivity, where negative values indicate a net uptake of CO_2 and positive values a net release of CO_2 .

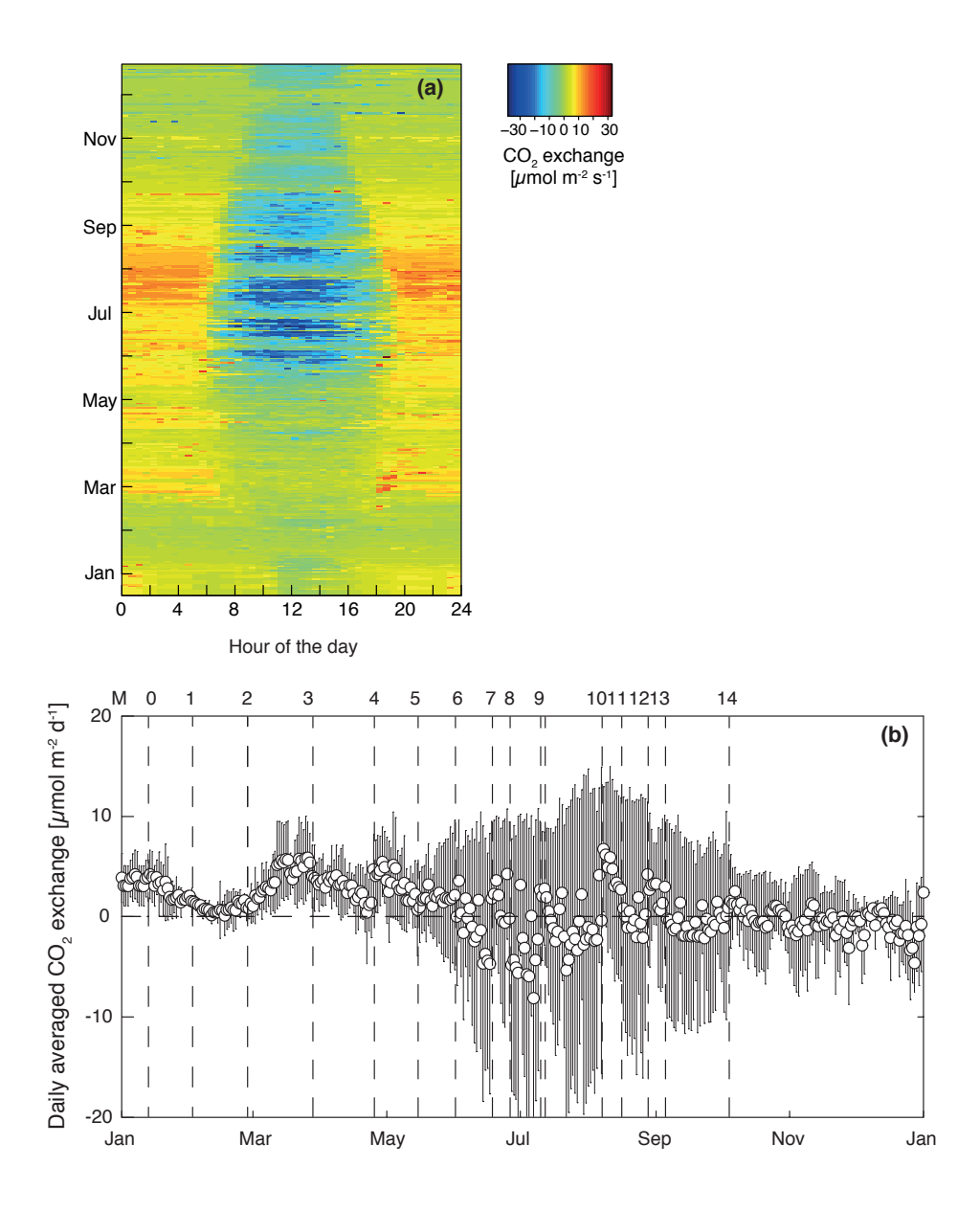


Figure 5: Net ecosystem exchange of carbon dioxide, **(a)** flux fingerprint visualizing gap-filled 30min averaged CO_2 exchange across each day in 2012, **(b)** daily averaged CO_2 exchange (gap-filled data \pm SD). The vertical dashed lines represent the specific management activities (M1 - M14). Negative fluxes indicated net uptake of CO_2 and positive values indicate net release of CO_2 .

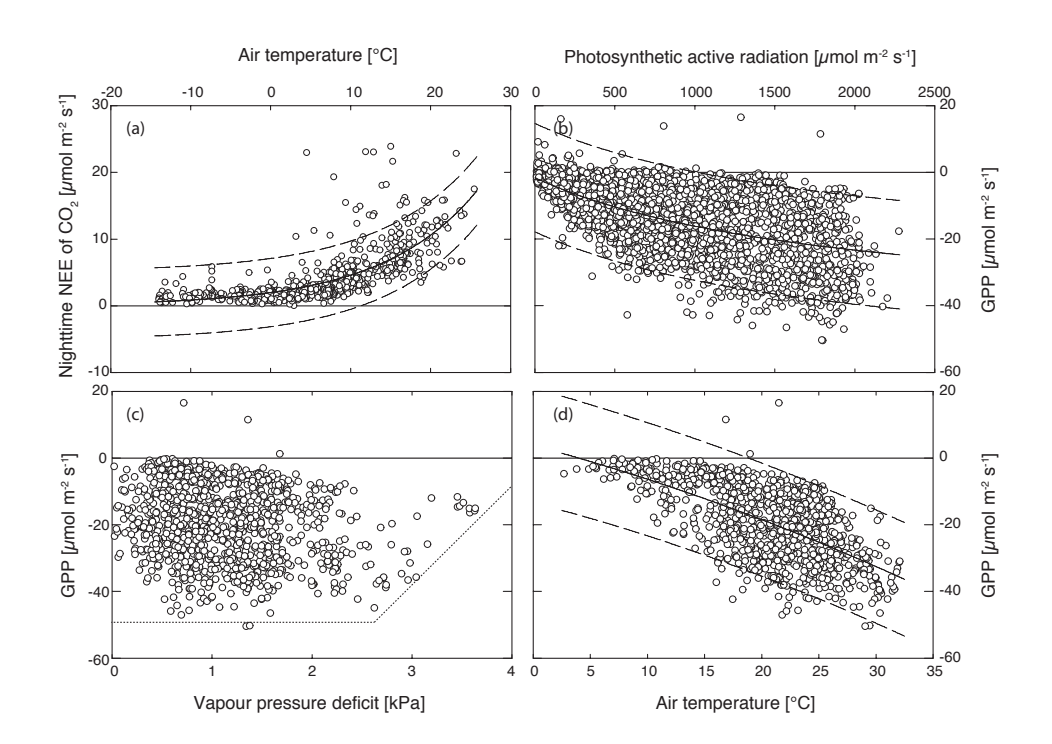


Figure 6: (a) Exponential relationship between measured nighttime NEE of CO $_2$ (R $_{eco}$) and air temperature in 2012 ($r^2=0.51,\ p<0.0001,\ n=820,\ y=1.98^{e0.08x}$); **(b)** hyperbolic light response curve of GPP versus photosynthetic active radiation (PAR) ($r^2=0.36,\ p<0.0001,\ n=2912,\ y=-44.39+(42.78\times1940.55)/(42.78+x)$); **(c)** reduced values of GPP were observed for values of vapor pressure deficit (VPD) exceeding 2.5kPa (shown for light saturated GPP, PAR > 1000 µmol m $^{-2}$ s $^{-1}$ and visualized by the dotted line, n=1062); and **(d)** the inverse quadratic response of light saturated GPP to air temperature (VPD < 2.5kPa, $r^2=0.40,\ p<0.001,\ n=1032,\ y=3.77-0.92x-0.009x^2$). Dashed lines indicate the 95% prediction bands of the curve fits.

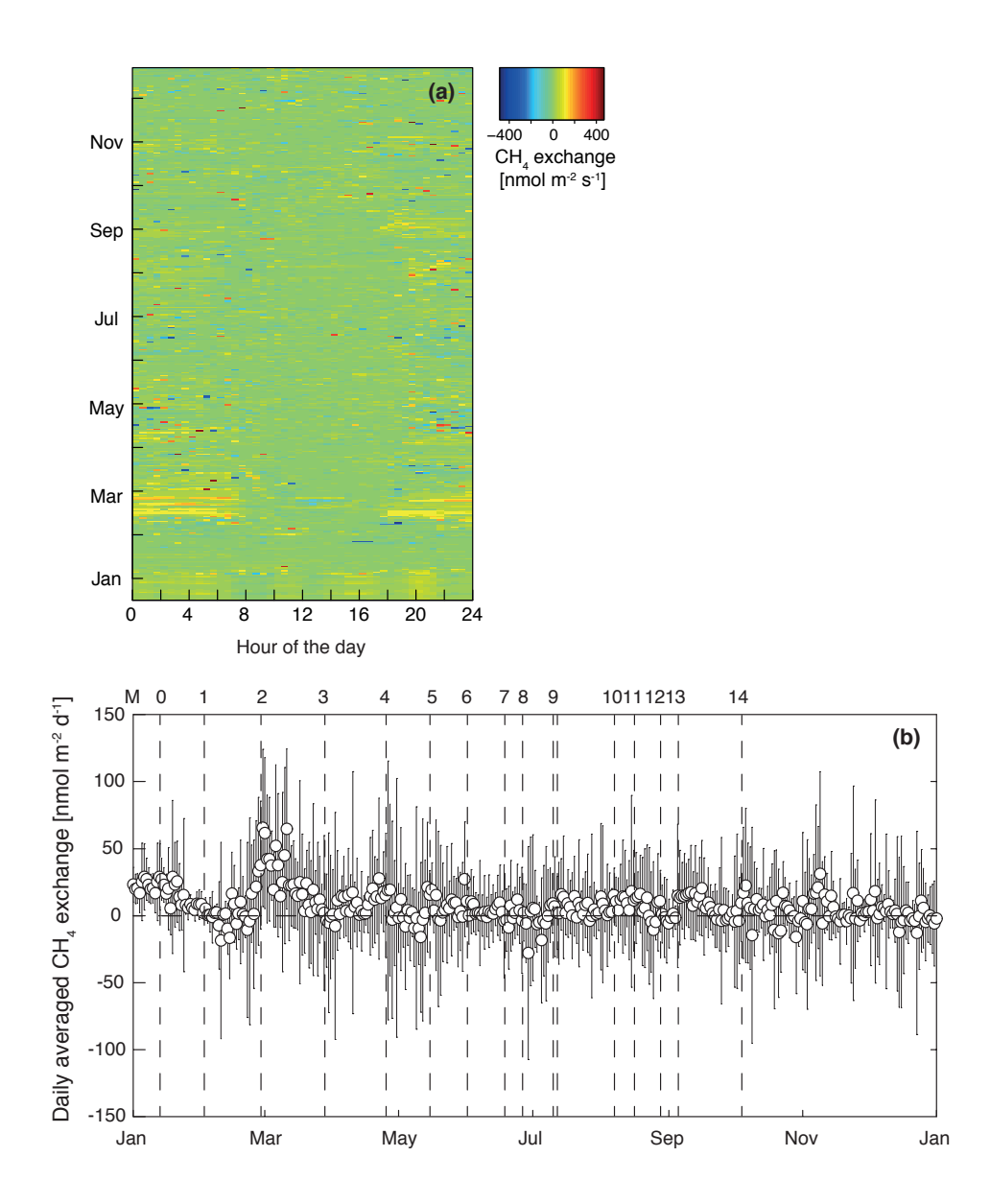


Figure 7: Net ecosystem exchange of methane: **(a)** flux fingerprint visualizing gap-filled CH_4 exchange across each day in 2012 in nmol m^{-2} s^{-1} , **(b)** daily averaged CH_4 exchange (gap-filled data \pm SD). The vertical dashed lines represent the specific management activities (M0 - M14). Negative fluxes indicated net uptake of CH_4 and positive values indicate net release of CH_4 .

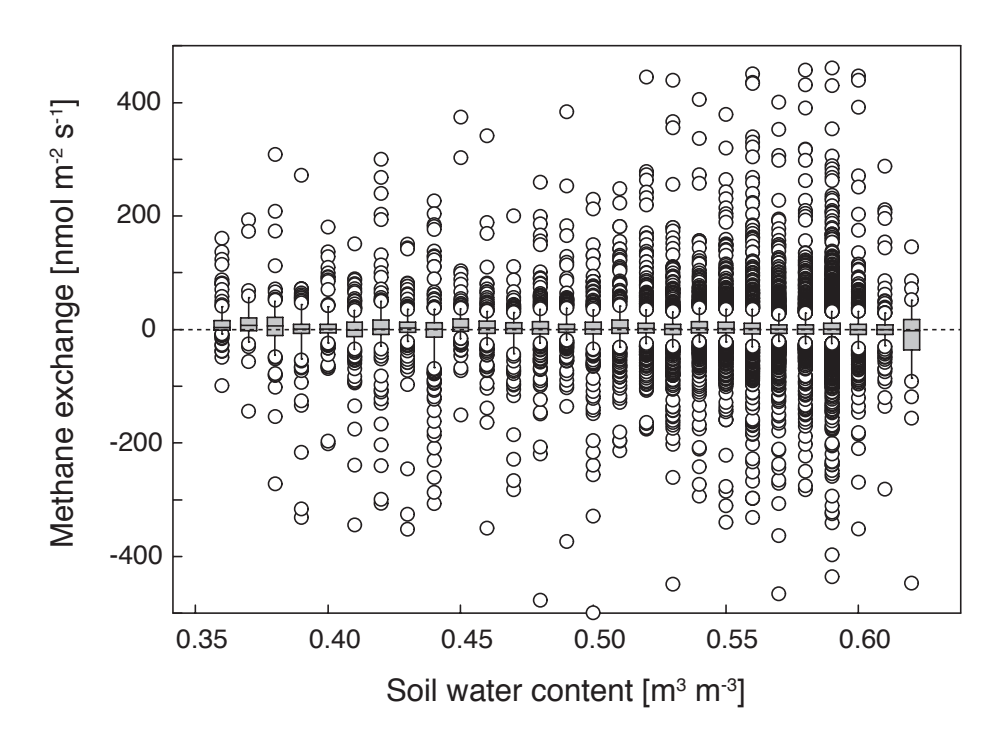


Figure 8: Response of binned CH₄ exchange to soil water content (0.05 m depth), indicating larger flux variation with higher soil water content. The last bin contains only 42 data points.

Table 1: Type of management activities and the respective dates at Chamau grassland site between January and December 2012. Each activity is identified by a specific ID (M0 – M14) and will be further used throughout the manuscript. Please note that M2 does not refer t specific management type but the time period during which the QCLAS had to be replaced, resulting in two weeks of missing N₂O and CH₄ flux data. Detailed information on nutrients contained in the organic fertilizers (manure and slurry). Well-mixed subsamples were sent t central aboratory (Labor fuer Boden- und Umweltanalytik, Eric Schweizer AG, Thun, Switzerland) for pH and dry matter (DM) determination and analysis of most important nutrients (e.g. C. N. P).

E	Date Ma	Management	Specification	Amount	Z	pH Dry	Dry matter (DM) Org. dry matter C org	g. dry matter		C:N N_tot N-NH4	tot N-N)3 P	$P-P_2O_5$), K	$K-K_2O$	Mg	Ca
							%	%		g	٠,		1 kg t-1	M kg t1 D	g kg¹ kg t¹ DM kg t¹ D	1 kg t1 DM	kg t1 DM	kg t' D
M	13.01.2012	organic fertilizer	manure application	26.8		7.79	16.71	79.11		14.3 32.	32.07 3.6	ľ	01 8.9	20.43	39.76	47.91	4.95	17.93
₹ 3	02.02.2012	ughing																
MZ	28.02.2012	no management	breakdown of the laser spectrometer															
,	16.03.2012	no management	restart of the laser spectrometer															
M3	28.03.2012	harrowing	power harrow															
	roll	rolling	OTT 440 F-4-															
		Sowing	OH 440 Extra - grass & wnite clover mixture															
	wos 2102.60.62	sowing	OH 440 EXIIA OH 440 EXIIA															
		9																
	llor	rolling																
Ž	25.04.2012	neral fertilizer	calcium ammonium nitrate fertilizer (13.5 % nitrate, 13.5 %															
			ammonium, Flora Düngemittel, Hanweller, Saar, Germany)	0.102 t°	27.50													
		molluscicide	snail bait (Steiner Ultra W-4935, Omya AG, Switzerland)															
M5	15.05.2012	resowing																
		resowing																
9W			residues left on the field															
		nning																
M Z	18.06.2012	. ;																
	SWS	swathing																
1	,	pressing round bales		į				;										;
2 E	26.06.2012	organic tertilizer cut	slurry distributed via hose spreader	ŝ	78.1	7.94	0.98	6.66	321.72	3.2 10	100.2 69.5	0.02	/T:II	75.59	133.96	161.42	8.13	32.5(
		eninning																
	10.07.2012 spinning	giinu																
	ids	Spinning																
	rde ons	symmig																
	Swi	aumig																
	SIIC	SIIO CHAILING																
	eard Croczoci	pressing round bales		5	- 00	9	00	6410	272 02 4 01	00 00			01.01	10.10		100	91.0	30 66
į	gro 2102.70.21	organic termizer	Sturry distributed via nose spreader	76		9.09	79.1	04.10	5/77.03	4.01 92.	7.04 66.	50:00			71.07	110.4	9.18	33.00
Ě	0 07.08.2012 cut																	
	08.08.2012 spinning	guiuu																
		guiuuds																
	09.08.2012 spir	Spinning																
	SWS.	swathing																
	loa	loading		ò		c t		200	100	00 00 00 00 00 00 00 00 00 00 00 00 00	0.0		10.01			000	000	,,,,,
į	M11 16.08.2012 orga M12 27.08.2012 cut	organic reruitzer cut	sturry distributed via nose spreader	8	5.67	61.1	7.81	67.60	381.17	4.78				74.67	91./0	78.57	9.08	30.33
		Spinning																
	28.08.2012 swathing	athing																
	loac	loading																
Ä	M13 05.09.2012 orga	organic fertilizer	slurry distributed via hose spreader	96	29.3	8.05	3.55	70.08	406.27	7.03 57.	57.78 31	<0.0001	01 11.07	7 25.37	59.6	71.82	7.76	32.1
	06.09.2012 herbicide	bicide	ASULAM (Agro Seller Discount AG, St. Gallen, Switzerland)															
Ě	M14 04.10.2012 cut																	
	05.10.2012 spinning	nning																
	06.10.2012 spinning	nning																
	SWE	swathing																
ļ	aud bue:	pressing round bales	S															

grass-white clover mixture "OH 440 Extra" (Otto Haueustein Samen AG) consisting of red clover (Trifolium pratense), white clover (Trifolium repens), english ryegrass (Lolium pretense), common meadow grass (Poa pratensis), red fescue (Festuca nubs) and common timothy

⁽Phieum pratense) but to excessive amounts of bluntleaf docks (Rumex obussfolius) amount of mineral fertilizer is given in tons

Fable 2: Descriptive statistics for gap-filled CO₂ (μmol m⁻² s⁻¹), N₂O and CH₄ fluxes (nmol m⁻² s⁻¹) per managementactivity in 2012. Each management is specified by the ID given in Table 1.

		; 05			GH₄			N ₂ O		ء
Management	min	mean ± SD	max	mir	mean ± SD	max	min	mean ± SD	max	
M0	-5.6	2.6 ± 2.3	22.9	-165.4	14.6 ± 26.2	391.6	-0.9	1.5 ± 1.0	13.9	096
M1	-14.9	0.9 ± 1.4	8.3	-436.1	1.9 ± 37.6	272.2	-19.9	7.6 ± 7.2	70.2	1248
M2	-6.7	3.9 ± 3.4	23.1	-276.9	26.6 ± 48.8	433.3	-64.3	4.6 ± 6.7	74.5	1392
M3	-14.1	2.9 ± 2.9	19.3	-373.6	7.7 ± 41.2	435.2	-31.6	4.8 ± 3.3	25.8	1344
Μ4	-8.1	3.5 ± 3.9	23.1	-477.6	2.3 ± 55.7	438.5	-27.6	6.4 ± 5.5	34.5	096
MS	-15.2	1.7 ± 4.9	12.6	-306.4	7.4 ± 37.9	255.8	-12.1	8.7 ± 9.1	70.2	816
W6	-31.1	-0.9 ± 9.7	32.1	-185.5	4.0 ± 21.9	156.3	-5.4	8.2 ± 5.0	68.3	816
M7	-22.1	1.6 ± 8.3	16.2	-134.8	0.8 ± 28.9	186.4	-1.4	4.1 ± 2.2	15.8	384
W8	-37.6	-3.6 ± 13.3	15.8	-340.2	-4.7 ± 44.5	307.9	-11.5	2.0 ± 2.7	40.0	624
6W	-35.5	-0.8 ± 12.5	22.8	-350.3	5.5 ± 32.7	373.6	-16.9	2.0 ± 2.5	26.0	1392
M10	-28.6	4.2 ± 9.7	23.9	-255.9	11.2 ± 36.2	383.6	-8.9	1.3 ± 3.5	63.7	431
M11	-28.7	-0.1 ± 12	15.5	-261.1	5.1 ± 38.4	252.5	-12.1	3.3 ± 3.4	26.7	529
M12	-23.5	2.1 ± 7.6	25.8	-175.8	0.9 ± 23.9	173.2	-2.4	2.8 ± 1.8	14.5	432
M13	-20.9	-0.7 ± 8.6	18.2	-331.2	6.9 ± 32.4	329.6	-47.7	1.9 ± 3.3	35.6	1392
M14	-30.9	-0.5 ± 3.9	22.8	-465.6	2.9 ± 37.2	460.8	-51.3	0.2 ± 1.6	30.9	4273
Overall	-37.6	1.1 ± 4.0	22.8	-465.6	6.2 ± 9.2	460.8	-64.3	4.0 ± 2.3	74.5	

Table 3: Statistics for the curve fittings of N_2O fluxes in relation to air and soil temperature (0.02 m depth and 0.15 m depth) as well as soil water content (SWC, 0.05 m depth). Numbers in parenthesis indicate the measurement depth (cm) of soil temperature. Stars indicate significance levels, $p < 0.05^*$, $p < 0.01^{**}$, $p < 0.001^{***}$. Empty cells are given when neither function (exponential or linear) could be fitted. The exponential function was as follows, $y = ax^*exp(bx)$.

Management ID	Driver Variable	n	r²	function	intercept	coefficient a	coefficient b
M0	Tair	11					
	SWC	11					
M1	Tair	25	0.4***	exp.		8.18	0.07
	SWC	25					
M2	Tair	12					
	SWC	12	0.14	linear	-15.37	30.8	
M3	Tair	28					
	SWC	28	0.18*	linear	-4.95	17.79	
M4	Tsoil (0.15)	20	0.22*	exp.		0.11	0.29
	SWC	20	0.19*	linear	-17.3	48.47	
M5	Tsoil (0.02)	17	0.08	exp.		0.07	0.3
	SWC	17	0.45**	linear	-30.93	85.81	
M6	Tair	17					
	SWC	17	0.06	linear	-1.9	16.67	
M7	Tair	8	0.36*	exp.		1.21	0.05
	SWC	8					
M8	Tair	13					
	SWC	13					
M9	Tair	29					
	SWC	29					
M10	Tair	9	0.02	exp.		0.003	0.27
	SWC	9					
M11	Tair	11					
	SWC	11	0.56**	linear	-24.49	52.18	
M12	Tair	9	0.23	exp.		0.5	0.08
	SWC	9					
M13	Tsoil (0.02)	26	0.34***	exp.		0.03	0.22
	SWC	26					
M14	Tair	99	0.48***	exp.		0.08	0.17
	SWC	99					

Table 4: Annual sums of CO_2 , CH_4 and N_2O derived after gap-filling and the respective global warming potentials in CO_2 -eq. calculated with a factor of 23 and 298 for CH_4 and N_2O respectively (IPCC, 2007a).

	CO ₂ -C	CH ₄ -C	N ₂ O-N	Cumulative
g m ⁻²	339	2.65	2.91	
	CO_2	CH ₄	N_2O	
g CO ₂ -eq. m ⁻²	1245	243	1363	2851
%	44	8	48	100

References

- Abdalla M, Jones M, Ambus P, Williams M (2010) Emissions of nitrous oxide from Irish arable soils: effects of tillage and reduced N input. *Nutrient Cycling in Agroecosystems*, **86**, 53-65.
- Ammann C, Spirig C, Leifeld J, Neftel A (2009) Assessment of the nitrogen and carbon budget of two managed temperate grassland fields. *Agriculture Ecosystems & Environment*, **133**, 150-162.
- Aubinet M, Vesala T, Papale D (2012) Eddy Covariance A practical guide to measurement and data analysis, Dordrecht, Heidelberg, London, New York, Springer.
- Baggs EM, Rees RM, Smith KA, Vinten AJA (2000) Nitrous oxide emission from soils after incorporating crop residues. *Soil Use and Management*, **16**, 82-87.
- Baldocchi D, Detto M, Sonnentag O, Verfaillie J, Teh YA, Silver W, Kelly NM (2012) The challenges of measuring methane fluxes and concentrations over a peatland pasture. *Agricultural and Forest Meteorology*. **153**, 177-187.
- Baldocchi D, Falge E, Gu LH *et al.* (2001) FLUXNET: A new tool to study the temporal and spatial variability of ecosystem-scale carbon dioxide, water vapor, and energy flux densities. *Bulletin of the American Meteorological Society*, **82**, 2415-2434.
- Baldocchi D, Meyers T (1998) On using eco-physiological, micrometeorological and biogeochemical theory to evaluate carbon dioxide, water vapor and trace gas fluxes over vegetation: a perspective. *Agricultural and Forest Meteorology*, **90**, 1-25.
- Ball BC (2013) Soil structure and greenhouse gas emissions: a synthesis of 20 years of experimentation. *European Journal of Soil Science*, **64**, 357-373.
- Blankinship JC, Brown JR, Dijkstra P, Hungate BA (2008) Effects of interactive global changes on methane uptake in an annual grassland. *J. Geophys. Res.*, **115**, G02008.
- Chen W, Wolf B, Bruggemann N, Butterbach-Bahl K, Zheng XH (2011) Annual emissions of greenhouse gases from sheepfolds in Inner Mongolia. *Plant and Soil*, **340**, 291-301.
- Dalal RC, Allen DE (2008) Greenhouse gas fluxes from natural ecosystems. *Australian Journal of Botany*, **56**, 369-407.
- Dengel S, Levy PE, Grace J, Jones SK, Skiba UM (2011) Methane emissions from sheep pasture, measured with an open-path eddy covariance system. *Global Change Biology*, **17**, 3524-3533.
- Eriksen J, Jensen LS (2001) Soil respiration, nitrogen mineralization and uptake in barley following cultivation of grazed grasslands. *Biology and Fertility of Soils*, **33**, 139-145.
- Eugster W, Moffat AM, Ceschia E et al. (2010) Management effects on European cropland respiration. *Agriculture Ecosystems & Environment*, **139**, 346-362.

- Eugster W, Pluss P (2010) A fault-tolerant eddy covariance system for measuring CH₄ fluxes. *Agricultural and Forest Meteorology*, **150**, 841-851.
- Eugster W, Senn W (1995) A Cospectral Correction Model for Measurement of Turbulent NO₂ Flux. *Boundary-Layer Meteorology*, **74**, 321-340.
- Falge E, Baldocchi D, Olson R *et al.* (2001) Gap filling strategies for defensible annual sums of net ecosystem exchange. *Agricultural and Forest Meteorology*, **107**, 43-69.
- Flechard CR, Neftel A, Jocher M, Ammann C, Fuhrer J (2005) Bi-directional soil/atmosphere N₂O exchange over two mown grassland systems with contrasting management practices. *Global Change Biology*, **11**, 2114-2127.
- Gilmanov TG, Soussana JE, Aires L *et al.* (2007) Partitioning European grassland net ecosystem CO₂ exchange into gross primary productivity and ecosystem respiration using light response function analysis. *Agriculture Ecosystems & Environment*, **121**, 93-120.
- Hansen S, Maehlum JE, Bakken LR (1993) N₂O and CH₄ fluxes in soil influenced by fertilization and tractor traffic. *Soil Biology & Biochemistry*, **25**, 621-630.
- Hartmann AA, Barnard RL, Marhan S, Niklaus PA (2013) Effects of drought and N-fertilization on N cycling in two grassland soils. *Oecologia*, **171**, 705-717.
- Hartmann AA, Niklaus PA (2012) Effects of simulated drought and nitrogen fertilizer on plant productivity and nitrous oxide (N₂O) emissions of two pastures. *Plant and Soil*, **361**, 411-426.
- Hatala JA, Detto M, Sonnentag O, Deverel SJ, Verfaillie J, Baldocchi DD (2012) Greenhouse gas (CO₂, CH₄, H₂O) fluxes from drained and flooded agricultural peatlands in the Sacramento-San Joaquin Delta. *Agriculture Ecosystems & Environment*, **150**, 1-18.
- Imer D, Merbold L, Eugster W, Buchmann N (2013) Temporal and spatial variations of CO₂, CH₄ and N₂O fluxes at three differently managed grasslands. *Biogesciences*, **10**, 5931-5945, doi:10.5194/bg-10-5931-2013
- IPCC (2007) Climate Change 2007: Synthesis Report. Contribution of Working Groups I, II and III to the Fourth Assessment, Geneva, Switzerland. IPCC
- Klumpp K, Bloor JMG, Ambus P, Soussana JF (2011) Effects of clover density on N₂O emissions and plant-soil N transfers in a fertilised upland pasture. *Plant and Soil*, **343**, 97-107.
- Kroon PS, Hensen A, Jonker HJJ, Zahniser MS, Van 'T Veen WH, Vermeulen AT (2007) Suitability of quantum cascade laser spectroscopy for CH₄ and N₂O eddy covariance flux measurements. *Biogeosciences*, **4**, 715-728
- Kroon PS, Schrier-Uijl AP, Hensen A, Veenendaal EM, Jonker HJJ (2010) Annual balances of CH_4 and N_2O from a managed fen meadow using eddy covariance flux measurements. *European Journal of Soil Science*, **61**, 773-784.

- Lal R (2010) Managing soils and ecosystems for mitigating anthropogenic carbon emissions and advancing global food security. *Bioscience*, **60**, 708-721.
- MacDonald JD, Angers DA, Rochette P, Chantigny MH, Royer I, Gasser MO (2010) Plowing a poorly drained grassland reduced soil respiration. *Soil Science Society of America Journal*, **74**, 2067-2076.
- Macdonald JD, Rochette P, Chantigny MH, Angers DA, Royer I, Gasser MO (2011) Ploughing a poorly drained grassland reduced N₂O emissions compared to chemical fallow. *Soil & Tillage Research*, **111**, 123-132.
- McManus JB, Zahniser MS, Nelson DD, Shorter JH, Herndon S, Wood E, Wehr R (2010) Application of quantum cascade lasers to high-precision atmospheric trace gas measurements. *Optical Engineering*, **49**.
- Mishurov M, Kiely G (2011) Gap-filling techniques for the annual sums of nitrous oxide fluxes. *Agricultural and Forest Meteorology*, **151**, 1763-1767.
- Mori A, Hojito M (2007) Grassland renovation increases N₂O emission from a volcanic grassland soil in Nasu, Japan. *Soil Science and Plant Nutrition*, **53**, 812-818.
- Mori A, Hojito M (2012) Effect of combined application of manure and fertilizer on N₂O fluxes from a grassland soil in Nasu, Japan. *Agriculture Ecosystems & Environment,* **160**, 40-50.
- Necpalova M, Casey I, Humphreys J (2013) Effect of ploughing and reseeding of permanent grassland on soil N, N leaching and nitrous oxide emissions from a clay-loam soil. *Nutrient cycling in agroecosystems*, **95**, 305-317.
- Neftel A, Ammann C, Fischer C *et al.* (2010) N₂O exchange over managed grassland: Application of a quantum cascade laser spectrometer for micrometeorological flux measurements. *Agricultural and Forest Meteorology*, **150**, 775-785.
- Ojima DS, Valentine DW, Mosier AR, Parton WJ, Schimel DS (1993) Effect of land-use change on methane oxidation in temperate forest and grassland soils. *Chemosphere*, **26**, 675-685.
- Palm CA, Alegre JC, Arevalo L, Mutuo PK, Mosier AR, Coe R (2002) Nitrous oxide and methane fluxes in six different land use systems in the Peruvian Amazon. *Global Biogeochemical Cycles*, **16**, 1073.
- Papale D, Reichstein M, Aubinet M *et al.* (2006) Towards a standardized processing of net ecosystem exchange measured with eddy covariance technique: algorithms and uncertainty estimation. *Biogeosciences*, **3**, 571-583.
- Reichstein M, Falge E, Baldocchi D et al. (2005) On the separation of net ecosystem exchange into assimilation and ecosystem respiration: review and improved algorithm. Global Change Biology, **11**, 1424-1439.
- Roth K (2006) Bodenkartierung und GIS-basierte Kohlenstoffinventur von Graslandböden. Diploma Thesis, University of Zurich, 132 pp.

- Sarkodie-Addo J, Lee HC, Baggs EM (2003) Nitrous oxide emissions after application of inorganic fertilizer and incorporation of green manure residues. *Soil Use and Management*, **19**, 331-339.
- Schaufler G, Kitzler B, Schindlbacher A, Skiba U, Sutton MA, Zechmeister-Boltenstern S (2010) Greenhouse gas emissions from European soils under different land use: effects of soil moisture and temperature. *European Journal of Soil Science*, **61**, 683-696.
- Schulze ED, Luyssaert S, Ciais P et al. (2009) Importance of methane and nitrous oxide for Europe's terrestrial greenhouse-gas balance. *Nature Geoscience*, **2**, 842-850.
- Sieber R, Hollenstein L, Odden B, Hurni L (2011) From classic atlas design to collaborative platforms The SwissAtlasPlatform Project. In: 25th International Conference of the ICA. Paris.
- Skiba U, Drewer J, Tang YS et al. (2009) Biosphere-atmosphere exchange of reactive nitrogen and greenhouse gases at the NitroEurope core flux measurement sites: Measurement strategy and first data sets. Agriculture Ecosystems & Environment, 133, 139-149.
- Skiba U, Hargreaves KJ, Beverland IJ, Oneill DH, Fowler D, Moncrieff JB (1996) Measurement of field scale N₂O emission fluxes from a wheat crop using micrometeorological techniques. *Plant and Soil*, **181**, 139-144.
- Snyder CS, Bruulsema TW, Jensen TL, Fixen PE (2009) Review of greenhouse gas emissions from crop production systems and fertilizer management effects. *Agriculture Ecosystems & Environment*, **133**, 247-266.
- Soussana JF, Allard V, Pilegaard K *et al.* (2007) Full accounting of the greenhouse gas (CO₂, N₂O, CH₄) budget of nine European grassland sites. *Agriculture Ecosystems & Environment*, **121**, 121-134.
- Teh YA, Silver WL, Sonnentag O, Detto M, Kelly M, Baldocchi DD (2011) Large greenhouse gas emissions from a temperate peatland pasture. *Ecosystems*, **14**, 311-325.
- Tuzson B, Hiller RV, Zeyer K, Eugster W, Neftel A, Ammann C, Emmenegger L (2010) Field intercomparison of two optical analyzers for CH₄ eddy covariance flux measurements. *Atmospheric Measurement Techniques*, **3**, 1519-1531.
- Vellinga TV, Van Den Pol-Van Dasselaar A, Kuikman PJ (2004) The impact of grassland ploughing on CO_2 and N_2O emissions in the Netherlands. Nutrient Cycling in Agroecosystems, **70**, 33-45.
- Webb EK, Pearman GI, Leuning R (1980) Correction of flux measurements for density effects due to heat and water-vapor transfer. *Quarterly Journal of the Royal Meteorological Society,* **106**, 85-100.
- Willems AB, Augustenborg CA, Hepp S, Lanigan G, Hochstrasser T, Kammann C, Muller C (2011) Carbon dioxide emissions from spring ploughing of grassland in Ireland. *Agriculture Ecosystems & Environment*, **144**, 347-351.
- Wohlfahrt G, Hammerle A, Haslwanter A, Bahn M, Tappeiner U, Cernusca A (2008) Seasonal and inter-annual variability of the net ecosystem CO₂

- exchange of a temperate mountain grassland: Effects of weather and management. *Journal of Geophysical Research-Atmospheres*, **113**.
- Zeeman MJ, Hiller R, Gilgen AK, Michna P, Plüss P, Buchmann N, Eugster W (2010) Management and climate impacts on net CO₂ fluxes and carbon budgets of three grasslands along an elevational gradient in Switzerland. *Agricultural and Forest Meteorology*, **150**, 519-530.
- Zona D, Janssens IA, Aubinet M, Gioli B, Vicca S, Fichot R, Ceulemans R (2013) Fluxes of the greenhouse gases (CO₂, CH₄ and N₂O) above a short-rotation poplar plantation after conversion from agricultural land. *Agricultural and Forest Meteorology*, **169**, 100-110.

Acknowledgements

I am deeply grateful to Nina Buchmann and Werner Eugster for their never ending and active willingness to support me during my PhD. Thank you Nina, for giving me the possibility to dive into physical sciences despite my economic background, for the great working environment and your open door policy (even on sundays!), and especially for your highly appreciated solution-oriented advices whenever help was needed. Thank you Werner, for introducing me to micrometeorology, statistics, R and scientific writing, and for being my first to last level support in many scientific aspects. I very much appreciated your help in the field: fighting trees, repairing winches, reprograming old-fashioned bernese instruments, ordering gas bottles and spreading optimism! Your indestructible patience while explaining me mathematical formulas (sometimes associated with an aura of logical distortion) and how to effectively phrase the first sentence in a manuscript, remains unforgettable.

I very much thank Peter and Thomas for giving me technical assistance before, during and after the field campaigns. Thank you Peter, for spending so many hours introcuding me to soldering, for setting up the experimental design and for retaining old-style measurement devices for my home collection! Thank you Thomas, for your fellowship while supervising Oliver and your tireless commitment on the Figaro/model aircraft topic. Your ideas of how to create a *field-work-conan* and of how to choose the right pinkish motorcycle are very much appreciated.

Euan, thank you for immediatly agreeing on being my co-referee and coming all the way down to Zürich.

Rolf, thank you for your isotopic analysis of the glass flasks, for the hours you spent

with me explaining how a mass-spec works and for your valuable input on the iso paper.

I would like to thank Hans-Ruedi Wettstein and his team for their support during the campaigns and for always providing valuable information about the ETH research station at Chamau.

Dennis, thank you for the great time Z'San Francisco and for all the diskrepiert discussions about anything and nothing. I very much enjoyed field work with you, especially referencing, calibrating, but also vial sampling, singing Schlager and waiting for the end!

Susanne, Rebecca and Anna always provided a positive working atmosphere and introduced me to real field work practice. Many thanks to Rebecca who explained almost everything to me! And thank you Susanne for your great support even over long distances!

A special thank goes to Ines. Thank you for performing the transect measurements and subsequent analysis and especially for pushing through the methane manuscript in these very last days with me.

I am especially grateful for my whole family and for their unceasing background support and faith in me during my PhD. You grounded me with adventurous discussions, lunches, dinners, vacation trips and many other invaluable aspects of life! Thank you for always having an open ear to my thoughts, although they were sometimes rather cryptic, and sharing your wisdom with me. Without you, I would have never been here where I am today!

The research presented in this thesis is funded by the Swiss National Science Foundation.

Jacqueline Véronique Stieger

Day of birth | 14 February 1986

Place of origin | Oberriet-Holzrhode (SG), Switzerland

Education

08/2010-10/2013	PhD Student, ETH Zürich, Zürich, Switzerland.
09/2011-04/2012	Certificate of Advanced Studies (CAS) Geographic Information Systems (GIS), ETH Zürich, Zürich, Switzerland.
09/2009-07/2010	Culture and Language studies, People's University of China 中国人民大学, Beijing, China.
03/2008-09/2009	MSc Geography, University of Bern, Bern, Switzerland. Master Thesis: Financing strategies and instruments of biogechnology and venture capital entreprises in Switzerland
10/2004-03/2008	BSc Geography, University of Bern, Bern, Switzerland. Bachelor Thesis: The pathdependency of biotechnology entreprises in Zürich and Basel. Major subject: Physical and economic geography Minor subjects: Biology and Geology
08/2000-08/2004	High school degree , <i>Kantonsschule Heerbrugg</i> , Heerbrugg, Switzerland. Major subject: Spanish Language and Culture

Professional Experience

08/2010-10/2013	Teaching Assistant , ETH Zurich, Zürich, Switzerland. Micrometeorological Field Course, MSc Level.
01/2009 – 08/2009	Administrative Assistant, OGG des Kantons Bern, Bern, Switzerland.
07/2008 – 07/2008	Administrative Assistant, oeku, Bern, Switzerland.
10/2007-05/2009	Administrative Assistant, femdat.ch. Bern. Switzerland.

Publications

- Hiller RV, Bretscher D, DelSotro T, Diem T, Eugster W, Hennenberger R, Hobi S, Hodson E, Imer D, Kreuzer M, Küzle T, Merbold L, Niklaus PA, Rihm B, Schellenberger A, Schroth MH, Schubert CJ, Siegrist H, **Stieger J**, Buchmann N, Brunner D (2013) Anthropogenic and natural methane fluxes in Switzerland synthesized within a spatially-explicit inventory. *Biogeosciences Discussions*, 2013, 10, 15181–15224
- 2013 Wolf S, Eugster W, Ammann C, Häni M, Zielis S, Hiller R, Stieger J, Imer D, Merbold L, Buchmann N (2013) Contrasting response of grassland versus forest carbon and water fluxes to spring drought in Switzerland. Environmental Research Letters, 2013, 8, 3, 035007

Selected Conference Contributions

- Jimenez MA, Cuxart J, Eugster W, Neininger B, **Stieger J**. Verification of a high-resolution mesoscale simulation over the Reuss Valley (Switzerland) using airborne generated data. *ISARRA 2013, Palma de Mallorca* (E), Talk, 18.–20.02.2013
- 2012 **Stieger J**, Eugster W, Siegwolf R, Buchmann N. Methane emission quantification at the farm scale using boundary-layer volume budgets. *AGU Fall Meeting 2012, San Francisco (USA)*, Talk, 06.12.2012
- 2012 **Stieger J**, Eugster W, Neininger B, Siegwolf R, Buchmann N. Methane from concentratione measurements to a regionally integrated emission estimate. *ACCENT-IGAC-GEIA Conference*, *Toulouse* (F), Poster, 11.–13.06.2012
- 2012 **Stieger J**, Eugster W, Buchmann N. Methane Emissions in Switzerland. Quantification of nocturnal methane emissions at the farm scale using boundary-layer volume budgets *Swiss Geoscience Meeting, Bern (CH)*, Talk, 17.12.2012
- 2011 **Stieger J**, Eugster W, Neininger B, Siegwolf R, Buchmann N. Variation of CH₄ emissions over agricultural areas. *TTorch Summer School, Hyytiälä (F)*, Poster, 27.09.–04.10.2011

Miscellaneous

- 2012 SRF Schweiz Aktuell: Jungforscher auf Methan-Jagd. 04.09.2012, 18:59 pm (http://www.srf.ch/player/tv/schweiz-aktuell/video/jungforscher-auf-methan-jagd?id=73caf515-e217-4e36-a09a-4a07df791ab5, date of access: 04.09.2013)
- 2011 SRF Einstein: Wie die Rinder das Klima beeinflussen. 08.09.2011, 21:08 pm (http://www.srf.ch/player/tv/einstein/video/wie-die-rinder-das-klima-beeinflussen?id=c3675435-c471-491d-8b92-0de46b92d892, date of access: 04.09.2013)



Eidgenössische Technische Hochschule Zürich Swiss Federal Institute of Technology Zurich

Diss. ETH No. 21538

